Synthesis, applications and conformational investigations of Neuropeptide Y analogues containing 2-(2-aminocyclopentyl) acetic acid and *trans*-pentacin

Dissertation

zur Erlangung des Doktorgrades

der Naturwissenschaften (Dr. rer. nat.)

der Fakultät für Chemie und Pharmazie

der Universität Regensburg

vorgelegt von

Pietro Di Stefano

aus

Palermo (Italien)

Regensburg 2012

Die Arbeit wurde angeleitet von: Prof. Dr. O. Reiser

Promotionsgesuch eingereicht am: 9. July 2012

Promotionskolloquium am: 30. July 2012

Prüfungsausschuß:

Vorsitzender:	Prof. Dr. F. Kees
1. Gutachter:	Prof. Dr. O. Reiser
2. Gutachter:	Prof. Dr. B. König
3. Prüfer:	Prof. Dr. J. Heilmann

Die vorliegende Arbeit wurde in der Zeit von Oktober 2008 bis Juli 2012 am Institut für Organische Chemie der Universität Regensburg unter der Leitung von Prof. Dr. O. Reiser angefertigt.

Meinem Lehrer, Herrn Prof. Dr. O. Reiser, danke ich herzlich für die Überlassung des interessanten Themas, die Möglichkeit zur Durchführung dieser Arbeit und seine stetige Unterstützung.

To my fiancée Ylenia, for her support and encouragement

Index

Abbreviations

Ac	acetyl	*e.e.*	enantiomeric excess
β-ACC	β-amino cyclopropanecarboxylic acid	Fmoc	9-fluorenylmethyl chloroformate
Aib	aminoisobutyric acid	HATU	2-(7-aza-benzotriazole-1-l)-1,1,3,3-tetramethyluronium) hexafluorophosphate
Bn	benzyl	HBTU	*O*-benzotriazole-N,N,N',N'-tetramethyluronium
Boc	tert-butyloxycarbonyl	HOAt	hydroxyazabenzotriazole
Bu	butyl	HOBt	hydroxybenzotriazole
d.e.	diastereoisomeric excess	LAH	lithium aluminiumhydride
d.r.	diastereoisomeric ratio	Me	methyl
DBU	1,8-Diazabicyclo [5.4.0]undec-7-ene	MeOH	methanol
DCC	*N*,*N*'-dicyclohexyl carbodiimide	MS	mass spectroscopy
DCM	Dichloromethane	NH_3	ammonia
DIPEA	diisopropylethylamine	Pg	protecting group
DMAP	dimethylaminopyridine	r.t.	room temperature
DME	dimethoxyethane	tert	tertiary
DMF	dimethylformamide	SPPS	solid phase peptide
DMSO	dimethylsulfoxide	TBS	*tert*-butyldimethylsilyl
EDC	*N*-(3-dimethylaminopropyl)-*N*-ethylcarbodiimide hydrochloride	TEMPO	2,2,6,6-tetramethylpyridine-*N*-ethylcarbodiimide
Et_3N	triethylamine	TFA	trifluoroacetic acid

α-Amino acids

Alanine	Ala	Leucine	Leu
Arginine	Arg	Lysine	Lys
Asparagine	Asn	Methionine	Met
Aspartic acid	Asp	Phenylalanine	Phe
Cysteine	Cys	Proline	Pro
Glutamine	Gln	Serine	Ser
Glutamic acid	Glu	Threonine	Thr
Glycine	Gly	Tryptophan	Trp
Histidine	His	Tyrosine	Tyr
Isoleucine	Ile	Valine	Val

I. Introduction

I. 0. Preface

"*When we look at a cell through a microscope or analyze its electrical or biochemical activity, we are, in essence, observing proteins*".[1]

Proteins are biochemical compounds produced by a process called "protein synthesis" in all living cells and constitute most of a cell's dry mass. Proteins and peptides are present in all living organism and appear as hormones, receptors, enzymes, etc. (**Table 1**)

Peptide Name	*Species*	*Peptide Sequence*
Thyrotropin-releasing hormone	Human	pGlu-His-Pro-NH_2
Gonadotropin-releasing hormone	Human	pGlu-His-Trp-Ser-Tyr-Gly-Leu-Arg-Pro-Gly-NH_2
Gastrin I	Human	pGlu-Gly-Pro-Trp-Leu-$(Glu)_5$-Ala-Try-Gly-Trp-Met-Asp-Phe-NH_2
Fertilization promoting peptide	Human	pGlu-Glu-Pro-NH_2
Growth-inhibition pentapeptide	Mouse	pGlu-Glu-Asp-Ser-Gly-OH
Caerulin-like peptide	Amphibian	pGlu-Asp-Tyr-(HSO_3)-Lys-Gly-Trp-Met-Asp-Phe-NH_2
Adipokinetic hormone	Insect	pGlu-Lys-Thr-Phe-Ser-Pro-Asp-Trp-NH_2
Leucosulfakinin-II	Insect	pGlu-Ser-Asp-Asp-Tyr-(SO_3H)-Gly-His-Met-Arg-Phe-NH_2
Corazonin	Insect	pGlu-Thr-Phe-Gly-Tyr-Ser-Arg-Gly-Trp-Thr-Asn-NH_2
Chitinase	Plant	pGlu-Cys-Glu-Thr-Thr-Ile-Tyr-Cys-Cys-Ser-Gly-His-NH_2

Table 1. Some examples of peptides.

An interesting property of proteins and peptides is the ability to fold into specific spatial conformations.[2] These structures are stabilized by weak bonds such as hydrogen bonding, Van Der Waals forces, and ionic interactions.[1,3] Their biological functions are associated with their final structure, therefore in order to understand the functions of proteins and peptides, it is necessary to know their three-dimensional structure.[4] The scientific field of medicinal chemistry and biochemistry utilizes different techniques such as X-ray crystallography, CD and two dimensional NMR spectroscopy to determine the structure of proteins and peptides (**Figure 1**).[5]

When a protein performs a biological activity, its conformation is called active conformation. Different factors such as pH, phosphorylation, ionic concentration, and the binding of a ligand, can favor several conformational changes.[6] There are different techniques to detect transitions between different conformations. Recently, an optical technique called second-harmonic generation (SHG) has been applied to probe structural dynamics as described by *Salafsky et al.*[7]

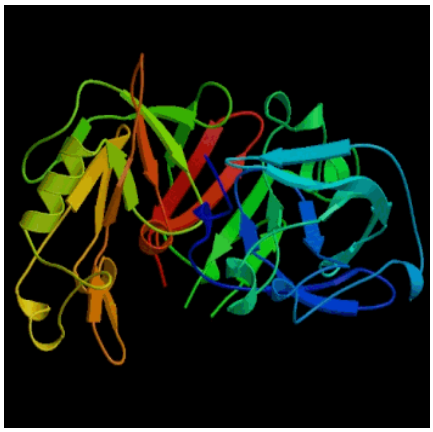

Figure 1. Three-dimensional structure of porcine pepsin. Pepsin was the first globular protein crystal successfully applied in X-ray diffraction.[8]

"*The discovery of peptide hormones, growth factors and neuropeptides implicated in vital biological functions of our organism has increased interest in therapeutic use of short peptides*".[9] **Table 2** shows some examples of active endogenous peptides. Therefore, peptide analogues and peptide mimetics have been widely investigated in order to obtain new useful ligands for SAR studies.[10]

Name	*Biological function*
Insulin	Decreases glucose level in blood.
Somatostatin	Inhibits the secretation of growth hormon, insulin and glucagon.
Oxytocin	Induces contraction of smooth muscles, especially uterine muscle.
Neurotensin	Causes constrictions of blood vessels.
Met-enkephalin	Morphine-like properties, analgesic

Table 2. Some examples of active endogenous peptides.[11]

Unnatural amino acids, because of their ability to induce folding, have been extensively used as building blocks for the design of new peptide analogues.[12] The synthesis of conformationally constrained γ-amino acids and their use as building blocks in foldamers will be the objective of this thesis.

I. 1. General information on peptides

Peptides are defined as "*amides derived from two or more amino carboxylic acid molecules (the same or different) by formation of a covalent bond from the carbonyl carbon of one to the nitrogen atom of another with formal loss of water*".[13] Because of the delocalization of the electrons, as shown by formula of resonance, the amide bond or peptide bond tends to be planar (**Figure 2**).

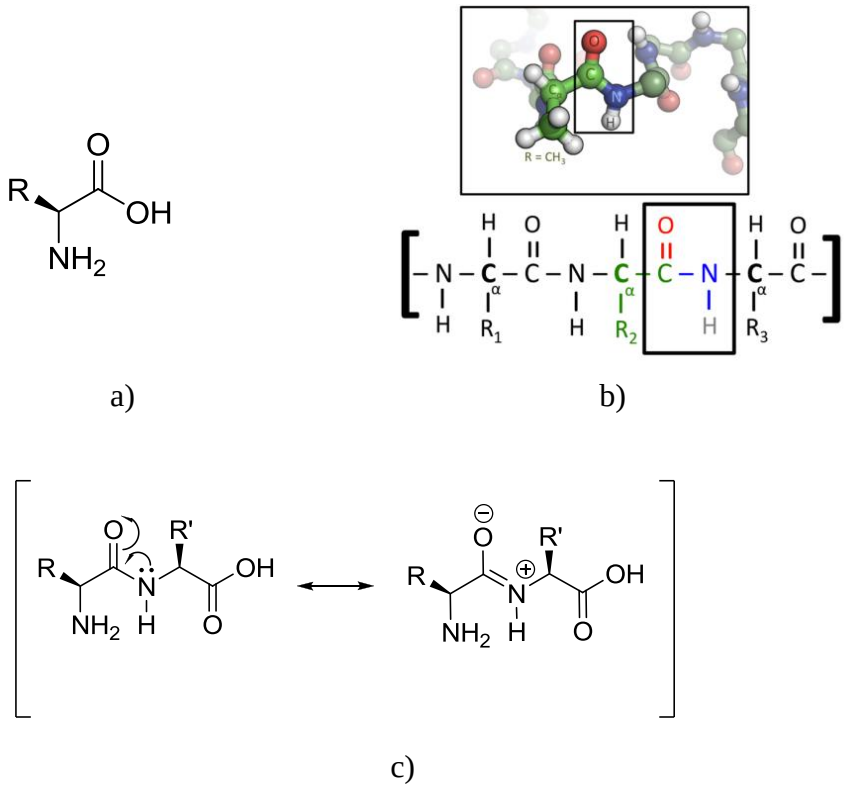

Figure 2. a) General formula of a α-amino acid; b) Sequence of a α-peptide and a peptide bond,[14] c) Formula of resonance of peptide bond.

The carbon atoms from the first one directly connected to the carboxyl group, are named using the greek letters: α, β, γ, δ, ϵ. In natural amino acids, the amino group is connected to the alpha carbon. If the amino group is connected to different carbon atoms along the chain, then this is usually an example of an unnatural amino acid.

Thus, it is called β-amino acid, when the amino group is on the beta carbon and so on. The spatial arrangement of the peptide depends on the orientation of the groups connected by three repeating bonds, which can be described by dihedral (or torsion) angles. These values describe the rotation about each of the three bonds and thus are the internal degrees of freedom of a protein or peptide.[15] The peptide dihedral angles are ω, φ and ψ. The first angle corresponds to the peptide bond and thus has a value close to 180 degrees. The dihedral angle φ describes the bond between the nitrogen and alpha carbon, and ψ describes the bond between alpha carbon and the carbon of the carboxylic group. The angles φ and ψ can have different values according to the final conformation. (**Figure 3**).[15]

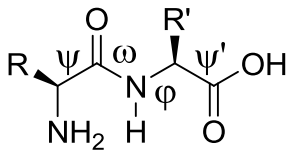

Figure 3. Dihedral angles.

All peptides have an amino end terminus called N-terminus and a carboxyl end terminus called C-Terminus. Peptides and proteins have four levels of organization that together give rise to their specific three-dimensional conformation. These levels of organization are classified as follows: primary structure, secondary structure, tertiary structure and quaternary structure.

I. 1. 1. Primary structure

The primary structure is a complete description of all peptide bonds which hold together the amino acids, and also it provides the location of any disulfide bonds, specifying the cysteines involved in these bonds. The primary structure is always denoted by writing the amino acid sequence, using the standard three-letter abbreviations in order, from the N-terminus to the C-terminus.[1]

I. 1. 2. Secondary structure

The secondary structure was proposed in 1951 by *Linus Pauling* and coworkers,[16,17] suggesting that a polypeptide chain does not remain in an elongated form in liquid phase, but it folds in a regular repetitive arrangement, stabilized by hydrogen bonds. The polypeptide chain folds up according to specific values of the dihedral angles ψ and φ, and to the steric hindrance of side groups.[15]

A method to predict the secondary structure of a polypeptide chain is the *Ramachandran plot*, that shows the possible values of the ψ and φ for each amino acid residue.[18] However, there are many proteins that have some domains with a defined structure and others which are not organized at all. A non-organized conformation is called a random coil. Three kinds of secondary structure can be observed: helices, sheets and turns.

I. 1. 2. 1. Helices

Helices are one of the most common secondary structures utilized by peptides and proteins. They consist of a helical structure, which is generally stabilized by hydrogen bonds. The helices are usually in the right-handed form, but in some cases the left-handed form has been observed.[19] There are different kinds of helices that can be classified according to the periodicity of the helix, where the most common one adopted by proteins is the α-helix. This structure is very compact, stabilized by the hydrogen bond between the carbonyl group of an *i* residue with the nitrogen of the residue *i*+4, forming a 13-membered ring (**Figure 4**).[20]

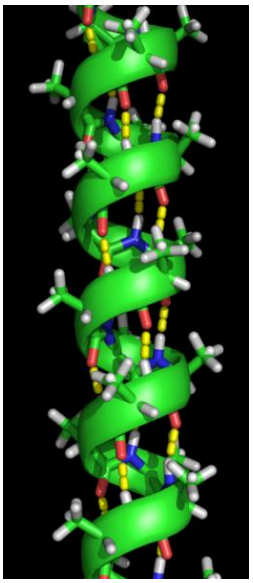

Figure 4. General representation of a α-helix. Hydrogen bonds are indicated with yellow color.[21]

The ability to form an α-helix depends on several factors, one of the most representative is the steric effect of side chains. Other helices are the 3_{10} helix and the Π-helix. The first one is stabilized by a hydrogen bond between the carbonyl group of an *i* residue with the nitrogen of the residue *i*+3, forming a 10-membered ring.

The Π-helix represents a rare class of helices. They have been found in 15% of known proteins, and present a hydrogen bond between an *i* residue and an residue *i*+5.[22] However, the Π-helix does not seem to always adopt a regular repetition like the α- and 3_{10}-helices.[23,20]

I. 1. 2. 2. β-Sheet

A β-Sheet consist of beta strands where hydrogen bonds are arranged parallel to each other, and the two fragments are far away from each other. This is a planar conformation, and the R groups are placed perpendicular to the plane of the peptide bonds. There are two types of β-sheet, the parallel type, where both fragments are oriented in the same direction and the anti-parallel, where they are oriented in opposite directions (**Figure 5**).[20]

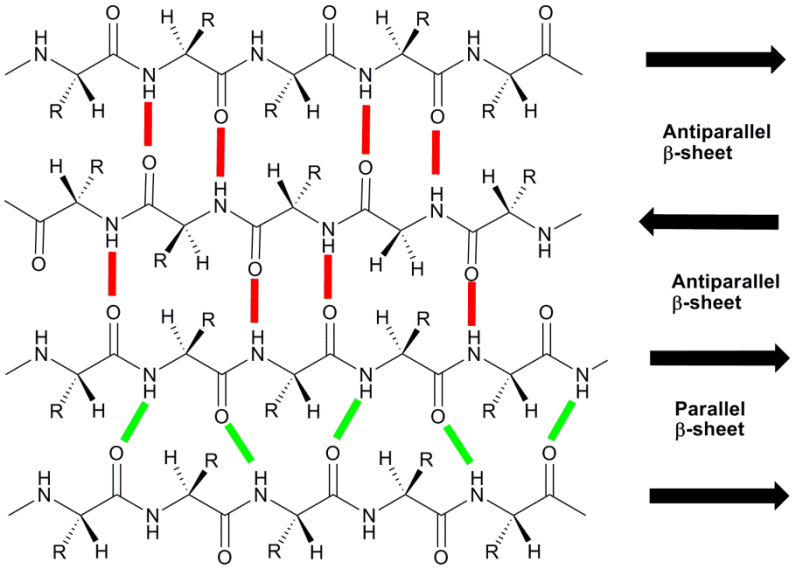

Figure 5. The parallel and anti-parallel β-sheet. Hydrogen bonds are indicated with red and green color [24]

I. 1. 2. 3. Turns

Turns are another kind of secondary structure that are formed at some points of a peptide sequence driven by a few hydrogen bonds.[25] There are different kinds of turns and they are classified on the base of the ring size of the hydrogen bond forming the turn.

β-Turns are most common and involve hydrogen bonding between the *i* residue and the *i+3* residue. On the basis of their backbone dihedral angles, three types of β-turn are known and are named type I, II and III (**Figure 6**). Moreover, there are also α-turns (hydrogen bonding between the *i* residue and the *i+4* residue), γ-turns (between the *i* residue and the *i+2* residue),[26] δ-turns (between the *i* residue and the *i+1* residue) and π-turns (between the *i* residue and the *i+5* residue).[27,20]

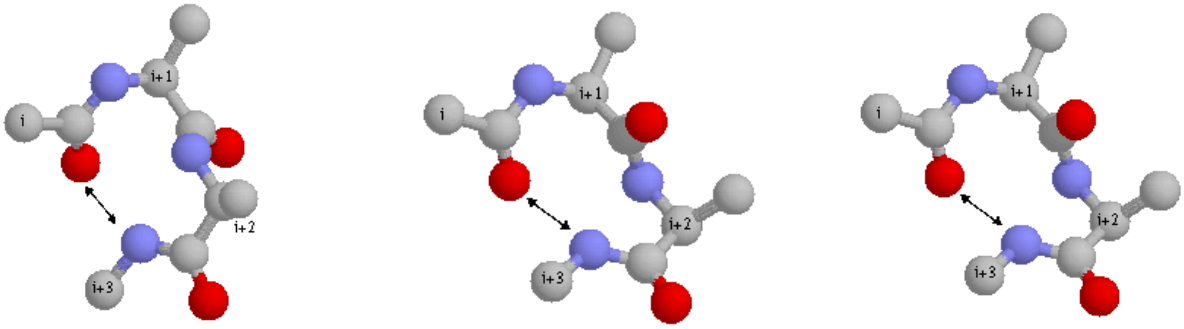

Figure 6. From left to right (β-turn-type I, β-turn-type II, β-turn type III).[24]

I. 1. 3. Tertiary structure

"*The tertiary structure of a protein is the spatial organization (including conformation) of an entire protein molecule consisting of a single chain*".[28] They derive from combinations of all regions with specific secondary structures. The tertiary structure is stabilized by secondary bonding, established between the side chains of amino acids such as the disulfide bond between cysteines.[29] The three-dimensional tertiary structure of proteins is very important for its function.[4]

I. 1. 4. Quaternary structure

"*Many protein molecules are composed of more than one subunit, where each subunit is a separate polypeptide chain and can form a stable folded structure by itself*".[20] The spatial organization of these polypeptide chains into more complex multi-subunits is called quaternary structure. The proteins can be defined globulars, if they fold in a spherical shape, and fibrous, if they maintain an elongated shape.[30,1]

I. 2. Synthesis of peptides

Peptide synthesis consists of coupling of a carboxyl group and an amino group between two amino acids. The mixture of two amino acids in solution at room temperature leads to the formation of a salt by a simple acid-base reaction. Therefore, it is necessary to convert the carboxylic acid to an activated form, favoring a nucleophilic attack by the amino group. In a typical peptide coupling reaction, a peptide coupling reagent (PCR)[31] reacts with the carboxylic group, generating a reactive intermediate, which will react with the amino group of a second amino acid, leading to the formation of a peptide bond as illustrated in **Scheme 1**.[32]

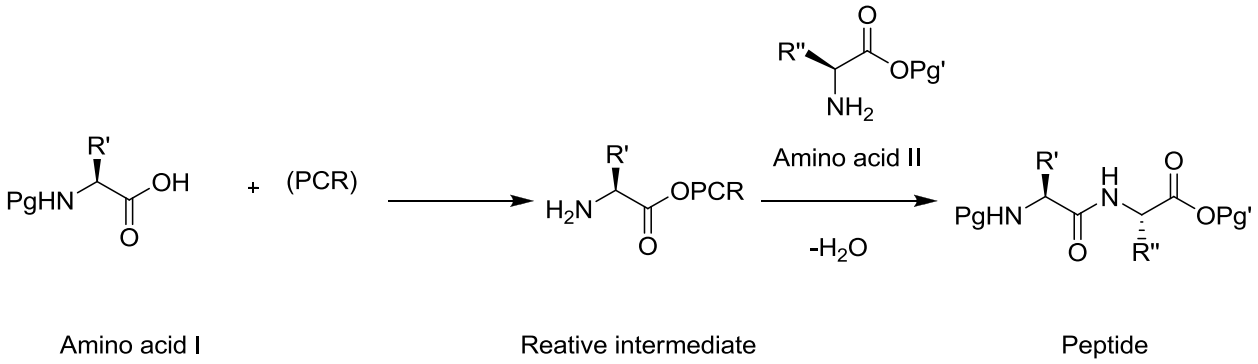

Scheme 1. Typical peptide coupling reaction. PCR (Peptide coupling reagent).

Activated forms of carboxylic acids for peptide coupling reactions are acid halides,[33] anhydrides,[34] activated amides,[35] and esters.[36] The carbodiimides **1** have especially attracted attention as peptide coupling reagents.[37] They have been widely used in peptide synthesis because of their moderate activity, which is important in peptide coupling to avoid secondary reactions (**Figure 7**). In 1955, *Sheehan et al.* suggested dicyclohexylcarbodiimide (DCC) **2** as peptide coupling reagent.[38] A great advantage is that the by-product *N,N'*-dicyclohexylurea is insoluble in most organic solvents and thus it is possible to separate it from the dissolved product by filtration.

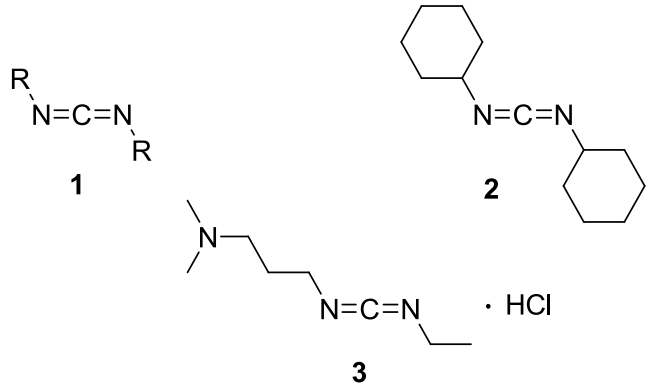

Figure 7. General formula of a carbodiimide **1**; Dicyclohexylcarbodiimide (DCC) **2**; *N*-(3-dimethylaminopropyl)-*N*-ethylcarbodiimide hydrochloride (EDC) **3**.

The general mechanism is shown in **scheme 2**. The carboxyl group of the N-protected amino acid **4** attacks the C=N bond of the general carbodiimide **1** leading to the *O*-acylisourea intermediate **5**. This highly reactive compound **5** reacts with a free amino group of a C-protected amino acid **6**, being a good nucleophile, determining the formation of peptide **7** and the dialkylurea by-product **8**.[39]

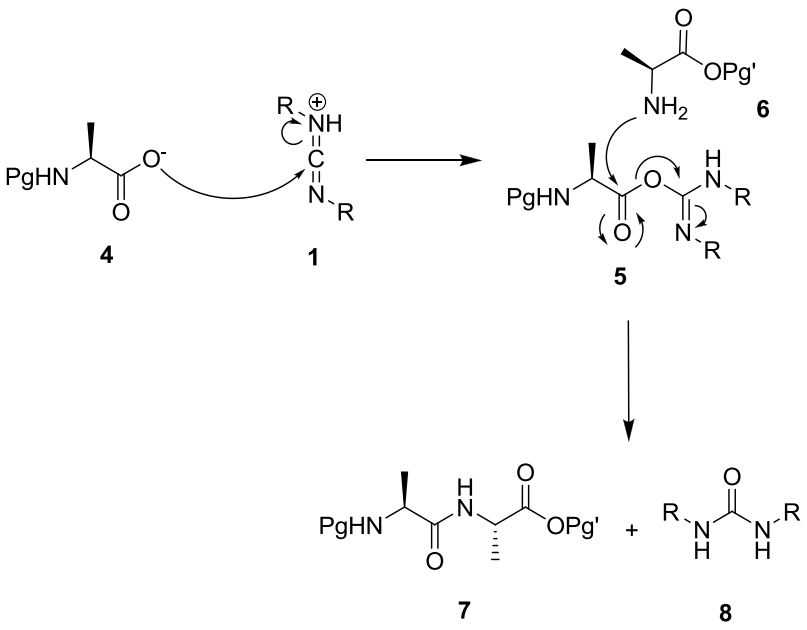

Scheme 2. Activation of a α-amino acid using a carbodiimide reagent.

Side reactions are a problem during peptide coupling. One of the most common side reactions during the coupling promoted by the carbodiimides is the racemization of a peptide sequence, because of their high reactivity. Racemization can occur in the course of a coupling reaction because of the formation of an oxazolone intermediate **10** from the *O*-acylisourea intermediate **9** (**Scheme 3**).[31] In the presence of a base, which is an important component in peptide couplings, compound **10** could be deprotonated in α-position giving the anion **11**, that is stabilized by resonance. Compound **11** could be reprotonated again, providing racemization of a peptide sequence **13**.

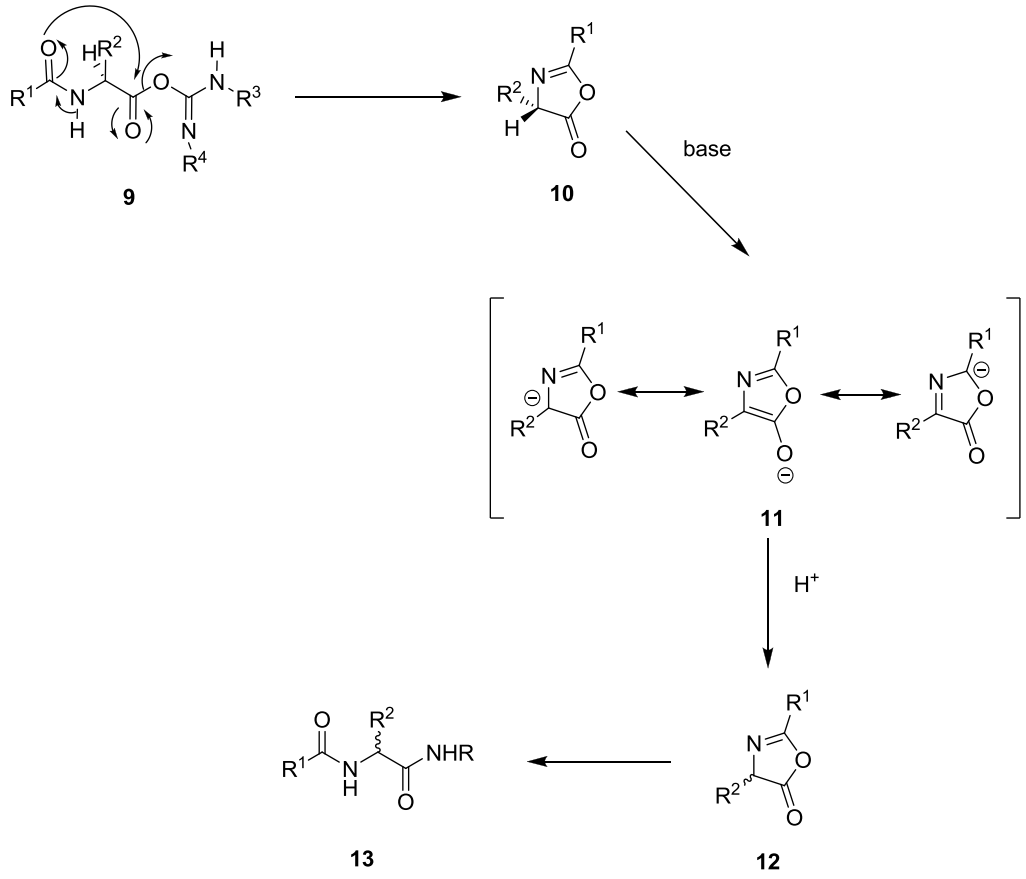

Scheme 3. Racemization of a peptide sequence by formation of oxazolone intermediate **10**.

Many of the side reactions can be avoided by using some additives or racemization suppressants.[40,31] The racemization suppressants intercept the *O*-acylisourea intermediate **9**, generating a reactive ester which reacts quickly with the amino group before racemization occurs. The most widely used are HOBt **14** and HOAt **15** (**Figure 8**).[41]

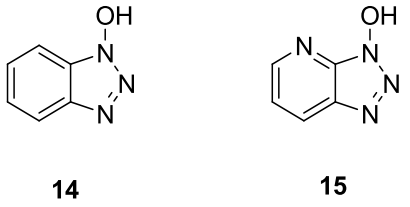

Figure 8. Structure of HOBt **14**, and HOAt **15**.

To avoid racemization many reagents similar to HOBt **14** have been developed.[42] Examples are phosphonium-based reagents such as BOP **16** and PyBOP **17** (**Figure 9**).[43] With the phosphonium-based reagents the racemization is minimal, and combining activation and coupling reagent, they can be used without prior activation by carbondiimides.

.

Compound **16** is also useful to prepare esters in mild conditions.[44]

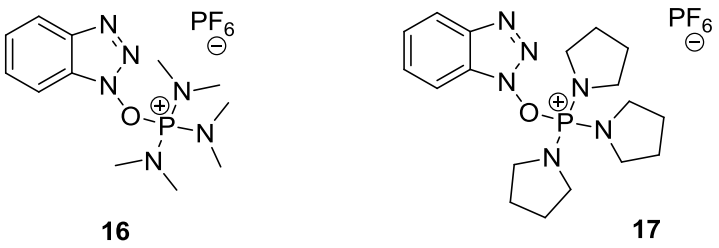

16 **17**

Figure 9. Phosphonium-based reagents BOP **16** and PyBOP **17.**

Other very popular coupling reagents are uronium salts, such as HBTU **18** and HATU **19**.[45] Both compounds crystallize as guanidinium *N*-oxide, as demonstrated by *Carpino et al.*, using X-ray crystallography studies (**Figure 10**).[46]

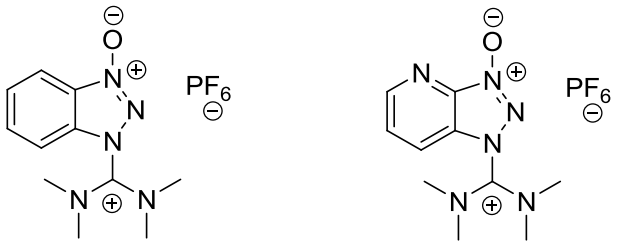

18 **19**

Figure 10. Guanidinium *N*-oxide structures of compounds **18** and **19**.

Peptides can either be synthesized in liquid-phase or in solid-phase. In liquid-phase peptide synthesis, it is possible to isolate and analyze the intermediate products after each amino acid addition.[47] Furthermore, the liquid-phase synthesis allows the development and application of new strategies such as the design of new protecting groups for the side chains and the use of new coupling reagents.[48] The synthesis of peptides in liquid phase is mainly used to synthesize small peptides, while for long sequence of peptides, the solid phase synthesis is mostly utilized.[47]

I. 2. 1. Solid phase peptide synthesis(SPPS)

"*Solid-phase peptide synthesis (SPPS) consists in the elongation of a peptidic chain anchored to a solid matrix by successive additions of amino acids which are linked by amide (peptide) bond formation between the carboxyl group of the incoming amino acid and the amino group of the amino acid previously bound to the matrix, until the peptide of the desired sequence and length has been synthesized*".[47] This procedure was introduced in 1963 by *Merrifield*, who showed the synthesis of a tripeptide on a solid phase.[49] Solid phase synthesis has many advantages, such as use of large excess of reagents, which leads to faster reaction (2-3 hours) and removal of by-products and excess of reagents by washing of the solid support since the peptide is anchored to it, leading to a more facile purification. **Scheme 4** shows the general scheme of SPPS using Fmoc as a N-protecting group, which is a base labile. The cleavage of the Fmoc group by an appropriate base (piperidine), leads to the free amine of a attached peptide or amino acid that will be coupled to a single activated N-protected amino acid. Then, the new N-protected peptide will be deprotected again, generating a new free N-terminal amine, which can be attacked by another activated amino acid.[50] For the cleavage of the peptide from the resin and deprotection of the side chain protection groups, a so called "cleavage cocktail" (1 mL per 30 mg resin) is used, which usually consists of TFA and different scavengers. The choice of the cleavage cocktail depends on the nature of the support and the nature of the protecting groups.[51] After that, the crude peptides are usually purified by preparative HPLC.[52] Development in SPPS has led to two main schemes of protection, the Boc/Bzl and Fmoc/*t*-Bu strategies, where Fmoc (base labile) and Boc (acid labile) are the protecting groups for the amino group, and *t*-Bu and Bzl groups are used to protect the side chains of several amino acids.[47] Furthermore, it is sometimes necessary to use different protecting groups for the side chains, depending on their nature, such as TBS and trityl group for alcohols, and Pbf or Pmc for guanidine groups.[53] Recently, microwave irradiation has been used for SPPS, especially for coupling of sterically hindered amino acids.[54] The microwave energy can prevent aggregation of preformed chains leading to faster reactions (reaction time 1.5–20 min), low degrees of racemization, and high yields of the final peptide product.[55]

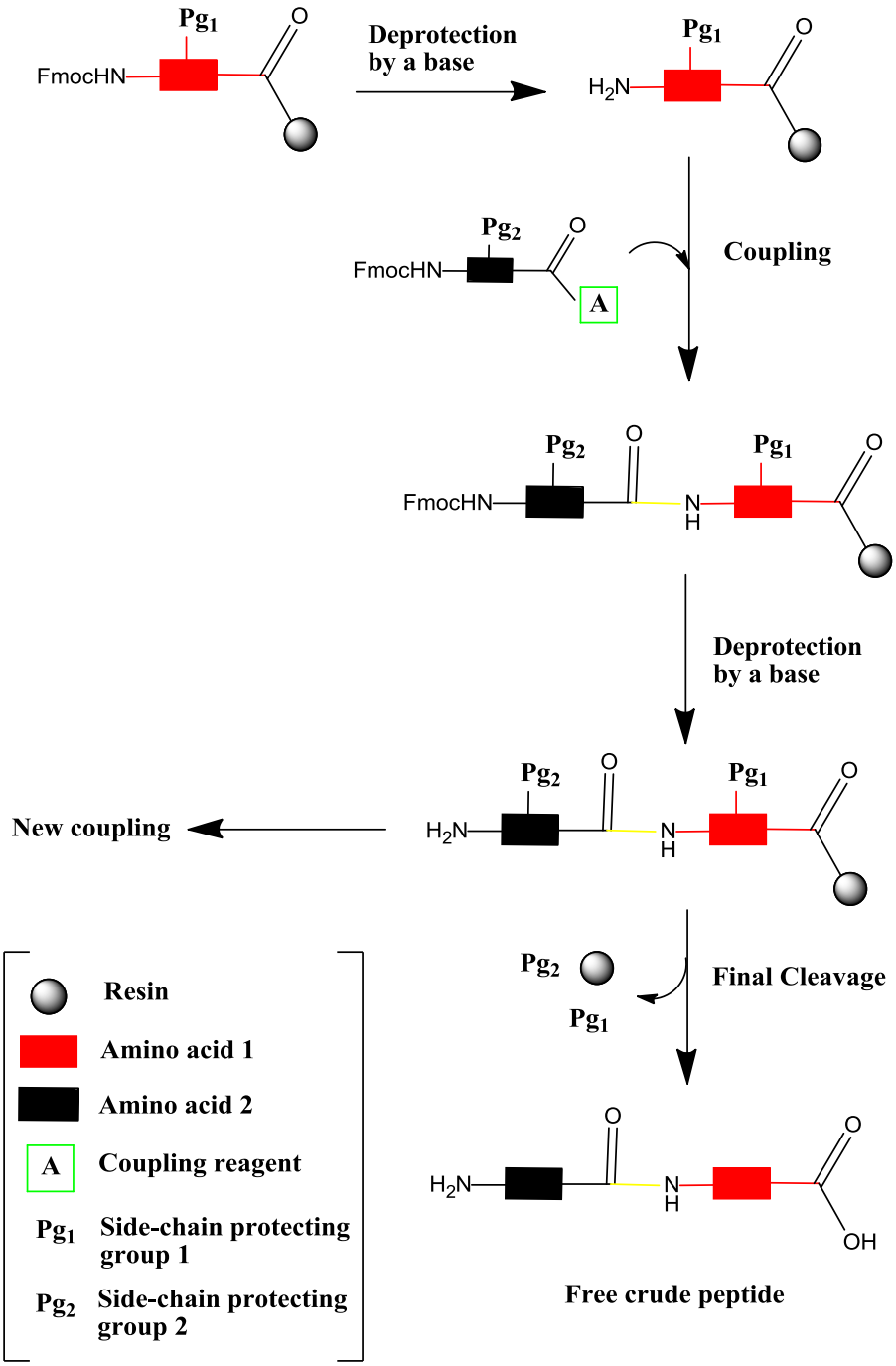

Scheme 4. General scheme of SPPS.

Solid supports for solid phase have to meet several requirements, such as uniform size of the particles, easily filterable, and moreover they have to be chemically inert and stable under the conditions of synthesis.[47] The supports for solid phase can be of three types: gel-type supports, surface-type supports and composites.[56] The gel-type supports are the most common, and consist of solvated polymers with different functional groups.

These includes polystyrene, polyacrylamide and polyethylene glycol (PEG).[57,56] For the Fmoc strategy, a common resin is Rink amide MBHA resin **20**, which is already derivatized with a Fmoc-amine.[58] Thus, the synthesis can be started before any prior preparation. There are some cases such as the Wang Type resin **21**, which need to be preloaded with the first amino acid (**Figure 11**).

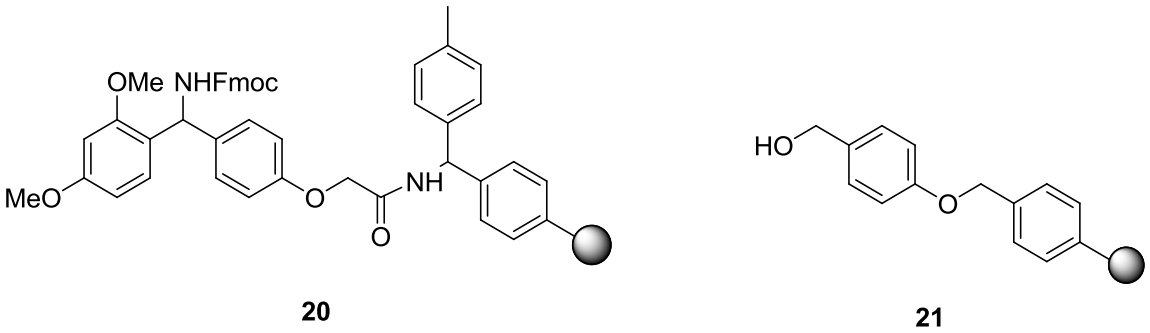

Figure 11. Structure of Rink amide MBHA resin **20** already Fmoc derivatized and Wang Type resin **21**.

Modern automated SPPS instrumentations are often used for the synthesis of short and long peptide sequences. It permits coupling with a yield of 99.99%, which leads to an overall yield of 99% for a 50 amino acid peptide.[59]

I. 3. Application of Peptides

Peptide research is a continuously growing field of medicinal chemistry and biochemistry. Peptides have intensively been used to prepare antibodies in animals, and inhibitors for protein tyrosine kinases against cancer and other diseases.[60] Furthermore, structure-activity-relationship (SAR) studies about different peptidic ligands, have increased the interest in the preparation of new synthetic peptides.[61] They have been used, for example, as probes for studies of protein-peptide interactions, and as peptidomimetics.[62,63]

"*Peptidomimetics are compounds whose essential elements (pharmacophore) mimic a natural peptide or protein in 3D space and which retain the ability to interact with the biological target and produce the same biological effect*".[63] They can be new compounds prepared by chemical synthesis, such as β-peptides,[64,65] or they can be designed by modification of an existing peptide such as incorporation of new compounds, in order to modify some molecular properties.[66]

Unnatural amino acids have been intensively studied in the area of peptide research, and have been used as pharmaceuticals. For example well-known are L-Dopa, which is used to alleviate the symptoms of Parkinson's disease, and D-Penicillamine for the treatment of arthritis.[67] Moreover, unnatural amino acids have become a very important class of building blocks to prepare foldamers and, in the design of new potent ligands for biological receptors by incorporation into biologically active peptides.[68,69] "*Foldamers are sequence-specific oligomers akin to peptides, proteins and oligonucleotides that fold into well-defined three-dimensional structures. They offer to the chemical biologist a broad pallet of building blocks for the construction of molecules that test and extend our understanding of protein folding and function*".[70] Foldamers have been intensively studied and have shown to have interesting properties.[71] The first application of unnatural amino acids into foldamers were reported by the groups of *Gellman* and *Seebach*.[72,64] Conformationally constrained *trans*-ACHC **22** was used by *Gellman et al*. to prepare different homooligomers, which showed a strong tendency to fold into a helical structure.[73] Moreover, even heterooligomers showed the ability to adopt well-defined conformations. Recently, *Gellman* also showed that β/γ-hybrid peptides **23**, which are composed of two different unnatural amino acids in alternate order, give stable secondary structure (**Figure 12**).[74]

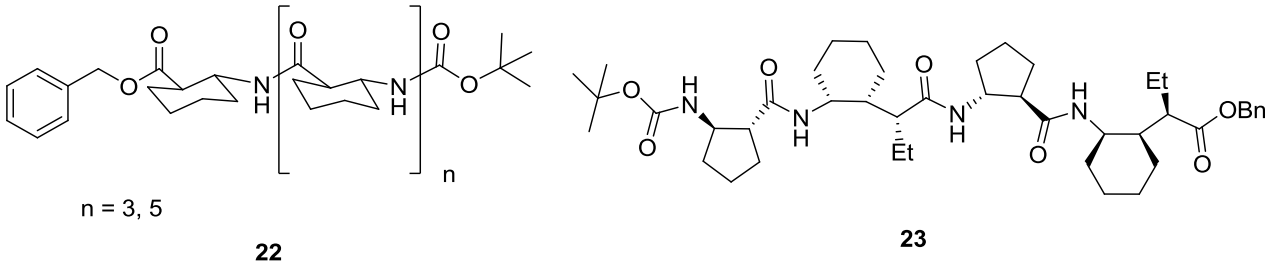

Figure 12. Examples of homooligomeric and heterooligomeric foldamers which give stable secondary structures.

Cyclic and bicyclic β-amino acids have been used to prepare potent analogues of natural peptides, and have shown interesting properties. For example, cispentacin derivative **24** has been incorporated into 6 positions of the gonadotropin releasing hormone as reported by *Mulzer et al.*,[75] and the bicyclic amino acid **25,** which was incorporated into different bioactive peptides such as enkephalin, somatostatin and growth hormone releasing factor (GRF) by *Nagai et al.*[76] (**Figure 13**).

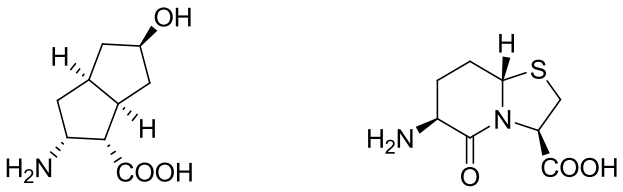

24 **25**

Figure 13. Unnatural amino acids incorporated in peptide analogues.

In both cases, different analogues showed some activity against the own receptor. β-ACCs **26** has been incorporated into different analogues such as neuropeptide Y (NPY),[77] calcitonin gene related peptide[78] and orexin peptide,[79] as reported by *Reiser et al*. Truncated NPY analogues **27** (residues 25-36) containing β-ACCs **26** in different positions in the *C*-terminus, showed good affinity and selectivity for the Y_1 receptor (**Figure 14**).[77]

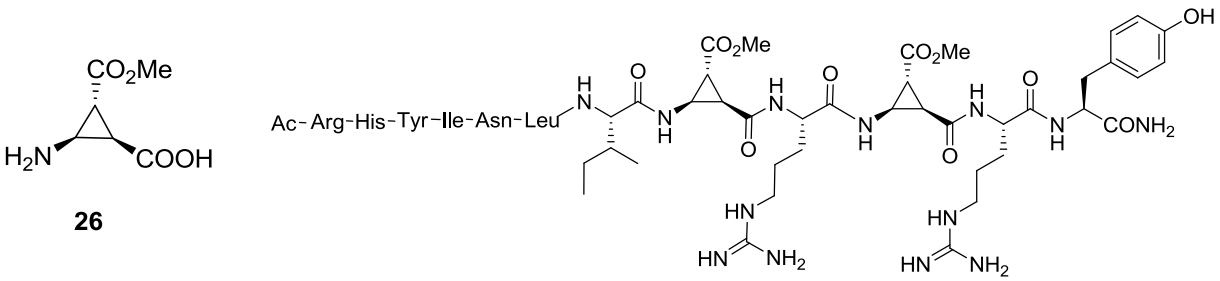

26 **27**

Figure 14. β-ACCs **26** as constrained β-amino acid analogues. Truncated NPY analogues **27** (residues 25-36) containing β-ACCs.

Cispentacin derivaties **28** were also incorporated in NPY analogues **29** in the group of *Reiser* (**Figure 15**), but unfortunately in this case, they showed affinities only in a high micromolar range.[80]

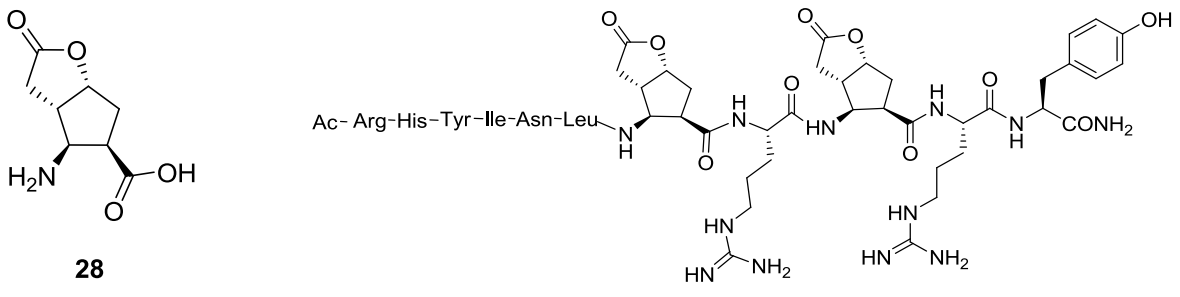

28 **29**

Figure 15. Cispentacin derivaties **28**; Truncated NPY analogues **29** containing compound **28**.

After several applications of β-amino acids in α-peptides in our research group, we focused on new conformationally constrained γ-amino acids as building blocks in the design of NPY analogues. On the basis, that differences in ring size can produce significant differences in the conformation of the resultant peptides and in the biological activity, as described by *Thompson et al.*,[81] γ-amino acids in which the backbone is constrained by a five-membered ring have been investigated. In this work *cis*-(**30**), *trans*-(**31**) and *trans*-(**32**) 2-(2-aminocyclopentyl) acetic acids were prepared in enatiomerically pure form (**Figure 16**).

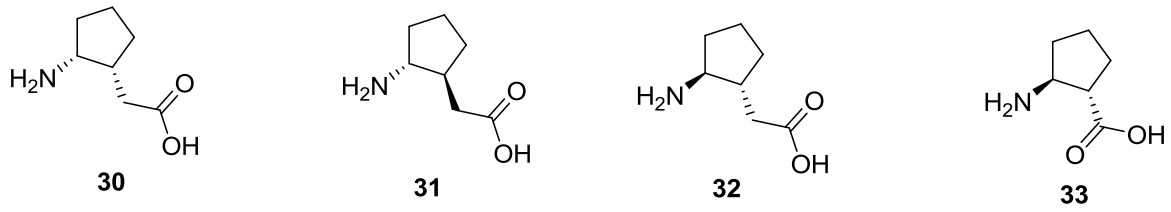

Figure 16. Different isomers of 2-(2-aminocyclopentyl) acetic acid and structure of *trans*-pentacin **33**

Furthermore, *trans*-pentacin **33** has also been introduced into NPY analogues in this work (**Figure 16**). *Gellman et al.* showed that β-peptides containing *trans*-pentacin **33** adopt a well-defined helical secondary structure.[82] In conclusion, the synthesis of NPY analogues containing different isomers of 2-(2-aminocyclopentyl) acetic acid and the *trans*-pentacin **33**, with their conformational investigations, and the testing of their biological activity against the different NPY receptors, is the aim of this work.

References Introduction

[1] Bruce, A.; Johnson, A.; Lewis, J.; Raff, M.; Roberts, K.; Walters, P. **(2002)** "The Shape and Structure of Proteins". *Molecular Biology of the Cell*, pp. 129; Fourth Edition.

[2] Kuntz, I. D. *J. Am. Chem. Soc.* **1972**, *94*, 4009.

[3] Pace, C. N.; Shirley, B. A.; Mcnutf, M.; Gajiwala, K. *FASEB J.* **1996**, *10*, 75.

[4] a) Nagata, K. Biosci. Biotechnol. Biochem. **2010**, *74*, 462. b) Perutz, M. F.; Kendrew, J. C.; Watson, H. C. *J. Mol. Biol.* **1965**, *13*, 669.

[5] Cai, X.; Dass, C. *Curr. Org. Chem*. **2003**, Volume 7, Number 18, 1841.

[6] a) Groban, E. S.; Narayanan A.; Jacobson *M. P. PLoS Comput. Biol.* **2006**, Volume 2, *4*, e32.; b) Tobi, D.; Bahar, I. *PNAS* **2005**, *102*, 18908.

[7] Salafsky, Joshua S. *J. Chem. Phys* **2006**, *125*, 074701.

[8] Picture reproduced with permission from: http://www.bio.davidson.edu/Courses/Molbio/MolStudents/spring2003/Kogoy/protein.html.

[9] Adessi, C. *Curr. Med. Chem.*, Volume 9, Number 9, May **2002**, *16*, pp. 963.

[10] a) Olson, G. L.; Bolin, D. R.; Bonner, M. P.; Bos, M.; Cook, C. M.; Fry, D. C.; Graves, B. J.; Hatada, M.; Hill, D. E.; Kahn, M.; Madison, V. S.; Rusiecki, V. K.; Sarabu, R.; Sepinwall, G.; Vincent, G. P.; Voss, M. E. *J. Med. Chem.***1993**, *36*, 3039; b) Gentilucci, L. *Curr. Top. Med. Chem.* **2004**, *4*, 19.

[11] Adapted from: De Pol, S.; *Dissertation*, Regensburg **2006**.

[12] Rajashekhar, B.; Kaise, E. T. *J. Biol. Chem.* **1986**, *261*, 13617.

[13] PAC, **1995**, *67*, 1307 *(Glossary of class names of organic compounds and reactivity intermediates based on structure (IUPAC Recommendations 1995))* on page 1356, White Book, p. 48.

[14] Picture reproduced with permission from: http://en.wikipedia.org/wiki/Protein;

[15] Richardson, J. *Adv. Prot. Chem.* **1981**, *34*, 174.

[16] Pauling, L.; Corey, R. B.; Branson, H. R. *Proc Natl Acad Sci USA* **1951**, *37*, 205.

[17] Pauling, L; Corey, R. B. *Proc Natl Acad Sci USA* **1951**, 37, 729.

[18] Ramachandran, G. N.; Ramakrishnan, C.; Sasisekharan, V. *J. Mol. Biol.* **1963**, *7*, 95.

[19] Novotny, M.; Kleywegt, G. J. J. Mol. Biol. **2005**, *347*, 231.

[20] Richardson, J. *Adv. Prot. Chem.* **1981**, *34*, 167.

[21] Picture reproduced with permission from: http://en.wikipedia.org/wiki/File:Alpha_helix.png.

[22] Cooley, R. B.; Arp, D. J.; Karplus, P. A. *J. Mol. Biol.* **2010**, *404*, 232.

[23] Rohl, C. A.; Doig, A. J. *Prot. Sci.* **1996**, *5*, 1687.

[24] Picture reproduced with permission from:
http://www.nku.edu/~russellk/tutorial/peptide/peptide.html.

[25] Toniolo C.; Benedetti, E. *CRC Crit Rev Biochem* **1980**, *9*, 1.

[26] Némethy, G.; Printz, M. P. *Macromolecules* **1972**, *5*, 755.

[27] Rose, G. A.; Gierasch, L. M.; Smith, J. A. J. *Adv. Prot. Chem.* **1985**, *37*, 1.

[28] PAC, **1996**, *68*, 2193 *(Basic terminology of stereochemistry (IUPAC Recommendations 1996))* on page 2220, White Book, p. 80.

[29] Wall, J. S. *J. Agr. Food Chem.***1971**, *19*, 619.

[30] Huggins, M. L. *Chem. Rev.***1943**, 32, 195.

[31] a) Han, S.-Y., Kim, Y.-A *Tetrahedron* **2004**, *60*, 2447. b) North, M. J. *J. Chem. Soc., Perkin Trans. I* **1999**, 2209. c) Humphrey, J. M., Chamberlin, A. R. *Chem. Rev.* **1997**, *97*, 2243.

[32] Kent, S. B. H. *Ann. Rev. Biochem.* **198**, *57*, 957.

[33] Montalbetti, C. A. G. N.; Falque, V. *Tetrahedron* **2005**, *61*, 10827.

[34] Rijkers, D. T. S.; Adams, H. P.; Hemker, H. C.; Tesser, G. I.; *Tetrahedron* **1995**, *51*, 11235.

[35] Pearson, C., Rinehart, K. L., Sugano, M. *Tetrahedron Lett.* **1999**, *40*, 411.

[36] a) Bodanszky, M.; Bednarek, M. *J. Protein Chem* **1989,** Vol. 8, No. 4. b) Babu, V. V. S.; Ananda, K.; Mathad, R. I. *Lett. Pept. Sci.* **2000,*7,*** 239.

[37] Mikolajczyk, M.; Kiezbasinski, P. *Tetrahedron* **1981**, *37*, 233.

[38] Sheehan, J. C. *J. Am. Chem. Soc.* **1955,** *77*, 1067.

[39] *Joullie, M. M.; Lassen, K. M. Arkivoc* **2010**, (viii), 189.

[40] Konig, W.; Geiger, R. *Chem. Ber*. **1970**, *103*, 788.

[41] a) Carpino, L. A. *J. Am. Chem. Soc.* **1993**, *115*, 4397.; b) Carpino, L. A.; El-Faham, A.; Minorb, C. A.; Albericio, F. *J. Chem. Soc., Chem. Commun.***1994**, 201.

[42] Di Fenza, A.; Rovero, P. *Letters in Peptide Science* **2002**, *9*, 125.

[43] Castro, B.; Dormoy, J. R.; Evin, G.; Selve, C. *Tetrahedron Lett.* **1975**, No. *14*, 1219.

[44] Kim, M. H.; Patel, D. V. *Tetrahedron Lett.* **1994**, *35*, 5603.

[45] Knorr, R.; Trzeciak, A.; Bannwarth, W.; Gillessen, D. Tetrahedron Letters **1989**, *30*, 1927.

[46] Carpino, L. A.; Imazumi, H.; El-Faham, A.; Ferrer, F. J.; Zhang, C.; Lee, Y.; Foxman, B. M.; Henklein, P.; Hanay, C.; Mugge, C.; Wenschuh, H.; Klose, J.; Beyermann, M.; Bienert, M. *Angew. Chem. Int.* Ed. **2002**, *41*, 441.

[47] Guzman, F.; Barberis, S.; Illanes, A. *Elettron J. Biotechn* ISSN: 0717-3458, **2007**, *10*, 279.

[48] a) Hiebl, J.; Alberts, D. P.; Banyard, A. F.; Baresch, K.; Baumgartner, H.; Bernwieser, I.; Bhatnagar, P. K.; Blanka, M.; Bodenteich, M.; Chen, T.; Esch, P. M.; Kollmann, H.; Lantos, I.; Leitner, K.; Mayrhofer, G.; Patel, R.; Rio, A.; Rovenszky, F.; Stevenson, D.; Tubman, K. D.; Undheim, K.; Weihtrager, H.; Welz, W.; Winkler, K. *J. Peptide Res.* **1999**, *54*, 54.; b) Nishiuchi, Y.; Inui, T.; Nishio, H.; Bodi, J.; Kimura, T.; Tsuji, F. I.; Sakakibara, S. *Proc. Natl. Acad. Sci. USA* **1998**, *95*, 13549

[49] Merrifield, R. B. *J. Am. Chem. Soc.* **1963**, *85*, 2149.

[50] Nilsson, B. L.; Soellner, M. B.; Raines, R. T. *Annu. Rev. Biophys. Biomol. Struct.* **2005**, *34*, 91.

[51]http://www3.appliedbiosystems.com/cms/groups/psm_marketing/documents/generaldocuments/cms_040654.pdf (April, 20th, 2012)

[52] Atherton, E.; Sheppard, R.C. (**1989**). *Solid Phase peptide synthesis: a practical approach*. Oxford, England**.**

[53] Isidro-Llobet, A.; Alvarez, M.; Albericio, F. *Chem. Rev.* **2009**, *109*, 2455.

[54] Palasek, S. A.; Cox, Z. J.; Collins, Z. M. *J. Pept. Sci.* **2007,** *13*, 143.

[55] a) Erdèlyi, M.; Gogoll, A. *Synthesis* **2002**, No. *11*, 1592.; b) Loffredo, C.; Assuncao, N. A.; Gerhardt, J.; Miranda, M. T. *J. Pept. Sci.* **2009**, *15*, 808.

[56] Meldal, M. *Method Enzymol* **1997**, *289*, 83.

[57] Labadie, J. W. *Curr. Opin. Chem. Biol.* **1998**, *2*, 346.

[58] Canne, L. E.; Botti, P.; Simon, R. J.; Chen, Y.; Dennis, E. A.; Kent, S. B. H. *J. Am. Chem. Soc.* **1999,** *121*, 8720.

[59] Amblard, M.; Fehrentz, J. A.; Martinez, J.; Subra, G. *Mol. Biotechnol.* **2006**, *33*, 239.

[60] a) Bulinski, J. C. *Int. Rev. Cytol.* **1986**, *103*, 281.; b) Fahad, A. Al-Obeidi; Lam, S. Kit *Oncogene* **2000**, *19*, 5690.

[61] Phikzicy, E.; Fields, S. *Microbiol. Mol. Biol. Rev.* **1995**, *59*, 94.

[62] Chapple, S. D.; Mason, D. J.; Joannou, C. L. *Infect. and Immun.* **1998**, Vol. 66, No *6*, 2434.

[63] Vagner, J.; Qu, H.; Hruby, V. J. *Curr Opin Chem Biol*. **2008**, *12*, 292.

[64] Seebach, D.; Overhand, M.; Kiihnle, Florian N. M. Martinoni, B. *HeIv. Chim. Acta* **1996**, *79*, 913.

[65] Milton, R. C.; Milton, S. C.; Kent, S. B. *Science* **1992**, *256*, 1445.

[66] Kharb, R.; Rana, M.; Sharma, P. G.; Yar, M. S. *J. Chem. Pharm. Res.* **2011**, *3*, 173.

[67] MA, James S. CHIMICA OGGI(*chemistry today,)* June **2003**, pp. 65.

[68] Nowick, J. S.; Lam, K. S.; Khasanova, T. V.; Kemnitzer, W. E.; Maitra, S.; Mee, H. T.; Liu, R. *J. Am. Chem. Soc.* **2002**, *124*, 4972.

[69] Soth, M. J.; Nowick, J. S. *Curr. Opin. Chem. Biol.* **1997**, *1*, 120.

[70] Goodman, C. M.; Choi, S.; Shandler, S.; DeGrado, W. F. *Nat. Chem. Biol.* **2007,** *3*, 252.

[71] a) Gellman, S.H. *Acc. Chem. Res* **1998**, *31*, 173.; b) Hill, D. J.; Mio, M. J.; Prince, R. B.; Hughes, T. S.; Moore, J. S. *Chem. Rev.* **2001**, *101*, 3893.

[72] Dado, G. P.; Gellman, S. H. *J. Am. Chem. Soc.* **1994**, *116*, 1054.

[73] Appella, D. H.; Christianson, L. A. ; Karle, I. L.; Powell, D. R.; Gellman, S. H. *J. Am.Chem. Soc.* **1996**, *118*, 13071.

[74] Guo, L.; Almeida, A. M.; Gellman,S. H. *J. Am. Chem. Soc.* **2010**, *132*, 7868.

[75] Langer, O.; Kählig, H.; Zierler-Gould, K.; Bats, J. W.; Mulzer, J. *J. Org. Chem.* **2002**, *67*, 6878.

[76] Nagai, U.; Sato, K.; Nakamura, R.; Kato, R. *Tetrahedron* **1993**, *47*, 3577.

[77] Koglin, N.; Zorn, C.; Beumer, R.; Cabrele, C.; Bubert, C.; Sewald, N.; Reiser, O.; Beck-Sickinger A. G. *Angew. Chem. Int. Ed.* **2003**, *42*, 202.

[78] Lang, M.; De Pol, S.; Baldauf, C.; Hofmann, H.-J.; Reiser, O.; Beck-Sickinger, A. G. *J. Med. Chem.* **2006**, *49*, 616.

[79] Lang, M.; Bufe, B.; De Pol, S.; Reiser, O.; Meyerhof, W.; Beck-Sickinger, A. G. *J. Pep. Sci.* **2006**, *12*, 258.

[80] Sahr, F.; *Dissertation*, Regensburg **2009**.

[81] Thompson, P. E.; Steer, D. L.; Aguilar, M. I.; Hearn, M.T.W. *Bioorg. Med. Chem. Lett.* **1998**, *8*, 2699.

[82] a) Appella, D. H.; Christianson, L. A.; Klein, D. A.; Richards, M. R.; Powell, D. R.; Gellman, S. H. *J. Am. Chem. Soc.* **1999,** *121*, 7574.; b) Appella, D. H.; Christianson, L. A.; Klein, D. A.; Powell, D. R.; Huang, X.; Barchi Jr, J. J.; Gellman, S. H. *Nature* **1997**, *387*, 381.

Chapter 1

1.1 Application and synthesis of γ-amino acids

1. 1. 1. γ-Amino acids in foldamers

After several years of extensive studies on β-amino acids in foldamers and peptide analogues, γ-amino acids have been investigated and have shown interesting properties. In the γ-peptide family, helices have been observed in oligomers with only four residues. It was also shown that going from α-peptides to β- and γ-peptides, more stable helices are obtained. Because of their high stability and diversity, γ-amino acids are a interesting class of unnatural amino acids in the field of foldamers.[1,2] Many foldamers containing γ-amino acids have been reported so far.[3,4] Interesting linear γ-peptides that form discrete secondary structures have been described by *Seebach et al.*[5] A series of (*R,R,R*)-γ-amino acids with side chains in the 2-, 3-, and 4-positions (**Figure 17**), were prepared and investigated. γ-Tetrapeptide **34**, and γ-hexapeptides **35** showed a (*M*)-2.6_{14} helix in the solid state and in MeOH solution (**Figure 18**).

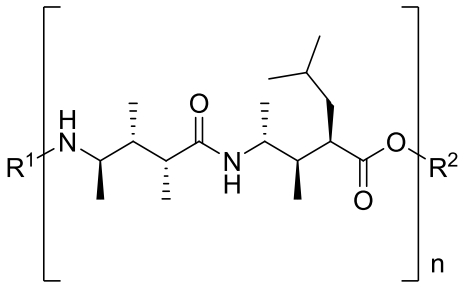

34 n = 2, R^1 = Boc, R^2 =Bn

35 n = 3, R^1 = H, R^2 = H

Figure 17. γ-2,3,4-Tetra- and hexapeptide derivatives **34** and **35** used for structure investigations.

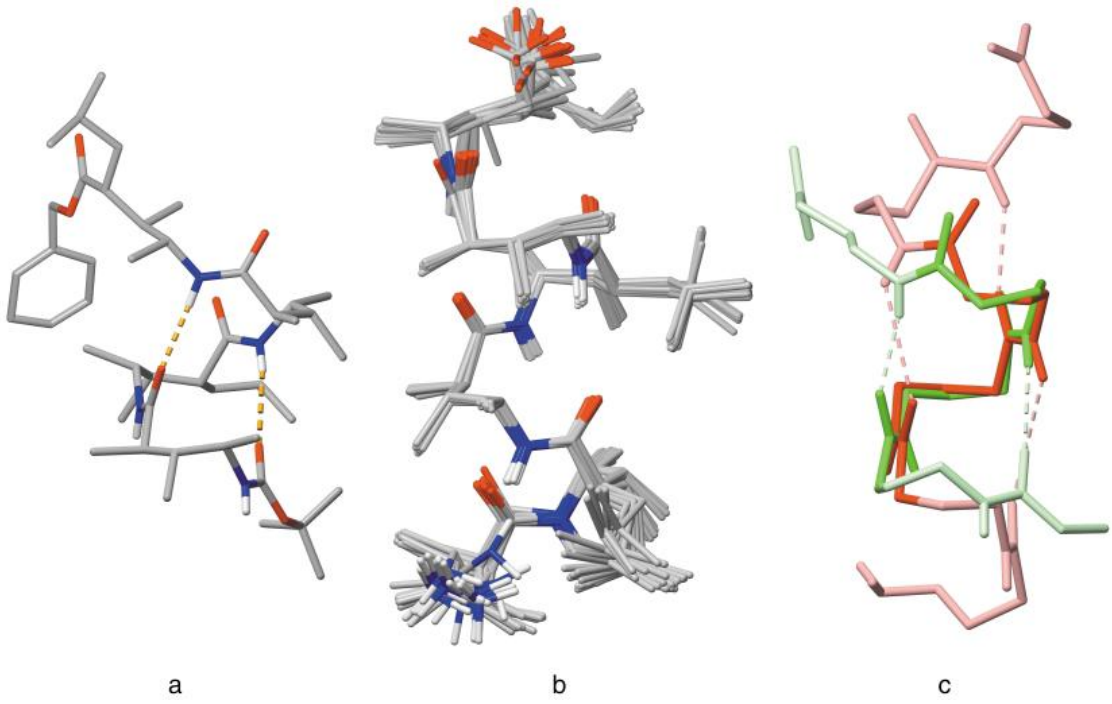

Figure 18. *"(M)-2.6$_{14}$ Helical structures of γ-peptides **33** and **34**. a) Structure of γ-tetrapeptide **33** in the crystal state determined by X-ray structure analysis. b) Bundle of 20 conformers of hexapeptide **34** in MeOH obtained by simulated annealing calculations using restraints from NMR data. c) Superposition of the peptide backbones from the X-ray diffraction structure (blue) and NMR structure (red)".*[6]

Foldamers containing cyclic γ-amino acids, being more conformationally restricted, have attracted more attention and have been intensively studied. Homo- and heterochiral tetrameric γ-peptides derivatives, in which the backbone is constrained by a five-membered ring, were prepared and investigated by *Smith et al*.[7] (**Figure 19**).

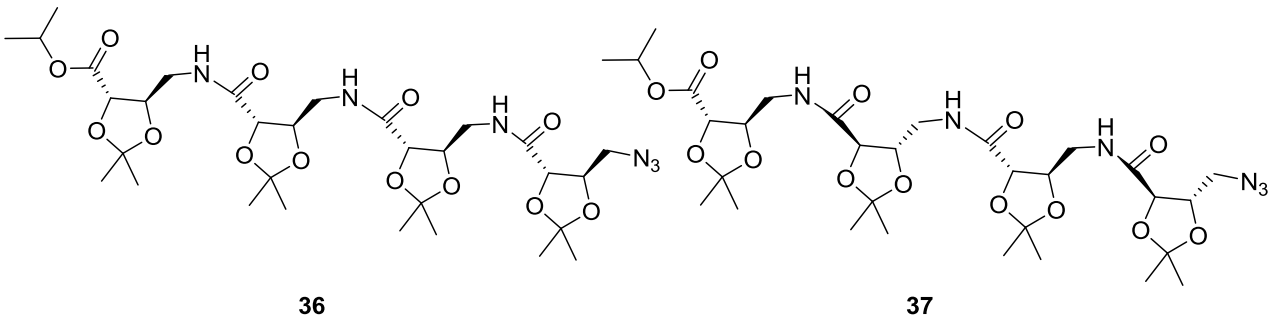

Figure 19. Homochiral γ-peptide **36** and alternating heterochiral γ-peptide **37**.

These peptides showed a bend-ribbon conformation in solution stabilized by intramolecular hydrogen bonds forming a 7-membered ring (**Figure 20**).

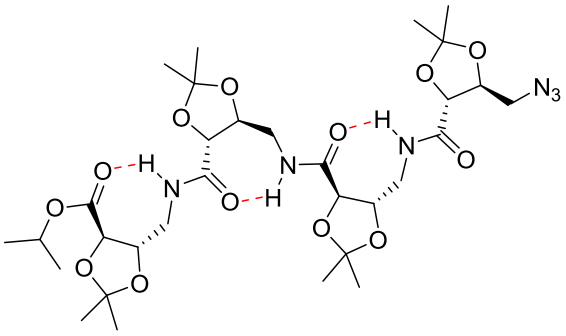

Figure 20. Observed bend-ribbon solution conformation of γ-peptide **36**.

Other γ-peptides using conformationally constrained γ-amino acids were prepared by *Gellman et al.*[8] A series of γ-peptides **40-44** were prepared by liquid phase method using a (Boc)-protected gabapentin **38** at the N-terminus and conformationally constrained γ-amino acid **39** (**Scheme 5**).

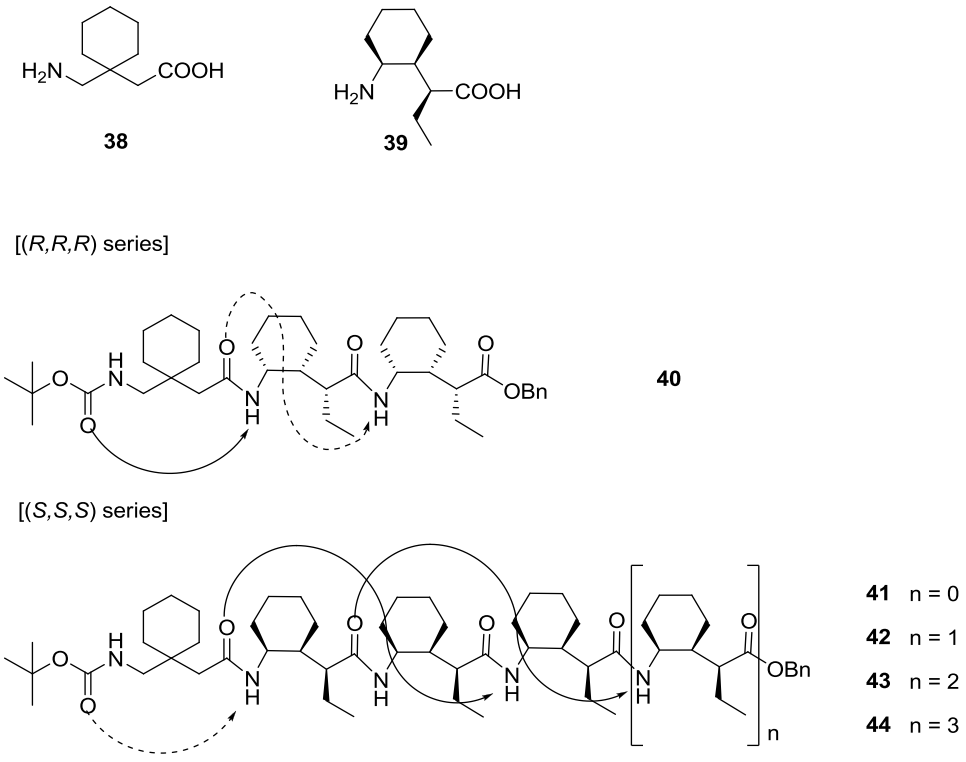

Scheme 5. Structure of gabapentin **38** and a unnatural γ-amino acid **39.** Structure of γ-peptides **40-44** (arrows indicate H-bonds in the crystal structure.[8]

The crystal structures of peptides **40**-**44** showed that segments derived from gabapantin **38** display the 14-helical conformation (**Figure 21**, the peptides **40**-**44** are numberd from **3** to **7**, from the original document).

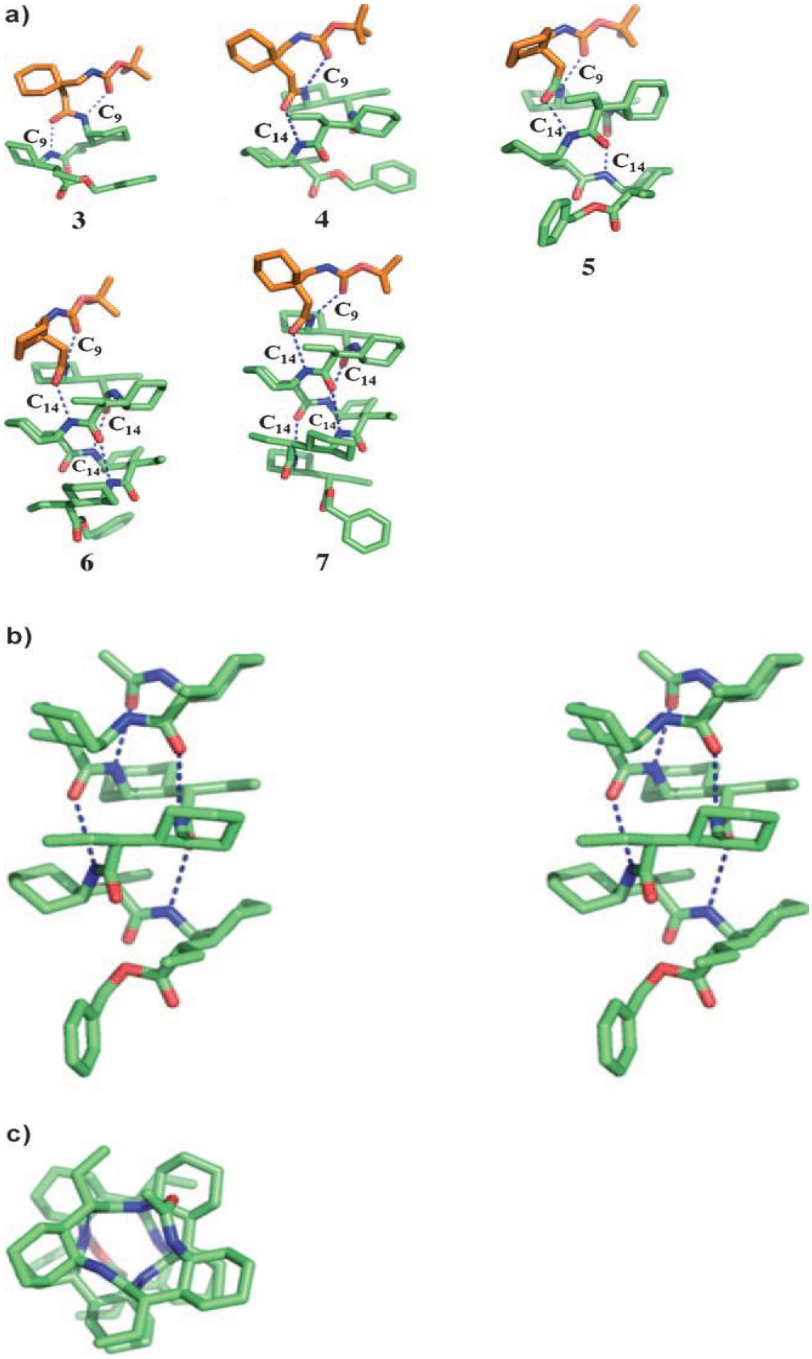

Figure 21. *"a) Crystal structures of **40-44** (**3-7** from the original document); b) Stereoview of the 14-helical segment of **40** (N-terminal gabapentin residue not shown; c) View along the helix axis of the 14-helical segment of **44.** Orange: Boc-protected gabapentin residue; green: residues derived from **44**; red: O, blue: N".*[9]

1. 1. 2. Application of γ-amino acids

"γ-Amino acids have attracted considerable attention as biologically active compounds in the central nervous system (CNS) of mammals".[10] The most known examples for natural γ-amino acids are GABA **45** (γ-aminobutyric acid), which is an inhibitory neurotransmitter in the central nervous system[11] and the γ-amino-β-hydroxybutyric acid (GABOB) **46**, which possess antitumor and antifungal activity.[12,13] Concerning the application of γ-amino acids as therapeutics, there are, for example the vigabatrin **47** and the baclofen **48**. The first one is an important anticonvulsant, while the baclofen is used in the treatment of spasticity and alcoholism, being a $GABA_B$ receptor agonist (**Figure 22**).[14]

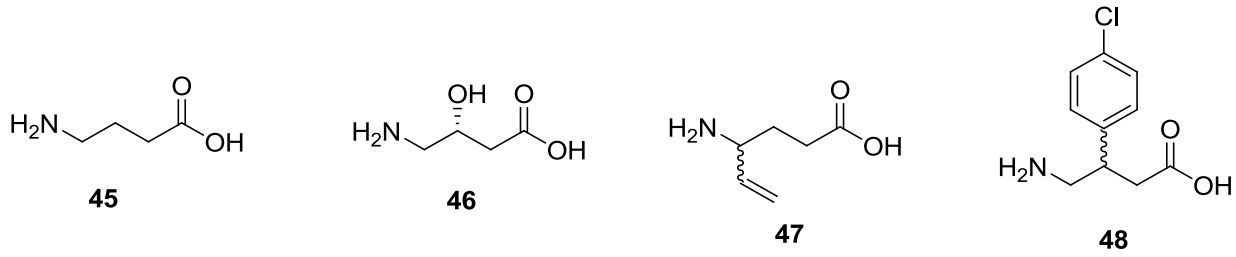

Figure 22. Some examples of γ-amino acids.

Foldamers derived from γ-peptides seem to have several promising applications. They display higher stability toward proteolytic enzymes than α-peptides, as shown by *Seebach et al.*[15] A group of γ-peptides were tested against 15 proteolytic enzymes and no degradation was observed after 48 h, while α-peptides usually degrade after 15 min. Furthermore, γ-amino acids have been used to design analogues of biological compounds. An interesting class of γ-amino acids, in which the backbone is constrained by a five-membered ring, as GABA analogues have been reported by *Allan et al.* (**Figure 23**).[16]

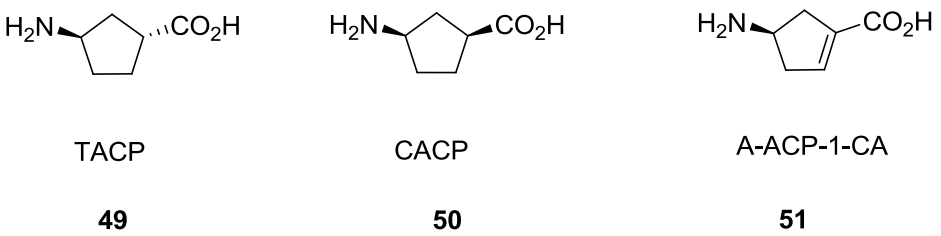

Figure 23. Cyclopentane GABA analogues.

All these analogues were tested at 100 μM against a GABA EC_{50} dose (50 μM), showing that cyclopentane GABA analogues TACP, CACP and 4-ACP-1-CA are potent $GABA_A$ agonists.

Additionally, *cis*- and *trans*-2-aminocyclopropyl**,** -cyclobutyl, -cyclopentyl, and -cyclohexylacetic acids as GABA analogues of restricted conformation were described by *Kennewell et al.*, but only the cyclopropyl and cyclobutyl series showed any significant biological activity (**Figure 24**).[17]

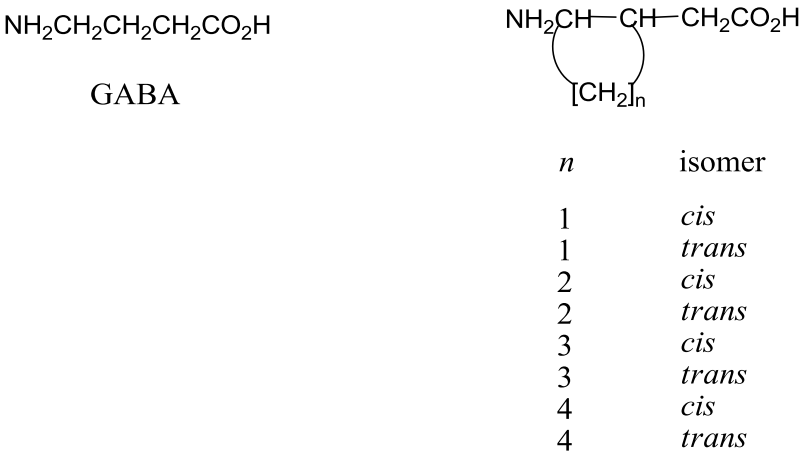

Figure 24. *cis*- and *trans*-2-aminocyclopropyl**,** -cyclobutyl, -cyclopentyl, and -cyclohexylacetic acids as GABA analogues.

Moreover, γ-peptides are able to mimic the β-turn of biologically active peptides as described by *Seebach et al*., showing different *N*-acyl γ-dipeptides with a good affinity for human somatostatin receptors.[18] Therefore, γ-amino acids could be a interesting class of building blocks in the design of new peptide analogues.

1. 1. 3. Synthesis of conformationally constrained γ-amino acids

Conformationally constrained γ-amino acids are a very important class of unnatural amino acids, which have been intensively investigated in order to generate new analogues, building blocks for peptidomimetics, as well as to study their properties in foldamers.[19] Therefore, over the last few years the stereoselective synthesis of new cyclic γ-amino acids has attracted interest.[10] An interesting synthetic route to prepare *trans*-cyclobutane and cyclopropane amino acids has been reported by *Kennewell et al.*[17] and is shown in **scheme 6**. *Trans*-cyclobutane 1,2-diethylester **52** was used as starting material for the cyclobutane series, while the synthesis of the cyclopropane series started with the *trans*-dimethylester **53**.

Partial hydrolysis of **52** and **53** yielded the mono-acids **54** and **55**, which were reduced by borane tetrahydrofurane complex, giving the *trans* isomers alcohols **56** and **57.** [20]

Tosylation of both alcohols has been carried out using *p*-toluenesulfonyl chloride and pyridine, obtaining the tosylates **58** and **59**. The treatment with potassium cyanide afforded the nitriles **60** and **61**, which have been converted first into the acid hydrazides **62** and **63**, then by *Curtius* rearrangement to the carbamates **64** and **65**, according to the methods of *Witiak et al.*[21] and *Hart et al*.[22] Compound **64** and **65** were hydrolized in sodium hydroxied solution, affording the amino acids **66** and **67**.

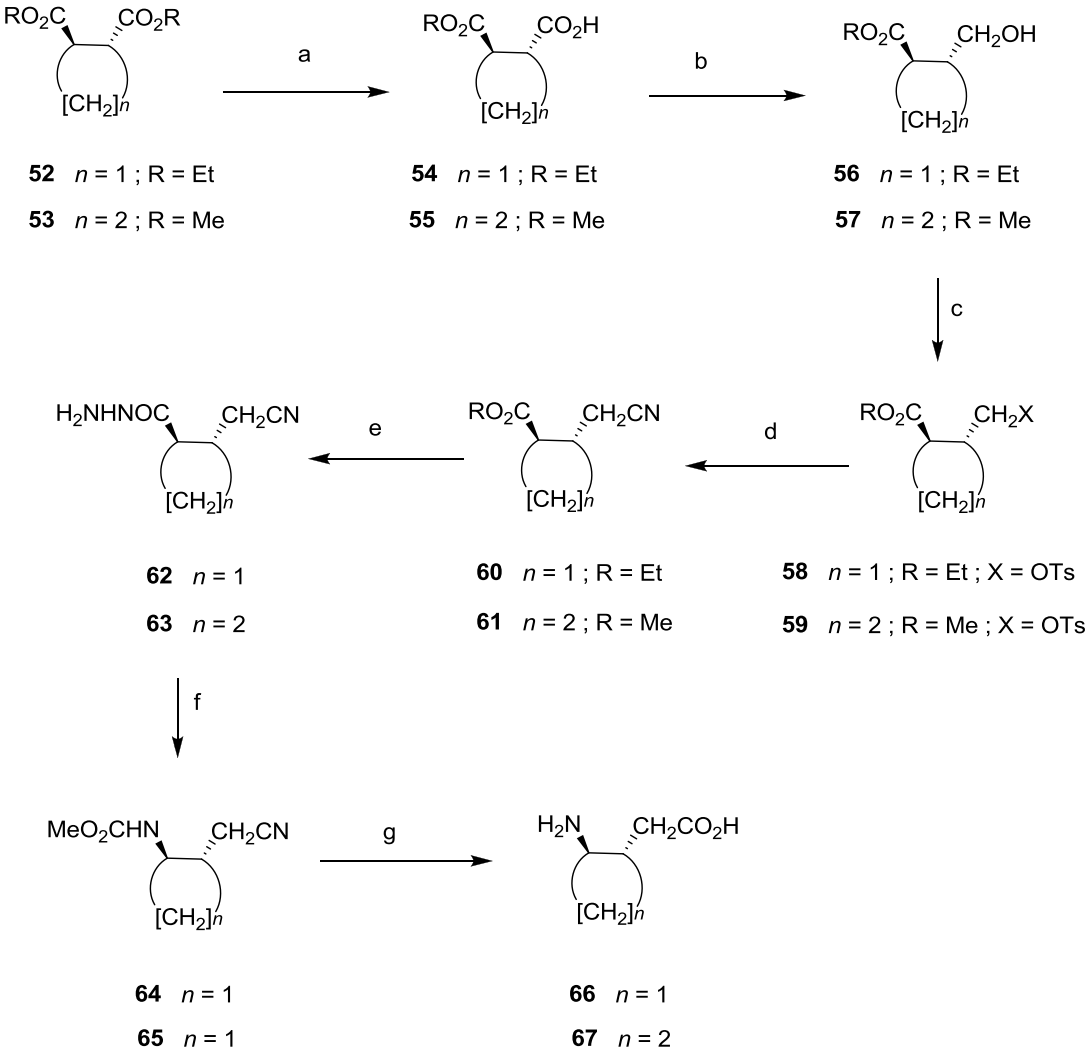

Scheme 6. Synthetic routes for *trans*-cyclobutane and cyclopropane γ-amino acids.
Reagents and conditions: a) NaOH-aq., EtOH, reflux, 2 h, 55%; b) BH_3THF-Et_2O, 0 °C, 1h, 95%; c) *p*-$MeC_6H_4SO_2Cl$-pyridine, 88%; d) KCN-DMSO, heat, 3 h, 75%; e) $NH_2NH_2\,H_2O$, EtOH, heat, 1 h, 58%; f) 1. $NaNO_2$,HCl, 0 °C, 1 h; 2. MeOH, reflux, 16 h, 78%; g) NaOH-aq., EtOH, reflux, 16 h, 60%.

An interesting synthetic rout toward the enantioselective synthesis of cyclic γ-amino acids has been shown by *Kessler et al.*[23] In this method, a sugar derived γ-amino acid was prepared from diacetone glucose **68** (**Scheme 7**).

This synthesis starts with the activation of an alcohol group in compound **68**, generating the triflyl activated diacetone glucose **69**, which will be converted into the azide **70**, followed by inversion of the configuration. After that, the exocyclic hydroxyl group was deprotected by acetic acid affording diol **71**. Then, the azide was reduced by hydrogenation and Fmoc protected producing compound **72**. Concluding, oxidation of the primary alcohol by TEMPO, sodium hypochlorite and KBr yielded γ-amino acid **73**.

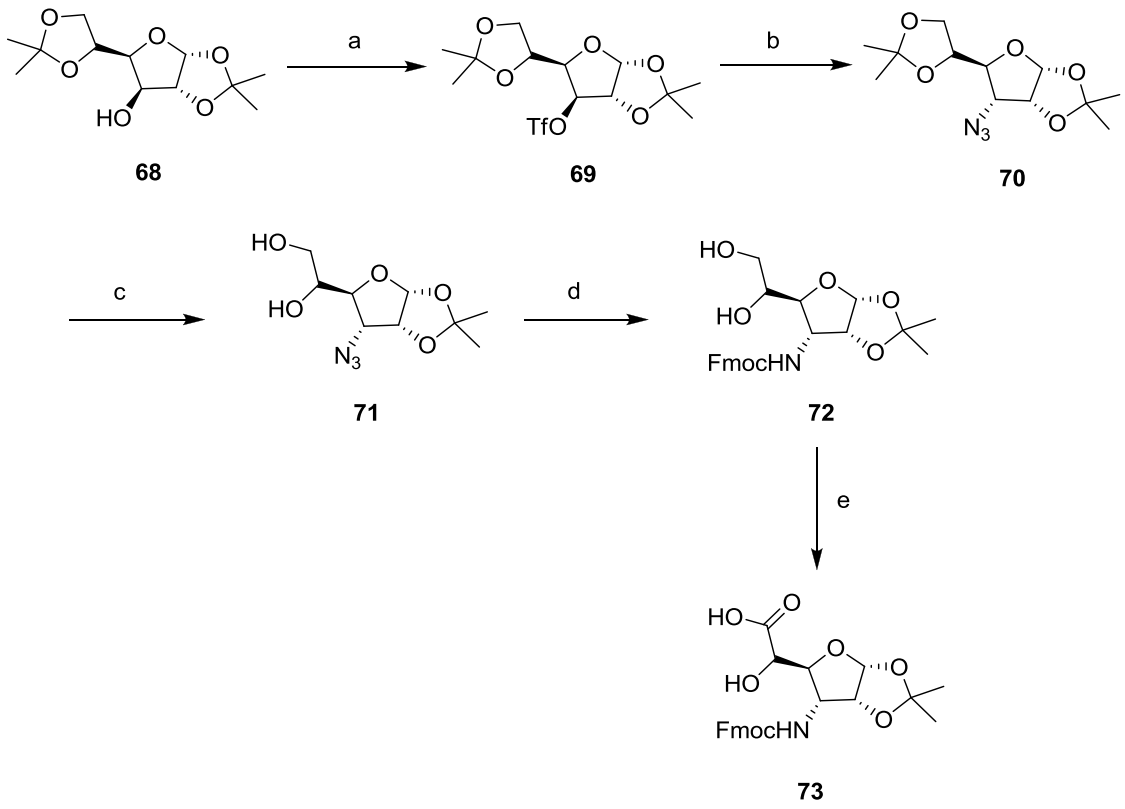

Scheme 7. Enantioselective synthesis of cyclic γ-amino acids from carbohydrates. Reagents and conditions: a) Tf_2O, pyridine, -10 °C, DCM, 1.5 h, 98%; b) NaN_3, Bu_4NCl (cat), 50 °C, DMF, 5 h, 70%; c) HOAc, 3 h, 65 °C, 77%; d) H_2, Pd/C, MeOH, FmocCl, $NaHCO_3$, THF, MeOH, r.t., 24 h, 90%; e) NaOCl, TEMPO (cat), KBr, DCM, sat. aq. $NaHCO_3$, Bu_4NCl, overnight, 62%.

Furthermore, the synthesis of different enantiomerically pure cyclopentane γ-amino acids has been reported. **Figure 25** presents different compounds prepared by *Ordònez et al*. in order to test them as GABA analogues.[10]

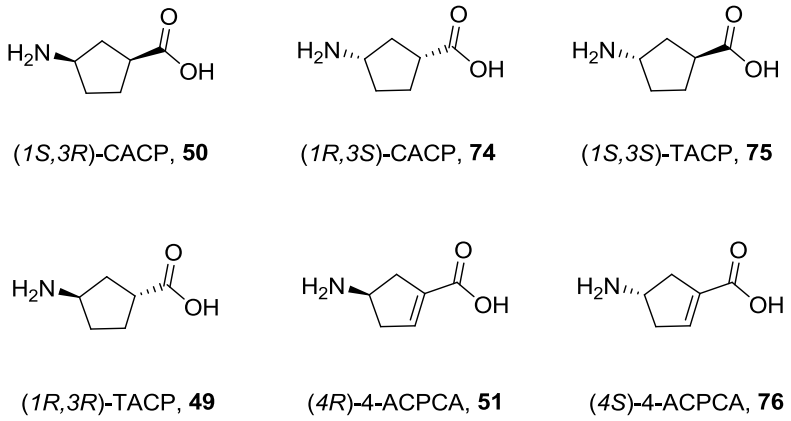

Figure 25. Cyclopentane γ-amino acids.

In most of the cases, the products in enantiomerically pure form were obtained starting from commercially available enantiopure starting materials, as in the case of compound **51** (**Scheme 8**),[24,25] or by enzymatic resolution as in the case of compound **50** (**Scheme 9**). Hydrolysis of enantiopure lactam (*1S,4R*)-**77** gave (*1R,4S*)-ACPECA **78** in quantitative yield, which was protected by Boc-anhydride and esterificated giving methyl ester (*1R,4S*)-**79** in 98% yield. Isomerization of the double bond in the presence of DBU provided the corresponding derivative (*4R*)-**80** in 95% yield, which was hydrolyzed in acidic conditions, yielding the (*4R*)-4-ACPCA **51**.[10]

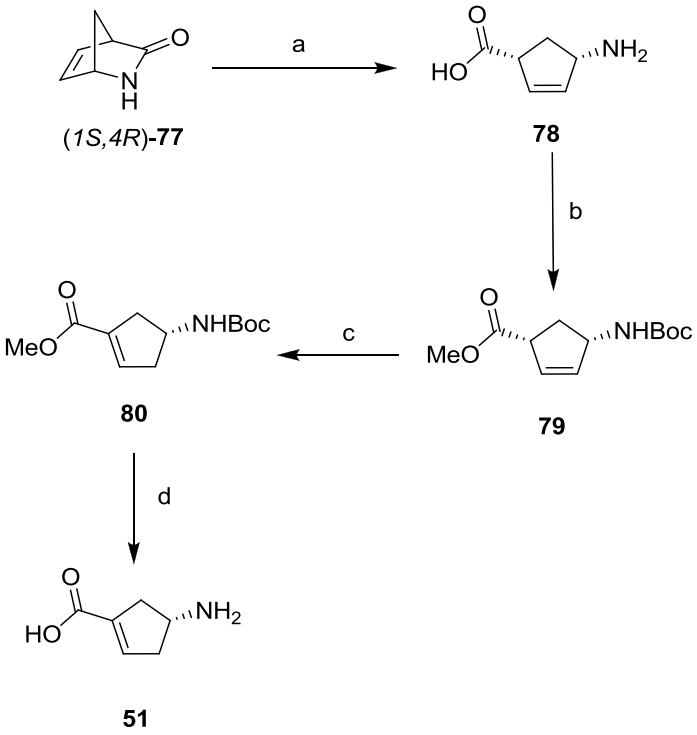

Scheme 8. Synthesis of (*4R*)-4-ACPCA **51** from commercially available enantiopure starting material **77**. Reagents and conditions: a) 6 M HCl, 12 h, quant. ; b) 1. $(Boc)_2O$, Et_3N, MeOH, r.t., 3 h; 2. CH_2N_2, DCM, 1h, 98%; c) DBU, THF, reflux, 10 h, 95%; d) 1. AcOH, HCl 1 M, 100 °C, 1 h, 77%.

The preparation of enantiomerically pure (*1R,3S*)-CACP **50** by enzymatic desymmetrization has been described by *Chenevert et al.*[26] The synthetic route starts with ozonolysis and simultaneously esterification of norbornene **81**, affording the diester **82** in 93% yield. Cholesterol esterase (CE) has been used to catalyze the partial hydrolysis of diester **82**, producing (*1R,3S*)-**83** in 95% yield and 90% *ee*. Ammonolysis of **83** using NH_3 in MeOH yielded amide **84** in 82% yield, which was converted into the amine under *Hoffmann* rearrangement conditions, affording (*1S,3R*)CACP-**50** in 92% yield.[27]

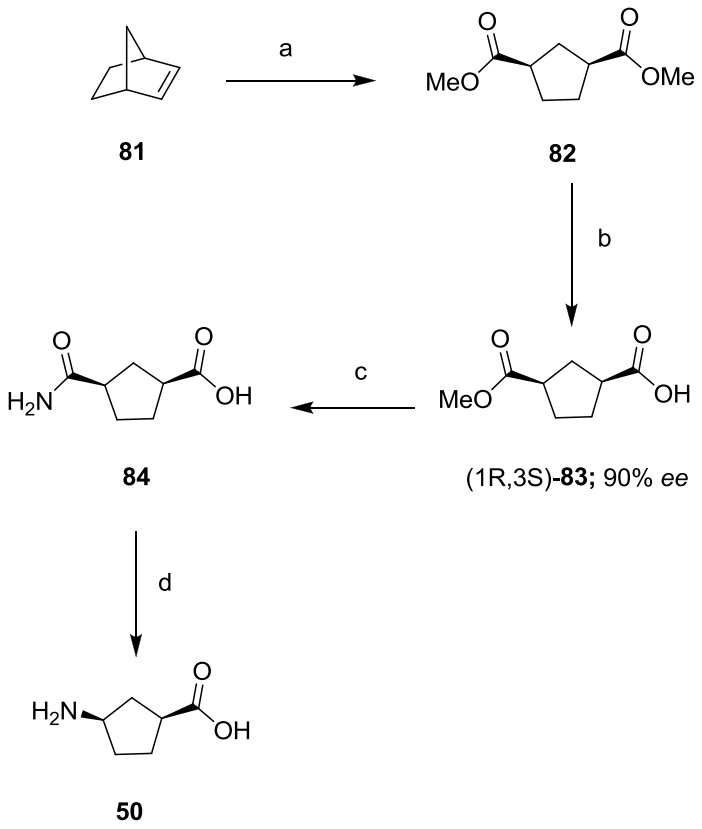

Scheme 9. Synthesis of (*1S,3R*)-CACP **50** by enzymatic resolution. Reagents and conditions: a) 1. O_3 , MeOH; 2. H_2O_2, HCO_2H; 3. MeOH/H^+, 93%; b) CE, phosphate buffer pH 7, 37 °C, MeOH, 95% c) NH_3, MeOH, 82%; d) $(CF_3CO_2)_2IC_6H_6$, MeCN, H_2O, 92%.

1. 2. Synthesis of the 2-(2-amino cyclopentyl) acetic acid derivative

At the beginning of this project, the focus was on the application of foldamers and NPY analogues containing the 2-(2-amino cyclopentyl) acetic acid derivative, precisely the 2-((*1S,2R,3R,5R*)-2-amino-3-(hydroxymethyl)-5-methoxycyclopentyl)acetic acid **85**, which has been described by *Florian Sahr* in his PhD thesis.[28] The γ-amino acid **85** has been synthesized by modifications of intramolecular 1,3-dipolar cycloaddition product **86**, which was obtained through several steps from cyclopropanation's product of 2-furoic methyl ester **87** (**Scheme 10**).

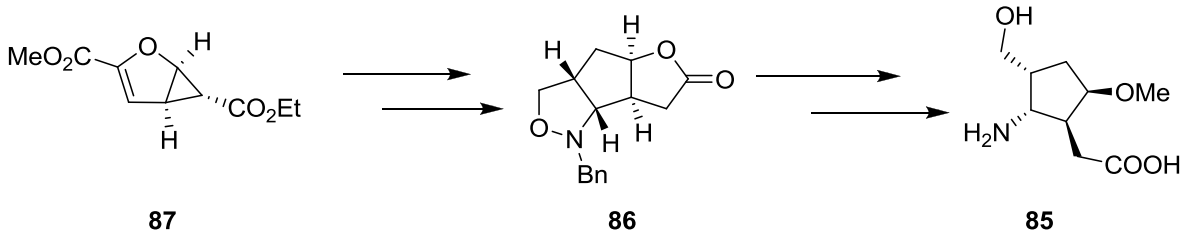

87 **86** **85**

Scheme 10. γ-Amino acid **85** obtained from intramolecular 1,3-dipolar cycloaddition product **86**, which is an important intermediate synthesized in several step from the compound **87**.

The entire synthesis consists first in the preparation of *anti*-4,5-disubstituted γ-butyrolactone aldehyde **88** (**Scheme 11**), which will then yield to the intramolecular 1,3-dipolar cycloaddition product **86**. The first step is the copper(I)-catalysed cyclopropanation of 2-furoic methyl ester **89** in presence of ethyl diazoacetate (EDA) and bis(oxazoline) ligand **90**, yielding cyclopropane derivaties **87** in 36% yield and 99% *ee*. Ozonolysis of compound **87** leads to the cleavage of the double bond, giving cyclopropane carbaldehyde **91** in 92% yield. *Sakurai* allylation of compound **91**, using *trimethylallylsilane* in the presence of *boron trifluoride etherate*, produced compound **92**, which in basic condition was converted into the free cyclopropane alcohol intermediate **93**. Compound **93**, being highly unstable, evolves to the *trans*-substituted lactone **88** in 41% yield, by a retro-aldol-lactonisation-cascade reaction.

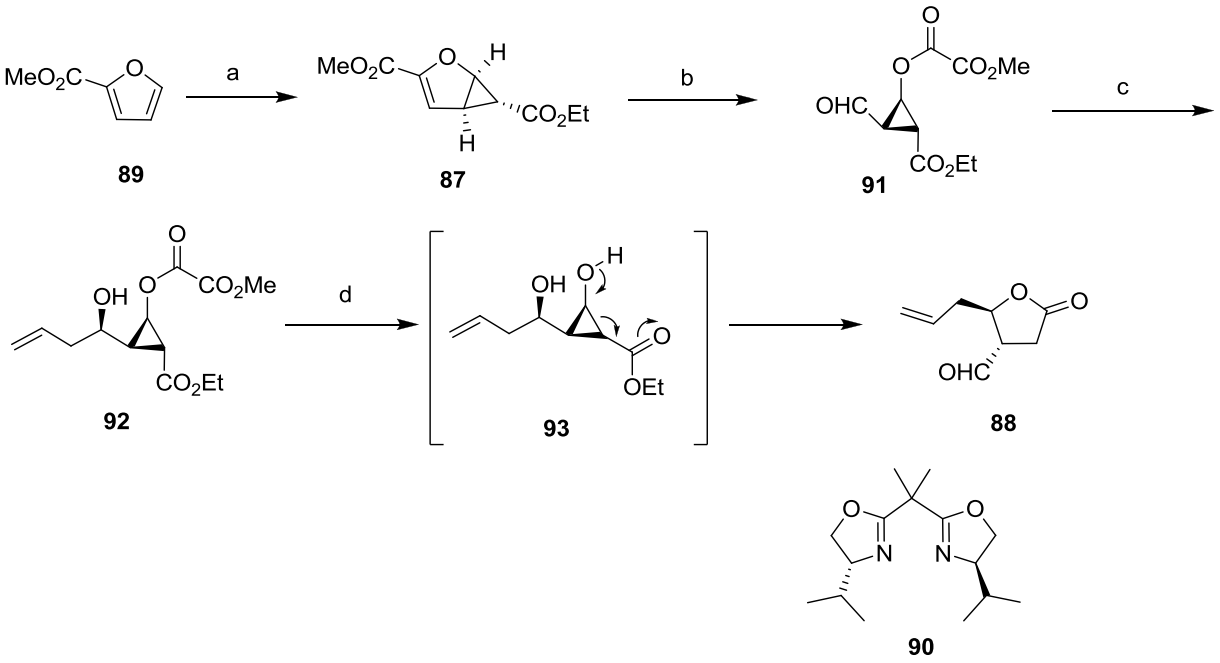

Scheme 11. Synthesis of *anti*-4,5-disubstituted γ-butyrolactone aldehyde **88**.[29] Reagents and conditions: a) $Cu(OTf)_2$, $PhNHNH_2$, compound **86**, ethyl diazoacetate (10% – 15% solution in DCM), 0 °C, 45%, after recrystallization 36% (99% *ee*). b) O_3, DCM, DMS, -78 °C → r.t., 24 h, 92%. c) Allyl trimethylsilane, $BF_3{\cdot}OEt_2$, DCM, -78 °C, 18 h; d) $Ba(OH)_2{\cdot}8H_2O$, MeOH, 0 °C, 24 h (41 %) over two steps.

The second part is the synthesis of compound **86** by an intramolecular 1,3-dipolar cycloaddition reaction (**Scheme 12**). γ-Butyrolactone **88** was treated with *N*-benzylhydroxylamine hydrochloride giving the nitrone **94**, which was not possible to purify because of its instability on silica gel and its poor crystallisation properties. Thus, crude **94** was dissolved in anhydrous benzene and refluxed for 24 hours, yielding a diastereomeric mixture of fused cycloadducts **86** and **95** in a 3:1 ratio.

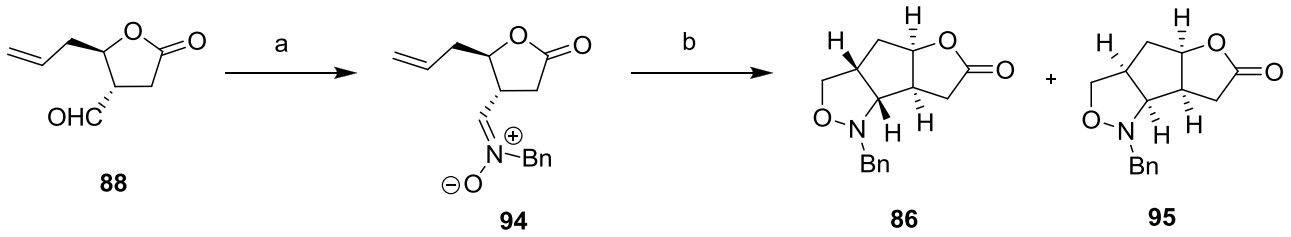

Scheme 12. Cycloaddition of nitrone **94**.[29] Reagents and conditions: a) *N*-benzylhydroxylamine hydrochloride, $NaOAc{\cdot}3H_2O$, ethanol/water (4:1), r.t., 2h; b) Benzene, reflux, 24 h, 55%.

The major diastereomer **86** was converted to a broad variety of protected unnatural-amino acids. Cispentacin derivatives with an annelated lactone **96**, as well as open chain products modified with protected alcohol groups **97** and protected guanidinium group **98**, were obtained (**Figure 26**).

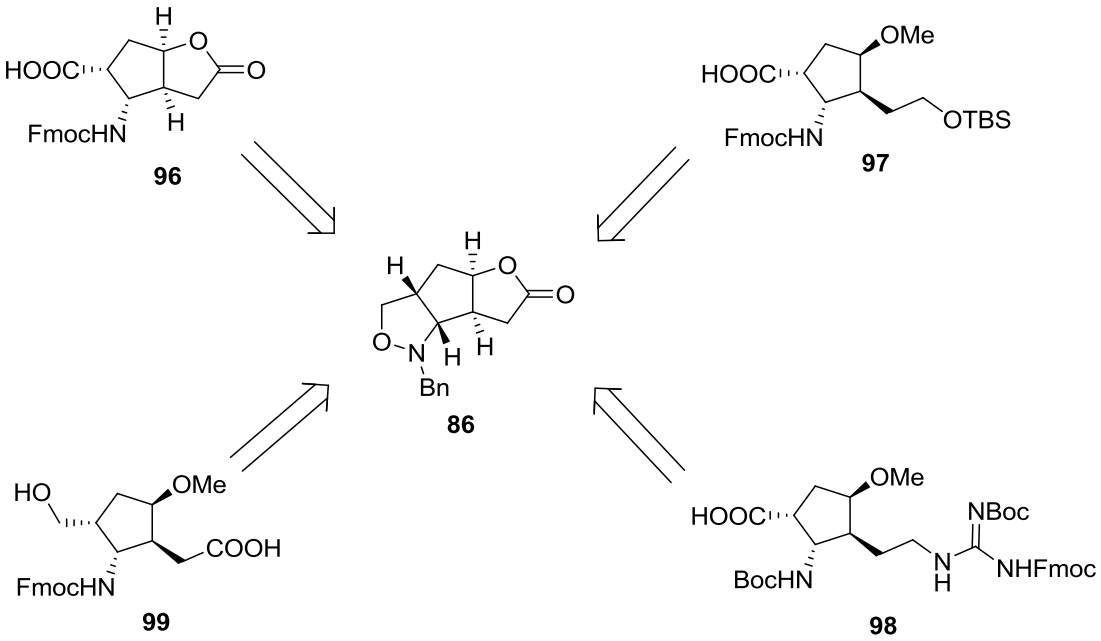

Figure 26. Different protected unnatural amino acids prepared from compound **86.**

Moreover, the 2-((*1S,2R,3R,5R*)-2-Fmoc-amino-3-(hydroxymethyl)-5-methoxycyclopentyl) acetic acid **99** with a cyclopentane backbone and a free alcohol group was also obtained from compound **86**. The synthetic route to obtain γ-amino acid **99** is shown in **Scheme 13**. The first step is the reduction of the lactone **86** using lithium aluminiumhydride, affording the diol **100** in quantitative yield. Then, a selective protection of the primary alcohol took place by TBSCl in the presence of triethylamine and a catalytic amount of DMAP, obtaining compound **101** in 92% yield. The secondary alcohol was protected as a methoxy group using iodomethane in the presence of sodium hydride as a base, yielding compound **102**. Protected diol intermediate **102** was oxidized under *Jones* oxidation conditions affording compound **103**. During this reaction, the acidic conditions will cleavage the silyl ether, realizing the primary alcohol, which is then oxidized to carboxylic acid. Subsequently, the isoxazoline moiety was opened by hydrogenation at atmospheric pressure catalysed by $Pd(OH)_2$-C, which allowed the removing of the benzyl group as well, affording a free hydroxyl group and free amine. Free γ-amino acid **85** was simultaneously protected with FmocOSu, yielding compound **99**.

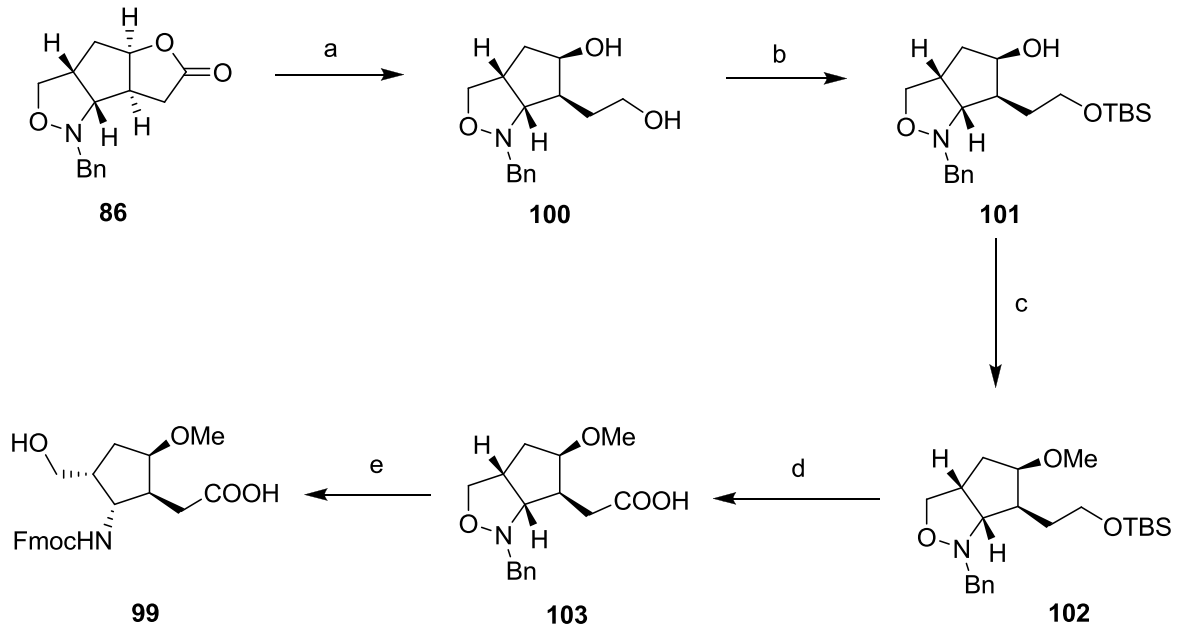

Scheme 13. Synthesis of Fmoc-2-((*1S,2R,3R,5R*)-2-amino-3-(hydroxymethyl)-5-methoxycyclopentyl)acetic acid **99**. Reagents and conditions: a) LAH, THF, 0 °C, 1 h, 98%; b) TBSCl, NEt_3, DMAP, DCM, 18 h, 92%; c) MeI, NaH, THF, 0 °C for 1 h, r.t. for 18h, 80%; d) *Jones* oxidation, acetone, 0°C – r.t., 6 h, 86%; e) 1. $Pd(OH)_2$-C, H_2, MeOH, overnight, 95%; 2. FmocOSu, $NaHCO_3$, acetone/water, r.t., 24 h, 58%.

As previously mentioned, the focus was on the synthesis of foldamers and NPY analogues containing γ-amino acid **85**. Fmoc protected γ-amino acid **99** was used to prepare different peptides by solid phase synthesis. Therefore, it was necessary to protect the primary alcohol group to avoid undesidered coupling to that position during the synthesis. The Fmoc/*t*Bu strategy has been chosen for this approach. The problem of this step was the difficulty to protect selectively the alcohol as a *t*-butyl ether in the presence of a free carboxylic acid. It was planned to protect simultaneously the primary alcohol and the carboxylic acid giving compound **104**. After that, a selective cleavage of *t*-butyl ester group would take place, giving compound **105**, as shown in **Scheme 14**.

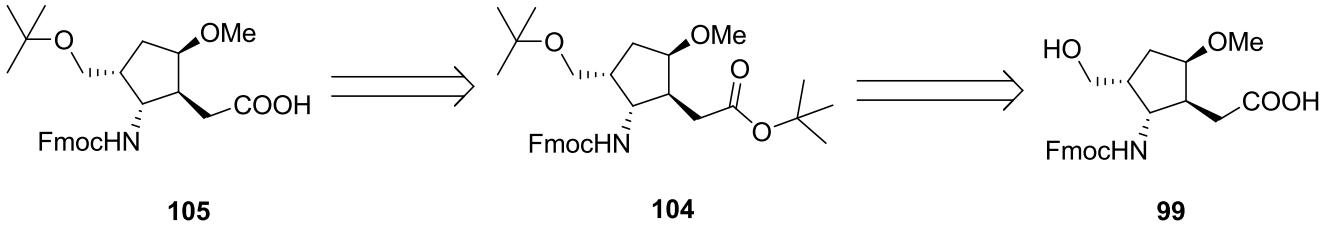

Scheme 14. Retrosynthetic scheme for *t*-butyl protected amino acid **105**.

The general reaction proceeds in the presence of trimethylsilyl triflate and a base, as described by *Bannwarth et al*.[29] The *t*-butyl ester **106** is converted into the trimethylsilyl ester **107**, which after aqueous workup yields the corresponding free carboxylic acid **108** (**Scheme 15**). The *t*-butyl ether is stable in the presence of trimethylsilyl triflate.

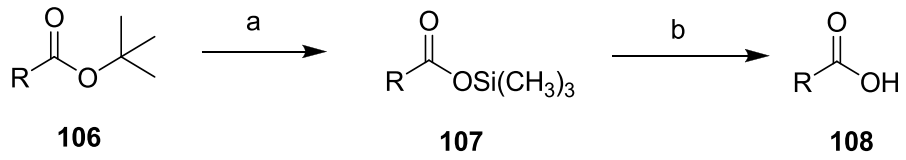

106 **107** **108**

Scheme 15. General selective cleavage of *t*-butyl ester **106**. Reagents and condition: a) Trimethylsilyl triflate, NEt_3; b) H_2O.

Unfortunately, the protection reaction did not give any good yield. Two different methods were tried: isobutylene in the presence of $BF_3{\cdot}OEt_2$ and H_3PO_4,[30] and *t*-BuOH in the presence of H_2SO_4 and $MgSO_4$ as drying agent.[31] In both methods the protection gave yields minor than 40% (**Scheme 16**).

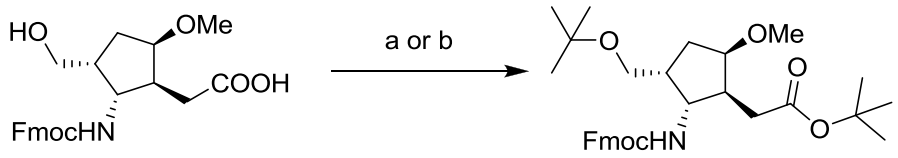

99 **104**

Scheme 16. Methods for *t*-butyl protection. Reagents and conditions: a) Isobutylene, $BF_3{\cdot}OEt_2$, H_3PO_4, DCM/THF, -78 °C, 5 days, 22%; b) H_2SO_4 (conc.), $MgSO_4$, *t*-BuOH, DCM, r.t., 36 h, 36%.

Therefore, it was decided to use another protecting group for the primary alcohol. Finally, γ-amino acid **99** was protected with TBSCl, providing the *O*-TBS group as described by *Koksch et al.*[32] The reaction was run in dry DMF, in the presence of imidazole and a catalytic amount of DMAP for 32 h at room temperature, affording the protected γ-amino acid **109** in ~80% yield (**Scheme 17**).

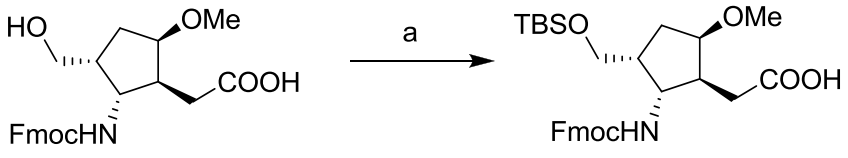

99 **109**

Scheme 17. Protection of primary alcohol **99**. Reagents and conditions: a) TBSCl, imidazole, DMAP, DMF, r.t., 32 h, 78.8%.

1. 2. 1. NPY analogues containing 2-(2-amino cyclopentyl) acetic acid derivaties

Compound **109** was used to synthesize alternated α-γ peptides and different NPY analogues **110** and **111** by SPPS (**Figure 27**). The synthesis was performed using Rink amide MBHA resin **20** (loading 0.6 mmol/g), HBTU in combination with HOBt and DIPEA as coupling reagents.

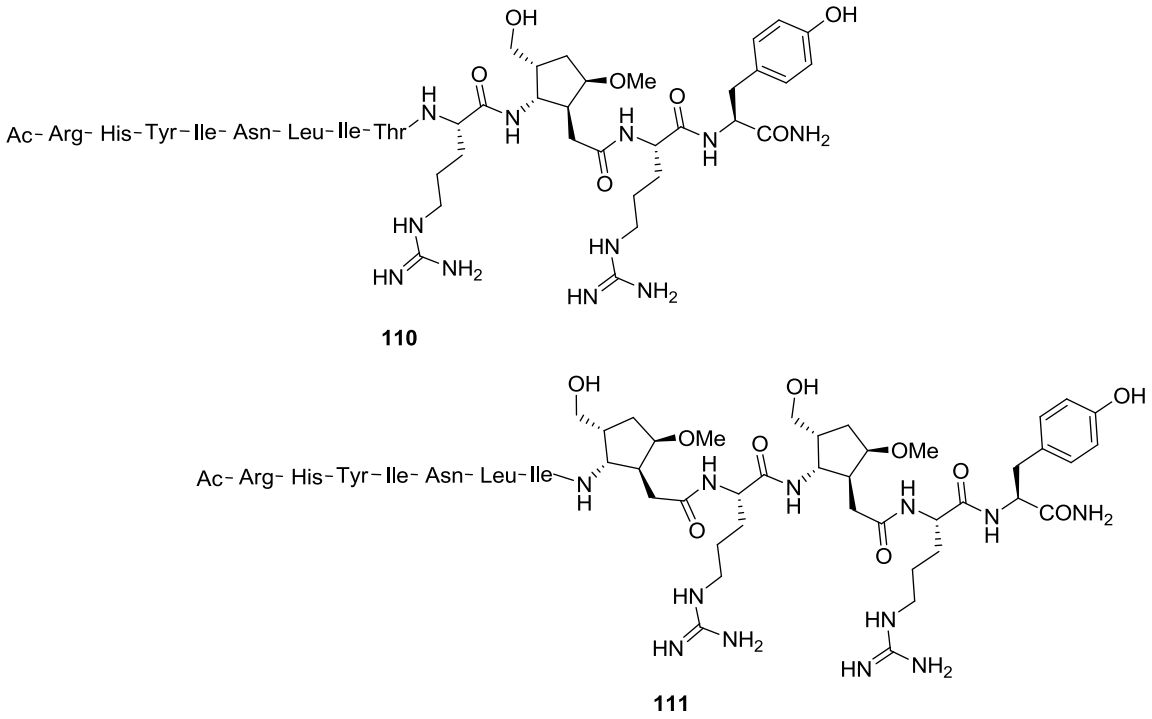

Figure 27. Structure of NPY analogues containing γ-amino acid **85**.

Unfortunately, the yields for each coupling were quite low, leading after 5-6 couplings to a final yield <10%. Other coupling reagents were tried, such as EDC in combination with HOBt, but also in this case the final yield was not good enough to obtain an analyzable amount of pure peptide. Therefore, the coupling of γ-amino acid **109** was investigated by synthesis in solution. A dipeptide **112** was prepared by coupling compound **109** and free *O*-benzyl ester alanine **113** in DMF/DCM 1:1, using different coupling reagents (**Scheme 18**).

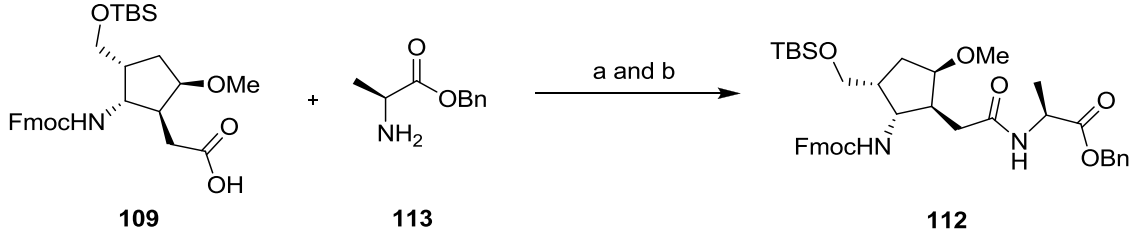

Scheme 18. Coupling in solution of the amino acid **109**. Reagents and conditions: a) HBTU/ HOBt, DIPEA, DMF/DCM (1:1), 0 °C for 1 h, overnight at r.t., 48%; b) EDC/HOBt, DIPEA, DMF/DCM (1:1), 0 °C, 1 h, overnight at r.t., 68%;

The couplings in solution showed that using EDC/HOBt, the yield (68%) was higher than using the HBTU/HOBt approach (48%). Therefore, it was planned to synthesize a α-γ-alternated peptide **114** by liquid phase synthesis, using EDC/HOBt as coupling reagent (**Figure 28**).

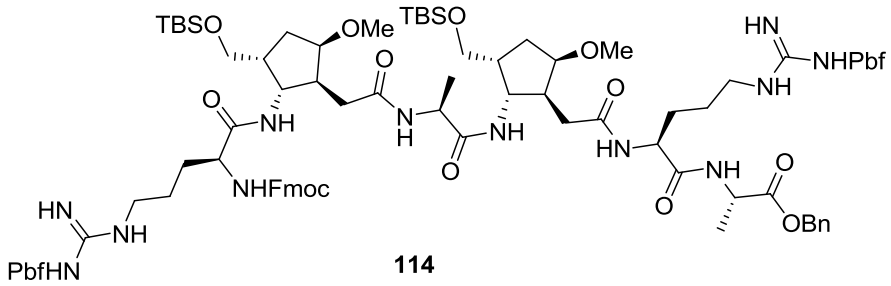

Figure 28. α-γ-Alternated peptide containing γ-amino acid **85**.

The synthesis of compound **114** has been carried out by coupling of two tripeptides **115** and **116**, which consist of Pbf-arginine, γ-amino acid **109** and alanine in a specific order (**Figure 29**). The tripeptides were prepared by a repeated cycle of coupling-deprotection steps in solution. The cleavage of Fmoc group was performed by stirring in 10% piperidine in DCM for 20 min, while hydrogenation in presence of Pd/C as catalyst was used to cleave the benzyl group.

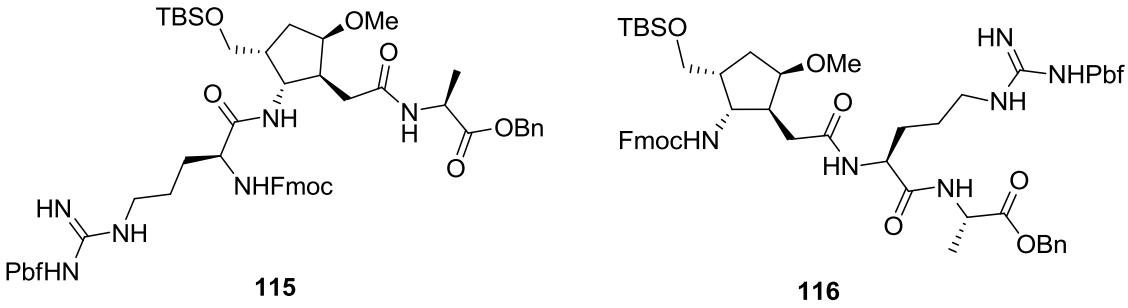

Figure 29. α-γ-Alternated tripeptides **115** and **116** prepared by liquid phase synthesis.

The final coupling produced a protected α-γ-hexapeptide in 60% yield, which was purified by preparative reversed HPLC. Furthermore, during the HPLC purification the TBS groups have been cleaved, due to the presence of TFA, affording compound **117** as confirmed by HPLC/MASS (**Figure 30**).

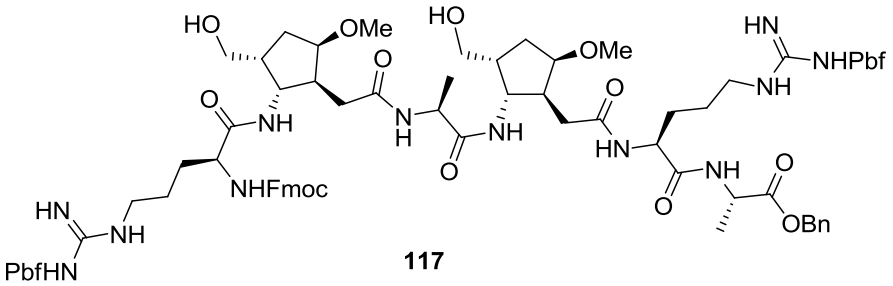

117

Figure 30. Structure of α-γ-hexapeptide **117**, after HPLC purification.

Unfortunately, the whole synthesis carried out only a small amount of pure peptide **117**, from which, after the cleavage of the protecting groups, it was not possible to isolate and analyze the free peptide. In conclusion, it was decided to cut off the research in this direction because of the difficult coupling, as well as the long and challenging synthesis of the γ-amino acid **109**. The research focus moved to the synthesis and application of the 2-(2-amino cyclopentyl) acetic acid without any side chains, which will be presented in the next paragraph.

1. 3. Synthesis of isomers of the 2-(2-amino cyclopentyl) acetic acid

As previously mentioned, during this project we focused on the synthesis of enantiomerically pure isomers of the 2-(2-amino cyclopentyl) acetic acid (**Figure 31**).

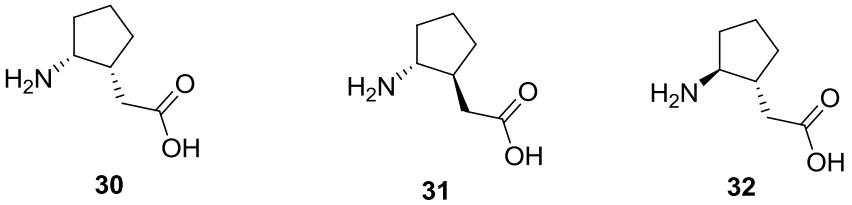

Figure 31. Isomers of the 2-(2-amino cyclopentyl) acetic acid.

A simple way to synthesize the *cis*-**30** and *trans*-**31** isomers has previously been described by *Kennewell et al.*,[17] with a slight modification to the method of *Booth et al.*[33] (**Scheme 19**). The oxime[34] **118** was hydrogenated over platinum oxide in ethanolic HCl[35], providing a mixture of isomers which were separated by distillation affording the *cis*-lactam **119** and the *trans*-amino-ester **120**. Then, hydrolysis of **119** and **120** yielded the *cis*-**30** and *trans*-**31** amino acids which were isolated by ion-exchange chromatography.

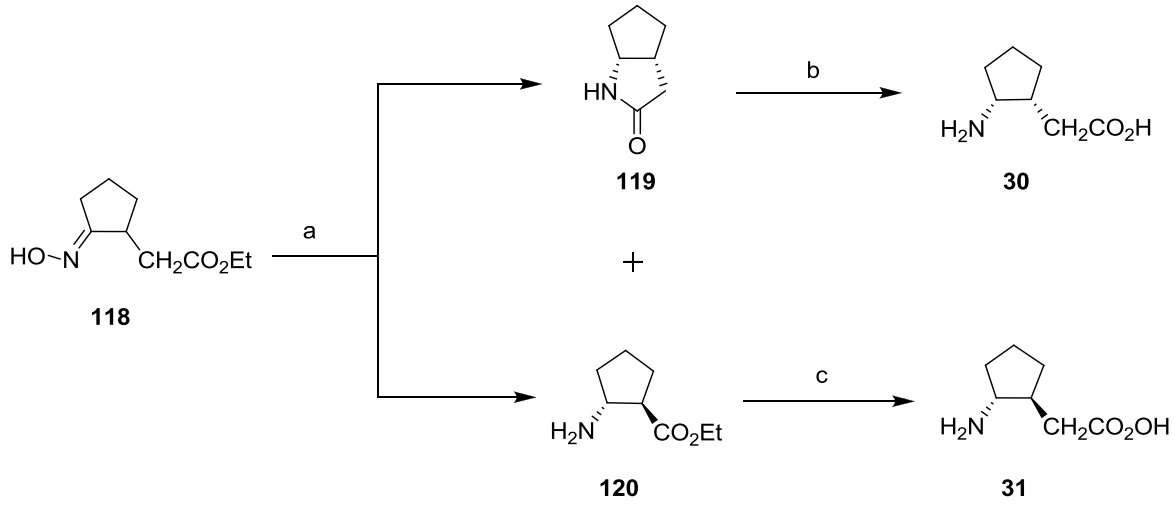

Scheme 19. General synthesis of isomers **30** and **31**. Reagents and conditions: a) 1. H_2-PtO_2-HCl-EtOH, 2. heat; b) NaOH-aq.-EtOH, heat, 24 h, 56%; c) NaOH-aq.-EtOH, heat, 1h, 80%.

The synthesis of compound **32** has been shown by *Page et al.*[36] (**Scheme 20**). Cyclopentene oxide[37] **121** was opened by sodium azide in ammonium chloride and aqueous ethanol, affording the azido cyclopentanol, which was reduced using triphenyl phosphine and simultaneously Boc-protected in situ, producing compound **122** in 22% yield over three steps. After that, compound **122** was ringclosed to the protected aziridine **123** in 75% yield, using *Mitsunobu* conditions.

Dimethyl malonate was used to open the aziridine system, by enolate generation, in a regioselective fashion yielding compound **124** as *trans*-isomer. Diester **124** was hydrolyzed in aqueous potassium hydroxide in order to convert first one of the methyl esters into the corresponding acid, and then into compound **125** as result of decarboxylation in xylene. Additionally, compound **125** was hydrolyzed in hydrochloric acid, affording the *trans*-2-(2-amino cyclopentyl) acetic acid **32** in 80% yield as HCl-salt.

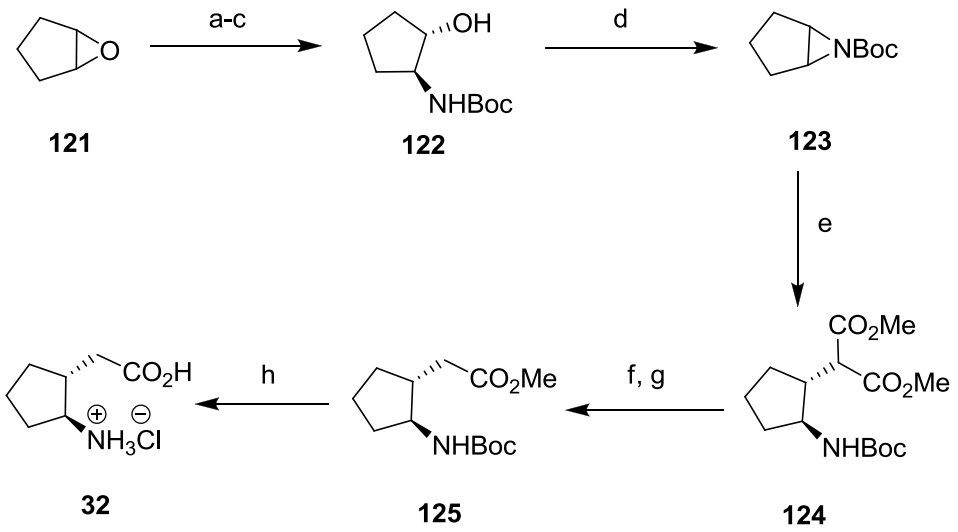

Scheme 20. Synthesis of isomer **32**, as described by *Page et al*. Reagents and conditions: a) NH_4Cl, NaN_3, EtOH–H_2O (1:1), reflux, overnight; b) PPh_3, toluene, reflux, 1.5 h; c) aq $NaHCO_3$, EtOAc, Boc_2O, 0 °C → r.t., overnight, 22% over three steps; d) PPh_3, DIAD, THF, –78 °C → r.t., 75%; e) NaH, dimethyl malonate, DME, reflux, 24 h, 95%; f) 1 M KOH, MeOH, $KHSO_4$; g) xylenes, reflux, 4 h 68%; h) 4 M HCl, r.t., 14 h, 80%.

In both described methods, the amino acids were obtained in good yield and with regioselective fashion, but not enantioselective. Thus, the products were obtained as racemic mixtures.

In this work the preparation of enantiomerically pure *trans* γ-amino acid **32** has been carried out by a synthetic route described by *Gellman et al*., using a common way to synthesize β-amino acids from α-amino acids by an *Arndt-Eistert* homologation (**Scheme 21**).[38] After formation of α-diazoketone **127** from Boc-protected α-amino acid **126** by reaction with diazomethane, the β-amino acid can be obtained as methyl ester **128** and as free carboxylic acid **129**, using different catalysts and conditions.

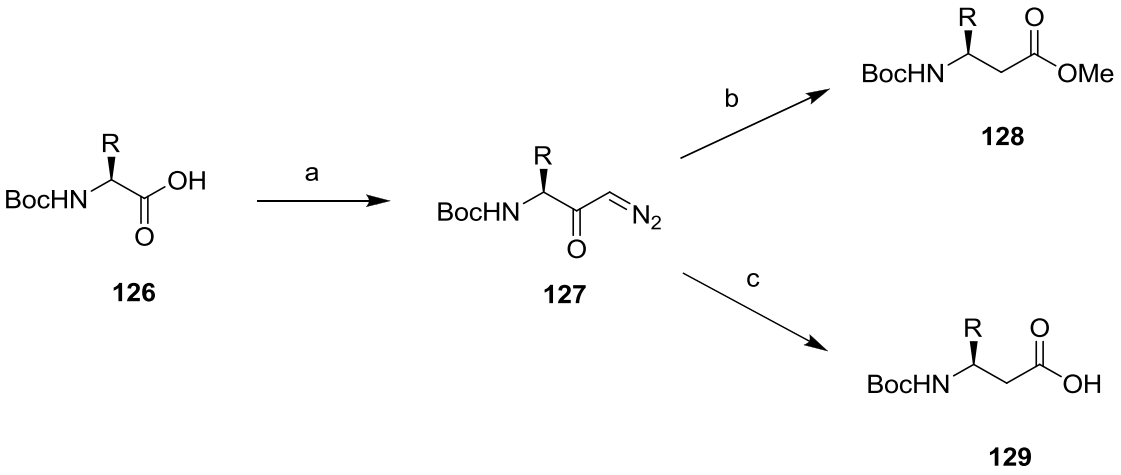

Scheme 21. *Arndt-Eistert* homologation of α-amino acid **126**.
Reagents and conditions: a) 1. $Et_3N/ClCO_2Et$, -15 °C; 2. CH_2N_2, -5 °C; b) Cat. $PhCO_2Ag$ in Et_3N/MeOH; c) Cat. CF_3CO_2Ag in THF/H_2O 9:1.

In our case, compound **32** is obtained as Fmoc-protected γ-amino acid **130** by a homologation of enantiomerically pure *trans*-Fmoc-pentacin **132** (**Scheme 22**).[39]

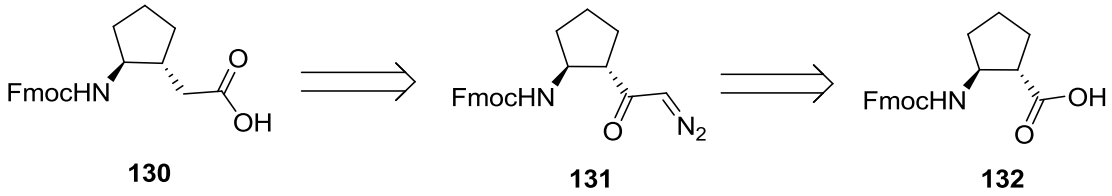

Scheme 22. Retrosynthetic scheme for *trans*-Fmoc-γ-amino acid **130**.

The synthetic route starts with the preparation of enantiomerically pure *trans*-Fmoc-pentacin **132**, which has also been described by *Gellman et al.* (**Scheme 23**).[40] In the first step, β-ketoester **133** was allowed to react with (*S*)-(-)-α-methylbenzylamine **134** to form enamine **135**. After that, $NaBH_3CN$ was added at 0 °C, giving, after formation of hydrochloric salt and recrystallization, the ethyl (*1S,2S*)-2-[(*S*)-phenylethyl]-aminocyclopentane carboxylate hydrochloride **136** in 29% yield and with a *d.e.* of 99%.[41,42] Then, compound **136** was hydrolyzed by stirring over LiOH, affording the (*1S,2S*)-2-[(*S*)-phenylethyl]-aminocyclopentanecarboxylic acid **137**. Removal of the chiral auxiliary has been performed by hydrogenation in autoclave (50 bar) and 10% Pd/C as catalyst. The resulting salt (*1S,2S*)-aminocyclopentanecarboxylic acid **33** was protected with Fmoc-OSu, affording the (*1S,2S*)-Fmoc-pentacin **132** in 85% yield.

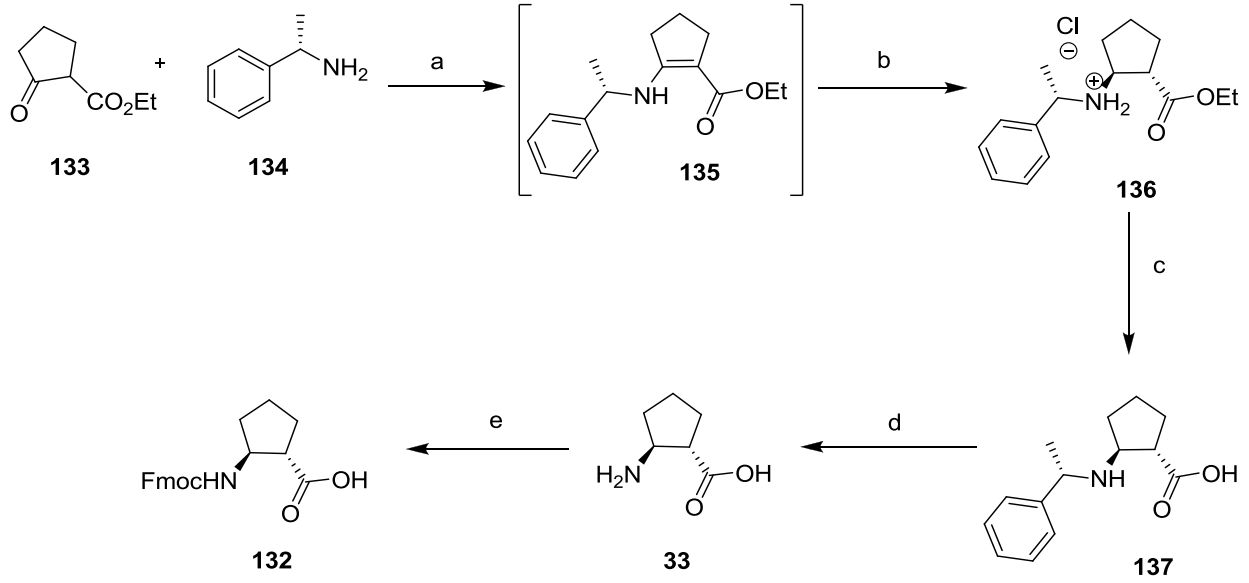

Scheme 23. Synthesis of *trans*-Fmoc-pentacin **132.** Reagents and conditions: a) AcOH, EtOH, reflux, 8 h; b) 1. $NaBH_3CN$; 2. HCl, recrystallization, 29%; c) LiOH, THF/MEOH/H_2O, 9 h, 0 °C, quant.; d) H_2 (50 bar) 10% Pd/C, EtOH, 48 h, quant.; e) Fmoc-OSu, $NaHCO_3$, Acetone/H_2O 1:1, overnight, 85% .

After that, *Arndt-Eistert* homologation[43] of compound **132** was carried out (**Scheme 24**). The *trans*-Fmoc-pentacin **132** was activated by isobutylchloroformate in the presence of *N*-methylmorpholine at -15 °C in THF. The mixture was allowed to warm to 0 °C, and freshly ethereal diazomethane solution,[44,45] prepared from *N*-methyl-nitroso-urea in 50% KOH, was added dropwise, affording the α-diazoketone **131** in 72% yield.[46] Subsequently, *Wolff*-rearrangement[47,48] of the α-diazoketone **131** in the presence of water and silver benzoate as catalyst, produced 2-((*1R,2S*)-2-Fmoc-aminocyclopentyl) acetic acid **130** in 35% yield.

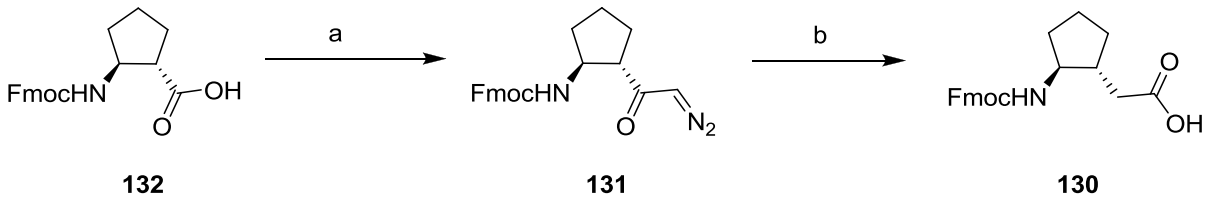

Scheme 24. Synthesis of 2-((*1R,2S*)-2-Fmoc-aminocyclopentyl) acetic acid **130**. Reagents and conditions: a) 1. IBCF/*N*-methylmorpholine, THF, -15 °C; 2. CH_2N_2, 0 °C, 4 h, 72%; b) cat. $PhCO_2Ag$, ultrasounds, dioxane/H_2O, 1 h, 35%.

The *Cis*-γ-amino acid **30** and *trans*-isomer **31** have also been successfully prepared. The synthesis of *cis*-hydrochloride salt compound **30** has previously been described by *Omar et al.*[49] In this work, the Fmoc-amino acid was prepared by a slight modification of the reported protocol (**Scheme 25**).

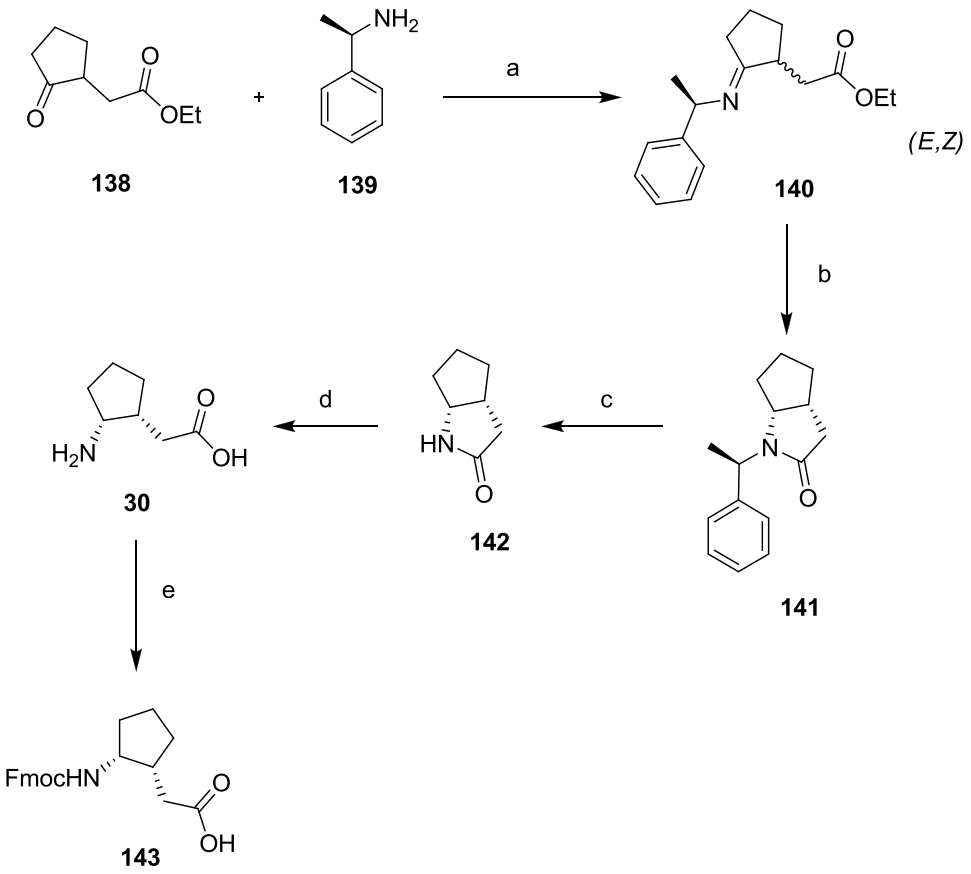

Scheme 25. Synthesis of 2-((1S,2S)-2-Fmoc-aminocyclopentyl) acetic acid **143**. Reagents and conditions: a) Benzene (abs.), reflux, 6 h, 78% ; b) 1. $NaBH_4$, 1 h, 0 °C ; 2. HCl, 0 °C, recrystallization, 55% ; 3. LiOH, THF/MeOH/H_2O, 0 °C, 9 h, quant.; c) Li/NH_3, -78 °C, THF/*t*BuOH, overnight, 77% ; d) 1 N HCl, 80 °C, 8 h, 55%; e) Fmoc-OSu, $NaHCO_3$, Acetone/H_2O 1:1, 18 h, 85%.

Racemic ethyl 2-(2-oxocyclopentyl)acetate[50] **138** was allowed to react with *R*-(+)-α-methylbenzylamine **139** using a *Dean-Stark*-trap, affording the imine mixture **140**. In this step theoretically four diastereoisomers are obtained as shown in **Figure 32.**

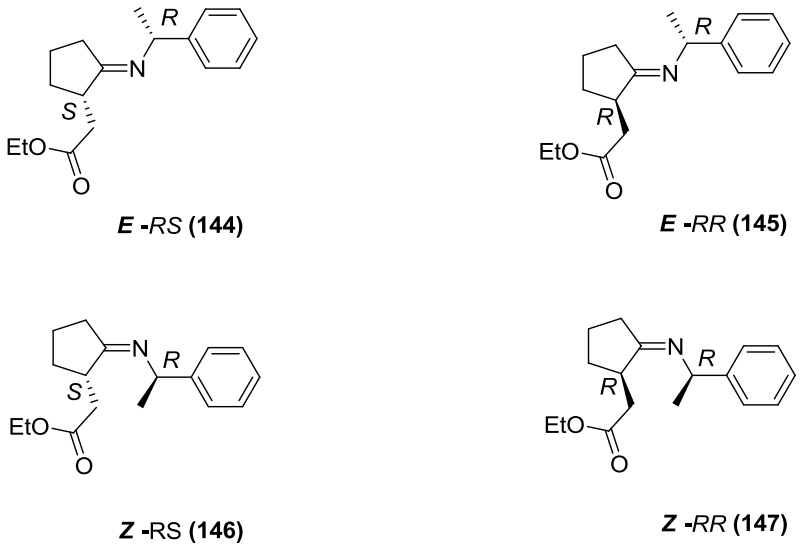

Figure 32. The imine mixture **140** consists of four diastereoisomers.

In the reported protocol, the imine mixture **140** was reduced by hydrogenation in autoclave in the presence of Raney-Nickel, yielding only the *cis*-phenylethylamino-cyclopentyl acetate in enantiomerically pure form. Unfortunately, we could not reproduce this step. Therefore, in this work it was planned to reduce the imine mixture **140** by another common way to synthesize α-amino acids from imines, by using $NaBH_4$ at 0 °C.[51] In these conditions, only two different isomers **148** and **149** were obtained in an 2:1 diastereomeric ratio, determined by ^{1}H-NMR (**Scheme 26**).

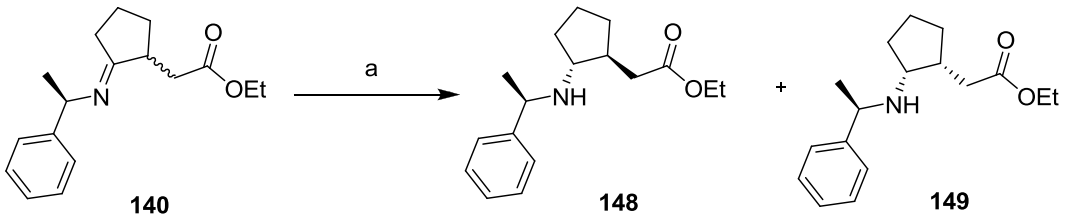

Scheme 26. Reduction of imine mixture **140** gave only two isomers **148** and **149**.
Reagents and conditions: a) $NaBH_4$, EtOH, 0 °C, 1 h, 55%.

NOESY analysis confirmed that the major isomer has the *trans*-configuration and the minor one has the *cis*-configuration (**Figure 33** and **Figure 34**).

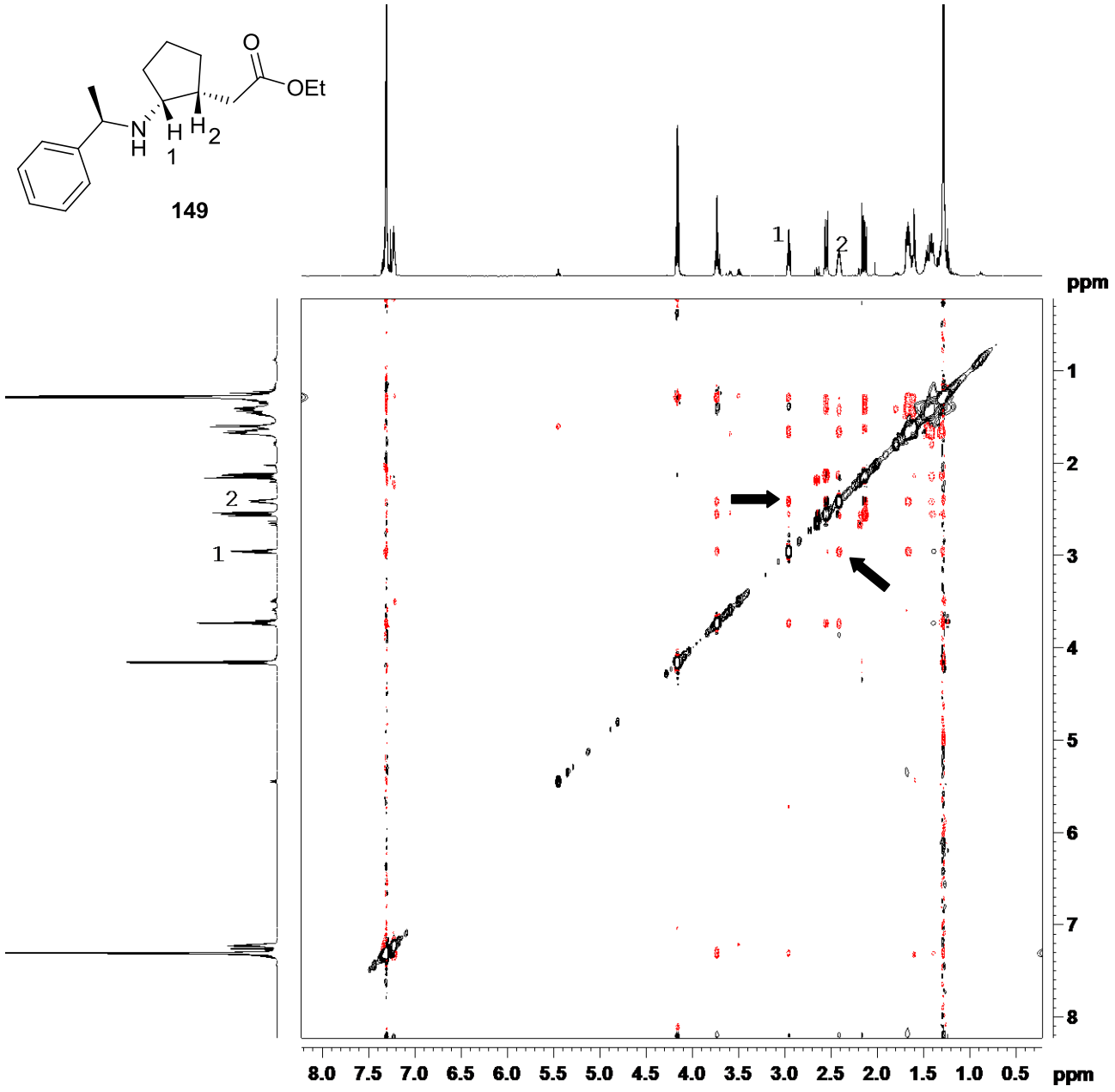

Figure 33. NOESY spectrum of compound **149** shows interaction between hydrogen 1 and 2. (*cis*-isomer).

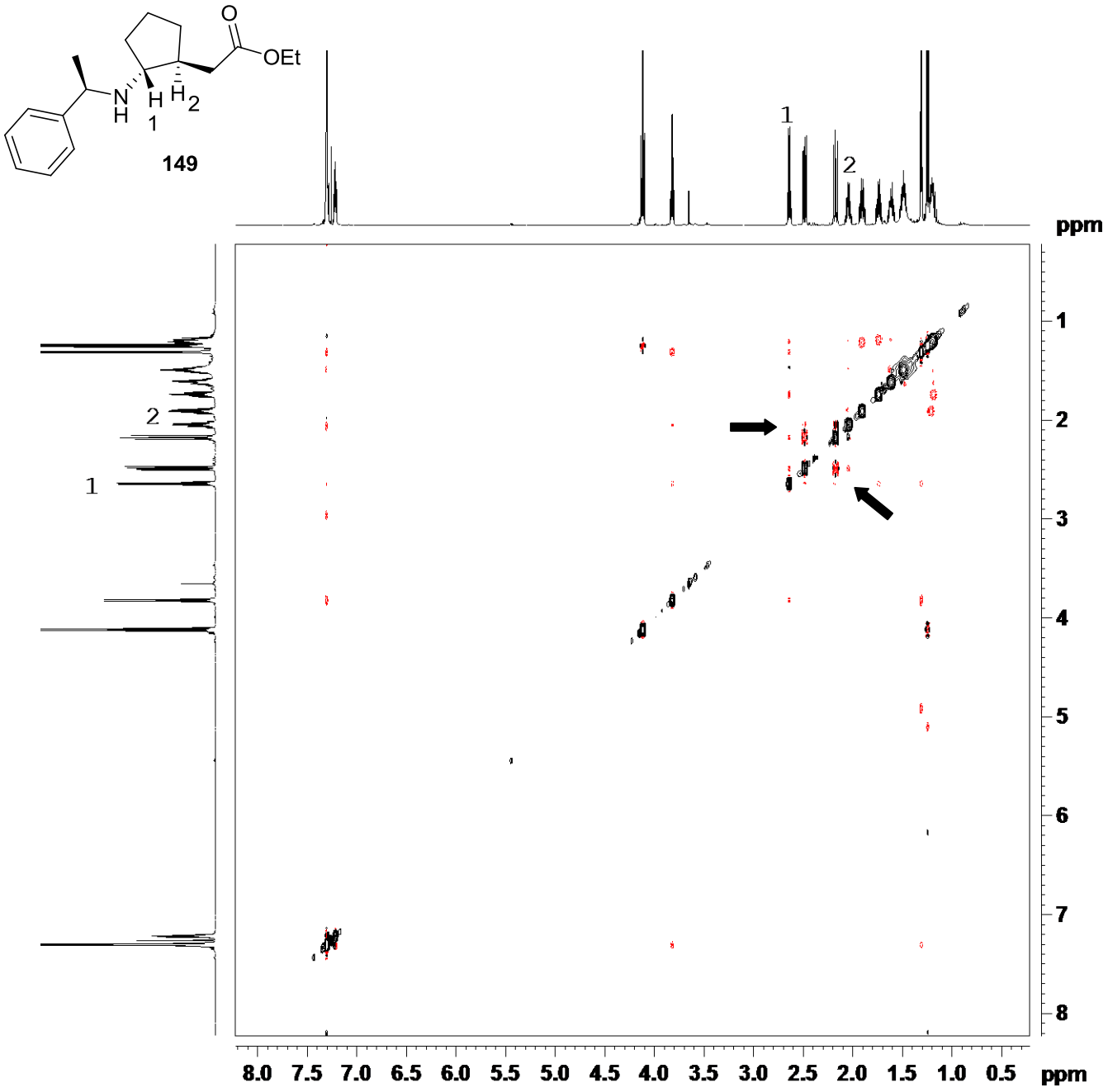

Figure 34. NOESY spectrum of compound **148** shows no interaction between hydrogen 1 and 2. (*trans*-isomer).

A freshly solution of HCl in ethyl acetate was added dropwise separately to solution of each phenylethylamino-cyclopentyl acetate **148** and **149** in diethyl ether cooled at 0 °C, affording after recrystallization the hydrochloride salts **150** and **151**. X-ray structure of these salts proved the corrected stereochemistry (**Figure 35**). The stereochemistry of compound **150** was exactly the opposite of *trans*-γ-amino acid **130**. Thus, the final Fmoc-amino acid synthesized by modifications of compound **150** will be the enantiomer of *trans*-γ-amino acid **130**.

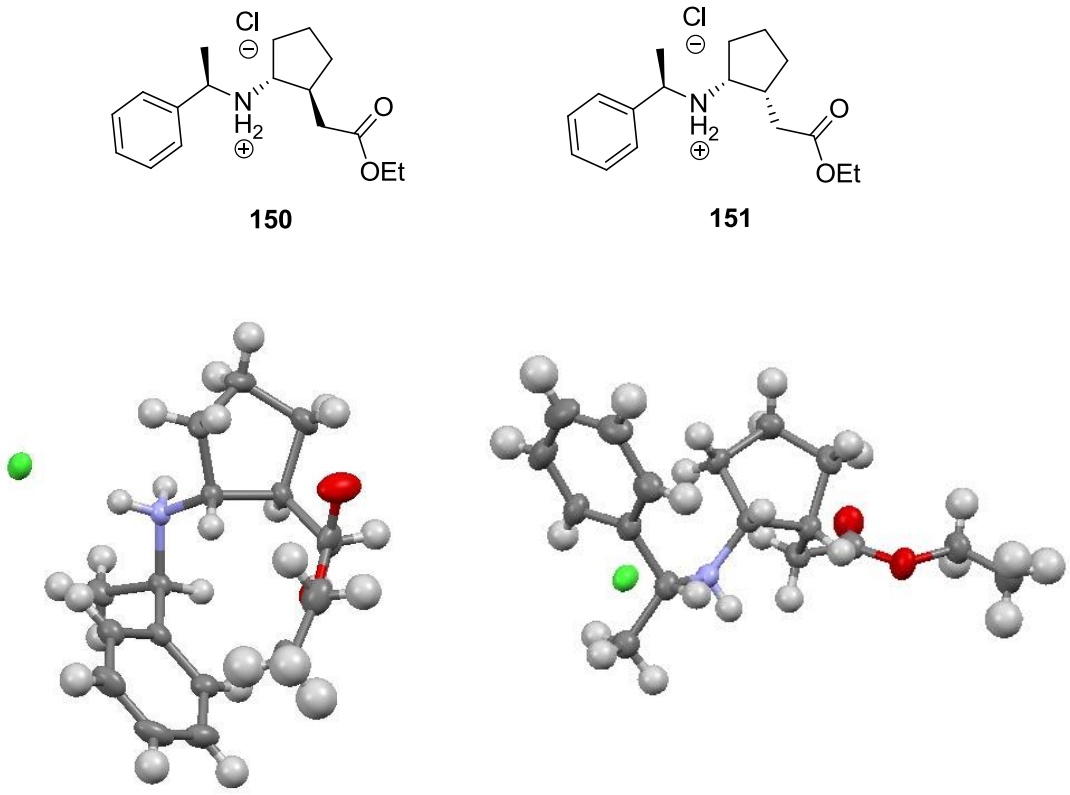

Figure 35. The hydrochloride salts of *trans*- and *cis*-ethyl 2-((*R*)-1-phenylethylamino)cyclopentyl)acetate (**150**, **151**); X-ray structures of compound **150** and **151**.

After that, the synthesis of Fmoc-γ-amino acids has been carried out by modifications of the hydrochloride salts **150** and **151**. **Scheme 27** shows the synthesis of *trans*-Fmoc-γ-amino acid **153**. The hydrochloride salts **150** was hydrolyzed in presence of LiOH, giving 2-((*1S,2R*)-2-((*R*)-1-phenylethylamino)cyclopentyl)acetic acid **152** in quantitative yield. Compound **152** was dissolved in ethanol, Pd/C (10 %) was added and the resulting mixture was shaken under H_2 (50 bar) at 50 °C for 48 h, affording 2-((*1S,2R*)-2-aminocyclopentyl)acetic acid **31**, which was protected with Fmoc-OSu, yielding the 2-((*1S,2R*)-2-Fmoc-aminocyclopentyl) acetic acid **153**.

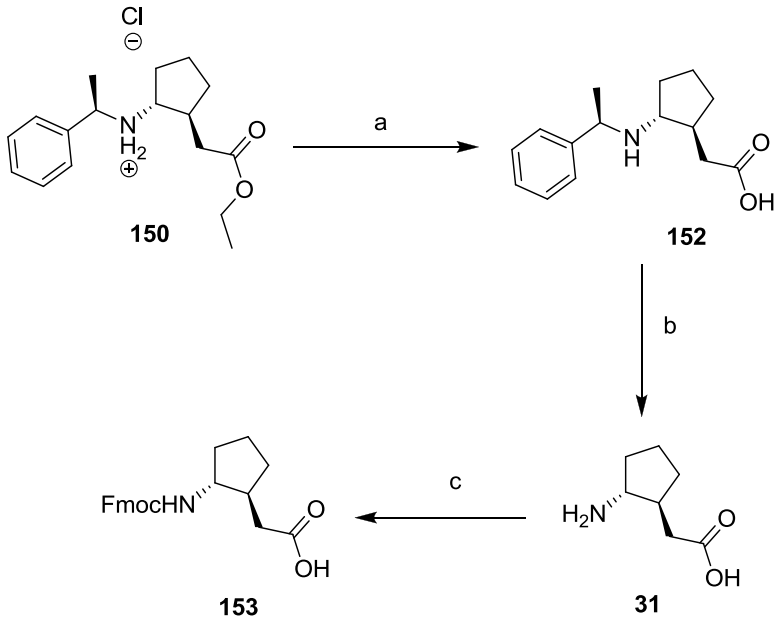

Scheme 27. Synthesis of 2-((*1S,2R*)-2-Fmoc-aminocyclopentyl) acetic acid **153**. Reagents and conditions: a) LiOH, THF/MEOH/H_2O, 9 h, 0 °C, quant.; b) H_2 (50 bar), 10 % Pd/C, 50 °C, EtOH, 48 h, 85%; c) Fmoc-OSu, $NaHCO_3$, Acetone/H_2O 1:1, 18 h, 85%.

The isomer **151** was used to prepare *cis*-Fmoc-amino acid **143**. The same route was tried, but because of *cis*-stereochemistry, lactamization took place during hydrolysis using LiOH, and the compound **151** was converted into lactam **141** in quantitative yield (**Scheme 28**).

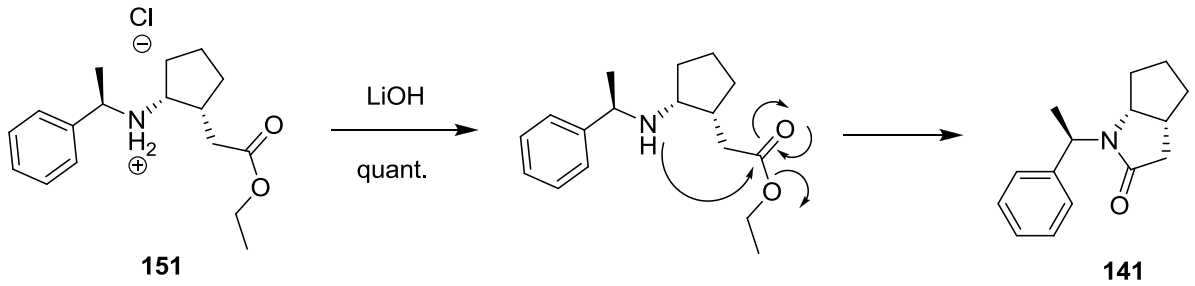

Scheme 28. Lactamization of compound **151**.

Therefore, a new synthetic route was planned to obtain Fmoc-protected *cis*-γ-amino acid **143** from lactam **141**, and it is shown in **Scheme 29**.

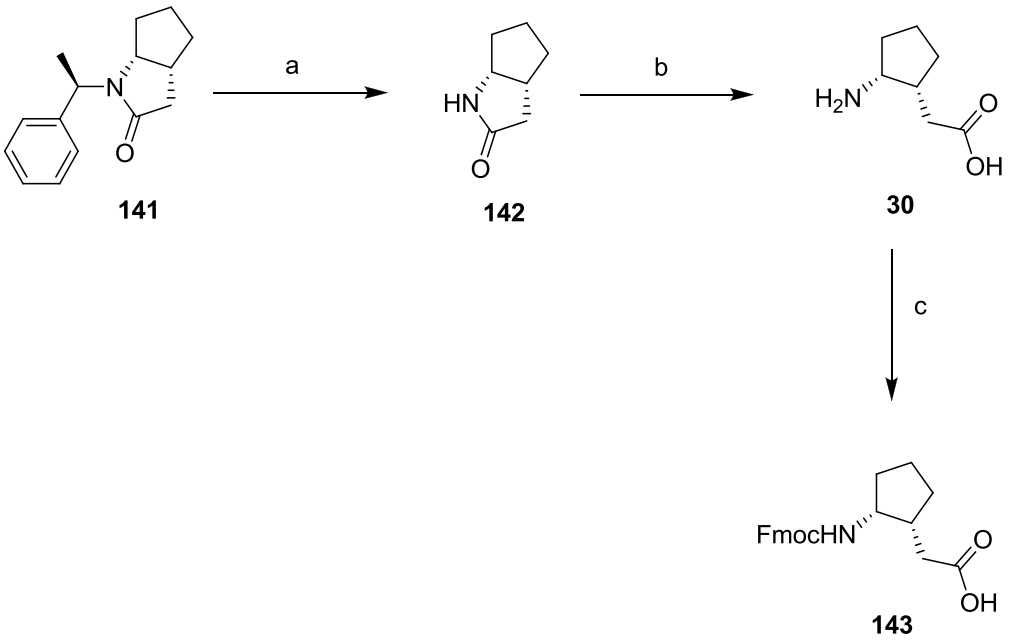

Scheme 29. New synthetic route to prepare 2-((*1R,2R*)-2-Fmoc-aminocyclopentyl) acetic acid **143**. Reagents and conditions: a) Li/NH_3, -78 °C, THF/*t*-BuOH, overnight, 77%; b) 1 N HCl, 80 °C, 8 h, 55% ; c) Fmoc-OSu, $NaHCO_3$, Acetone/H_2O 1:1, 18 h, 85%.

Debenzylation of compound **141** was carried out by *Birch* reaction.[52] The reaction was run at -78 °C in liquid ammonia and lithium, then *t*-BuOH was added together with compound **141** in THF. Lactam **142** was obtained in 77% yield.[53,54] Compound **142** was hydrolysed[54] in 1 N HCl, giving the 2-((*1R,2R*)-2-aminocyclopentyl) acetic acid **30**, which was protected with Fmoc-OSu, affording the 2-((*1R,2R*)-2-Fmoc-aminocyclopentyl) acetic acid **143** in 85% yield. In conclusion, in this work three isomers of 2-(2-Fmoc-aminocyclopentyl) acetic acid were prepared in enantioselective form, and were used to synthesize different NPY analogues by solid phase synthesis. Furthermore, *trans*-pentacin **33** was an important intermediate compound for the synthesis of γ-amino acid **130** and thus it has also been prepared in good amount in this work. As mentioned in the introduction, on the base of its good result in foldamers as shown by *Gellman et al.*,[55] NPY analogues containing compound **33**, and in different combination with the γ-amino acids **30**, **31** and **32** have also been prepared. The synthesis and conformational analysis of NPY analogues containing β and γ-amino acid will be presented in the next chapter.

Chapter 2

2. 1. Synthesis and conformational investigation of NPY analogues

2. 1. 1. Structure inducing moieties in NPY analogues

"Neuropeptide Y (NPY) is one of the most abundant neuropeptides in the central nervous system".[56] NPY was isolated in 1982 from a porcine brain by *Tatemoto et al.*,[57] and it is a important member of a peptide family, together with peptide YY (PYY) and pancreatic polypeptide (PP). The peptides in this family consist of 36 amino acids, have a high content of tyrosine, and an amide group at the C-terminus.[58] The three peptides show a high homology in their peptide sequence, especially between NPY and PYY, and a bit less with pancreatic polypeptide (PP).[59] NPY has been found in nonsympathetic neurons in several organs such as the gastrointestinal tract, salivary glands, the urinogenital system, and the heart.[60] In the periphery, it has been found in the sympathetic nervous system, co-stored with norepinephrine.[61] NMR studies on NPY have shown that it consists of a C-terminal part folded into an α-helical conformation and a N-terminal part which is unfolded.[62] Contrary to the structure of avian PP, which consists of a β-turn type II that connects a type II polyproline helix to an amphiphilic α-helix, as confirmed by X-ray crystallography.[63] The activities of NPY are mediated through G-protein-coupled receptors of class A (rhodopsin-like) (**Figure 36**).[64] These receptors are metabotropic, and can thus open and close ion channels.

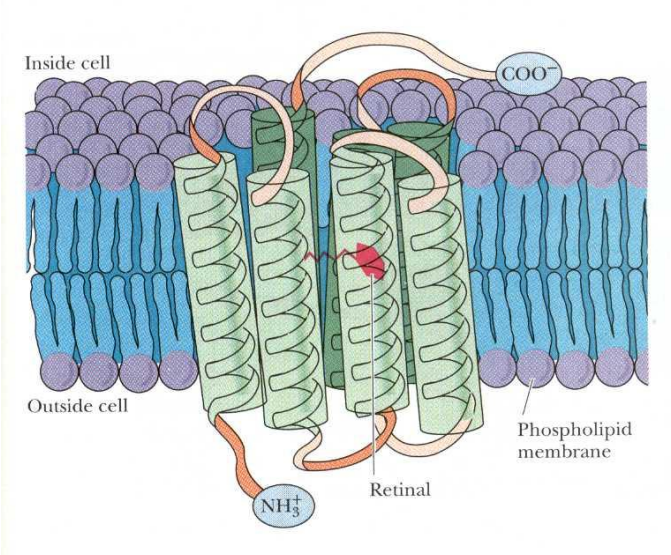

Figure 36. Structure of receptors rhodopsin-like GPCR family.[67]

Contrary to ionotropic receptors which open the channels directly, in this case after binding of the ligand, a series of reactions mediated by a intracellular second messenger lead to a channel-opening or other cellular effects.[65]

In this class of receptor, the intracellular second messenger is usually the cyclic adenosine monophosphate (cAMP), but some studies showed NPY receptors can also couple with phospholipase C, releasing the Ca^{2+} from intracellular stores.[66]

"*Five receptor subtypes have been cloned in mammals (Y_1, Y_2, Y_4, Y_5, and y6)".*[68] NPY and PYY show a high affinity for Y_1, Y_2 and Y_5 receptor subtypes, while the PP prefers the Y_4 receptor.[69] On the base of the degree of amino acid sequence identity, the receptors can be organized into three subfamilies, which are called subfamilies Y_1, Y_2 and Y_5.[70] These subtypes of NPY receptors have an important role in many different processes such as stimulation of feeding, regulation of blood pressure, anxiety, stress, depression, memory and learning processes [71] (**Table 3**). Furthermore, they perform other biological functions such as vasoconstriction in periphery, modulation of pain and epileptic seizures.[72]

Receptors	*Physiological implications*
Y_1	Regulation of blood pressure, food intake, seizure regulation, anxiety, pain sensitivity, depression.
Y_2	Regulation of blood pressure, food intake, seizure regulation, anxiety, hypothalamic regulation of bone formation, pain sensitivity, depression, regulation of the motility of the gastrointestinal tract.
Y_4	Food intake, regulation of the motility of the gastrointestinal tract.
Y_5	Food intake, seizure regulation, anxiety.

Table 3. Physiological effects mediated by different NPY receptors.[73]

The development of subtype-selective ligands for each receptor could help shed light on the working of each receptor, since NPY shows a different affinity towards each of them.[74] Subtype selective agonists and antagonists have been synthesized and tested.[75] Several non peptidic as well as peptidic, selective ligands are shown in **table 4**.

Compounds	*Properties*
1. NPY(18–36)	Antagonized NPY effects on rat cardiac ventricular membranes[76] and myocytes, canine purkinje fibers, and NMDA response in rat hippocampus. Partial agonist at Y_1 receptors and full agonist at Y_2 receptors.[77,78]
2. *N*-α-Ac-[3-(2,6-dichlorobenzyl-Tyr27, D-Thr32] NPY(27–36), PYX1 *N*-α-Ac-[3-(2,6-dichlorobenzyl)-Tyr27,36, *D*-Thr32] NPY(27–36), PYX2	Bound to rat brain bearing predominantly Y_2 receptors and antagonized NPY effects on HEL cells. PYX_2 also antagonized NPY-induced feeding. Demonstrated for the time that decapeptide based compounds can also interact with NPY receptors. Found to be weak or inactive antagonist by other investigators.[79]
3. [*D*-Trp32] NPY.	Antagonized NPY-induced feeding in rats and mice.[80,81] Reported to be a weak[82] and potent[83] Y_5 selective ligand. Also reported to be weak agonist on feeding.[82]
4. Antagonists based on centrally truncated NPY analogs: e.g. 1. Des-AA7–24[*D*-Ala5, Aoc6, *D*-Trp32]NPY; 2. Des-AA6–24[Aca5, Ala28] NPY.	Antagonized NPY effects on HEL cells, and NPY-induced hypertension in rats.[84] Only moderately potent and nonselective.
5. [*D*-Tyr27,36, *D*-Thr32]NPY(27–36).	Antagonized rat food intake induced by both food deprivation and exogeneous NPY. Receptor affinities or selectivity not reported.[85]
6. Nonapeptide antagonists: e.g. 1. Des-Asn29[Trp28, 32, Nva] NPY(27–36); 2. [Pro30, Tyr32, Leu34] NPY(28–36).	Moderately potent Y_1 receptor antagonist, $Y_1 > Y_2$;[86] Potent Y_1 receptor antagonist, $Y_1 > Y2$.[87]

Table 4. List of some peptide and non peptide antagonists.[88]

Some studies have established that specific positions on the NPY sequence, such as the two arginines in positions 33 and 35 and the tyrosine amide in position 36, are fundamental to the recognition process by the respective receptor. Therefore, removing these amino acids, the corresponding analogue loses its selectivity and thus its activity.[89] It has also been shown that substitutions close to these positions allows to obtain analogues which fold in a different conformation and have different selectivity for some receptor subtypes. For example, the introduction of a proline residue in position 34 reduced the Y_2 receptor affinity, but maintains the affinity toward the Y_1 and Y_5 receptors.[90,81] Moreover, the introduction of the turn-inducing Ala-Aib sequence in positions 31 and 32, led to a Y_5-selective analogue as reported by *Cabrele et al*.[91]

In order to rigidify the peptide backbone and to stabilize any distinct secondary structure in NPY analogues, new conformationally constrained amino acids as building blocks have been investigated. As previously mentioned in the introduction, the two enantiomers of β-ACC **26** were introduced in the C-terminus (residues 25-36) of the NPY in position 32 and 34.[92] These analogues showed a good affinity and selectivity to the Y1 receptor subtype. Furthermore, depending on the position of the substitution and the absolute configuration of β-ACC **26**, different affinity and selectivity have been observed. (**Table 5**).

Peptide	*Sequence*	Y_1	Y_2	Y_5
154	Ac-RHYINLITRQRY-NH_2	>1000	21	>1000
155	Ac-RHYINL-IT-R-(+)-RY-NH_2	37(±20)	>1000	724
156	Ac-RHYINL-IT-R(–)RY-NH_2	>1000	>1000	>1000
157	Ac-RHYINLI(+)RQRY-NH_2	>1000	>1000	>1000
158	Ac-RHYINLI(–)RQRY-NH_2	>1000	>1000	>1000
159	Ac-RHYINL-I(+)-R(–)RY-NH_2	50(±10)	>1000	617
160	Ac-RHYINL-R(+)-R(–)RY-NH_2	29(±13)	>1000	118

Table 5. Sequence and affinities of NPY analogues containing β-ACC (where (+) = **(+)β-ACC** and (–) = **(–)β-ACC)**. The affinities are expressed as K_i values [nM].[93]

On the base of these results with β-ACC, different NPY analogues containing isomers of 2-(2-aminocyclopentyl) acetic acid and *trans*-pentacin **33** in position 32 and 34 were prepared. Their synthesis will be presented in the next paragraph.

2. 1. 2. NPY analogues containing isomers of the 2-(2-amino cyclopentyl) acetic acid

Different NPY analogues containing isomers of the 2-(2-amino cyclopentyl) acetic acid have been prepared in collaboration with the group of *Prof. Dr. Chiara Cabrele* at University of Bochum. Fmoc-protected unnatural γ-amino acids **130**, **153**, **143** and **132** have been used to synthesize truncated NPY analogues (residues 25-36) by solid phase synthesis using Fmoc chemistry. Recently, the synthesis and conformational analysis on α-β-γ foldamer containing *trans*-pentacin **33** and a γ-amino acid in which the backbone is constrained by a six-membered ring has been reported by *Gellman et al.*, and these peptides showed to adopt an a-helix like conformation in water.[94] On the base of these results, NPY analogues containing *trans*-pentacin **33** in combination with the γ-amino acids **30**, **31** and **32** as α-β-γ foldamers were prepared and investigated. **Figure 37** shows two NPY analogues containing compounds **30** and **33**.

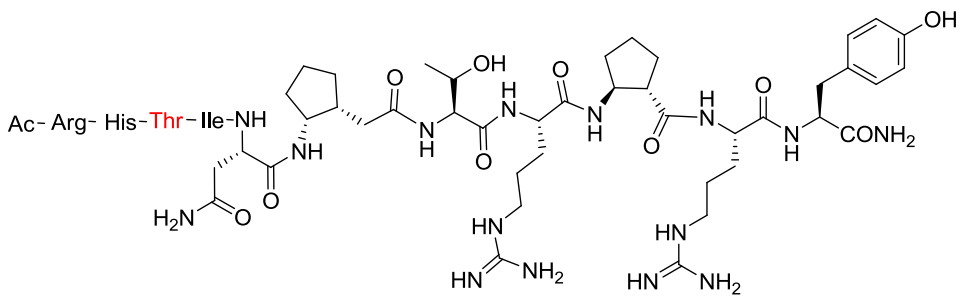

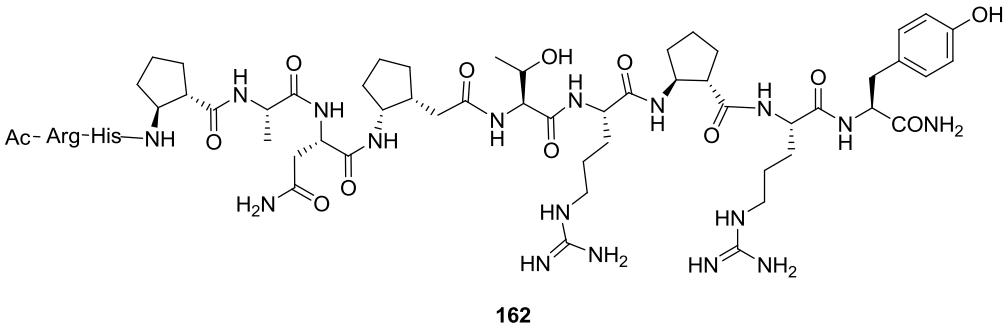

Figure 37. Structure of the NPY analogues containing unnatural amino acids **30** and **33** as α-β-γ foldamers.

In peptide **161**, the original structure of NPY has been modified in three positions. Tyrosine in position 28 was replaced with a threonine. The *cis*-γ-amino acid **30** has been introduced in position 31, and *trans*-pentacin **33** in position 34. In peptide **162**, *cis*-γ-amino acid **30** was introduced in position 31, and *trans*-pentacin **33** in position 34 and 28.

Moreover, NPY analogues containing only a unnatural amino acid have been prepared and are shown in **Figure 38**.

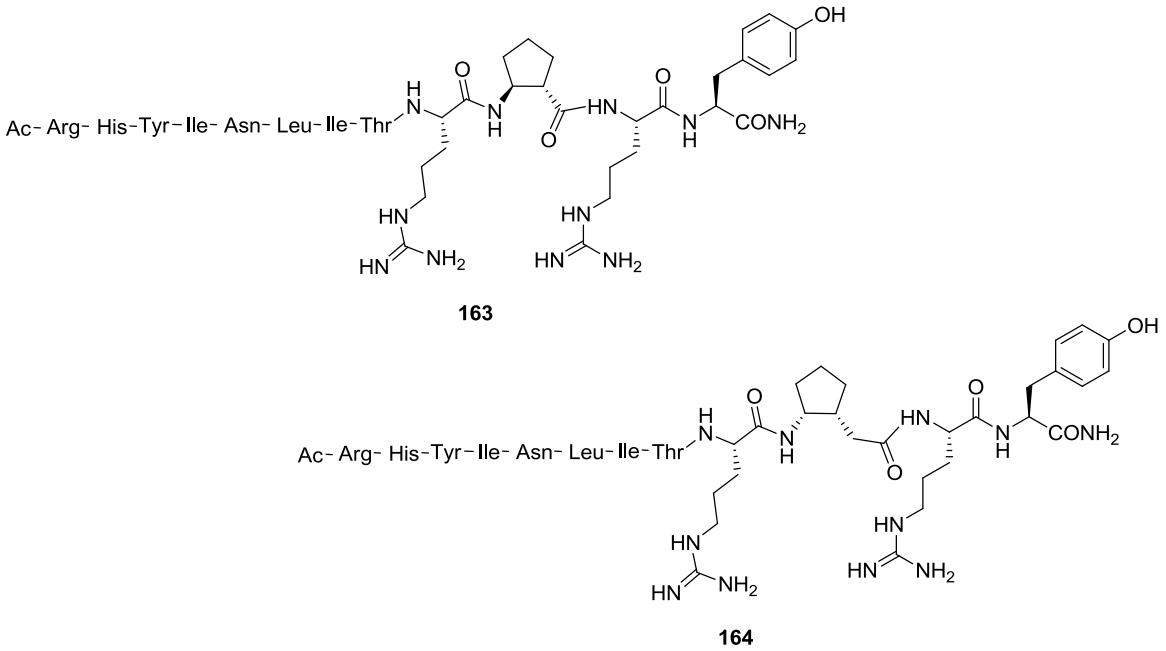

.

Figure 38. Structure of the NPY analogues containing unnatural amino acids **33** and **30** in position 34.

In this case, only a unnatural amino acid has been introduced in position 34. *trans*-pentacin **33** in peptide **163**, and *cis*-γ-amino acid **30** in peptide **164**.

All crude peptides have been characterized by MS and analytical HPLC, confirming that the main peaks correspond to the desired peptides (**Figure 39** and **Figure 40**).

Ac-Arg[1]-His[2]-Thr[3]-Ile[4]-Asn[5]-(1S,2S-ACPA)[6]-Thr[7]-Arg[8]-(1S,2S-ACPC)[9]-Arg[10]-Tyr[11]-NH_2 **161**

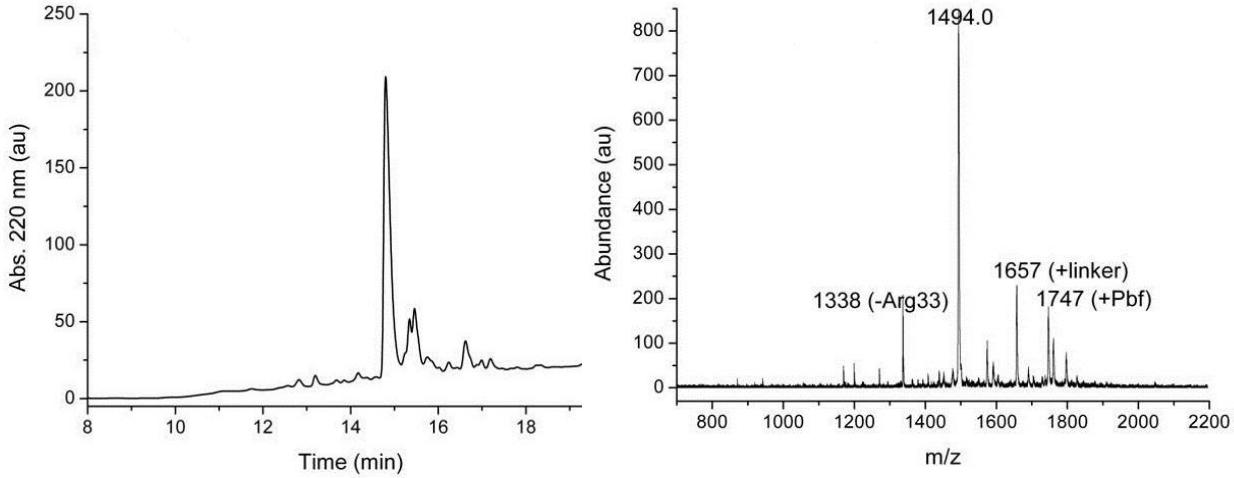

Ac-Arg[1]-His[2]-(1S,2S-ACPC)[3]-Ile[4]-Asn[5]-(1S,2S-ACPA)[6]-Thr[7]-Arg[8]-(1S,2S-ACPC)[9]-Arg[10]-Tyr[11]-NH_2 **162**

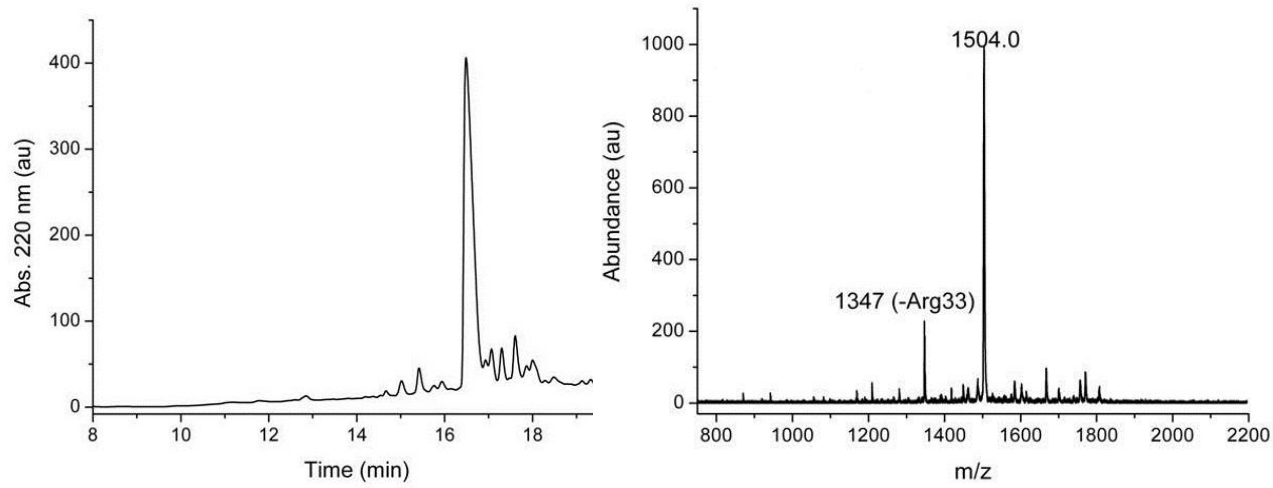

Figure 39. Characterization of the crude peptides **161** and **162** by HPLC-MS.

Ac-Arg[1]-His[2]-Tyr[3]-Ile[4]-Asn[5]-Leu[6]-Ile[7]-Thr[8]-Arg[9]-(*1S,2S*-ACPC)[10]-Arg[11]-Tyr[12]-NH_2 **163**

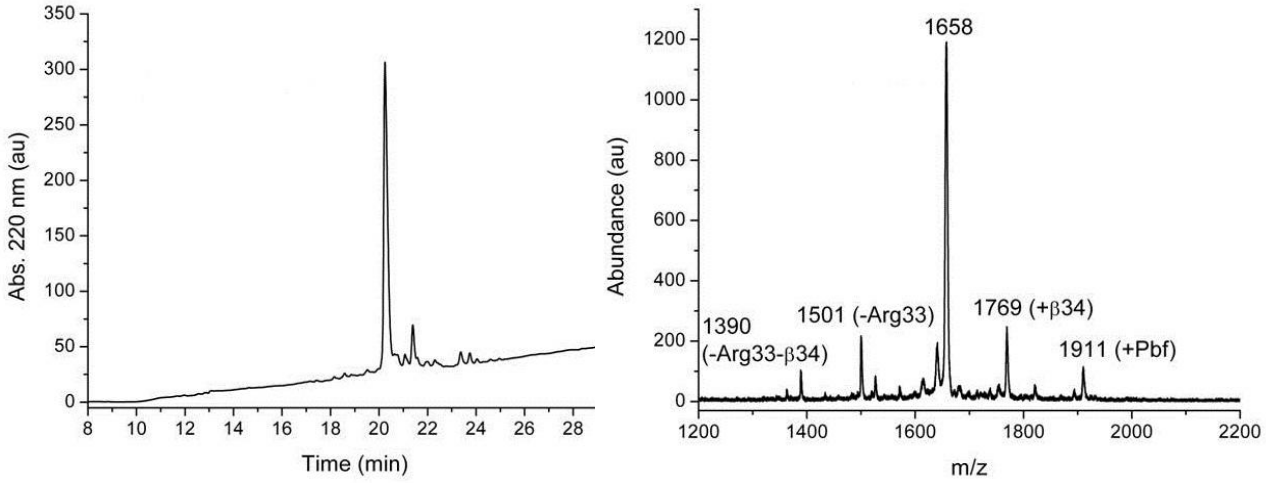

Ac-Arg[1]-His[2]-Tyr[3]-Ile[4]-Asn[5]-Leu[6]-Ile[7]-Thr[8]-Arg[9]-(1S,2S-ACPA)[10]-Arg[11]-Tyr[12]-NH_2 **164**

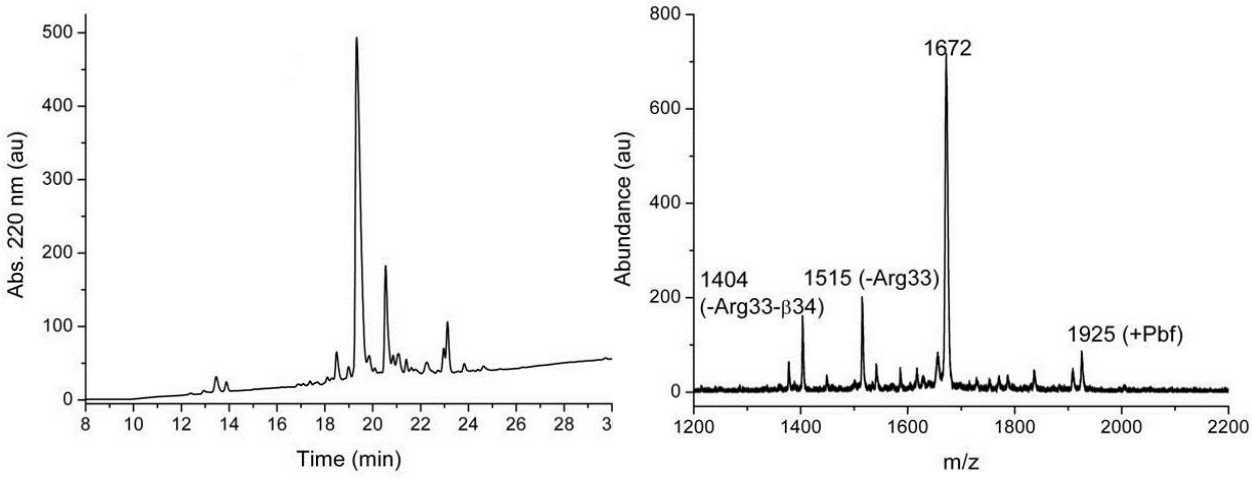

Figure 40. Characterization of the crude peptides **163** and **164** by HPLC-MS.

NPY analogues containing the *trans*-isomers **31** and **32** were also prepared. Peptides **165** and **166** contain two substitutions. *Trans*-pentacin **33** in position 34, and the *trans*-γ-amino acids in position 31. *Trans*-isomer **31** was introduced in peptide **165**, while its enantiomer *trans*-isomer **32** in peptide **166**. Therefore, these peptides are diastereoisomers (**Figure 41**).

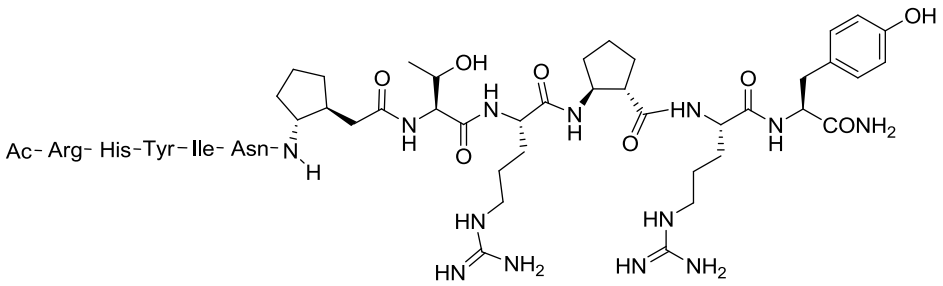

165

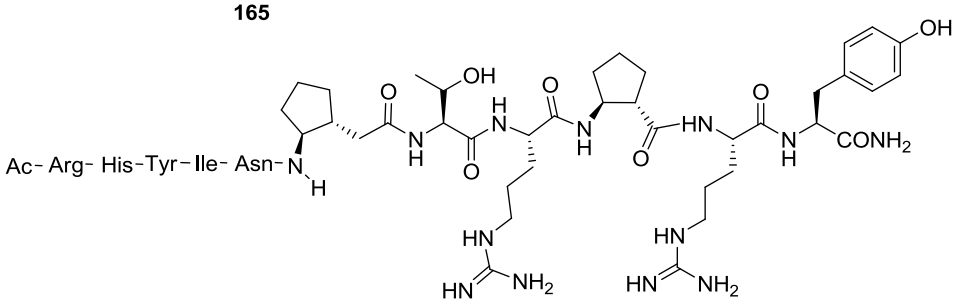

166

Figure 41. Structure of the NPY analogues containing unnatural amino acids **31**, **32** and **33**.

Analytical HPLC of crudes NPY analogues **165** and **166** displayed very good chromatogramms, showing a main peak which corresponds to the product and only few impurities (**Figure 42** and **43**).

Ac-Arg^{1}-His^{2}-Tyr^{3}-Ile^{4}-Asn^{5}-(*1S,2R*-ACPA)^{6}-Thr^{7}-Arg^{8}-(1S,2S-ACPC)^{9}-Arg^{10}-Tyr^{11}-NH_2 **165**

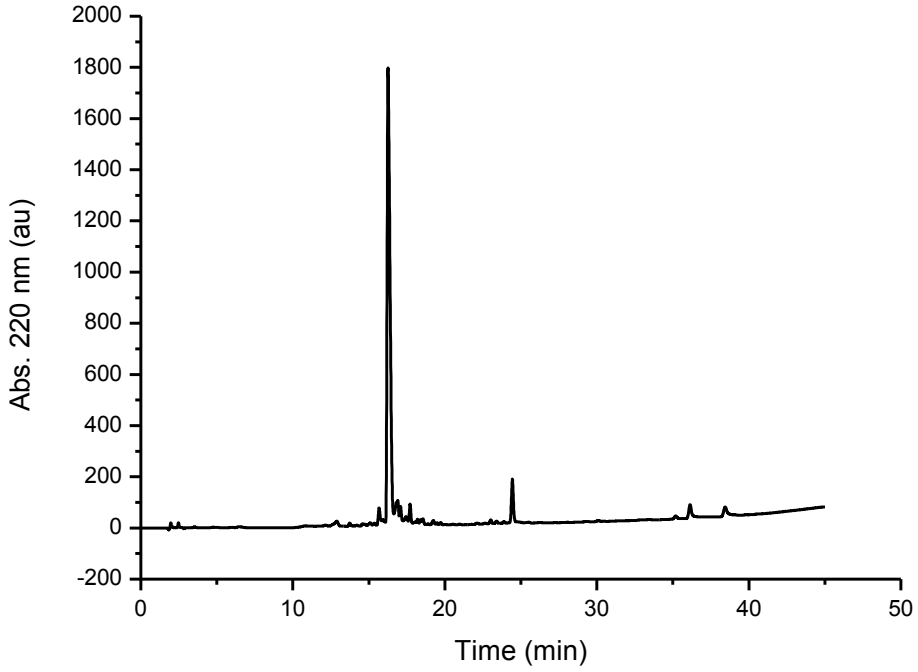

Figure 42. Analytical HPLC of crude NPY analogue **165**.

Ac-Arg[1]-His[2]-Tyr[3]-Ile[4]-Asn[5]-(*1R,2S*-ACPA)[6]-Thr[7]-Arg[8]-(1S,2S-ACPC)[9]-Arg[10]-Tyr[11]-NH_2 **166**

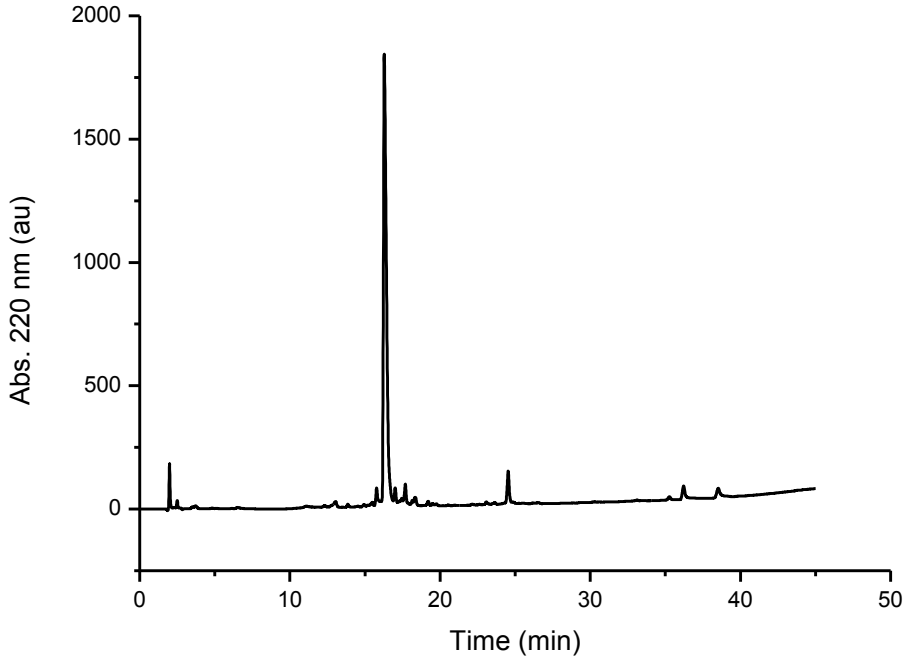

Figure 43. Analytical HPLC of crude NPY analogue **166.**

Concluding, in the last part of this work *trans*-γ-amino acid **31** and **32** have also been introduced in position 34 into the structure of NPY segment, generating the analogues **167** and **168** as shown in **figure 44**.

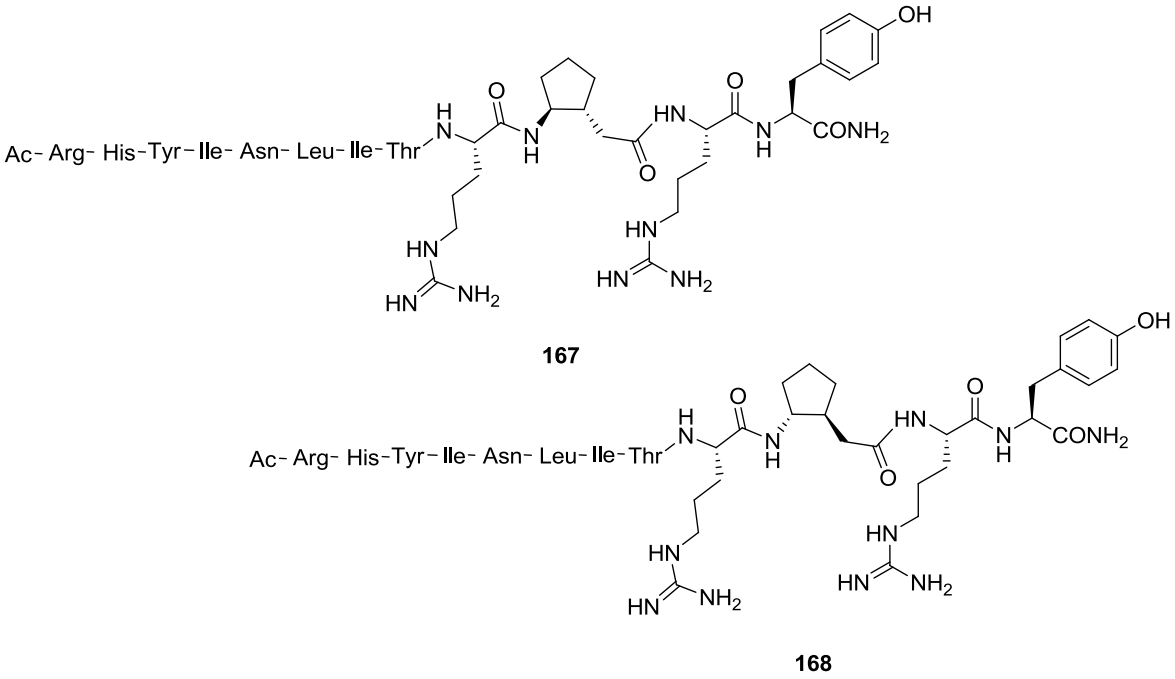

Figure 44. Structure of the NPY analogues containing unnatural amino acids **31** and **32** in position 34.

Analytical HPLC of crude NPY analogues **167** and **168** are shown in **figure 45**.

Ac-Arg[1]-His[2]-Tyr[3]-Ile[4]-Asn[5]-Leu[6]-Ile[7]-Thr[8]-Arg[9]-(*1R,2S*-ACPA)[10]-Arg[11]-Tyr[12]-NH_2 **167**

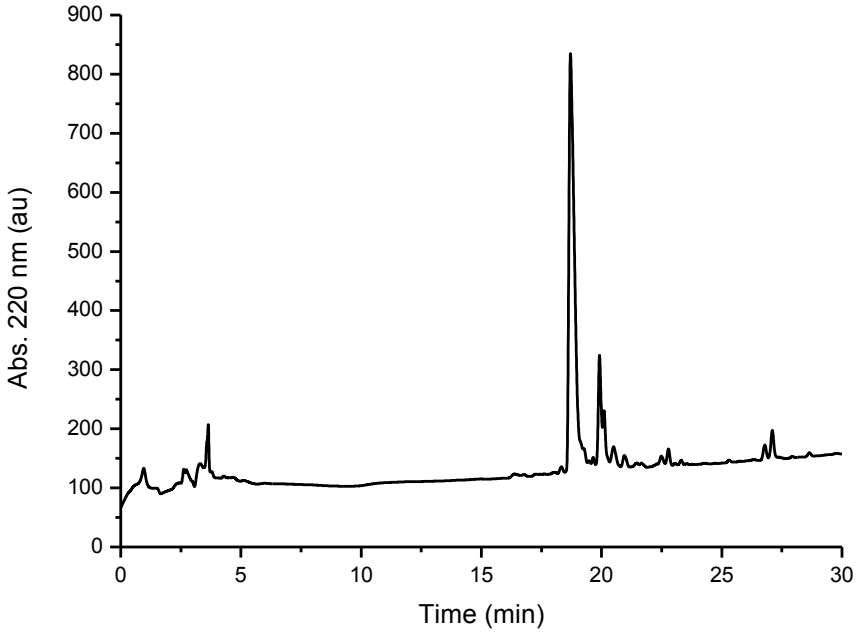

Ac-Arg[1]-His[2]-Tyr[3]-Ile[4]-Asn[5]-Leu[6]-Ile[7]-Thr[8]-Arg[9]-(*1S,2R*-ACPA)[10]-Arg[11]-Tyr[12]-NH_2 **168**

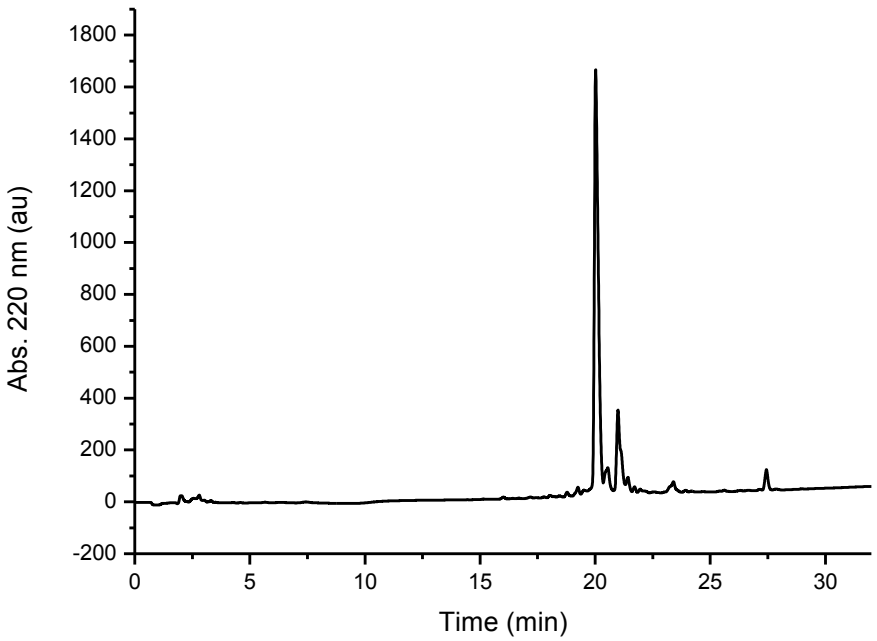

Figure 45. Analytical HPLC of the crudes NPY analogues **167** and **168**.

The synthesis of all peptides was performed using Fmoc-Rink-amide MBHA resin (loading: 0.45 mmol/g), HBTU in combination with HOBt and DIPEA as coupling reagents. Peptide cleavage from the resin and simultaneous side-chain deprotection has been performed by mixture TFA/water/TIS/thioanisole. All peptide crudes were purified by preparative *reversed* phase *HPLC*, affording the pure peptides with a high degree of purity (86-98%). After purification, NPY analogues were subjected to conformational investigation, which will be introduced in the next paragraph.

2. 2. Conformational Investigations

Peptides and proteins fold into a defined conformation which depends in principal on the kind of amino acids in their sequence.[95] Conformational analysis of the three dimensional structure of a peptide allows the understanding of its physical, chemical and biological properties.[96] This investigation consists of the characterization of the secondary structure and structural investigations at atomic resolution. The last one is obtained by X-ray crystallography, which allows a direct way to observe the structure of the peptide. Actually, the analysis of the secondary structure is the most common for the characterization of peptides. The techniques used to investigate the three dimensional structure are circular dichroism, 1D and 2D NMR spectroscopy.[96]

2. 2. 1. Circular dichroism

Circular dichroism is an important spectroscopic technique to investigate the secondary structure of peptides, proteins and nucleic acids. The principle of CD spectroscopy is based on the different absorption of the left and right circularly polarized components of light by an optically active substance such as a peptide. When these components are recombined, a projection of the resulting amplitude yields an ellipse. The extent of this ellipticity is then measured, giving a CD spectrum.[97] Concerning a peptide, the UV-CD spectropolarimeter measures the ellipticity in the absorption band of amide bonds (180-250 nm). The absorption $\pi \rightarrow \pi^*$ of amides can change according to the presence of hydrogen bond, and thus on the presence of any secondary structure.[98]

The CD spectrum shows some curves that are the results of the combination of absorbance of the orientated chromophores in the three dimensional arrangement, therefore each peptide secondary structure will give a specific curve. **Figure 46** shows the typical CD spectra for some secondary structures of α-peptides. The analysis are performed in solvents which do not absorb in amide band, such as methanol, trifluoroethanol, water and acetonitrile.

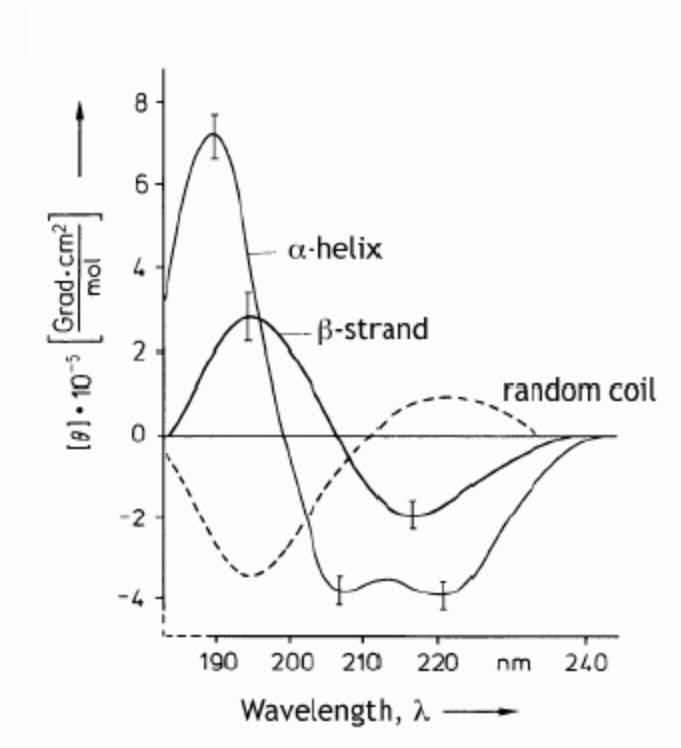

Figure 46. CD spectra of the common secondary structures seen for α-peptides.[99]

The ellipticity can be calculated by the *Beer-Lambert* law: $\theta = CD_{measured}/(C \cdot l \cdot n)$, where θ is the ellipticity in deg $cm^2 \cdot dmol^{-1}$, C is the concentration in $mol \cdot L^{-1}$, l is the length of the cell in cm and n is the number of amino acids.

Circular dichroism can suggest if and which secondary structure the peptide adopts, but it does not give any information about which amides are involved in hydrogen bonding.[100] NMR analysis can give a lot of information concerning this last point.

2. 2. 2. NMR investigations

Nuclear Magnetic Resonance (NMR) spectroscopy is a useful technique to investigate the secondary structure of peptides and proteins in solution. It allows the analysis on an atomic level, especially concerning the presence and location of hydrogen bonding. Important information are obtained from 1D and 2D NMR spectra.[101]

2. 2. 2. 1. 1D-proton NMR spectra

1D-proton NMR spectra are used to identify the protons that are involved in an intramolecular hydrogen bonding. The NMR analysis can be influenced by different factors: the choice of solvent, hydrogen deuterium exchange and the variation of temperature. The solvent can influence the ability of a peptide to adopt a secondary structure, thus peptides often show different conformations in different solvents.[102]

Hydrogen deuterium exchange studies give information on the presence and on which part of the peptide is stabilized by hydrogen bonding. A secondary structure in solution can modify the proton exchange, producing a slower exchange rate of labile protons, which can be measured by time dependent NMR-spectroscopy. This measurement is not possible in small molecules where proton exchange is too fast. The experiments are conducted in the presence of deuterated solvents, encouraging the exchange between the deuterium with amide protons of the peptide. In this moment the exchange rates are measured. Longer exchange time with deuterium indicates that the protons are blocked and stabilized by hydrogen bonding. Contrary to protons which are not involved in hydrogen bonding, where the exchange time is much shorter.[103,101] NMR analysis can also be influenced by variation of temperature, which can modify the hydrogen-bonded state of amide protons.[104] This information is obtained from the temperature coefficient ($\Delta\delta/\Delta T$). For these studies, it is fundamental that no aggregation occurs and thus they are conducted in a specific concentration to avoid it. Generally, if amide protons exchange slowly with the deuterium and have a temperature coefficient more positive than -4.5 ppb/K, then they are involved in a hydrogen bonding. Contrary to protons not involved in a hydrogen bonding that exchange rapidly and have a temperature coefficient more negative than -4.5 ppb/K.[105,106]

2. 2. 2. 2. Information from 2D-proton NMR spectra

2D NMR investigation allows to obtain structural information on peptides and proteins.[107] A typical 2D spectrum displays the diagonal peaks, which are peaks in a 1D-NMR, and the cross peaks which indicate couplings between the protons.[108] The COSY (*correlation spectroscopy*), TOCSY (*total correlation spectroscopy*), ROESY(*rotating-frame overhauser spectroscopy*) and NOESY (*nuclear overhauser effect spectroscopy*) experiments are very useful in peptide analysis. *"The COSY displays [^{1}H,^{1}H]-correlations due to scalar (through-bond) coupling"*.[101] Therefore, it allows to identify vicinal protons. *"A TOCSY experiment contains all cross peaks due to protons of the same spin system"*.[101] In this case, it is not necessary that the two nuclei are directly coupled, but the cross peaks are observed also between nuclei which are connected by a chain of couplings. This is very useful to identify large interconnected networks of spin couplings such as the side chains of amino acids.[109] Coupling by spatial interaction are shown by NOESY and ROESY. *"Cross peaks in the NOESY are due to dipolar couplings resulting from interactions of spins via space and hence only depend on the distance but not on the number of intervening bonds"*.[101] Therefore, hydrogen atoms of different amino acids which are far away in the primary structure, can be very close in a three dimensional structure and give spatial interactions. A NOE peak usually is displayed when two protons are within 5 Å, but it depends also on other factors such as molecular weight. Sometimes, the protons are within 5 Å, but the NOE is close to zero. This is due to the cross-relaxation rate constant which becomes negative as the correlation time increases. For peptides with high molecular weight, it is better to use ROESY, which is very similar to NOESY, but in this case the cross-relaxation rate constant is always positive.[108] The presence of NOE or ROE peaks between protons which are far away in the sequence, indicates that the peptide or protein folds in a specific conformation stabilized by hydrogen bonding. Furthermore, NMR analysis can suggest which kind of secondary structure is adopted by the peptide. Concerning to this, interatomic distances, the three-bond coupling constants $^3J_{HN\alpha}$, intensity and kind of contacts in NOESY or ROESY spectrum are a very useful tool to predict a kind of secondary structure.[110] **Table 6** shows sequential (between the *i* residue and the *i+1* residue) and medium (between the *i* residue and *i+2*, *i+3*, and *i+4*) range ^{1}H-^{1}H distances for identification of secondary structure.

Contacs	*α-Helix*	*3_{10} Helix*	*β Antiparallel*	*β Parallel*	*Type I Turn*	*Type II Turn*
$d_{\alpha N}$	3.5	3.4	2.2	2.2	3.4/3.2	2.2/3.2
$d_{\alpha N}$ (*i, i+2*)	4.4	3.8			3.6	3.3
$d_{\alpha N}$ (*i, i+3*)	3.4	3.3			3.1-4.2	3.8/4.7
$d_{\alpha N}$ (*i, i+4*)	4.2					
d_{NN}	2.8	2.6	3.3	4.0	2.6/2.4	4.5/2.4
d_{NN} (*i, i+2*)	4.2	4.1			3.8	4.3
$d_{\alpha\beta}$ (*i, i+3*)	2.5-4.4	3.1-5.1				

Table 6. Useful sequential and medium range ^{1}H-^{1}H distances (in Å) for identification of secondary structure in polypeptide chains. For the helices, β sheets, and turns, no number is given for distances >4.5 Å.[111]

Some more information about the secondary structure are given from spin-spin coupling constants $^{3}J_{HN\alpha}$, which is directly related to the backbon dhiedral angle φ, and from the intensity of NOE peaks. Generally, values of coupling constant minor than 5 Hz indicates a turn or helical structure, while values higher than 6 Hz are characteristic of extended or unordered conformation.[110] **Table 7** summarizes the sequential and medium range proton-proton NOEs and the spin-spin coupling constants $^{3}J_{HN\alpha}$ in some common secondary structures.

Distances	*βαβp*	*α-Helix*	*3_{10} Helix*	*Turn I*	*Turn II*	*Turn I'*	*Turn II'*	*Half-Turn*
$d_{\alpha N}$ (*i, i+4*)								
$d_{\alpha\beta}$ (*i, i+3*)								
$d_{\alpha N}$ (*i, i+3*)								
d_{NN} (*i,i+2*)								
$d_{\alpha N}$ (*i, i+2*)								
d_{NN}								
$d_{\alpha N}$								
$^{3}J_{HN\alpha}$	9 9 9 9 9 1 2 3 4 5	4 4 4 4 4 4 4 1 2 3 4 5 6 7	4 4 4 4 4 4 1 2 3 4 5 6	4 9 1 2 3 4	4 5 1 2 3 4	7 5 1 2 3 4	7 9 1 2 3 4	4 9 1 2 3 4

Table 7. The sequential and medium range proton-proton NOE's and the spin-spin coupling constants $^{3}J_{HN\alpha}$ in some common secondary structures. The numbers at the bottom represent the amino acid residues in the given secondary structure. The thickness of the line is proportional to the intensity of the NOE.[110]

2. 3. Conformation analysis of NPY segment and analogues

Conformational investigation of Neuropeptide Y has allowed to know its structure. COSY and TOCSY studies allowed to assign all chemical shift for each protons and to confirm the α-helical folding by NOESY and ROESY analysis.[112] *Gurrath et al.* showed the conformational analysis of two C-terminal segments, NPY (13-36) and NPY (18-36), by CD measurement, 2D NMR and conformational refinement of NMR-derived structure by molecular mechanism simulations.[113] **Table 8** shows all chemical shift for NPY segment (18-36).

Residue	*NH*	H^{α}	H^{β}	$H^{\beta 1}$	H^{γ}	$H^{\gamma 1}$	H^{δ}	$H^{\delta 1}$
Ala^{18}	-	4.17	1.57 CH_3^{β}	-	-	-	-	-
Arg^{19}	8.48	4.36	1.83		1.68		3.25	
Tyr^{20}	7.75	4.50	3.15/3.10		-	-	-	-
Tyr^{21}	7.53	4.40	3.15		-	-	-	-
Ser^{22}	7.86	4.28	4.08	4.03	-	-	-	-
Ala^{23}	7.94	4.26	1.61 CH_3^{β}	-	-	-	-	-
Leu^{24}	7.99	4.31	1.88	1.76	1.78	-	1.11 CH_3^{δ}	105 CH_3^{δ}
Arg^{25}	8.17	4.04	1.94		1.75	1.66	3.22	
His^{26}	8.11	4.46	3.47		-	-	-	-
Tyr^{27}	8.36	4.35	3.35		-	-	-	-
Ile^{28}	8.71	3.78	2.03	1.02 CH_3^{γ}	1.92	1.42	0.95 CH_3^{δ}	-
Asn^{29}	8.21	4.42	3.12	2.88	-	-	-	-
Leu^{30}	8.00	4.15	1.85		1.70	-	0.94 $CH_3^{\delta 2}$	
Ile^{31}	8.41	3.91	1.92	0.89 CH_3^{γ}	1.47	1.24	0.78 CH_2^{δ}	-
Thr^{32}	8.11	4.10	4.46	-	1.42 CH_3^{γ}	-	-	-
Arg^{33}	7.95	4.23	2.08		1.89	1.84	3.26	
Gln^{34}	8.13	4.18	2.25		2.57	2.47	-	-
Arg^{35}	7.95	4.21	1.80	1.72	1.48		3.12	
Tyr^{36}	7.81	4.68	3.32	2.98	-	-		-

Table 8. ^1H Assignment of NPY (18-36) in TFE-d_2/H_2O 9:1 at T = 308 K.[114]

Furthermore, the group of *Gurrath* reported some more structural information on the NPY segment derived from CD spectroscopy studies. The CD spectrum in aqueous solution showed a typical unfolded conformation, but the presence of TFE induced helix formation with a maximum helix content of 80%, in the presence of 30% of TFE, as revealed by typical CD spectrum with two negative minima at 222 and 208 nm (**Figure 47**).

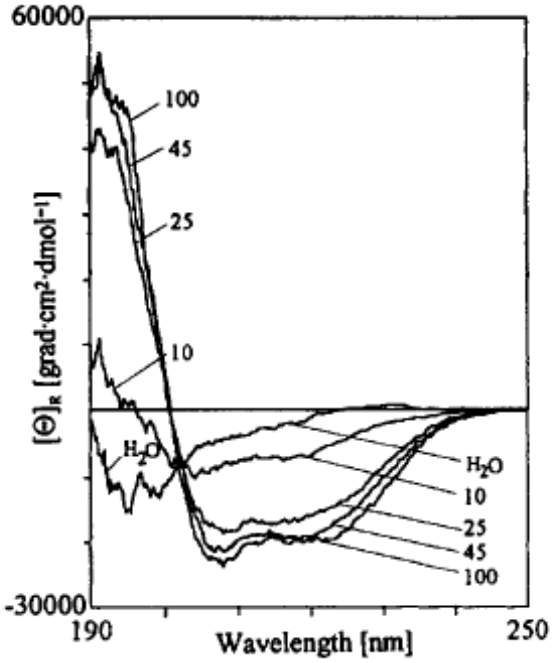

Figure 47. CD spectra of NPY(18-36) segment in water/TFE mixtures. TFE percentages are indicated on the spectra.[115]

In the last 20 years, the synthesis of NPY segments as well as analogues and its conformational analysis has attracted interest. *Aguilar et al.* reported the conformation analysis on NPY (18-36) analogues, containing a single D-amino acid substitution, in hydrophobic environments by CD spectroscopy.[116] The CD spectra were recorded in phosphate buffer, and in mixture with organic solvent (**Figure 46**).

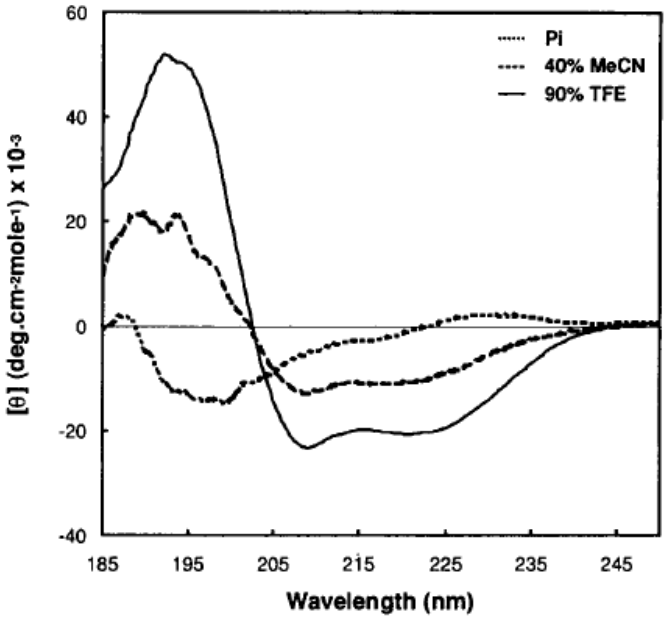

Figure 48. CD spectra of NPY (18-36) measured in 15 mM organophpsphate buffer, 40% acetonitrile in buffer, and 90% TFE in buffer.[117]

The results showed that NPY (18-36) does not adopt any helical structure in buffer, but the α-helical content was increased in presence of organic solvents. This result confirms that the conformation adopted by NPY segment in solution is influenced by the solvent conditions. CD spectra were recorded for each analogues using the same buffer condition, indicating the importance of central region of NPY segment for the maintenance of the α-helical conformation, while the D-amino acid substitutions within N- and C-terminal regions do not influence the secondary structure. Concluding, CD spectra measured in the same condition detect several information about the conformation changing as a result of introduction of new building blocks on the NPY sequence. Therefore, CD as well as NMR studies are an important tool for the conformational analysis of NPY analogues.[118,113]

2. 4. Conformation analysis of NPY analogues containing the 2-(2-amino cyclopentyl) acetic acid

NPY analogues have been investigated by CD- as well as NMR spectroscopy. All CD spectra were recorded in water, and in 20% of methanol and TFE in water. Being very soluble in water, no much organic solvent was used for the analysis, but only the necessary amount to stabilize any conformation (20-30%). Furthermore, the CD were measured in phosphate buffer 50-100 mM at pH 7.4, and in 20% of methanol and TFE in buffer. The peptide concentration for each analysis was 0.3 mM. NMR spectra were recorded in water, with 10% of D_2O. 1D NMR experiments were acquired at five different temperatures (283, 288, 293, 303 and 313 K), in order to have a good dispersion of signals. This temperature was used to record the 2D experiments. The complete sequence-specific resonance assignment has been done by using COSY, TOCSY and ROESY spectra. Furthermore, the NOE peaks intensities were converted into distance, and were classified as strong (1.8-2.7 Å), medium (1.8-3.3 Å) and weak (1.8-5 Å).[111]

*2. 4. 1 Results on NPY analogues **161** and **162***

2. 4. 1. 1. CD studies

As already mentioned, NPY analogues **161** and **162** contain two different unnatural amino acids, the *trans*-pentacin **33** and the *cis*-γ-amino acid **30**. Thus, these analogues can be considered as α-β-γ foldamers. The CD spectra of compound **161** are shown in **figure 49.**

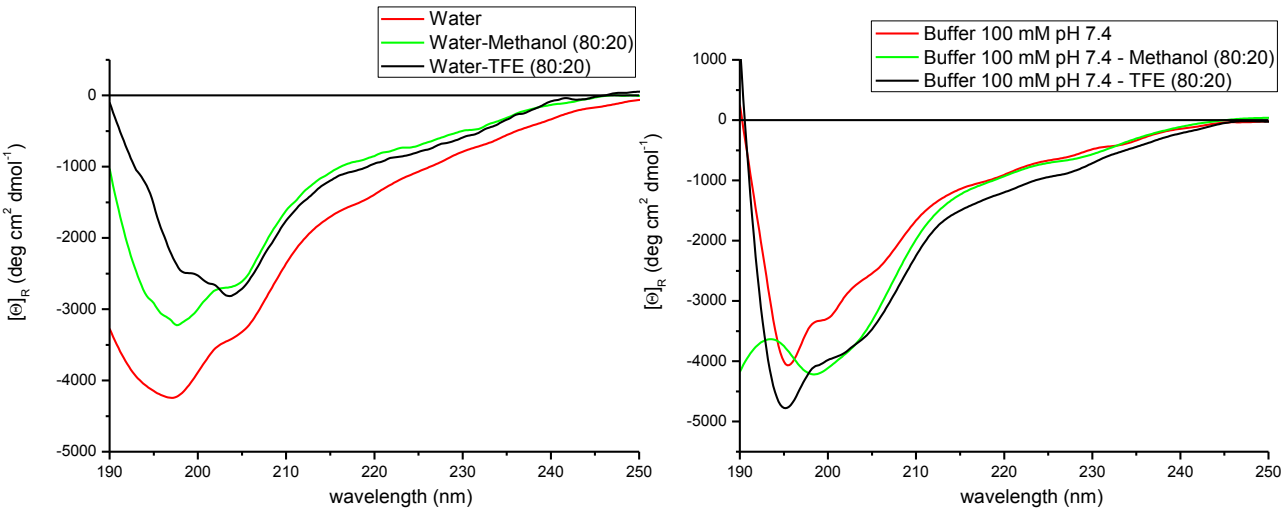

a) b)

Figure 49. CD spectra of compound **161**. a) CD spectrum in water, and in 20% of methanol and TFE in water; b) CD spectrum in phosphate buffer and in 20% of methanol or TFE in buffer.

All CD spectra showed only negative bands. The peptide **161** in water displays a broad band with a minimum at 197 nm and a shoulder at about 205 nm (panel a of **Figure 49**).

The CD curve obtained in the presence of 20% methanol is very similar to that in water, however with reduced intensity. This suggests that methanol does not significantly change the conformation adopted in water. In presence of 20% TFE, the CD curve shows a minimum at about 205 nm, as already detected in water and water/methanol, whereas the minimum at 197 nm disappears almost completely. These results suggest that the two CD signals at 205 nm and 197 nm are probably related to two different conformations, which are both present in water and water/methanol, whereas TFE seems to stabilize the conformation related with the CD contribution as 205 nm. By using phosphate buffer at pH 7.4 in place of water, there is a blue-shift of the CD bands (from 205 nm to 200 nm, and from 197 nm to 195 nm). Interestingly, the band at shorter wavelength, which disappears in water/TFE, is still present in buffer/TFE, whereas it disappears in buffer/methanol. Apparently, the effect of the two organic solvents on the conformation is different at acidic (water) and slightly basic pH (buffer).

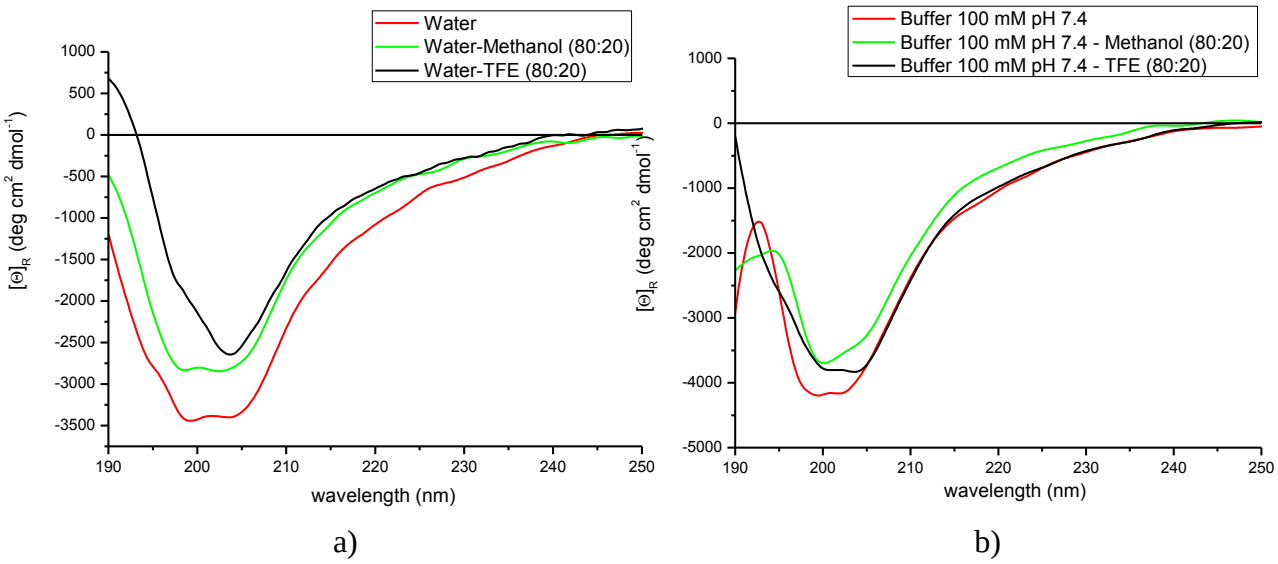

a) b)

Figure 50. CD spectra of compound **162**. a) CD spectrum in water and in 20% of methanol and TFE in water; b) CD spectrum in phosphate buffer and in 20% of methanol and TFE in buffer.

Peptide **162** is expected to be more structured than peptide **161**, having one more unnatural amino acid unit in its structure. Comparison of the CD spectra of **162** (**Figure 50**) and **161** (**Figure 49**) in water and in the presence of organic solvent reveals that the band at 197 nm in water and water/methanol is less pronounced for the peptide **162** than for the peptide **161**. Moreover, the CD spectrum of **162** in water/TFE shows a more positive contribution below 200 nm than peptide **161**, leading to a crossover at 194 nm (panel a of **Figure 50**). As already observed for peptide **161**, the effect of TFE on the conformation of peptide **162** is different in buffer and in water. Indeed, in water/TFE the band at 197 nm is not present but it reappears in butter/TFE (panel b of **Figure 50**). Instead, the CD shape in water/methanol is similar to that in buffer/methanol, with the only difference found in the relative intensity between the two bands. The CD spectra of compounds **161** and **162** are reminiscent of the disordered state of α-peptides, being characterized by a broad negative band centered below 200 nm. However, the comparison of the CD spectra of α-peptides with those of peptides containing unnatural building blocks is critical. As already mentioned, *Gellman et al.* reported a conformational analysis on a α-β-γ foldamer with the alternated sequence αγααβα by CD and NMR spectroscopy, showing that this peptide (numbered with **1** in **Figure 51**) adopts an α-helix-like conformation in aqueous solution.[94]

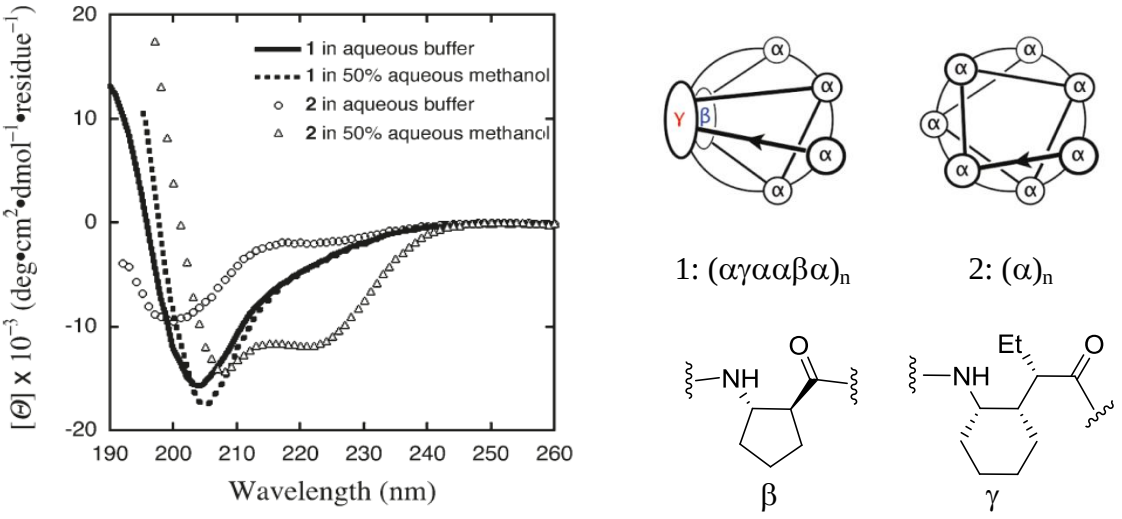

Figure 51. CD spectrum for α-β-γ peptide **1** and α-peptide **2** reported by *Gellman et al.*[119]

The CD spectrum of this foldamer displays a negative band at about 205 nm and a positive band below 190 nm with a crossover at 196 nm (**Figure 51**).For our peptides **161** and **162**, this CD curve should be a better reference than those of α-peptides, especially for the peptide **162** that also contains a similar alternated sequence (ααγααβααγαα). Indeed, the CD spectrum with most similarity to that of the peptide **1** of *Gellman at al.* is that of peptide **162** in water/TFE, being the only one with a crossover. This could suggest that the two foldamers may adopt a similar conformation.

2. 4. 1. 2. NMR studies

Peptide **161** and **162** have been investigated by NMR spectroscopy. The best dispersion of signals was obtained at 283 K for both peptides, thus this temperature was used to record 2D experiments. Under these conditions all amide protons and side chains could be identified, confirming the right sequence. Moreover, the temperature dependency and hydrogen/deuterium exchange were analyzed by 1D NMR. **Table 9** shows the temperature coefficients (Δδ/ΔT) found in the NPY analogue **161**, for the amide protons of two threonines in position 28 and 32, asparagine in position 30, *cis*-γ-amino acid **30** in position 31, arginine in position 33 and *trans*-pentacin **33** in position 34. No temperature coefficients could be determined for the other amide protons due to signal overlap. Moreover, it should be noted that the amide protons of the two threonines were also overlapped.

Temperature	*NH-Thr*[28/32]	*NH-Asn*[30]	*NH-**30***[31]	*NH-Arg*[33]	*NH-**33***[34]
283.0 K	8.0237	8.3232	7.7731	8.1924	7.8147
288.0 K	8.0359	8.3374	7.7835	8.2041	7.8344
293.0 K	8.0495	8.3537	7.7965	8.2181	7.8571
298.0 K	8.0631	8.3689	7.8082	8.2298	7.8799
303.0 K	8.0756	8.3829	7.8193	8.2420	7.9002
313.0 K	8.1012	8.4140	7.8419	8.2687	7.9423
Δδ/ΔT (ppb/K)	2.58	3.02	2.29	2.54	4.25

Table 9. Temperature coefficients (Δδ/ΔT) for the NPY analogue **161**.

The temperature coefficients for peptide **161** show all positive values with a maximum of 4.2 ppb/K for the amide proton of *trans*-pentacin **33** and a minimum of 2.29 ppb/K for the amide proton of γ-amino acid **30** in position 31 (**Table 9**). Usually, the temperature coefficients are negative for protons involved in hydrogen bonding, as the formation of a H-bond leads to a downfield shift. Indeed, for structured proteins the temperature coefficients of H-bonded amide protons are between -4.6 and -1 ppb/K.[104] However, temperature coefficients between -28 and 12 ppb/K have been observed for partially folded peptides, which have been attributed to a conformational change during the warming.[120] Obviously, this makes the use of these temperature coefficients as indicators of H-bonds for partially folded peptides very difficult, although some studies showed that amide protons involved in a strong intramolecular hydrogen bond display temperature coefficients < 3 ppb/K, while for a weak intramolecular hydrogen bond the values are > 8 ppb/K.[121]

In contrast, Andersen and coworkers proposed the use of a different parameter that relates the chemical shift deviation of the amide protons (CSD-NH) from the random coil value with the temperature coefficients: if the correlation (R^2) between these two values is > 75%, it can be assumed that the peptide adopts a single ordered conformation in the cooled state, which unfolds upon warming.[120] R^2 values > 95% are characteristic for helices and β-hairpins. The slope of the linear fit reflects the unfolding facility (steeper means easier to unfold).

To evaluate the correlation between the CSD-NH values and the temperature coefficients for peptide **161**, the CSD-NH values for the natural residues were first calculated by using the random coil values reported by *Wright et al.*[122] The chemical shift deviations are derived from the lowest temperature included in the experiment and are reported in **Table 10**. The linear regression of the three experimental CSD-NH values and of the corresponding temperature coefficients is shown in **Figure 52**.

	NH-Thr[28/32]	*NH-Asn*[30]	*NH-Arg*[33]
Δδ/ΔT (ppb/K)	2.58	3.02	2.54
CSD-NH (ppm)	-0.4963	-0.4368	-0.4976

Table 10. Temperature coefficients (Δδ/ΔT) and chemical shift deviation of the amide protons (CSD-NH) for the NPY analogue **161.**

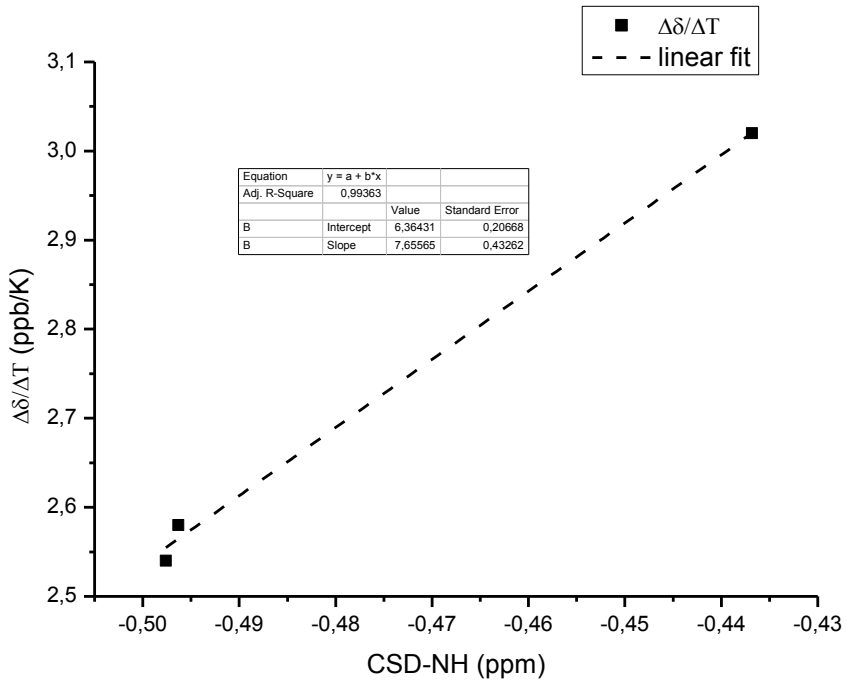

Figure 52. Correlation between temperature coefficients (Δδ/ΔT) and the NH shift deviation from the random coil expectation value (CSD-NH).

The correlation was found to be > 99%, which would indicate that the NPY analogue **161** adopts an ordered conformation at 283 K, which however easily unfolds to a random coil state upon heating up to 313 K. Deuterium/proton exchange experiment have been performed in pure deuterium oxide, and as a result, all amide protons, were already exchanged after 12 min at 283 K (**Figure 53**).

However, a broad peak is present at 8.21 ppm, which could be the amide proton of arginine in position 33, although slightly shifted. Furthermore, other two broad peaks are present at 7.43 ppm and 6.69 ppm, which would be close to the signals of side-chain amide of asparagine at position 30. It was noted that the phenyl ring signals of tyrosine in position 36 are downfield shifted. This might suggest a conformational change of the peptide upon lyophilization: in fact, the NMR probe in H_2O/D_2O (9:1) used for the 2D experiments needed to be lyophilized before dissolving it in D_2O. To prove this hypothesis, the NMR probe in D_2O was lyophilized again and then dissolved in D_2O/H_2O (8:2). A new 1D NMR was recorded, which showed a very different signal dispersion when compared to the first NMR sample. As shown in **Figure 53**, not only most signals are shifted, but also broad signals are present, which might be an indication of peptide aggregation. The latter hypothesis would explain, why some amide protons did not fully exchanged in D_2O: indeed, it is expected that aggregation protects polar groups from contacts with the solvent.

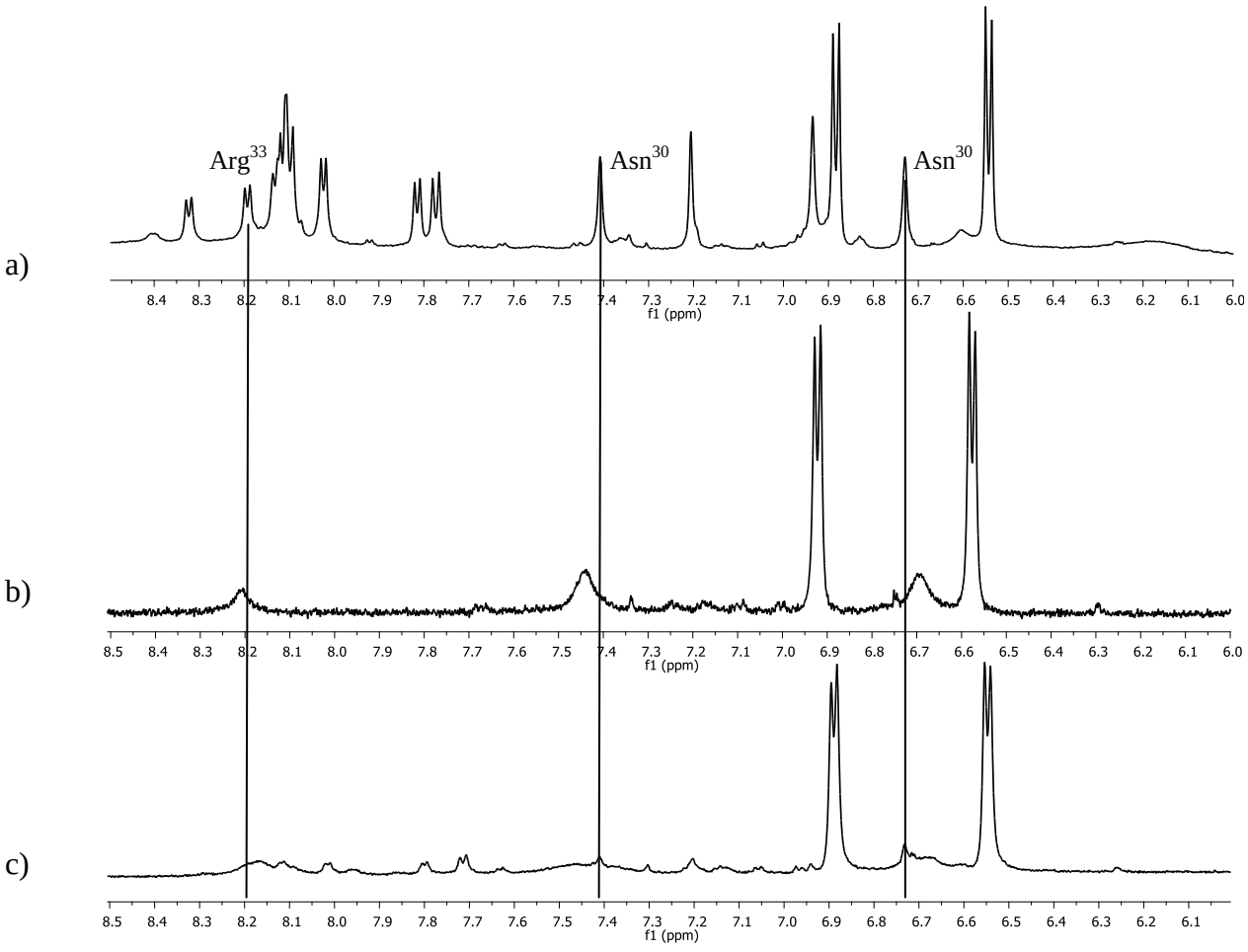

Figure 53. Deuterium/proton exchange studies. a) NMR sample in H_2O/D_2O 9:1 prepared with the peptide obtained after HPLC purification and lyophilization; b) NMR sample in 100% D_2O, obtained after lyophilization from the first NMR sample; c) NMR sample in H_2O/D_2O 8:2, obtained after lyophilization from the NMR sample in 100% D_2O. (Vertical lines show the shifted signals).

Further information on the conformation of the peptide is given from the spin-spin coupling constants $^{3}J_{NH\alpha}$. **Table 11** shows all spin-spin coupling constants for peptide **161**.

Protons	$^{3}J_{HN\alpha}$ *(Hz)*
HNα-Thr$^{28/32}$	6.6
HNα-Asn^{30}	6.9
*HNα-**30***^{31}	8.5
HNα-Arg^{33}	6.8
*HNα-**33***^{34}	7.0

Table 11. Vicinal coupling constants for H^{N}, H^{α} of peptide **161** in H_2O/D_2O (90:10).

All coupling constants show values higher than 6 Hz, excluding the presence of a typical α-helix. Furthermore, the coupling constant for HNα in *cis*-γ-amino acid **30** shows a value of 8.5 Hz, which is typical for antiparallel β-sheet. This might indicate that the γ-amino acid adopts a straight, β-strand-like conformation, alternatively it might be involved in a turn motif. 2D NMR experiments allowed to assign all resonances and also to detect all contacts. Moreover, the intensities of all NOE peaks were converted into distances. Sequential and medium range proton-proton distances in peptide **161** are summarized in **tables 12**.

Contacts	*Distances (Å)*	$d_{\alpha N}$ *(i,i+1)*	$d_{\beta N}$ *(i,i+1)*	$d_{\gamma N}$ *(i,i+1)*	d_{NN} *(i,i+1)*	$d_{\alpha\gamma}$ *(i,i+1)*	$d_{\alpha\gamma}$ *(i,i+2)*	$d_{\beta\beta}$ *(i,i+1)*
Hα Ile^{29}-HN Asn^{30}	3.2	Medium						
HN **33**^{34}-Hα Arg^{35}	2.8	Medium						
Hα **30**^{31}-HN Thr^{32}	3.4	Weak						
Hα Arg^{33}-HN **33**^{34}	3.1	Medium						
Hα Asn^{30}-HN **30**^{31}	2.9	Medium						
Hα Thr^{32}-HN Arg^{33}	2.9	Medium						
Hα Thr^{28}-HN Ile^{29}	3.2	Medium						
Hβ Ile^{29}-HN Asn^{30}	4.4		Weak					
Hβ Asn^{30}-HN **30**^{31}	4.3		Weak					
Hγ Ile^{29}-HN Asn^{30}	4.4			Weak				
Hγ Thr^{32}-HN Arg^{33}	4.5			Weak				
Hγ Thr^{28}-HN Ile^{29}	4.6			Weak				
HN Asn^{30}-HN **30**^{31}	4.7				Weak			
HN Arg^{33}-HN **33**^{34}	4.3				Weak			
HN Ile^{29}-HN Asn^{30}	4.8				Weak			
HN Thr^{32}-HN Arg^{33}	4.7				Weak			
Hγ Ile^{29}-Hα Asn^{30}	4.3					Weak		
Hγ Thr^{32}-Hα **33**^{34}	4.5						Weak	
Hβ Arg^{35}-Hβ Tyr^{36}	4.7							Weak

Distances	*Ac-Arg^{26}-His^{27}-Thr^{28}-Ile^{29}-Asn^{30}-**30**^{31}-Thr^{32}-Arg^{33}-**33**^{34}-Arg^{35}-Tyr^{36}-NH$_2$*
$d_{\alpha N}$ *(i, i+1)*	
$d_{\beta N}$ *(i, i+1)*	
$d_{\gamma N}$ *(i, i+1)*	
d_{NN} *(i, i+1)*	
$d_{\alpha\gamma}$ *(i, i+1)*	
$d_{\alpha\gamma}$ *(i, i+2)*	
$d_{\alpha\beta}$ *(i, i+1)*	

Table 12. All sequential and medium range proton-proton NOEs in peptide **161** (the different line thickness reflects the weak and medium NOE intensity)

ROESY analysis of peptide **161** showed many contacts (*i,i+1*) of medium and weak intensity, and only one contact $d_{\alpha\gamma}$ (*i,i+2*) of weak intensity between the side chain of Thr^{32} and the Hα of **33**^{34}.

No contacts (*i,i+3)*, and (*i,i+4)* were observed, suggesting an extended conformation, at least for the N-terminal region of the peptide. Instead, the detection of the indicated NH-NH backbone-to-side-chain and side-chain-to-side-chain contacts within the segment 29-34, suggests the presence of a folded structure at the C-terminus of the peptide. These results would fit with the interpretation of the CD data, based on the presence of a structural motif and a flexible backbone related to the CD bands at 205 nm and 197 nm, respectively (**Figure 49**).

CD studies of peptide **162** suggested that this peptide could adopt a conformation similar to that of the α-β-γ peptide reported by *Gellman et al.*, displaying a similar CD signature in water/TFE (**Figure 50** and **Figure 51**). As for peptide **161**, the best dispersion of signals in 1D NMR was obtained at 283 K. Temperature coefficients and chemical shift deviations have been determined and are shown in **table 13**.

Temperature	*NH-Asn*[30]	*NH-**30***[31]	*NH-Thr*[32]	*NH-Tyr*[36]
283.0 K	8.2948	7.5917	8.1907	8.0933
288.0 K	8.3189	7.6144	8.2079	8.1179
293.0 K	8.3388	7.6342	8.2208	8.1359
303.0 K	n.d	7.6723	n.d.	n.d
313.0 K	n.d.	7.7085	n.d	n.d.
Δδ/ΔT (ppb/K)	4.00	6.88	3.01	4.26
CSD-NH (ppm)	-0.4652	-	-0.3293	-0.4967

Table 13. Temperature coefficients (Δδ/ΔT) and chemical shift deviation (CSD-NH) for the NPY analogue **162**.

The NMR spectrum of peptide **162** displayed signals overlap, making the peak assignment difficult. Temperature coefficients have been determined for the amide protons of asparagine in position 30, threonine in position 32, tyrosine in position 36 and *cis*-γ-amino acid **30** in position 31. They show positive values between 3.00 and 6.88 ppb/K, suggesting an equilibrium between hydrogen bonded (folded) and non-hydrogen bonded state (unfolded).[123]

The values are higher than in peptide **161**. In particular, the value for the amide proton of *cis*-γ-amino acid **30** in position 31 is almost 7 ppb/K, while it was 2.29 ppb/K in peptide **161**.
The correlation between CSD-NH values and the corresponding temperature coefficients was found to be > 99%. Thus likely to peptide **161**, peptide **162** could adopt an ordered conformation in the cooled state which unfolds upon warming (**Figure 54**).

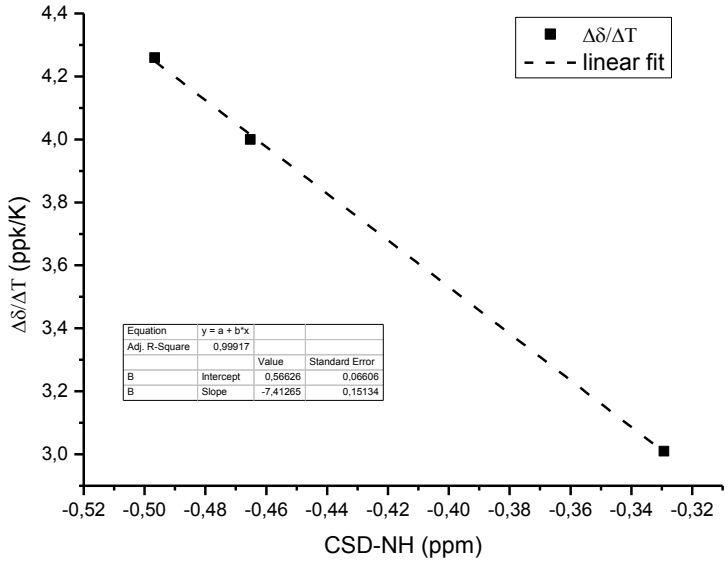

Figure 54. Correlation between temperature coefficients (Δδ/ΔT) and the NH shift deviation from the random coil expectation value (CSD-NH).

Deuterium/proton exchange experiment performed in pure deuterium oxide showed results very similar to those of peptide **161**, with the presence of the broad peaks around 8.21, 7.69 and 6.75 ppm (**Figure 55**).

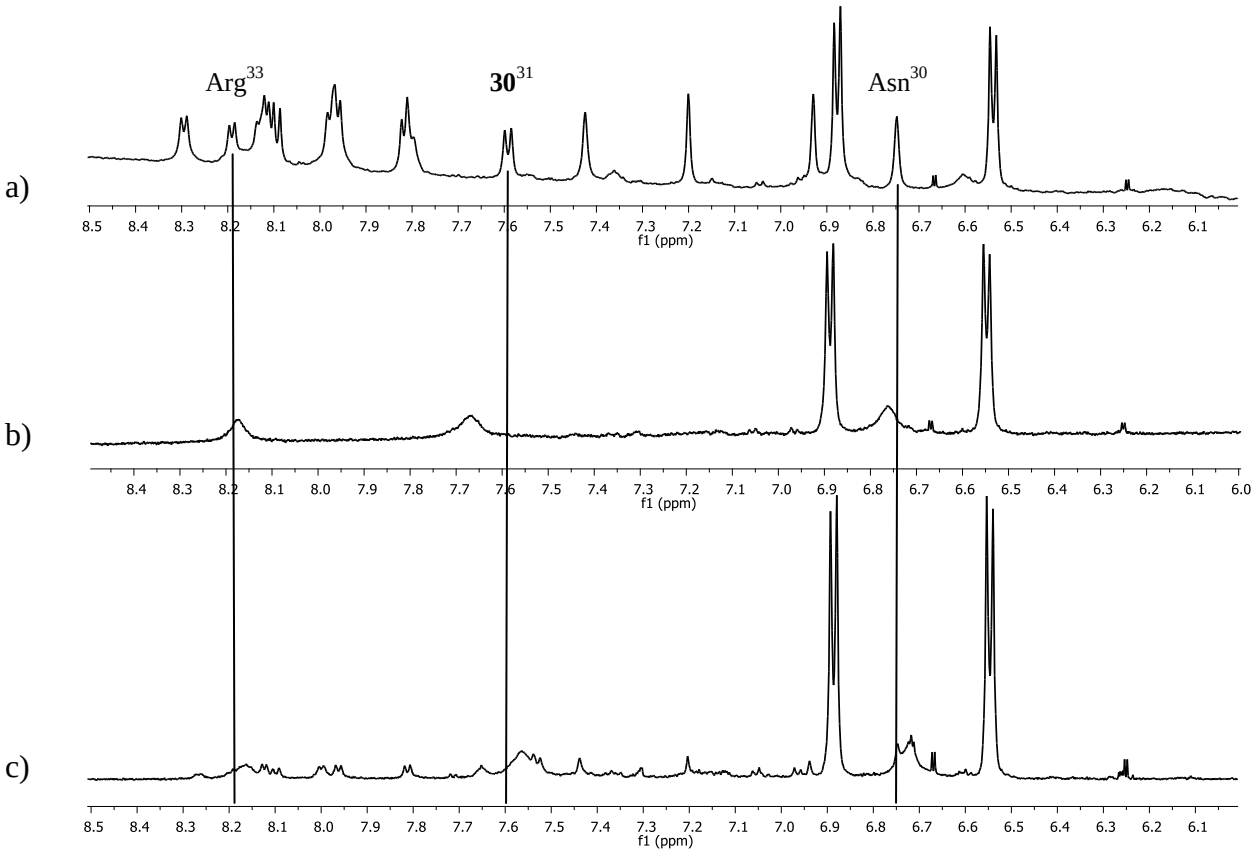

Figure 55. Deuterium proton exchange studies. a) NMR sample in H_2O/D_2O 9:1 prepared with the peptide obtained after HPLC purification and lyophilization; b) NMR sample in 100% D_2O, obtained after lyophilization from the first NMR sample; c) NMR sample in H_2O/D_2O 8:2, obtained after lyophilization from the NMR sample in 100% D_2O. (Vertical lines show the shifted signals).

Moreover, the spectrum obtained after repeated lyophilization is much less dispersed, suggesting also in this case aggregation of the peptide after freeze-drying. Further, coupling constants were calculated and showed values higher than 6 Hz, thus excluding a typical α-helix conformation (**Table 14**).

Protons	$^3J_{HN\alpha}$ *(Hz)*
HNα-Asn^{30}	7.0
*HNα-**30***^{31}	8.4
HNα-Arg^{33}	6.9
HNα-Tyr^{36}	8.1

Table 14. Vicinal coupling constants for H^N, H^α of peptide **162** in H_2O/D_2O (90:10).

It is interesting to note that the values of the coupling constants are very close to those of the same amino acids in peptide **161**, which could suggest a similar conformation in this region. For peptide **162** also the coupling constant of the C-terminal tyrosine could be determined, which is 8.1 Hz, thus indicating a β-strand- or turn-like conformation, as for the γ-amino acid **30** at position 31. Sequential and medium range proton-proton distances in peptide **162** are summarized in **tables 15**.

Contacts	*Distances (Å)*	$d_{\alpha N}$ *(i,i+1)*	$d_{\beta N}$ *(i,i+1)*	$d_{\gamma N}$ *(i,i+1)*	d_{NN} *(i,i+1)*	d_{NN} *(i,i+5)*	$d_{\beta\delta}$ *(i,i+1)*
Hα Ile^{29}-HN Asn^{30}	3.0	Medium					
HN **33**^{34}-Hα Arg^{35}	3.0	Medium					
Hα **33**^{28}-HN Ile^{29}	3.3	Medium					
Hα His^{27}-HN **33**^{28}	4.4	Weak					
Hα Asn^{30}-HN **30**^{31}	3.1	Medium					
Hα **30**^{31}-HN Thr^{32}	3.4	Weak					
Hα Arg^{35}-HN Tyr^{36}	3.1	Medium					
Hα Arg^{33}-HN **33**^{34}	3.2	Medium					
Hβ Ile^{29}-HN Asn^{30}	4.4		Weak				
Hβ Asn^{30}-HN **30**^{31}	4.4		Weak				
Hγ Ile^{29}-HN Ans^{30}	4.2			Weak			
Hγ Thr^{32}-HN Arg^{33}	4.7			Weak			
HN Asn^{30}-HN **30**^{31}	4.5				Weak		
HN Ile^{29}-HN Asn^{30}	4.0				Weak		
HN **30**^{31}-HN Thr^{32}	3.8				Weak		
HN Arg^{33}-HN **33**^{34}	3.9				Weak		
HN Asn^{30}-HN Arg^{35}	4.7					Weak	
Hδ Ile^{29}-Hβ Asn^{30}	4.3						Weak

Distances	*Ac-Arg^{26}-His^{27}-**33**^{28}-Ile^{29}-Asn^{30}-**30**^{31}-Thr^{32}-Arg^{33}-**33**^{34}-Arg^{35}-Tyr^{36}-NH$_2$*
$d_{\alpha N}$ (*i, i+1*)	
$d_{\beta N}$ (*i, i+1*)	
$d_{\gamma N}$ (*i, i+1*)	
d_{NN} (*i, i+1*)	
d_{NN} (*i, i+5*)	
$d_{\beta\gamma}$ (*i, i+1*)	

Table 15. All sequential and medium range proton-proton NOEs in peptide **162** (the different line thickness reflects the weak and medium NOE intensity).

ROESY analysis showed contacts (*i,i+1*) of medium and weak intensity, but also one contact (*i,i+5*) of weak intensity between Asn^{30} and Arg^{35}. By comparing the NOE contacts of the peptides **161** and **162**, it was noted that seven and five side-chain-to-backbone NOEs were found for peptides **161** and **162**, respectively. The NOEs γ^{29}-N^{30}, β^{30}-N^{31}, γ^{32}-N^{33} were common to both peptides, whereas the NOEs of peptide **161** involving γ^{29}-α^{30} and the residue pairs 32-34 and 35-36 were not found in peptide **162**. In contrast, in the latter peptide the NOEs β^{29}-N^{30} and δ^{29}-β^{30} were detected. Apparently, a slightly different spatial distribution of the side chains around positions 29 and 30 is present in the two peptides, which is attributed to the presence of the additional unnatural amino acid at position 28 in peptide **162**. However, it is interesting to note that there are also some differences in the C-terminal region, although the sequence is identical: indeed, the NOEs between the residue pairs 32-34 and 35-36 are present only in peptide **161**, while the long-range (*i,i+5*) NH-NH connectivity is present only in peptide **162.**

*2. 4. 2. Results on NPY analogues **163** and **164***

2. 4. 2. 1. CD studies

In NPY analogues **163** and **164**, only one unnatural amino acid has been introduced in position 34, which is the *trans*-pentacin **33** in peptide **163**, and *cis*-γ-amino acid **30** in peptide **164**. These compounds are more similar to NPY (25-36), and thus CD spectra of the NPY segment in different solvents can be used as reference. The CD spectra of compound **163** are shown in **figure 56**.

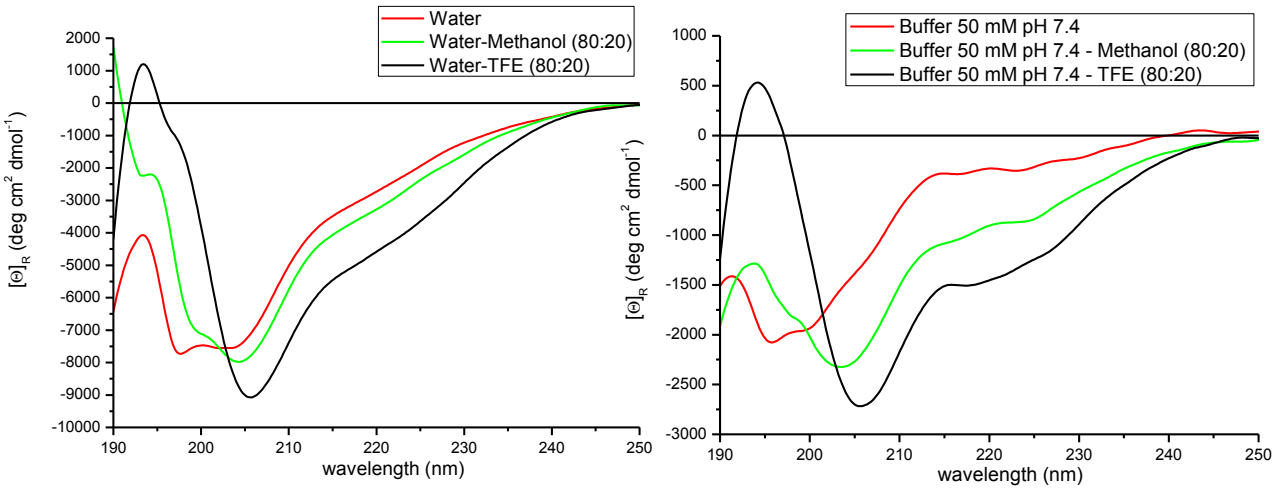

Figure 56. CD spectra of compound **163**. a) CD spectrum in water and in 20% of methanol and TFE in water; b) CD spectrum in phosphate buffer and in 20% of methanol and TFE in buffer.

The CD spectrum of peptide **163** in water displays two negative bands at 197 and 204 nm (panel a of **Figure 56**). In presence of organic solvents, the curves change significantly. In particular, in presence of methanol, the relative intensity of the two bands (which are slightly red-shifted) is modified from about 1:1 to >1 at the expenses of the band at 197 nm. In presence of TFE, the curve assumes a shape similar to that of a 3_{10} helical conformation, displaying a minimum at 206 nm with a negative shoulder at 220 nm, and a maximum at 195 nm. The curve of peptide **163** in buffer is similar to the curve shown in water, but it displays reduced intensity and blue-shift (panel b of **Figure 56**). The CD spectrum in buffer /methanol displays the same shape but minor intensity compared with that in water/methanol. This holds also for the buffer/TFE mixture.

Therefore, these results suggest that the conformation of peptide **163** is not affected by the pH; in water or buffer the peptide chain is highly flexible, however, upon addition of methanol or TFE, a helical structure is stabilized.

CD spectra of compound **163** have been compared with CD signature of NPY segment (25-36) as shown in **Figure 56**.

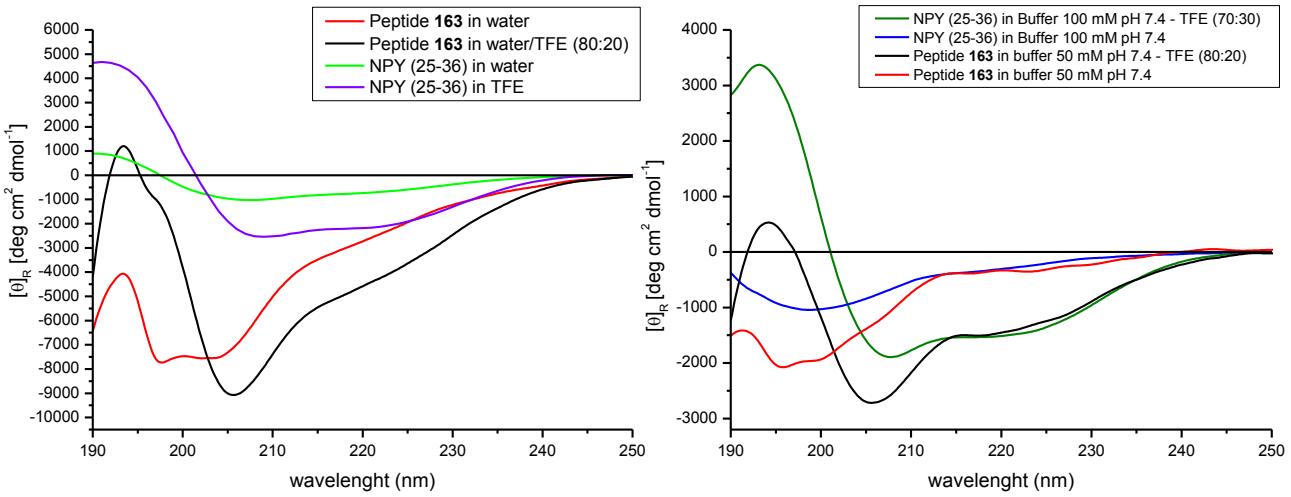

a) b)

Figure 57. CD spectra of peptide **163** in comparison with NPY segment (25-36).

It is interesting to see that the presence of the unnatural amino acid induces a different conformation to the NPY sequence: indeed, in the presence of TFE the native sequence is α-helical prone, whereas the peptide **163** is 3_{10}-helix-like. The CD spectra of compound **164** are shown in **figure 58**.

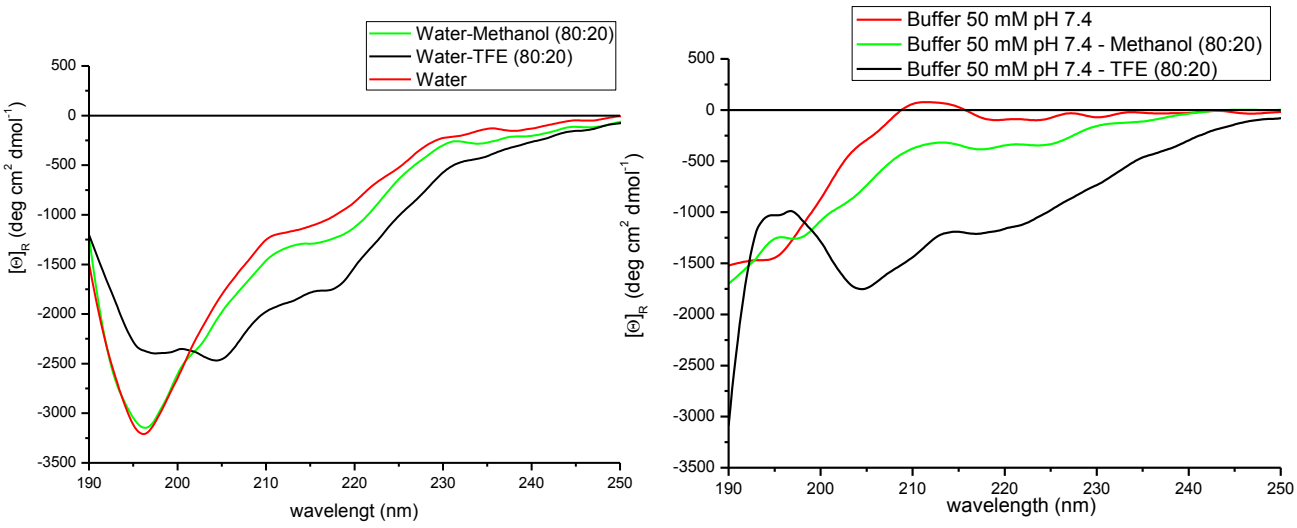

a) b)

Figure 58. CD spectra of compound **164**. a) CD spectrum in water and in 20% of methanol and TFE in water; b) CD spectrum in phosphate buffer and in 20% of methanol and TFE in buffer.

The conformational properties of peptide **164** are very different from those of the peptide **163**. Indeed, the minimum at 196 nm and a weak shoulder at 215 nm observed in water and water/methanol suggest a highly flexible structure. Also the weak CD intensity of the spectra in buffer and buffer/methanol are indicative of lack of ordered structure. In contrast, both in water/TFE and buffer/TFE mixtures the peptide is more ordered, as suggested by the negative CD bands at 218 nm and 205 nm. In water/TFE the minima are slightly blue-shifted and an additional minimum at 197 nm is detectable, probably reflecting the presence of a disordered fraction. The CD signature of peptide **164** has also been compared with the CD signature of the NPY segment (25-36) (**Figure 59**).

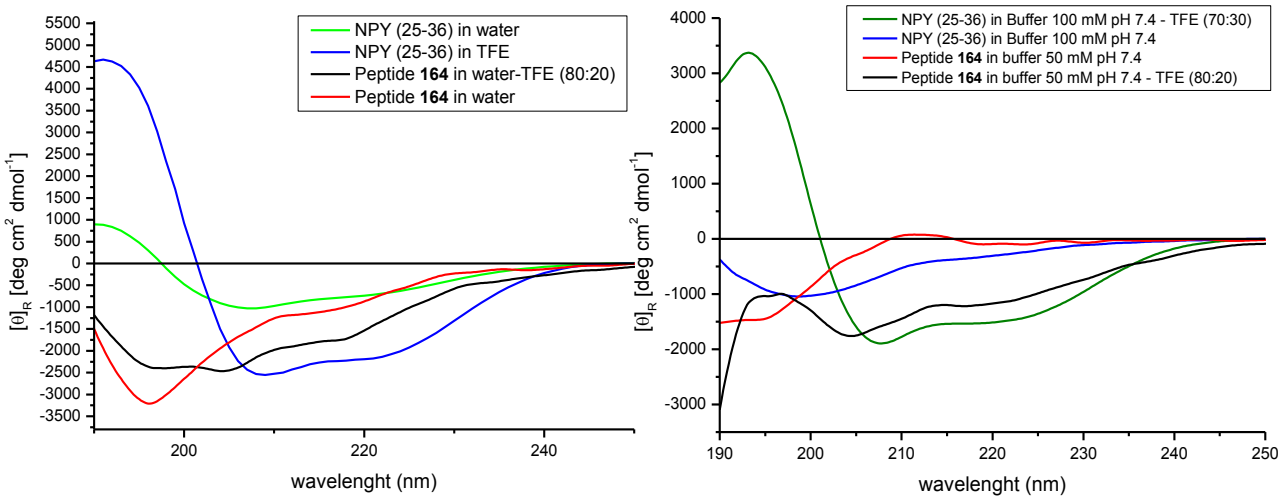

Figure 59. CD spectra of peptide **164** in comparison with NPY (25-36).

It is interesting to note that the CD spectra of the native sequence and of the peptide **164** in buffer/TFE are almost superimposable in the range 205-225 nm, suggesting a similar helical conformation. Peptide **163** and **164** were obtained in very less amount < 0.8 mg, thus not enough for NMR analysis.

*2. 4. 3. Results on NPY analogues **165** and **166***

2. 4. 3. 1. CD studies

NPY analogues **165** and **166** contain two substitutions, *trans*-pentacin **33** in position 34, and a *trans*-γ-amino acids in position 30. Peptide **165** contains the γ-amino acid **31**, while its enantiomer γ-amino acid **32** has been introduced in peptide **166**. Therefore, these analogues can be considered as α-β-γ foldamers. Accordingly, their CD spectra in water and water/organic solvent are reminiscent of those of the α-β-γ foldamer **161**, as shown in **figure 60**.

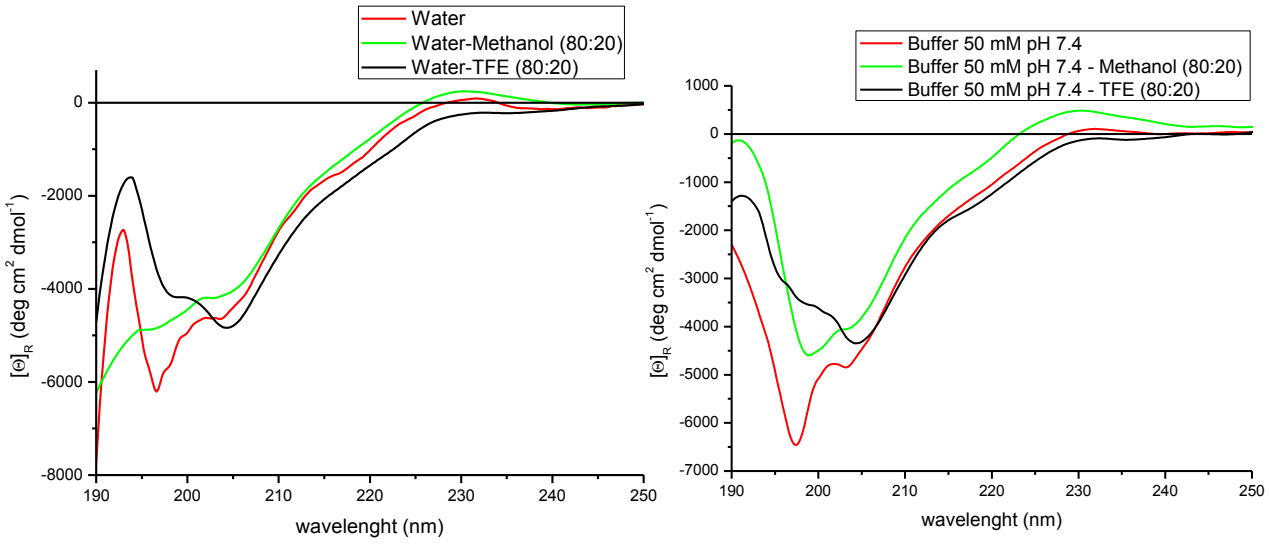

a) b)

Figure 60. CD spectra of compound **165**. a) CD spectrum in water and in 20% of methanol and TFE in water; b) CD spectrum in phosphate buffer and in 20% of methanol and TFE in buffer.

Interestingly, in the case of the peptide **165** there are no significant changes in the CD shape, going from acidic to slightly basic conditions in presence of methanol or TFE. This suggests that the combination of the two building blocks **33** and **31** induce a conformation that is pH-independent. Further, the CD spectra of compound **166** are given in **figure 61**.

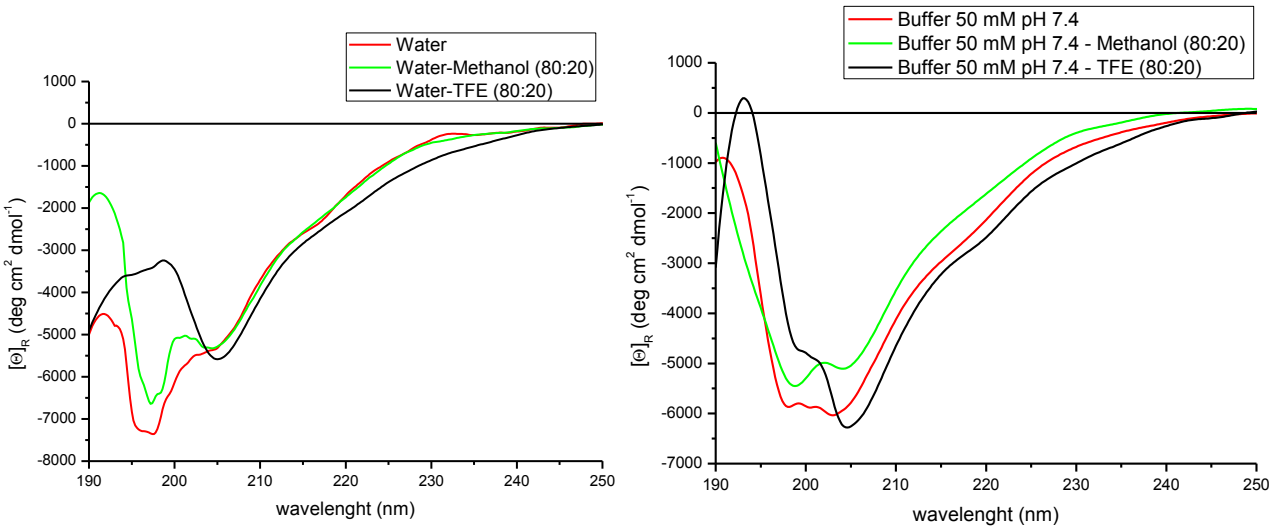

a) b)

Figure 61. CD spectra of compound **166**. a) CD spectrum in water and in 20% of methanol and TFE in water; b) CD spectrum in phosphate buffer and in 20% of methanol and TFE in buffer.

In water and water/organic solvent they are comparable to those of peptide **165**, suggesting that the presence of the enantiomer of the γ-amino acid does not induce a different conformation. However, it should be noted that in buffer and buffer/methanol the band at 197 nm is less intense than for peptide **165**, and that the CD curve in buffer/TFE has a more positive contribution below 200 nm than that of the peptide **165**, suggesting a more ordered structure for the peptide **165** in slightly basic conditions. It is also interesting to compare the curves of peptide **165** and **166**, with the curves of the peptide **161**, which has the *cis*-γ-amino acid **30** in position 30, and therefore we can see the effect of the configuration. **Figure 62** and **63** show the curves of peptide **165**, **166** and **161** in different solvents.

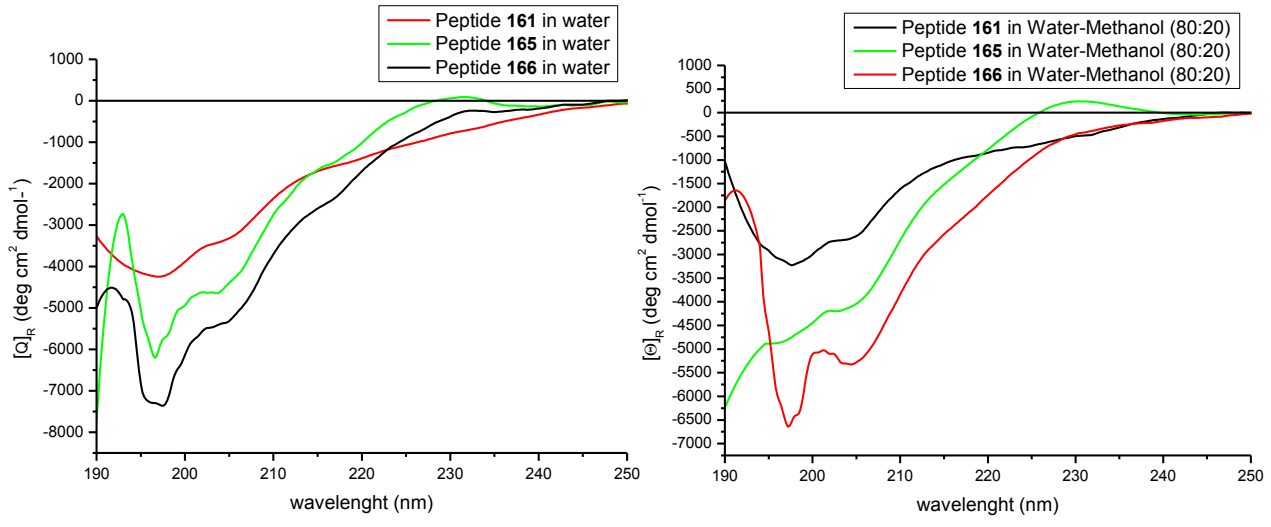

a) b)

Figure 62. CD spectra of peptide **165** and **166** in comparison with peptide **161** in water and water/20% methanol.

It appears clear that all three peptides are similar in water or water/methanol (**Figure 62**). In contrast, the peptides **165** and **166** seem to possess the highest helix propensity when dissolved in water/TFE or buffer/TFE (**Figure 63**, panels a and d). However, in the absence of any organic solvent the peptide **166** is probably more ordered than the peptide **165** at physiologic pH, as suggested by the relative intensity of the minima at 197 nm and 205 nm, which is about 1:1 for **166** and >1 at the expenses of the minimum at 205 nm for **165** (**Figure 63**, panel b).

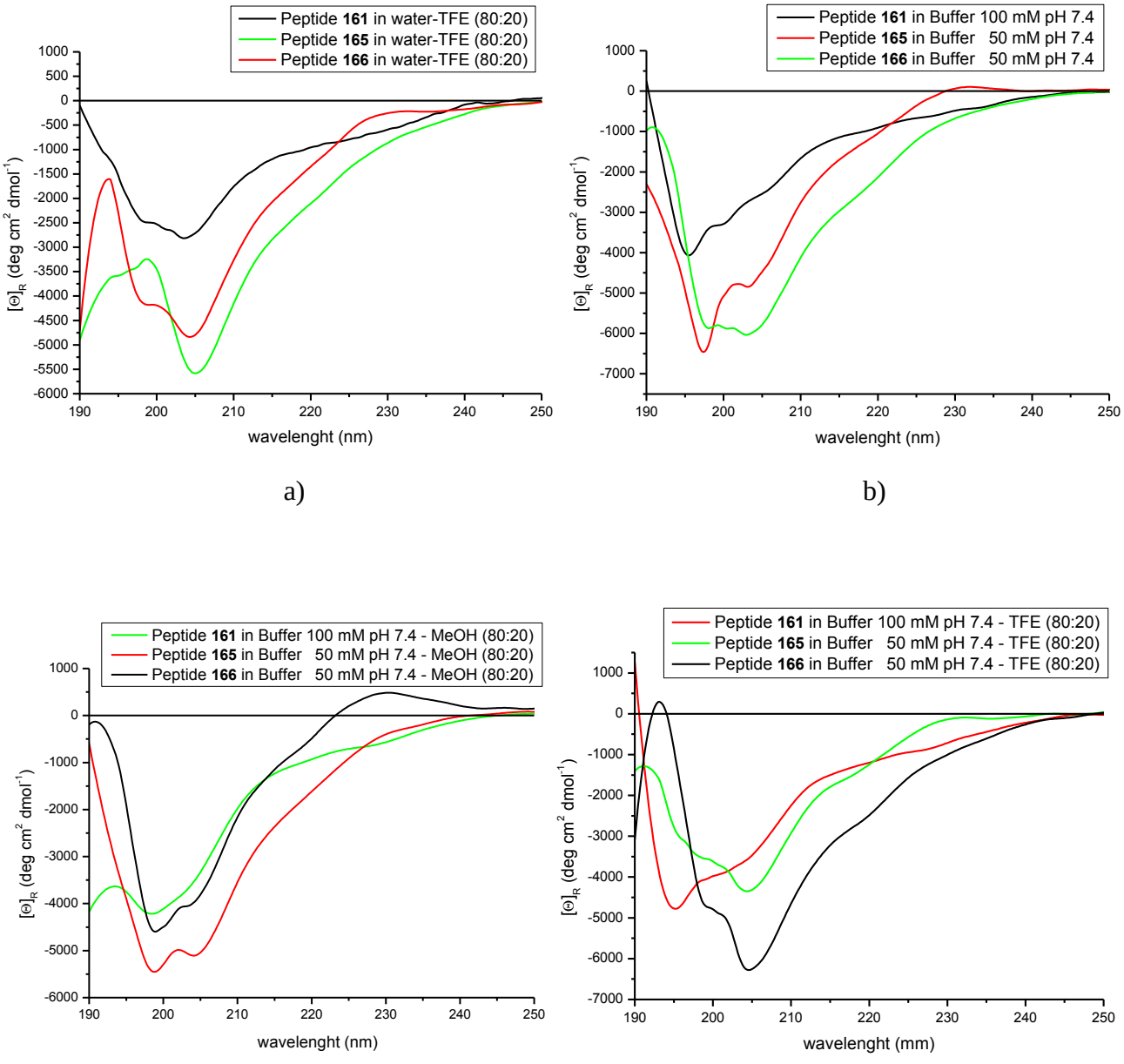

Figure 63. CD spectra of peptide **165** and **166** in comparison with peptide **161** in water/TFE, in phosphate buffer, and in 20% of methanol and TFE in buffer.

2. 4. 3. 2. NMR studies

Peptide **165** and **166** have also been investigated by NMR spectroscopy. In comparison with the peptides **161** and **162**, the NMR spectrum of peptide **165** showed better signals dispersion. The analysis at different temperatures showed the best dispersion at 313 K, which is a quite high temperature for a small peptide. This might indicate that the peptide aggregates at low temperatures or that an ensemble of differently stable conformations exists in equilibrium.

Due to the high temperature used to study the conformation, the peptide was not subjected to further heating for the determination of the temperature coefficients. Nevertheless, the 1D NMR spectra recorded from 283 K to 313 K were used to look at the correlation between the Δδ/ΔT and the CSD-NH values (**Table 16**), which in this case is expected to be small, due to the fact that the peptide in the cooled state (283 K) is less ordered than after warming (313 K). Indeed, the correlation was found to be only 17%, as shown in **Figure 64**, which confirms the presence of unordered structure and/or different conformers in the cooled state.

Temperature	*NH-His*^{27}	*NH-Tyr*^{28}	*NH-Ile*^{29}	*NH-Asn*^{30}	*NH-**31***^{31}	*NH-Arg*^{33}	*NH-**33***^{34}	*NH-Arg*^{35}	*NH-Tyr*^{36}
283.0 K	8.3143	n.d.	7.9724	n.d.	7.7306	8.1326	7.7839	8.0997	8.0997
288.0 K	8.3345	8.2162	7.9924	8.2162	7.7621	8.1551	7.8011	n.d.	n.d.
293.0 K	8.3529	n.d.	8.0098	n.d.	7.7913	8.1754	7.8163	n.d.	n.d.
298.0 K	8.3722	n.d.	8.0281	n.d.	n.d.	8.1963	n.d.	n.d.	n.d.
303.0 K	8.3894	8.2506	8.0442	8.2756	7.8501	8.2156	7.8501	8.1572	8.1828
313.0 K	8.4204	8.2726	8.0711	8.3085	7.8752	8.2487	7.9007	8.1803	8.2151
Δδ/ΔT (ppb/K)	3.53	2.25	3.29	3.69	4.82	3.87	3.89	2.68	3.84
CSD-NH (ppm)	-0.4757	-	-0.5476	-	-	-0.5574	-	-0.5903	-0.4903

Table 16. Temperature coefficients (Δδ/ΔT) and chemical shift deviations (based on the δ values at 283 K) for the NPY analogue **165**.

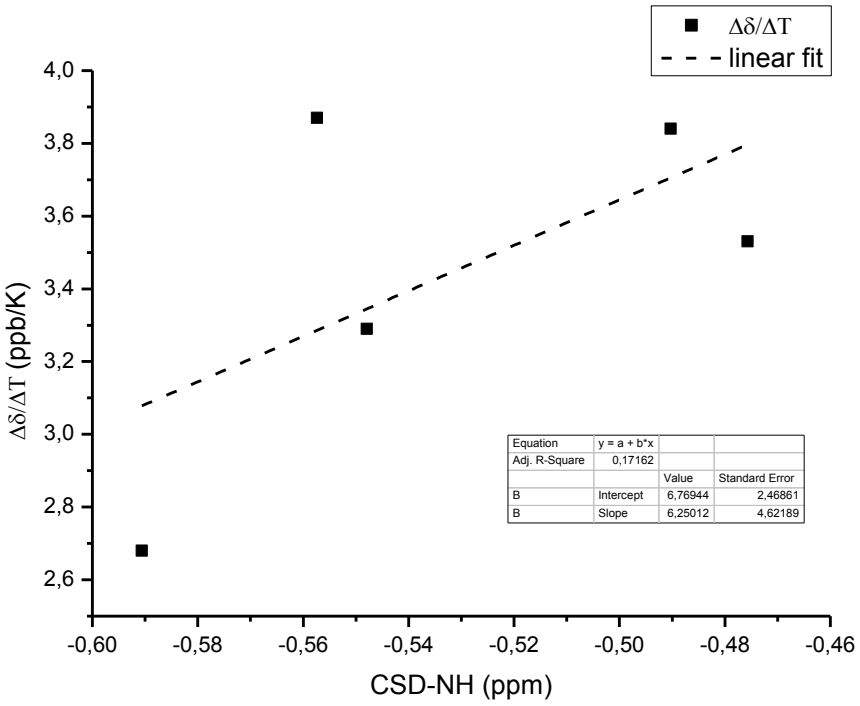

Figure 64. Correlation between temperature coefficients (Δδ/ΔT) and the NH shift deviation from the random coil expectation value (CSD-NH).

The deuterium/proton exchange experiment showed the presence of a broad signal at 8.14 ppm, similarly to the peptides **161** and **162**. But, contrary to the latter peptides, the 1D NMR spectrum of the re-lyophilized peptide **165** was comparable to that recorded before freeze-drying, the broad signal at 8.14 ppm in D_2O could belong to the amide proton of Thr^{32} (**Figure 65**).

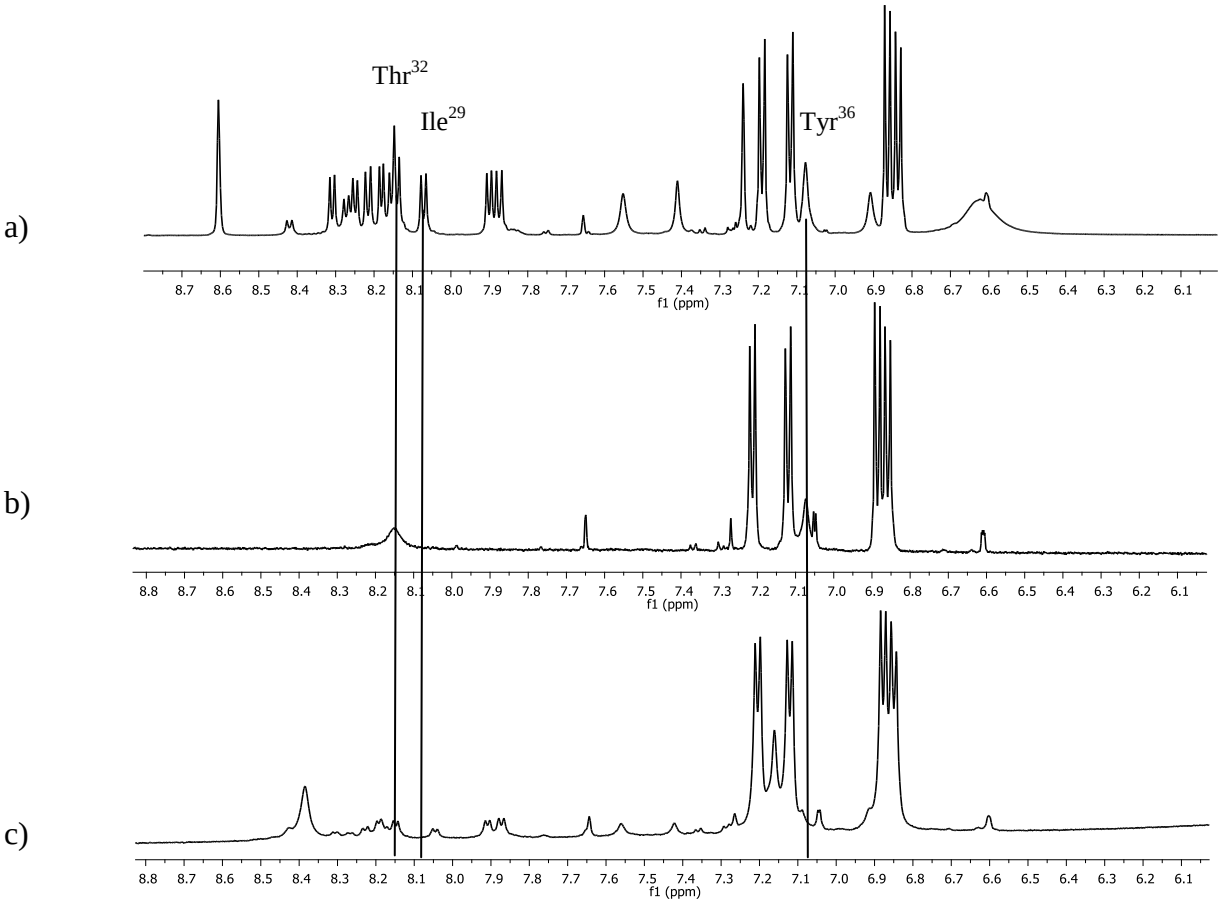

Figure 65. Deuterium proton exchange studies. a) NMR sample in H_2O/D_2O 9:1 prepared with the peptide obtained after HPLC purification and lyophilization; b) NMR sample in 100% D_2O, obtained after lyophilization from the first NMR sample; c) NMR sample in H_2O/D_2O 8:2, obtained after lyophilization from the NMR sample in 100% D_2O. (Vertical lines show the shifted signals).

The coupling constants showed values higher than 6 Hz, thus excluding a typical α-helix structure (**Table 17**). The values of 8.0 Hz for Tyr^{36} and 8.2 Hz for **33**^{34} suggest possible β-strand- or turn-like conformations for these two residues.

Protons	$^{3}J_{HN\alpha}$ *(Hz)*
HNα-His^{26}	7.8
HNα-Tyr^{28}	7.4
HNα-Ile^{29}	7.7
HNα-Asn^{30}	7.2
*HNα-**31***^{31}	7.2
HNα-Arg^{33}	7.3
*HNα-**33***^{34}	8.2
HNα-Arg^{35}	6.1
HNα-Tyr^{36}	8.0

Table 17. Vicinal coupling constants for H^N, H^α of peptide **165** in H_2O/D_2O (90:10).

ROESY studies on peptide **165** showed contacts (*i,i+1*) of medium and weak intensity. Additionally two contacts $d_{\alpha\gamma}$ (*i, i+2*) involving the pairs 29-31 and 32-34 were observed, as for peptide **161**. (**Table 18**).

Contacts	*Distances (Å)*	$d_{\alpha N}$ *(i,i+1)*	$d_{\beta N}$ *(i,i+1)*	$d_{\gamma N}$ *(i,i+1)*	d_{NN} *(i,i+1)*	$d_{\alpha\gamma}$ *(i,i+2)*	$d_{\delta N}$ *(i,i+1)*	$d_{\varepsilon N}$ *(i,i+1)*
Hα **31**^{31}-HN Thr^{32}	3.6	Weak						
Hα Asn^{30}-HN **31**^{31}	3.5	Weak						
Hα Ile^{29}-HN Asn^{30}	2.9	Medium						
Hα Tyr^{28}-HN Ile^{29}	3.8	Weak						
Hα Thr^{32}-HN Arg^{33}	4.3	Weak						
Hα Arg^{33}-HN **33**^{34}	4.2	Weak						
Hα **33**^{34}-HN Arg^{35}	2.9	Medium						
Hα Arg^{26}-HN His^{27}	3.2	Medium						
Hβ Asn^{30}-HN **31**^{31}	4.3		Weak					
Hβ Arg^{33}-HN **33**^{34}	4.7		Weak					
Hβ Ile^{29}-HN Asn^{30}	4.2		Weak					
Hβ Tyr^{28}-HN Ile^{29}	4.1		Weak					
Hβ His^{27}-HN Tyr^{28}	4.4		Weak					
Hγ Ile^{29}-HN Asn^{30}	4.1			Weak				
HN Asn^{30}-HN **31**^{31}	4.4				Weak			
HN Arg^{33}-HN **33**^{34}	4.2				Weak			
Hγ Thr^{32}-Hα **33**^{34}	4.4					Weak		
Hγ Ile^{29}-Hα **31**^{31}	4.4					Weak		
Hδ **31**^{31}-HN Thr^{32}	4.2						Weak	
Hε Tyr^{28}-HN Ile^{29}	4.2							Weak

Distances	*Ac-Arg^{26}-His^{27}-Tyr^{28}-Ile^{29}-Asn^{30}-**31**^{31}-Thr^{32}-Arg^{33}-**33**^{34}-Arg^{35}-Tyr^{36}-NH$_2$*
$d_{\alpha N}$ (*i, i+1*)	
$d_{\beta N}$ (*i, i+1*)	
$d_{\gamma N}$ (*i, i+1*)	
d_{NN} (*i, i+1*)	
$d_{\alpha\gamma}$ (*i, i+2*)	
$d_{\delta N}$ (*i, i+1*)	
$d_{\varepsilon N}$ (*i, i+1*)	

Table 18. All sequential and medium range proton-proton NOEs in peptide **165** (the different line thickness reflects the weak and medium NOE intensity).

ROESY analysis showed that most contacts $d_{\alpha N}$ (*i,i+1*) are of weak intensity within the segment 28-34, which suggests that the backbone structure is more flexible than in peptides **161** and **162**, where the contacts $d_{\alpha N}$ (*i,i+1*) are mainly of medium intensity.

Moreover, fewer contacts between amide protons d_{NN} (i, i+1), but more contacts $d_{\beta N}$ (*i,i+1*) of weak intensity within the segment 27-31 were detected, suggesting a different conformation in this region. This is supported by the presence of one contacts (*i,i+2*) between Ile^{29} and **31**^{31}, which was absent in peptide **161**. Also NOEs such as $d_{\delta N}$ and $d_{\varepsilon N}$ (*i,i+1*) were found for peptide **165**, which were not detected in the ROESY spectra of peptides **161** and **162**.

1D NMR analysis of peptide **166** at different temperatures showed good dispersion of signals at 313 K, thus this temperature was used to record 2D experiments. As already discussed for peptide **165**, also peptide **166** was not subjected to warming for the calculation of the temperature coefficients. However, a correlation between the CSD-NHs for the cooled state at 283 K and the corresponding $\Delta\delta/\Delta T$ values obtained upon heating up to 313 K (**Table 19**) was determined. Likely to peptide **165**, also in this case the correlation was very poor (about 37%), as shown in **Figure 66**.

Temperature	*NH-Ile*[29]	*NH-Asn*[30]	*NH-**32***[31]	*NH-Thr*[32]	*NH-Arg*[33]	*NH-**33***[34]
283.0 K	7.9023	8.2125	7.7378	n.d.	8.1812	7.7836
288.0 K	7.9194	8.2287	7.7468	n.d.	8.1939	7.8046
293.0 K	7.9367	8.2445	7.7582	n.d.	8.2073	7.8267
298.0 K	7.9567	8.2619	7.7699	8.1096	8.2216	7.8506
303.0 K	7.9717	8.2744	7.7801	8.1214	8.2333	7.8711
313.0 K	8.0022	8.3034	7.8033	8.1492	8.2586	7.9121
Δδ/ΔT ppb	3.33	3.03	2.18	2.64	4.07	4.28
CSD-NH (ppm)	-0.6177	-0.5475	-	-	-0.5088	-

Table 19. Temperature coefficients (Δδ/ΔT) and chemical shift deviation for the NPY analogue **166**.

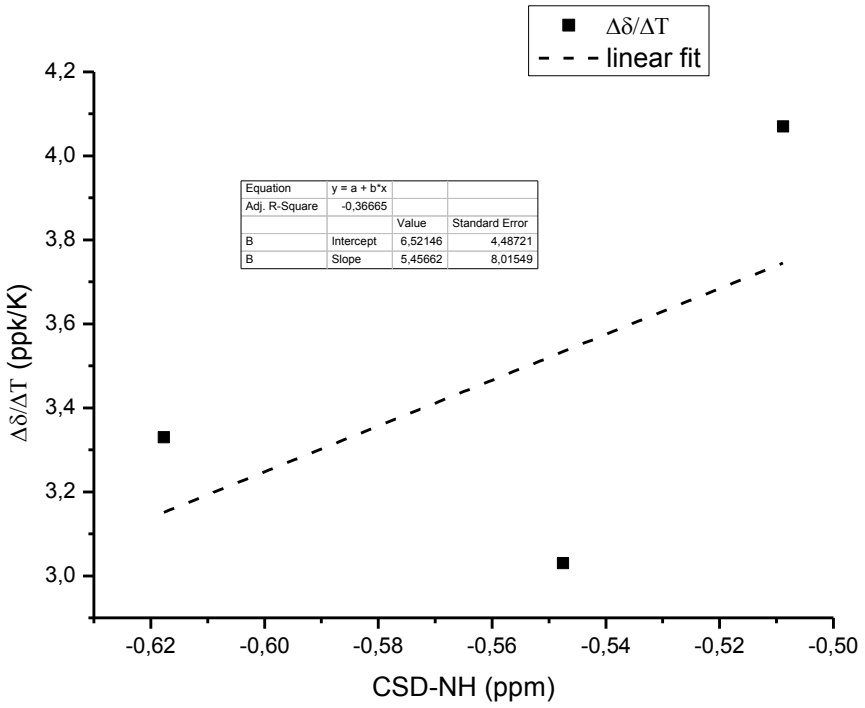

Figure 66. Correlation between temperature coefficients (Δδ/ΔT) and the NH shift deviation from the random coil expectation value (CSD-NH).

In deuterium/proton exchange experiment performed in pure deuterium oxide the peptide **166** showed a very broad peak over the region 8.1-8.4 ppm and centered at 8.2 (**Figure 67**). The 1D NMR spectrum recorded after lyophilization of the sample in pure D_2O was not identical to that of the sample in water: in particular, the signals dispersion was still very good and with sharp signals, but some signals were shifted and/or new ones appeared. Therefore, the peptide **166** clearly changed its conformation upon lyophilization, as already observed for peptides **161** and **162**. However contrarily to the latter, peptide **166** did not show any tendency to aggregate, similarly to peptide **165**.

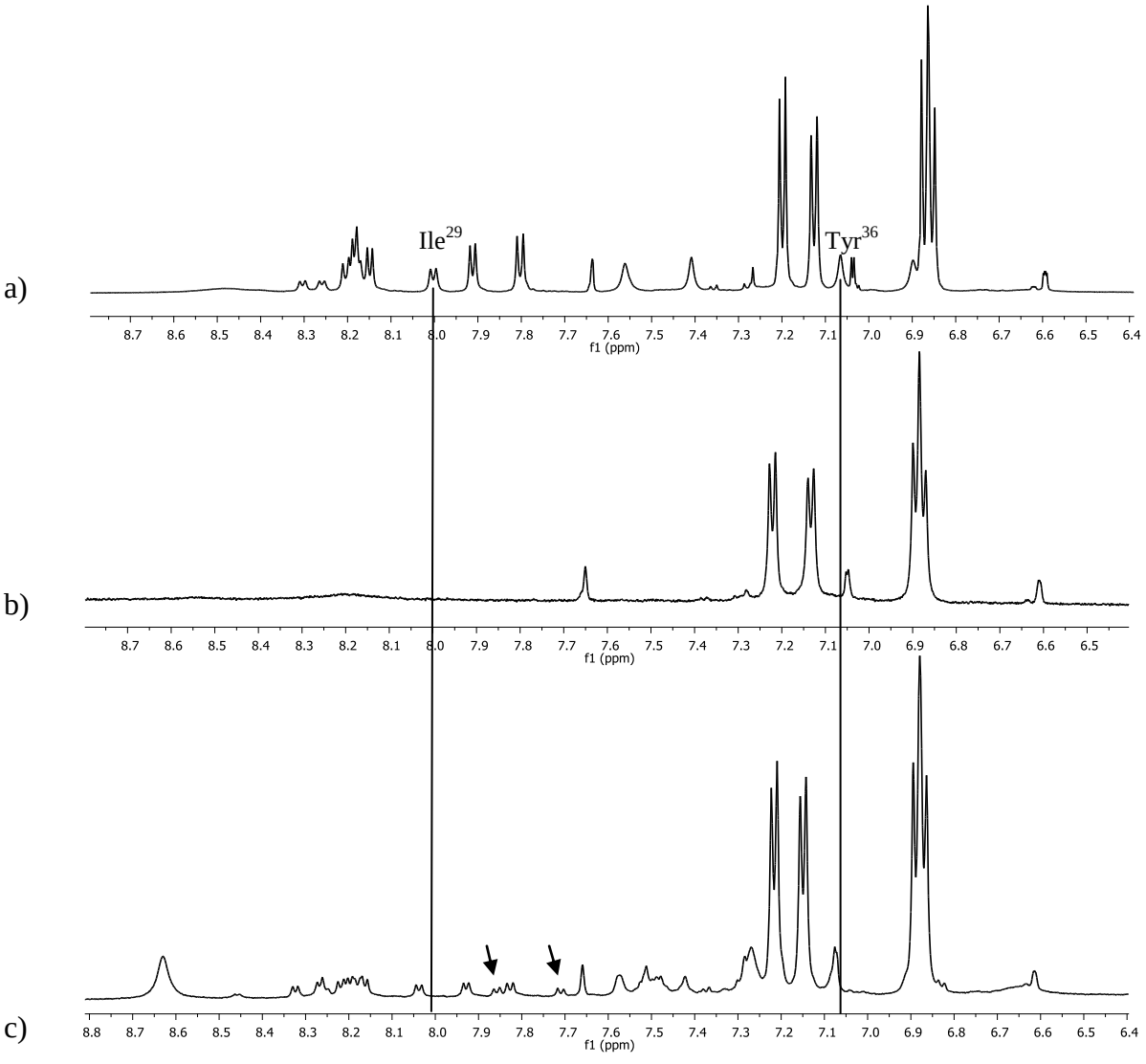

Figure 67. Deuterium proton exchange studies. a) NMR sample in H_2O/D_2O 9:1 prepared with the peptide obtained after HPLC purification and lyophilization; b) NMR sample in 100% D_2O, obtained after lyophilization from the first NMR sample; c) NMR sample in H_2O/D_2O 8:2, obtained after lyophilization from the NMR sample in 100% D_2O. (Vertical lines show the shifted signals; the arrows indicate new signals).

The coupling constants of this peptide are higher than 6 Hz, and, as for the peptides **161** and **162**, furthermore the coupling constant for *trans*-γ-amino acid **32** at the position 31 was again >8 Hz, suggesting a β-strand- or turn-like conformation (**Table 20**).

Protons	$^{3}J_{HN\alpha}$ *(Hz)*
HNα-Ile^{28}	7.6
HNα-Asn^{30}	7.5
*HNα-**33***^{31}	8.4
HNα-Thr^{32}	6.8
HNα-Arg^{33}	6.9
HNα-**33**^{34}	7.2

Table 20. Vicinal coupling constants for H^N, H^α of peptide **166** in H_2O/D_2O (90:10).

ROESY analysis showed contacts (*i,i+1*) of medium and weak intensity, and one contact (*i,i+2*) of weak intensity, involving positions 29 and 31 (**Table 21**).

Contacts	*Distances (Å)*	$d_{\alpha N}$ *(i,i+1)*	$d_{\beta N}$ *(i,i+1)*	d_{NN} *(i,i+1)*	$d_{\gamma N}$ *(i,i+1)*	$d_{\gamma N}$ *(i,i+2)*	$d_{\delta N}$ *(i,i+1)*
Hα Ile^{29}-HN Asn^{30}	3.4	Medium					
Hα **33**^{34}-HN Arg^{35}	3.0	Medium					
Hα **32**^{31}-HN Thr^{32}	3.8	Medium					
Hα Arg^{33}-HN **33**^{34}	4.0	Weak					
Hα Asn^{30}-HN **32**^{31}	3.9	Medium					
Hα Tyr^{28}-HN Ile^{29}	4.2	Weak					
Hβ Ile^{29}-HN Asn^{30}	4.5		Weak				
Hβ Tyr^{28}-HN Ile^{29}	4.3		Weak				
Hβ Asn^{30}-HN **32**^{31}	4.3		Weak				
Hβ Arg^{33}-HN **33**^{34}	4.6		Weak				
HN Asn^{30}-HN **32**^{31}	4.5			Weak			
HN Arg^{33}-HN **33**^{34}	4.2			Weak			
Hγ Ile^{29}-HN Asn^{30}	4.7				Weak		
Hγ **32**^{30}-HN Thr^{31}	4.8				Weak		
Hγ Ile^{29}-HN **32**^{31}	4.8					Weak	
Hδ **32**^{31}-HN Thr^{32}	4.6						Weak
Hδ Tyr^{28}-HN Ile^{29}	4.8						Weak

Distances	*Ac-Arg^{26}-His^{27}-Tyr^{28}-Ile^{29}-Asn^{30}-**32^{31}**-Thr^{32}-Arg^{33}-**33^{34}**-Arg^{35}-Tyr^{36}-NH$_2$*
$d_{\alpha N}$ (*i, i+1*)	
$d_{\beta N}$ (*i, i+1*)	
d_{NN} (*i, i+1*)	
$d_{\gamma N}$ (*i, i+1*)	
$d_{\gamma N}$ (*i, i+2*)	
$d_{\delta N}$ (*i, i+1*)	

Table 21. All sequential and medium range proton-proton NOEs in peptide **166** (the different line thickness reflects the weak and medium NOE intensity).

The presence of contacts $d_{\alpha N}$ (*i,i+1*) of medium intensity suggests a more ordered structure than peptide **165**. However, the same contacts $d_{\beta N}$ (*i,i+1*) were found within the segment 28-31, suggesting structural similarities between the two peptides. Therefore, the presence of the different enantiomer of the *trans*-γ-amino acid at position 31 does not induce a different conformation.

*2. 4. 4. Results on NPY analogues **167** and **168***

2. 4. 4. 1. CD studies

In the NPY analogues **167** and **168**, only one unnatural amino acid has been introduced in position 34, the (*1R,2S*)-configured *trans*-γ-amino acid **32** in peptide **167**, while its enantiomer *trans*-γ-amino acid **31** in peptide **168**. CD spectra of crude peptides were measured in water and in 20% methanol or TFE in water. As for the monosubstituted NPY analogues **163** and **164**, the CD spectra of the NPY segment (25-36) in different solvents can be used as reference for these peptides. The CD spectra of compounds **167** and **168** are shown in **figure 68**.

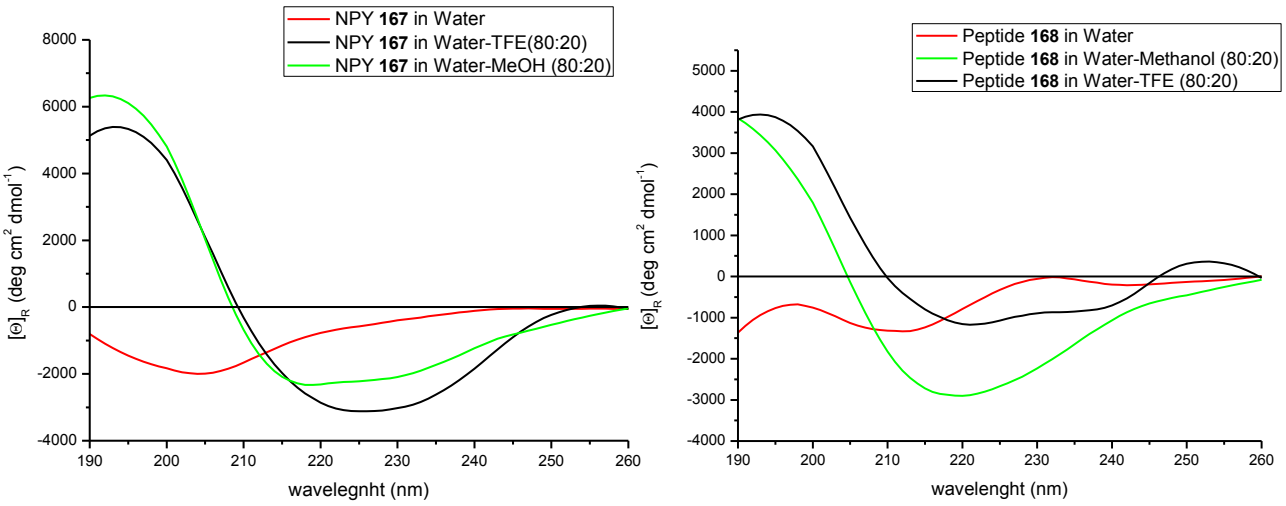

a) b)

Figure 68. CD spectra of compounds **167** (a) and **168** (b) in water and in 20% methanol or TFE in water. (These spectra were recorded at the Ruhr-University of Bochum).

Both peptides show a low-intensity spectrum in water, which is characterized by a negative band at 210 nm for peptide **168**, and a blue-shifted one for peptide **167** (205 nm). One negative contribution around 210-215 nm has been previously found for the monosubstituted NPY analogue **164** that contains the *(1S,2S)*-configured *cis*-γ-amino acid **30** at position 34. However, the latter displayed an additional predominant minimum at 195 nm, which would suggest that peptide **164** was more disordered than peptide **168** in water. In contrast, a negative CD contribution at 205 nm was found, other than for peptide **167**, also for peptides **161**, **162**, **163**, **165** and **166**: however, the latter analogues showed an additional minimum around 195 nm, which would suggest that they were more disordered than peptide **167** in water. In fact, the water CD spectrum of peptide **167** reminds that of a 3_{10}-helix, whereas only the TFE CD spectra of the other peptides do it, confirming the superior folding propensity of peptide **167** versus the others.

In 20% MeOH, the curves of both peptides assume a shape similar to that of β-turn type II, displaying a maximum at 195 nm and a minimum close to at 220 nm (the additional shoulder at 230 nm for peptide 168 might be due to the aromatic residues).[124]

In presence of TFE, the CD signature of peptide **167** is similar to that in methanol, but the minimum is red-shifted to 225 nm and becomes more intense, suggesting a superior structure-stabilizing effect of TFE over MeOH. In contrast, the curve of the peptide **168** in TFE shows a reduced intensity of the minimum at 220 nm. Moreover, an exciton splitting at 235 nm (neg.) and 250 nm (pos.) is detected, which should be attributed to the two tyrosine side chains. The CD spectra of peptides **167** and **168** have been compared with the CD signature of the NPY segment (25-36), as shown in **figure 69**.

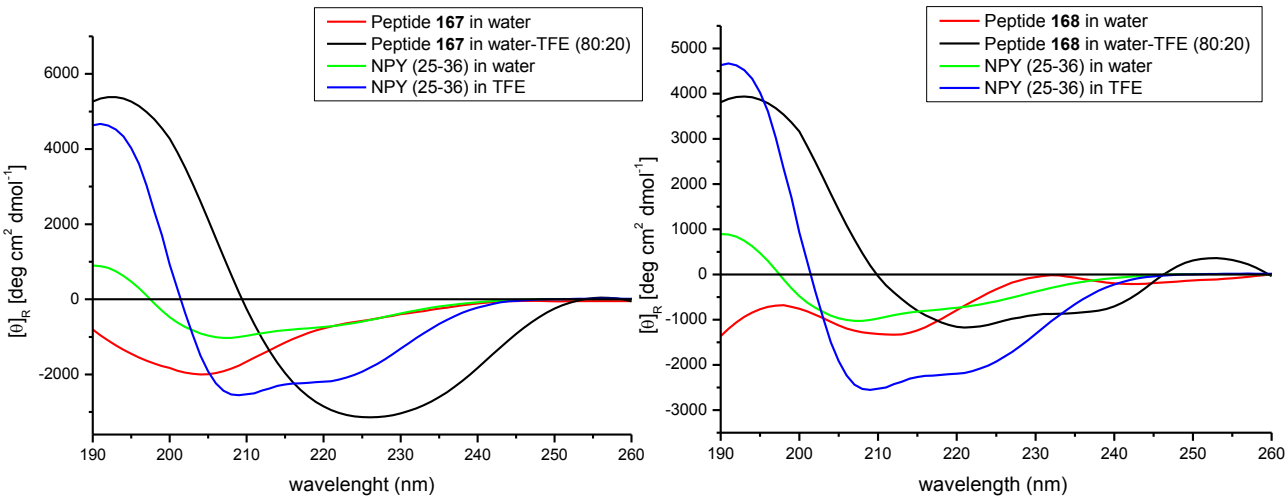

Figure 69. CD spectra of peptides **167** and **168** in comparison with NPY (25-36).

The presence of the *trans*-isomer in position 34 induces a different conformation to the NPY sequence: indeed, in TFE the native sequence is α-helical, whereas the peptides **167** and **168** are likely to build a turn. However, peptide **167** and the NPY segment have similar spectra in water, both reminiscent of a 3_{10}-helix, although the band at 205 nm of peptide **167** is more negative, probably because of higher content of disordered structure. As mentioned above, peptides **164** and **168** present both a CD contribution around 210-215 nm, but peptide **164** is apparently less ordered than peptide **168**, as indicated by the band at 195 nm (**Figure 70**, panel a). Instead, peptide **167** displays a minimum at 205 nm.

This suggests that the γ-amino acid at position 34 can induce different conformations, depending on the configuration of the cyclopentane ring. This is true not only in water, but also in the presence of MeOH or TFE (**Figure 70**, panels b and c). NMR studies are currently ongoing in the Reiser group.

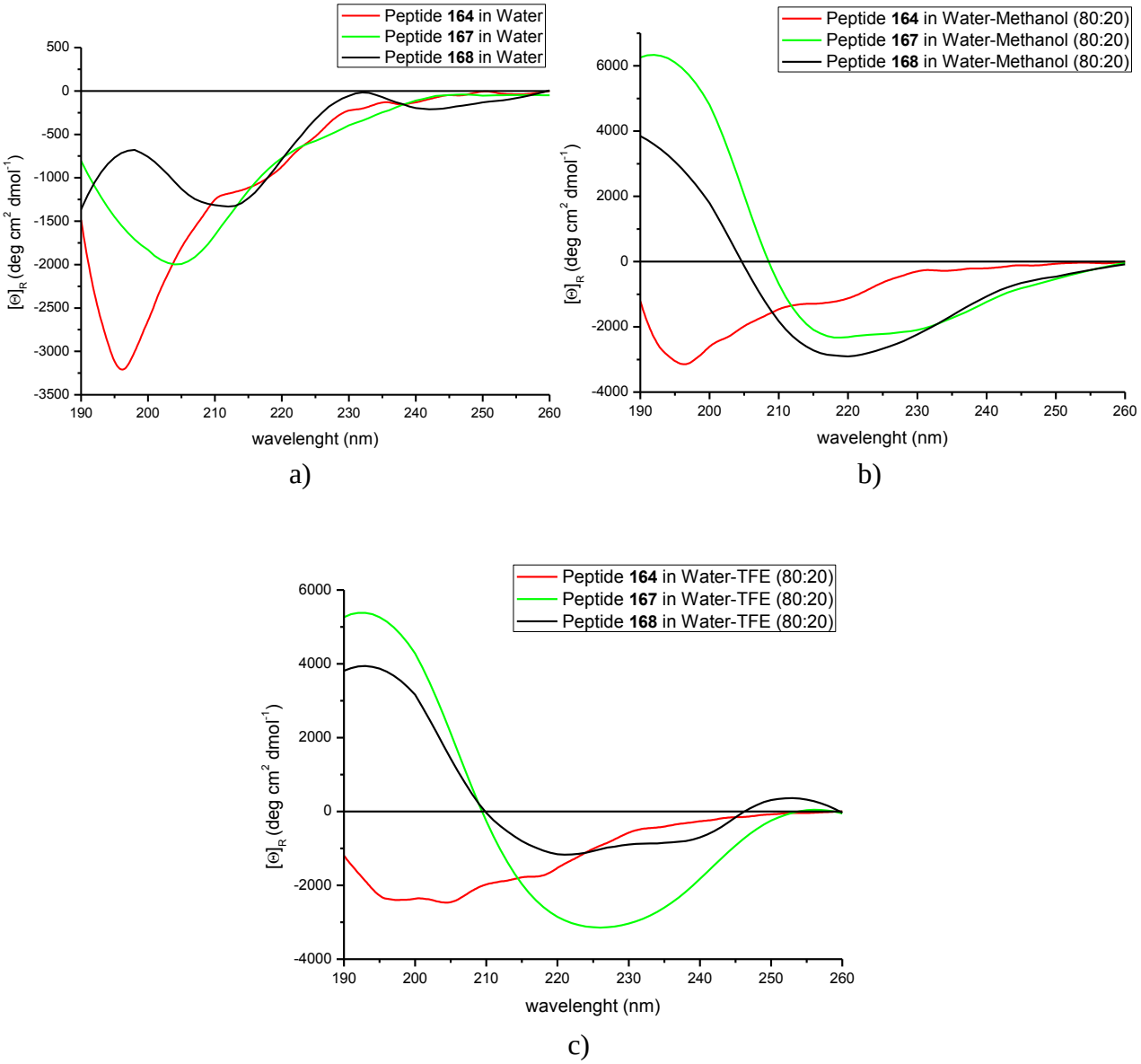

Figure 70. CD spectra of peptides **167** and **168** in comparison to peptide **164**.

Summary

In this work conformationally constrained γ-amino acids in which the backbone is constrained by a five-membered ring have been prepared and utilized as building blocks in the design of NPY analogues. Stereoisomers **130**, **143** and **153** of 2-(2-Fmoc-amino cyclopentyl) acetic acid were synthesized in enantiomerically pure form (**Figure 71**).

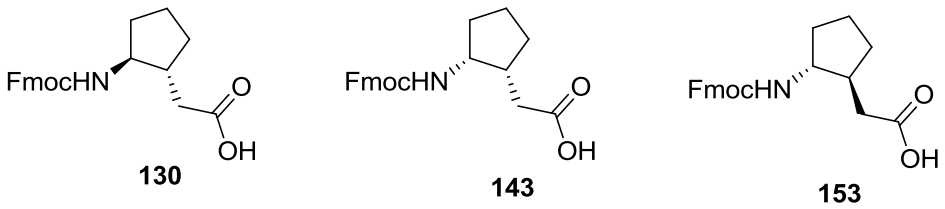

Figure 71. Isomers of the 2-(2-amino cyclopentyl) acetic acid

γ-Amino acid 1**30** has been prepared by an *Arndt-Eistert* homologation of enantiomerically pure *trans*-Fmoc-pentacin **132** as described by *Gellman et al.* (**Scheme 30**).[43]

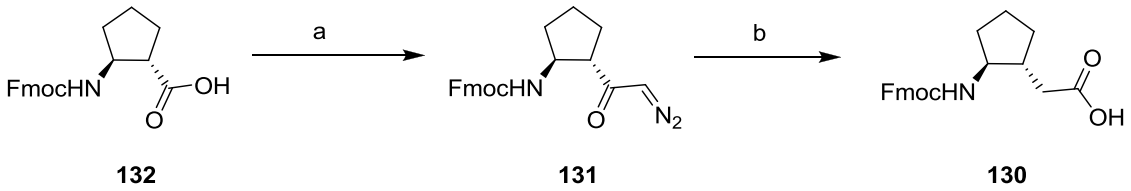

Scheme 30. Synthesis of 2-((*1R,2S*)-2-Fmoc-aminocyclopentyl) acetic acid **132**.
Reagents and conditions: a) 1. IBCF/*N*-methylmorpholine, THF, -15 °C; 2. CH_2N_2, 0 °C, 4 h, 72%; b) cat. $PhCO_2Ag$, ultrasounds, dioxane/H_2O, 1 h, 35%.

Trans-(**153**) and *cis*-(**143**) isomers have been synthesized by modifications of the hydrochloride salts of *trans*- and *cis*-ethyl 2-((*R*)-1-phenylethylamino)cyclopentyl)acetate (**150** and **151**), obtained by selective reduction of imine mixture **140** (**Scheme 31**).

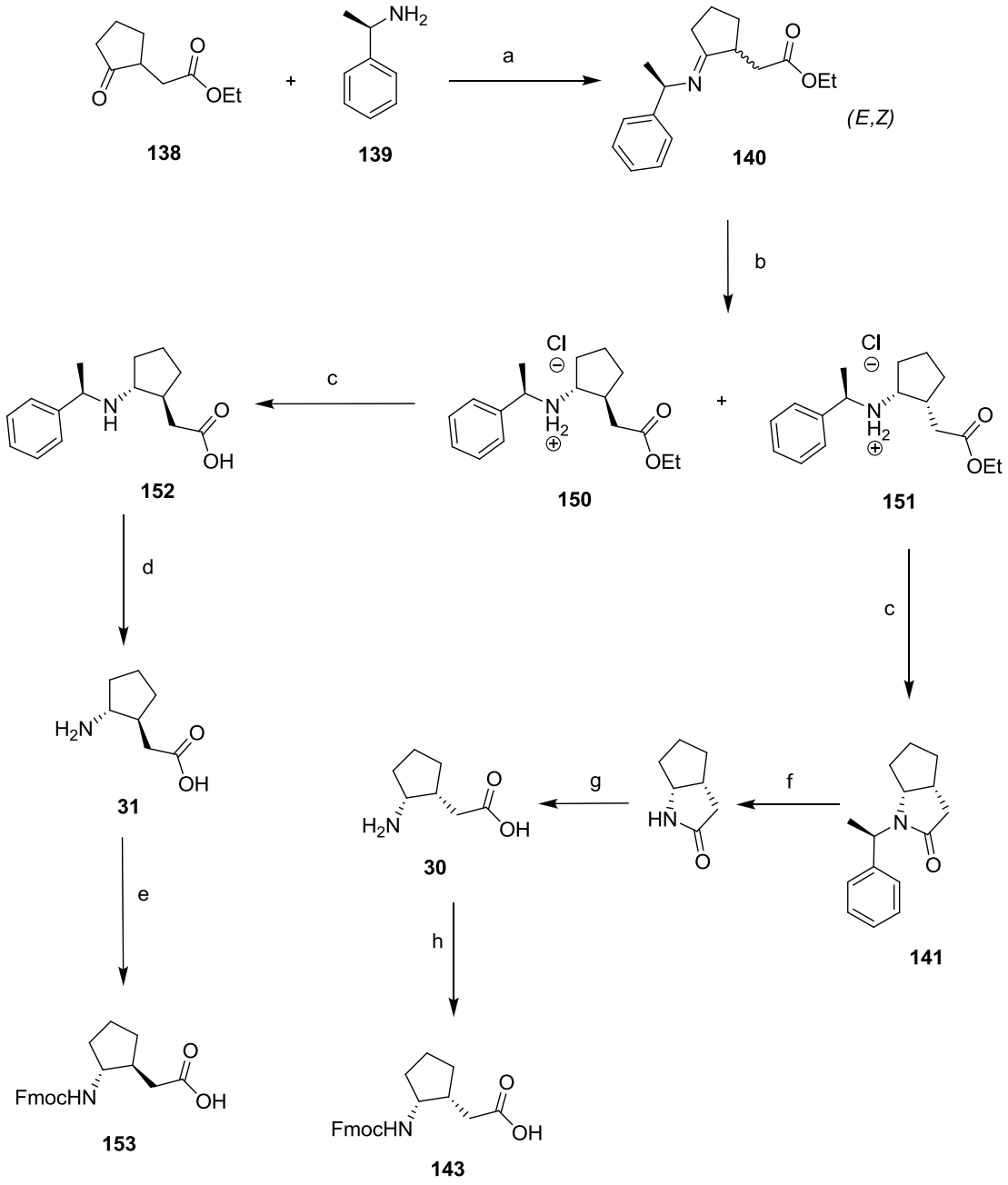

Schema 32. Synthesis of Fmoc-protected *cis*-(**143**) and *trans*-(**153**) 2-(2-amino cyclopentyl) acetic acid. Reagents and conditions: a) Benzene (abs.), reflux, 6 h, 78%; b) 1. $NaBH_4$, EtOH, 0 °C, 1 h; 2. HCl, recrystallization, 55%; c) LiOH, THF/MEOH/H_2O, 9 h, 0 °C, quant.; d) H_2 (50 bar), 10 % Pd/C, 50 °C, EtOH, 48 h, 85%; e) Fmoc-OSu, $NaHCO_3$, Acetone/H_2O 1:1, 18 h, 70%; f) Li/NH_3, -78 °C, THF/*t*BuOH, overnight, 73% ; g) 1 N HCl, 80 °C, 8 h, 52%; h) Fmoc-OSu, $NaHCO_3$, Acetone/H_2O 1:1, 18 h, 72%.

NPY analogues containing isomers of the 2-(2-amino cyclopentyl) acetic acid and in combination with *trans*-pentacin **33** have been prepared by solid phase synthesis and investigated by CD- and NMR spectroscopy (**Figure 72**).

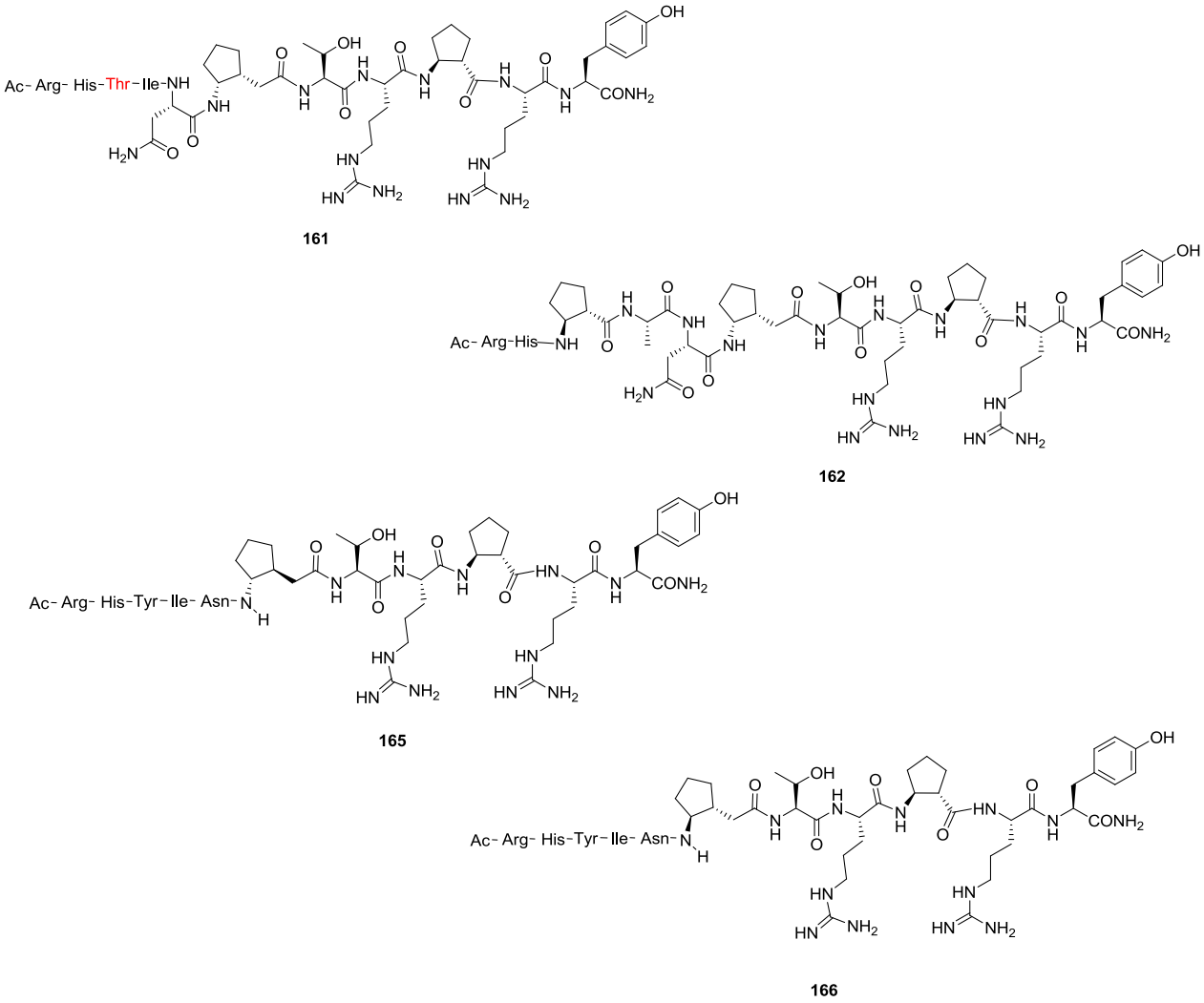

Figure 72. Structure of NPY analogues containing *trans*-pentacin **33** in position 34, in combination with isomers of the 2-(2-amino cyclopentyl) acetic acid in position 31 and 28.

Conformational analysis of peptides **161**, **162**, **165** and **166** suggests the presence of a flexible conformation in water. However the detection of one/two (*i*,*i*+*2*) contacts or of one (*i*,*i*+*5*) contact, like in peptide **162**, indicates the presence of turn-like or loop motifs.

Further, CD studies showed that in buffer and in organic solvents peptide **165** and **166** seem to possess the highest helix propensity, suggesting that the *trans*-isomers of the 2-(2-amino cyclopentyl) acetic acid are more able to induce an ordered conformation (**Figure 69**).

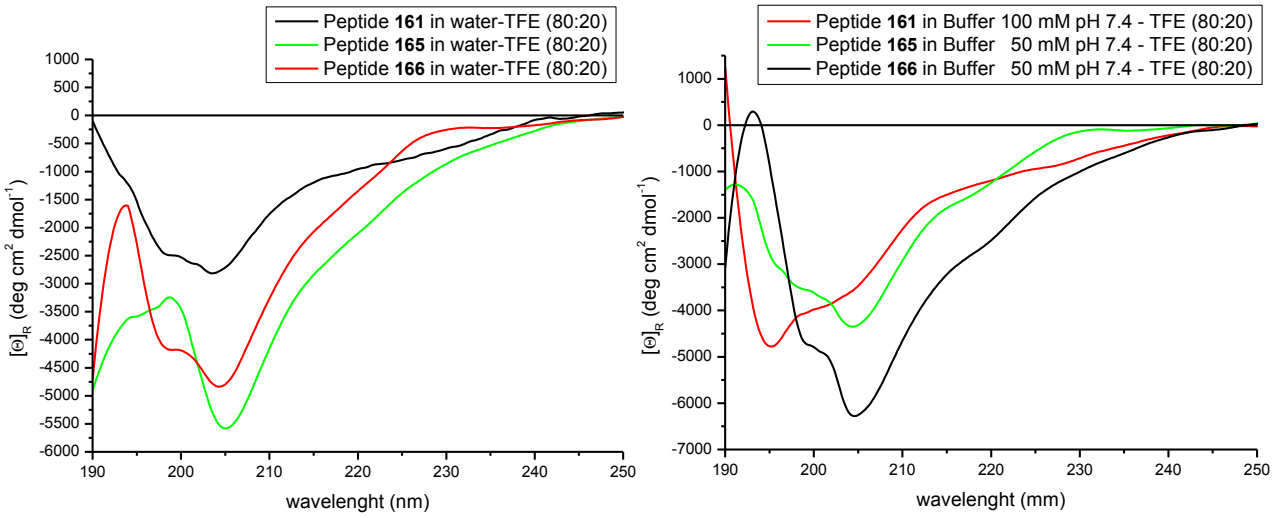

Figure 69. CD spectra of peptide **165** and **166** in comparison with peptide **161** in water/TFE and in 20% of TFE in buffer.

Different results were obtained with NPY analogues containing only one unnatural amino acid in position 34 (**Figure 70**).

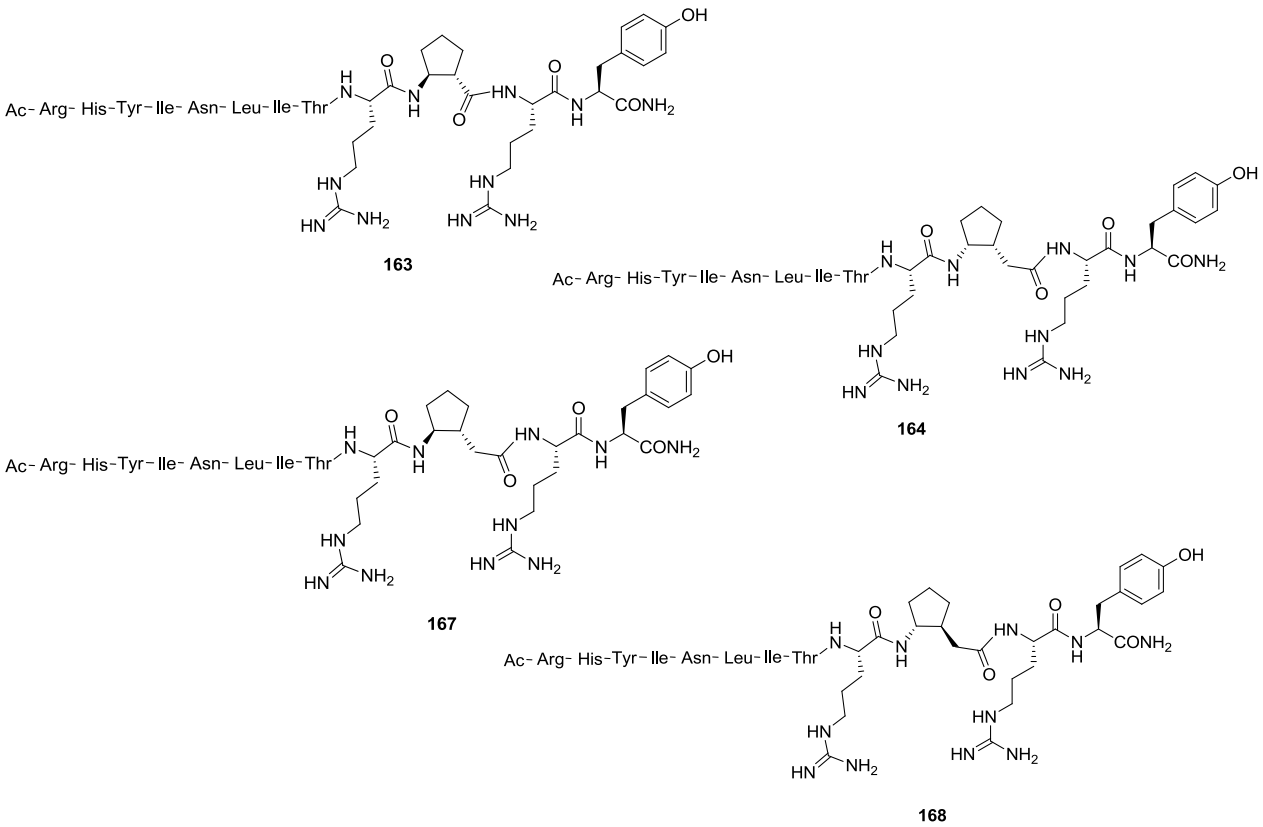

Figure 70. Structure of NPY analogues containing *trans*-pentacin **33** and isomers of the 2-(2-amino cyclopentyl) acetic acid in position 34.

CD studies on peptide **163**, which contain *trans*-pentacin **33** in position 34, suggested a conformation highly flexible in water or buffer, while a 3_{10} helical conformation is likely in organic solvents (**Figure 71**).

The introduction of the γ-amino acids at position 34 induces different conformations, depending on the configuration of the cyclopentane ring. The presence of *cis*-isomer (peptide **164**) induces a flexible structure in water, while a helical conformation similar to that of NPY native sequence was observed in buffer/TFE. (**Figure 71**)

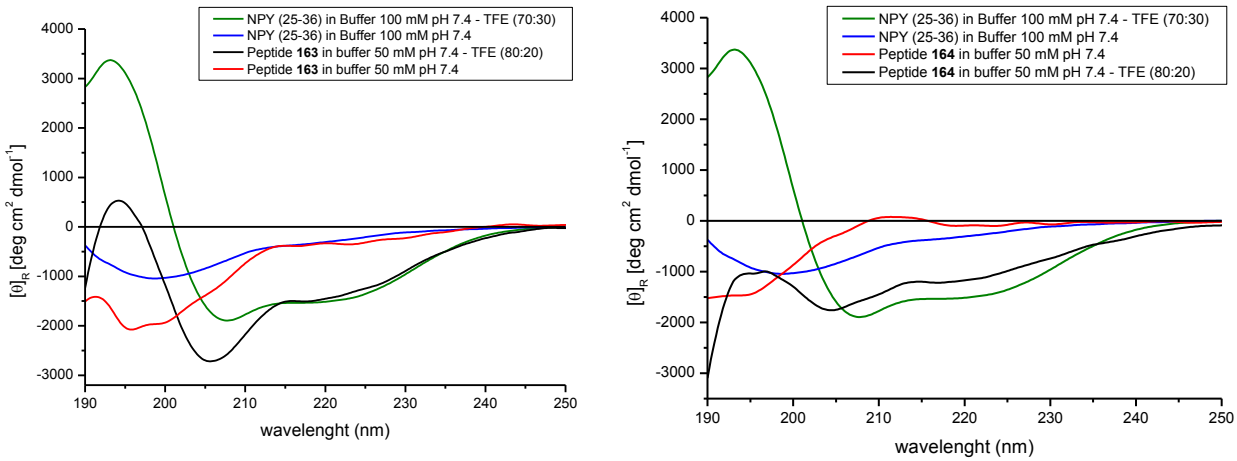

Figure 71. CD spectra of peptide **163** and **164** in comparison with NPY (25-36), in buffer and in 20% of TFE in buffer.

Peptides containing the *trans*-isomers in position 34 showed to adopt a more ordered structure. CD studies on NPY **167** and **168** suggest the presence of a stable β-turn type II in methanol or TFE. However, when the *trans*-γ-amino acids were present at position 31, together with the *(1S,2S)*-configured *trans*-pentacin **33** at position 34, there were no significant changes in the conformational preferences, as shown for the peptides **165** and **166**.

Concluding, the 2-(2-amino cyclopentyl) acetic acid is able to induce different conformational properties on the structure of NPY, depending on the position of the substitution and the absolute configuration. The biological activity of all NPY analogues will be tested against the own receptors, in collaboration with University of Leipzig.

References Chapters 1 and 2

[1] Bouillère, F.; Laurent, S. T.; Kouklovsky, C; Alezra, V. *Amino Acids* **2011,** *41*, 687.

[2] Seebach, D.; Hook, D. F.; Glattli, A. *Biopolymers (Peptide Science)* **2006**, *84*, 23.

[3] Hanessian,S.; Luo, X.; Schaum, R.; Michnick, S.- *J. Am. Chem. Soc.*, **1998**, *120*, 8569.

[4] Hintermann, T.; Gademann, K.; Jaun, B.; Seebach, D. *Helv. Chim. Acta*, **1998**, *81*, 983.

[5] Seebach, D.; Brenner, M.; Rueping, M.; Schweizer, B.; Jaun, B. *Chem. Commun.* **2001**, 207.

[6] Picture taken from: http://dx.doi.org/10.1039/B008377L. *Reproduced by permission of The Royal Society of Chemistry.*

[7] Kothari, A.; Khurram, M.; Qureshi, N.; Beck, E. M.; Smith, M. D. *Chem. Commun.*, **2007**, 2814.

[8] Guo, L.; Zhang, W.; Reidenbach, A. G.; Giuliano, M. W; Guzei, I. A.; Spencer, L. C.; Gellman, S. H. *Angew. Chem. Int. Ed*. **2011**, *50*, 5843.

[9] Picture reproduced with permission from ref. **8**.

[10] Ordonez, M.; Cativiela, C. *Tetrahedron: Asymmetry* **2007**, *18*, 3.

[11] Otzuka, M.; Obata, K.; Miyata, Y.; Tanaka, Y.; *J. Neurochem.* **1971,** *18*, 287.

[12] Maccari, M.; Maggi, G. C. *Brit. J. Pharmacol.* **1965**, *24*, 462.

[13] Qureshi, A.; Colin, P. L.; Faulkner, D. *Tetrahedron* **2000**, *56*, 3679.

[14] Ramachandran & Shekhar, *Future Med. Chem.* **2011**, *3*, 139.

[15] Frackenpohl, J.; Arvidsson, P. I.; Schreiber, J. V.; Seebach, D. *Chem Bio Chem* **2001**, *2*, 445.

[16] Locock, Katherine E. S.; Johnston, Graham A. R.; Allan, Robin D. *Neurochem Res* **2009**, *34*, 1698.

[17] Kennewell, Peter D.; Matharu, Saroop S.; Taylor, John B.; Westwood, R. *J. Chem. Soc. Perkin Trans. I* **1982,** pp. 2553.

[18] Seebach, D.; Schaeffer, L.; Brenner, M.; Hoyer, D. *Angew Chem Int Ed* **2003**, *42*, 776.

[19] Trabocchi, A.; Guarna, F.; Guarna, A. *Curr. Org. Chem.* **2005**, *9*, 1127.

[20] Yoon, N. M.; Pak, C. S.; Brown, H. C.; Krishnamurthy, S.; Stocky, T. P. *J. Org. Chem.*, **1973**, *38*, 2786.

[21] Witiak, D. T.; Sinha, B. K.; Lee, O. S.; Feller, D. R. *J. Med. Chem.* **1972**, *15*, 803.

[22] Hart, R. W.; Gibson, R. E.; Chapman, J. D.; Reuvers, A. R.; Sinha, B. K.; Griffiths, R. K.; Witiak, D. T. *J. Med. Chem.* **1975**, *18*, 323.

[23] Gruner, S. A. W.; Truffault, V.; Voll, G.; Locardi, E.; Stöckle, M.; Kessler, H. *Chem. Eur. J.* **2002**, *8*, 4365.

[24] Qiu, J., Pingsterhaus, J. M., Silverman, R. B. *J. Med. Chem.* **1999**, *42*, 4725.

[25] For the preparation of (*1S,4R*)- and (*1R,4S*)-**71** via resolution of rac-**69** with lactamase, see: Smith, M. E. B., Lloyd, M. C., Derrien, N., Lloyd, R. C., Taylor, S. J. C., Chaplin, D. A., Casy, G., McCague, R. *Tetrahedron: Asymmetry* **2001**, *12*, 703.

[26] Chenevert, R., Martin, R.; *Tetrahedron: Asymmetry* **1992**, *3*,199.

[27] For the preparation of **76** by resolution using (*S*)-α-methylbenzylamine, see: Milewska, M. J., Połonski, T. *Tetrahedron: Asymmetry* **1994**, *5*, 359.

[28] Sahr, F.; *Dissertation,* Regensburg **2009**.

[29] Trzeciak, A.; Bannwarth, W. *Synthesis* **1996**, *12*, 1433.

[30] Cohen, N.; Eichel, W. F.; Lopresti, R. J.; Neukom, C.; Saucy, G. *J. Org. Chem.* **1976**, *41*, 3505.

[31] Wright, S. W.; Hageman, D. L.; Wright, A. S.; McClure, L. D. *Tetrahedron Letters* **1997**, *42*, 7345.

[32] Cadicamo, C. D.; Asante, V.; Ammar, M. A.; Borelli, C.; Korting, H. C.; Kokscha, B. *J. Pept. Sci.* **2009,** *15*, 272.

[33] Booth, H.; King, F. E.; Mason, K. G.; Parrick, J.; Whitehead; R. L. St. D. *J. Chem. Soc.* **1959,** 1050.

[34] Linstead, R. P.; Meade, E. M. *J. Chem. Soc.* **1934**, 935.

[35] Freifelder, M. *' Practical Catalytic Hydrogenation,'* Wiley-Interscience, New York, **1971,** p.264.

[36] Page, M. F. Z.; Jalisatgi, S. S.; Maderna, A.; Hawthorne, M. F. *Synthesis* **2008**, *4*, 555.

[37] Goodman, L.; Benitez, A.; Baker, B. R. *J. Am. Chem. Soc.* **1958**, *80*, 1680.

[38] Seebach, D,; Overhand, M.; Kühnle, F. N. M.; Martinoni, B.; Oberer, L.; Hommel, U.; Widmer, H. *Helv. Chim. Acta* **1996**, *79*, 913.

[39] Gellman, S. H.; Woll, M. G.; Lai, J. R.; Murray, J. Patent, No.: US 6,958,384 B2, Oct. 25, **2005**.

[40] LePlae, P. R.; Umezawa, N.; Lee, H.-S.; Gellman, S. H. *J. Org. Chem.* **2001,** *66*, 5629.

[41] Wrobel, J. E.; Ganem, B. *Tetrahedron Letters* **1981**, *36*, 3447**.**

[42] Lee, H.-S.; LePlae, P. R.; Porter, E. A.; Gellman, S. H. *J. Org. Chem.* **2001**, *66*, 3597.

[43] Arndt, F.; Eistert, B. *Ber. Dtsch. Chem. Ges.* **1935**, *68*, 200.

[44] *Organic Syntheses*, Coll. Vol. *2*, p.461 (**1943**); Vol. 15, p.48 (**1935**).

[45] *Organic Syntheses*, Coll. Vol. *2*, p.165 (**1943**); Vol. 15, p.3 (**1935**).

[46] Ye, T.; McKervey, M. A. *Chem. Rev.* **1994**, *94*, 1091.

[47] Meier, H.; Zeller, K.-P. *Angew. Chem. Int. Ed. Engl.* **1975**, *14*, 32.

[48] Kirmse, W. *Eur. J. Org. Chem.* **2002**, *14*, 2193.

[49] Omar, F.; Frahm, A. W. *Arch. Pharm.* (Weinheim) **1989**, *322*, 461.

[50] Segrer, A.; Viterbo, G.; Parisi, G. *J. Am. Chem. Soc.* **1957**, *79*, 3503.

[51] Quitt, P.; Hellerbach, J.; Vogler, K. *HeIv. Chim. Acta,* Vol. XLVI, Fasciculus I **1963**, *32*, 327.

[52] a) Birch, A. J.; "117. Reduction by dissolving metals. Part I". *J. Chem. Soc.* **1944,** 430. b) Birch, A. J.;"212. Reduction by dissolving metals. Part II". *J. Chem. Soc.* **1945**, 809. c) Birch, A. J.; "119. Reduction by dissolving metals. Part III". *J. Chem. Soc.* **1946**, 593. d) Birch, A. J.; "25. Reduction by dissolving metals. Part IV". *J. Chem. Soc.* **1947,** 102. e) Birch, A. J.; "327. Reduction by dissolving metals. Part V". *J. Chem. Soc.* **1947,** 1642. f) Birch, A. J.; Mukherji, S. M.; "532. Reduction by dissolving metals. Part VI. Some applications in synthesis". *J. Chem. Soc.* **1949,** 2531.

[53] Resek, J. E. *J. Org. Chem.* **2008**, *73*,9792.

[54] Galeazzi, R.; Mobbili, G.; Orena, M. *Tetrahedron 55* **1999**, 261.

[55] a) Appella, D. H.; Christianson, L. A.; Klein, D. A.; Richards, M. R.; Powell, D. R.; Gellman, S. H. *J. Am. Chem. Soc.* **1999,** *121*, 7574.; b) Appella, D. H.; Christianson, L. A.; Klein, D. A.; Powell, D. R.; Huang, X.; Barchi Jr, J. J.; Gellman, S. H. *Nature* **1997**, *387*, 381.

[56] Leroux, P. *J. Comp. Neurol.* **2002**, *442*, 35.

[57] a) Tatemoto, K.; Carlquist, M.; Mutt, V. *Nature* **1982**, *296*, 659.; b) Tatemoto, K. *Proc. Natl. Acad. Sci. USA* **1982**, *79*, 5485.

[58] Larhammar, D. *Regul. Peptides* **1996**, *62*, 1.

[59] Kimmel, J. R.; Hayden, L. J.; Pollock, H. G. *J. Biol. Chem*. **1975,** *250*, 9369.

[60] a) Mattiasson, A.; Ekblad, E.; Sundler, F.; Uvelius, B. *Cell Tissue Res* **1985**, *239*, 141.
b) Ekstrism, J.; Ekman, R.; Luts, A.; Sundler, F.; Tobin, G. *Regulatory Peptides* **1996**, *61***,** 125.
c) Grundemar, L.; Hakanson, R. *Gen. Pharmac.* **1993**, *4*, 785.

[61] McDonald, J. K. *Crit Rev Neurobiol*. **1988**, *4*, 97.

[62] Bader, R.; Bettio, A.; Beck-Sickinger, A. G.; Zerbe, O. *J. Mol. Biol.* **2001**, *305*, 307.

[63] Blundell, T. L.; Pitts, J. E.; Tickle, I. J.; Wood, S. P.; Wu, C.-W. *Proc. Natl. Acad. Sci. USA* **1981**, *78*, 4175.

[64] Wraith, A.; Törnsten, A.; Chardon, P. *Genome Res.* **2000**, *10*, 302.

[65] Michel, M. C.; Beck-Sickinger, A.; Cox, E.; Doods, H. N.; Herzog, H.; Larhammar, D.; Quirion, R.; Schwartz, T.; Westfall, T. *Pharmacol. Rev.* **1998**, *50*, 143.

[66] Herzog, H.; Hort, Y. J.; Ball, H. J.; Hayes, G.; Shine, J.; Selbie, L. A. *Proc. Natl. Acad. Sci. USA* **1992**, *89*, 5794.

[67] "Building Gene Families", *Science* **1997**, Vol. 278, no. 5338 p. 615.

[68] Berglund, M. M.; Lundell, I.; Cabrele, C.; Serradeil-Le Gal,C.; Beck-Sickinger, A. G.; Larhammar, D. *Biochem. Pharmacol.* **2000**, *60*, 1815.

[69] Berglund, M. M.; Lundell, I.; Eriksson, H.; Söll, R.; Beck-Sickinger, A. G.; Larhammar, D. *Peptides* **2001**, *22*, 351.

[70] Larhammar, D.; Salaneck, E. *Neuropeptides* **2004**, *38*, 141.

[71] Silva, A. P.; Cavadas, C.; Grouzmann, E. *Clin. Chim. Acta* **2002**, *326*, 3.

[72] a) Cabrele, C.; Beck-Sickinger, A. G. *J. Pept. Sci***. 2000**, *6*, 9-122; b) Inui, A. *Trends Pharmacol. Sci.* **1999**, *20*, 43.

[73] Adapted from: Gehlert, D. R. *Neuropeptides* **2004**, *38*, 135.

[74] Wahlestedt, C.; Reis, D. J. *Annu. Rev. Pharmacol. Toxicol.* **1993**, *32*, 309.

[75] Brennauer, A.; Dove, S.; Buschauer, A. *Handb. Exp. Pharmacol.* **2004**, *162*, 505.

[76] Balasubramaniam, A.; Sherriff, S. *J. Biol. Chem.* **1990**, *265*,14724.

[77] Edvinson, L.; Erlinge, D.; Sun, X. Y.; Hedner, T. *Pharmacol. Toxicol.***1994**, *74*,193.

[78] Michel, M. C.; Gaida, W.; Beck–Sickinger, A. G.; Wieland, H. A.; Doods, H.; Durr, H.; Jung, G.; Schnorrenberg, G. *Mol. Pharmacol*. **1992**, *42*, 642.

[79] Beck, B.; Stricker–Krongrad, A.; Musse, N.; Nicolas, J. P.; Burlet, C. *Neurosci. Lett*. 1994, *181*, 126.

[80] Balasubramaniam, A.; Sheriff, S.; Johnson, M. E.; Prabhakaran, M.; Huang, S.-G.; Fischer, J. E.; Chance, W. T. *J. Med. Chem*. **1994**, *37*, 811.

[81] Broqua, P.; Wettstein, J. G.; Rocher, M-N.; Gauthier-Martin, B.; Riviere, P. J. M.; Junien, J-L.; Dahl, S. G. *Brain Res*. **1996**, *724*, 25.

[82] Gerald, C.; Walker, M. W.; Criscione, L. et. al. *Nature* **1996**, *382*, 168.

[83] Hu, Y.; Bloomquist, B. T.; Cornfield, L. J. et. al. *J. Biol. Chem*. **1996**, *271*, 26315.

[84] Balasubramaniam, A.; Ujhelyi, M.; Borchers, M.; Huang, Y.; Zhai, W.; Zhou, Y.; Johnson, M.; Sheriff, S. and Fischer, J.E. *J. Med. Chem*. **1996**, *39*, 1142.

[85] Myers, R. D.; Wooten, M. H.; Ames, C. D.; Nyce, J. W. *Brain Res. Bull*. **1995**, *37*, 237.

[86] Balasubramaniam, A.; Zhai, W.; Tao, Z.; Huang, Y.; Fischer, J. E.; Eden, P.; Taylor, J. E.; Kar, L.; Samarasinghe, S. D.; Johnson, M. E. *Peptides* **1996**, *17*, 1113.

[87] Leban, J. J.; Heyer, D.; Landavazo, A.; Matthews, J.; Aulabaugh, A.; Daniels, A. J. *J. Med. Chem* **1995**, *38*, 1150.

[88] Adapted from: Balasubramaniam, A. *Peptides* **1997,** *3*, 445.

[89] Mörl, K.; Beck-Sickinger, A. G. *A. Handb. Exp. Pharmacol.* **2004**, *162*, 479.

[90] Fuhlendorff, J.; Gether, U.; Aakerlund, L.; Langeland-Johansen, N.; Thgersen, H.; Melberg, S. G.; Olsen, U. B.; Thastrup, O. *Proc. Natl. Acad. Sci*. USA **1990,** *87*, 182.

[91] Cabrele, C.; Langer, M.; Bader, R.; Wieland, H. A.; Doods, H. N.; Zerbe, O.; Beck-Sickinger, A. *J. Biol. Chem*. **2000**, *275*, 36043.

[92] Koglin, N.; Zorn, C.; Beumer, R.; Cabrele, C.; Bubert, C.; Sewald, N.; Reiser, O.; Beck-Sickinger A. G. *Angew. Chem. Int. Ed.* **2003**, *42*, 202.

[93] Adapted from ref. **92**.

[94] Sawada, T.; Gellman, S. H. *J. Am. Chem. Soc.* **2011**, *133*, 7336.

[95] Guzzo, A. V. *Biophys. J.* **1965**, vol. 5, 809.

[96] Marshall, G. R.; Beusen, D. D.; Nikiforovich, G. V. *"Peptides: Synthesis, Structures and Applications"*, Ed.: Gutte, B.; (**1995**), Cap. 5, pag. 193.

[97] Perczel, A.; Hollòsi, M. in *"Circular Dichroism and conformational Analysis of Biomolecules"*, Ed.: Fasman, G. D.; Plenum Press, New York, **1996**.

[98] Kelly, S. M.; Price, N. C. *Current Protein and Peptide Science* **2000**, *1*, 349.

[99] Adapted with permission from: Greenfield, N.; Fasman, G. *Biochemistry*, **1969**, *8*, 4108. Copyright 1969, American Chemical Society

[100] Toniolo, C.; Polese, A.; Formaggio, F.; Crisma, M.; Kamphuis, J. *J. Am. Chem. Soc.* **1996**, *118*, 2744.

[101] http://www.oci.uzh.ch/group.pages/zerbe/PeptidNMR.pdf (April, 15th ,**2012**)

[102] Awasthi, S. K.; Shankaramma, S. C.; Raghothama, S.; Balaram, P. *Biopolymers* **2001**, *58*, 465.

[103] Markus, M. A.; Dayie, K. T.; Matsudaira, P.; Wagner, G. *J. Magn. Reson.* **1994**, B *105*, 192.

[104] Cierpicki, T.; Otlewski, J. *J. Biomol. NMR* **2001**, *21*, 249.

[105] Baxter, N. J.; Williamson, M. P. *J. Biomol. NMR* **1997**, *9*, 359.

[106] Liang, G. B.; Rito, C. J.; Gellman, S. H. *J. Am. Chem. Soc.* **1992**, *114*, 4440.

[107] Wuthrich, K. *J Biol Chem* **1990,** *265*, 22059.

[108] Lambert, J. B.; Mazzola, E. P. (**2004**) Nuclear Magnetic Resonance Spectroscopy: *An introduction to principles, applications, and experimental methods*. Upper Saddle River, N.J: Pearson/Prentice Hall.

[109] Griesinger, C.; Otting, G.; Wuthrich, K.; Ernst, R. R. *J. Am. Chem. SOC.* **1988**, *110*, 7870.

[110] Wüthrich, K. (**1986**) *NMR of Proteins and Nucleic Acids*, New York: Wiley.

[111] Wüthrich, K.; Billeter, M.; Braun, W. *J. Mol. Biol.* **1984**, *180*, 715.

[112] a) Monks, S. A.; Karagianis, G.; Howlett, G. J.; Norton, R. S. *J. Biomol. NMR* **1996**, *8*, 379.; b) Darbon, H.; Bernassau, J. M.; Deleuze, J.; Chenu, J.; Roussel, A.; Cambillau, C. *Eur. J. Biochem.* **1992**, *209*,765.

[113] Gurrath, M.; Bisello, A.; Bollazzo, K.; Chung, C-W.; Mammi, S.; Peggion, E. *J. Pept. Sci.* **1996**, *2*, 176.

[114] Adapted from ref. **113**.

[115] Picture reproduced with permission from ref. **113**.

[116] Lazoura, E.; Maidonis, L.; Bayer, E.; Hearn, M. T. W.; Aguilar, M-I. *Biophys. J.* **1997**,*72*, 238.

[117] Picture reproduced with permission from ref. **116**.

[118] Jois, S. D. S.; Balasubramaniam, A. *Peptides* **2003**, *24*, 1035.

[119] Reprinted with permission from (Sawada, T.; Gellman, S. H. *J. Am. Chem. Soc.* **2011**, *133*, 7336). Copyright **2011** American Chemical Society.

[120] Andersen, N. H.; Neidigh, J. W.; Harris, S. M.; Lee, G. M.; Liu, Z.; Tong, H. *J. Am. Chem. Soc.* **1997**, *119,* 8547.

[121] Bordessa, A.; *Dissertation,* Regensburg **2008**.

[122] Merutka, G.; Dyson, H. J.; Wright, P. E. *Journal of Biomolecular NMR* **1995**, 5, 14.

[123] a) Dado, G. P.; Gellman, S. H.; *J. Am. Chem. SOC.* **1993**,*115*, 4228; b) Gellman, S. H.; Dado, G. P.; Liang, G. B.; Adams, B. R. *J. Am. Chem. Soc.* **1991**, *113*, 1164.

[124] Dumy, P.; Eggleston, I. M.; Esposito, G.; Nicula, S.; Mutter, M. *Biopolymers* **1996**, *39*, 297.

Experimental part

Instruments and general techniques

^{1}H-NMR spectra were recorded on Bruker Avance 300 (300 MHz) and Bruker Avance 600 (600 MHz). The chemical shifts are reporter in δ (ppm) relative to chloroform ($CDCl_3$, 7.26 ppm), dimethylsulfoxide (DMSO-d_6, 2.49 ppm), methanol-d_3 or methanol-d_4 (CD_3OH, 3.34 ppm), deuterium oxide (D2O, 4.79 ppm). The spectra were analysed by first order, the coupling constant (*J*) are reported in Hertz (Hz). Characterisation of signals: s = singlet, bs = broad singlet, d = doublet, t = triplet, q = quartet, m = multiplet, bm = broad multiplet, dd = double doublet, dt = double triplet, ddd = double double doublet. Integration is determined as the relative number of atoms. Diastereomeric ratios were determined by comparing the integrals of corresponding protons in the ^{1}H-NMR spectra.

^{13}C-NMR spectra were recorded on Bruker Avance 300 (75.5 MHz) and Bruker Avance 600 (150.9 MHz). The chemical shifts are reported in δ (ppm) relative to chloroform ($CDCl_3$, 77 ppm), dimethylsulfoxide (DMSO-d_6, 39.52 ppm), methanol-d_3 or methanol-d_4 (CD_3OH, 49 ppm). ^{13}C NMR resonance assignment were aided by the use of the DEPT 135 (DEPT = distortionless enhancement by polarisation transfer) or HSQC (Heteronuclear Single Quantum Correlation) techniques to determine the number of hydrogens attached to each carbon atom and is declared as: + = primary or tertiary (positive DEPT signal intensity or straight line in HSQC), - = secondary (negative DEPT signal or dot line in HSQC) and quat = quaternary (no DEPT signal intensity) carbon atoms. In some cases DEPT 90 spectra were recorded to distinguish between primary and tertiary carbon atoms and HMBC (Heteronuclear Multiple Bond Correlation) to distinguish between quaternary carbon and aromatic CH.

2D-NMR spectra (COSY, NOESY, ROESY, TOCSY, HMBC, HSQC) were recorded on Bruker Avance 600 (600 MHz).

IR spectra were recorded with a Bio-Rad Excalibur series FT-IR.

MS spectra were recorded in the mass spectroscopy department of the University of Regensburg.

Optical rotations were measured on a Perkin-Elmer-polarimeter 241 with sodium lamp at 589 nm in the specified solvent. Concentration is indicated as [g/100ml].

CD spectra were measured on a JASCO model J-710/720 at the Institute of Analytical Chemistry of the University of Regensburg (research group of Prof. Dr. O. Wolfbeis) at 21°C between 260 and 190 nm in the specified solvent, with 8 scans. The length of the rectangular cuvette was 0.1 mm, the resolution was 0.2 nm, the band width 1.0 nm, the sensitivity 10-20 mdeg, the response 0.25 s, the speed 20 nm/min. The background was substracted for each spectrum. The absorption value is measured as molar ellipticity per residue (deg cm^2 $dmol^{-1}$). The spectra were smoothed by adjacent averaging algorithm or FFT filter with the Origin 8.0 program.

Thin layer chromatography (TLC) was performed on alumina plates coated with silica gel (Merck silica gel 60 F 254, layer thickness 0.2 mm) or glass plates coated with flash chromatography silica gel (Merck silica gel 60 F 254, layer thickness 0.25 mm). Visualisation was accomplished by UV light (wavelength l= 254 nm), permanganate solution, ninhydrin/acetic acid solution, vanillin/H_2SO_4 solution, anisaldehyde solution or Draggendorf-Munier reagent.

Column chromatography was performed on silica gel Geduran SI 60 (70-230 mesh) purchased from Merck and flash chromatography on flash-silica gel 60 (230-400 mesh ASTM) purchased from Merck. All solvents were distilled before use. Other chemicals were purchased from commercial suppliers and used as received. All reactions with oxygen or moisture sensitive reactants were performed under nitrogen atmosphere.

HPLC-chromatography analytical and preparative reverse Phase HPLC was performed on Agilent equipment 1100/1 (Böblingen, Germany) by using the column: Phenomenex Luna C18(2), 3 μm, 2.00 x 150 mm and a Nucleodur 100-5 C18, 5 μm, 21 x 250 mm, (Macherey–Nagel; Dueren, Germany). The flow rate was 0,3 mL/min for the analytical HPLC runs and 16 mL/min for preparative applications. The binary solvent system (A/B) was: (A) ACN, (B) 0.0059% TFA in water. The absorbance was detected at 220 nm.

Melting point were measured by Automated Melting Point System of the SRS (Stanford Research System). All samples were analyzed in a range between 25 °C and 400 °C.

Elemental analysis: microanalytical department of the University of Regensburg.

Solid phase peptide synthesis

(*General procedure for the preparation of peptides*)

The syntheses of peptides was carried out using 50 mg Fmoc-Rink-amide MBHA resin (loading: 0.45 mmol/g) in a 5-ml syringe with teflon-frit for each peptide. Swelling of the resin in DMF/NMP 8:2 for 30 min.

Double coupling with Fmoc-AA-OH/HOBt/HBTU/DIPEA 5:5:4.8:10 eq. in DMF/NMP 8:2 (2x40 min.) for all natural amino acids (protecting groups: trityl for Asn and His, tBu for Thr and Tyr, Pbf for Arg). Double coupling with Fmoc-*trans*-pentacin **132** /HOBt/HBTU/DIPEA 3:3:2.8:6 eq. DMF/NMP 8:2 (2x60 min.) Single coupling with Fmoc-ACPA-OH /HOBt/HBTU/DIPEA 3:3:2.8:6 eq. DMF/NMP 8:2 (60 min.) Fmoc cleavage with 40% piperidine in DMF/NMP 8:2 for 3 min, followed by 20% piperidine in DMF/NMP 8:2 for 10 min. Acetylation of the N-terminus with Ac_2O/DIPEA 10:10 eq. in DMF/NMP 8:2 (2X20 min.) After each coupling/Fmoc-cleavage step washings with DMF (5x). After completion of the peptide-chain assembly washings with DMF (5x), DCM (5x), Et_2O (5x). Peptide cleavage from the resin and simultaneous side-chain deprotection: treatment of the peptide-resin with the mixture TFA/water/TIS/thioanisole 90:3:4:3 for 3 h, then filtering-off of the resin and precipitation of the peptide from ice-cold Et_2O. Recovery of the peptide by centrifugation at 3 °C for 8 min, then repeated ether-washing/centrifugation cycles (3-4 times). Peptide drying under nitrogen flow.

NMR analysis

NOE peaks intensities were converted into distances. Calibration of the unknown interproton distances was done using the peak intensity and distance of a proton pair with a fixed distance r_{ref} as reference by:

$$r_{(1-2)} = r_{ref} \cdot (V_{ref}/V_{1-2})^{1/6}$$

where $r_{(1-2)}$ is the unknown distance between protons 1 and 2, r_{ref} is the reference distance (aromatic vicinal proton-proton distances Hδ,Hε of tyrosine: 2.48 Å), V_{ref} is the integral of NOE peak of the reference protons and V_{1-2} is the integral of NOE peak between proton 1 and 2 calculated in NOESY or ROESY spectrum.

Preparation of compounds

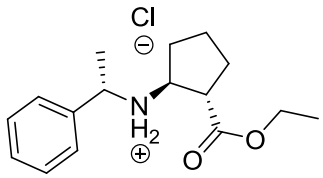

(*1S,2S*)-2-(ethoxycarbonyl)-N-((*S*)-1-phenylethyl)cyclopentanaminium chloride (136)[40]

To a stirred solution of α-ketoester **133** (40 mL, 270 mmol, 1 equiv) in absolute ethanol (320 mL) under N_2 was added (*S*)-(-)-α-methylbenzylamine **134** (69.6 mL, 540 mmol, 2 equiv) and glacial acetic acid (30.8 mL, 540 mmol, 2 equiv). The reaction mixture was stirred at room temperature until the formation of the enamine was complete (2 h; monitored by TLC, 7:3 hexane/EtOAc, *Rf* = 0.22). The reaction mixture was diluted with 640 mL of absolute ethanol and heated to 72 °C, and sodiumcyanoborohydride (42.4 g, 675 mmol, 2.5 equiv) was then added to the reaction mixture in five portions over a 5 h period. The disappearance of enamine was monitored by TLC. Through the course of the reaction a solid formed on the surface that hindered efficient mixing of additional sodium cyanoborohydride. This solid could be broken up with a spatula or by use of a mechanical stirrer. When the reaction was complete (6-8 h), 200 mL of H_2O was added, and the ethanol was removed via rotary evaporation. The resulting mixture was extracted with diethyl ether (700 mL). The ethereal solution was passed through a plug of silica, eluting with an additional 1.5 L of ether. The filtrate was concentrated, the resulting oil was dissolved in EtOAc (1.2 L), and 4 N HCl in dioxane (65 mL) was added dropwise at room temperature with stirring. The resulting solution was stored at 0 °C for 1 h. A white precipitate formed during this time. The solid was isolated by filtration and washed with EtOAc (200 mL). This solid could be purified by recrystallization from ethanol (75 g of solid in 450 mL ethanol). The resulting solid was filtered and washed with acetonitrile and then recrystallized from acetonitrile (27 g in 400 mL).

After filtration and drying, compound **136** (23 g, 73.7 mmol) was obtained as a white crystalline solid (29% yield). ^{1}H NMR indicated the diastereomeric excess to be > 99%.

mp: 240-241 °C; **[α]^{20}** (measured) = 42.3 (*c* 0.19 , MeOH); (**[α]^{20}** not reported in literature).
^{1}H NMR (CD_3OD, 300MHz) δ 7.53-7.40 (m, 5H), 4.44 (q, *J* = 6.6 Hz, 1H), 4.14 (m, 2H), 3.80 (dt, *J* = 8.1 Hz, 6.4 Hz, 1H), 3.11 (m, 1H), 2.27-2.00 (m, 2H), 1.89-1.59 (m, 7H), 1.24 (t, *J* = 7.2 Hz, 3H); **^{13}C NMR** (CD_3OD, 300MHz) δ 137.8, 130.6, 130.5, 128.7,62.4, 60.4, 59.1, 48.6, 31.8, 31.1, 25.1, 20.2, 14.4; **IR** (neat): 2748, 2673, 2476, 1719, 1598, 1465, 1369, 1189, 1155, 1035, 856, 767, 707. **MS (ES-MS):** m/z (%) = 261.9 (100) [M+H$^+$], 303.1 (20) [MH$^+$ + MeCN], 637.3 (5) [2MH$^+$+TFA]. **HR-MS (ES-MS):** 262.1802 ($C_{16}H_{24}NO_2$ [M+H]$^+$: calcd. 262.1802).

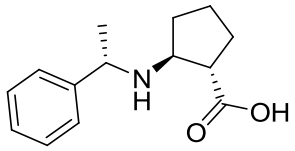

(*1S*,*2S*)-2-((*S*)-1-phenylethylamino)cyclopentanecarboxylic acid (137)[40]

Compound **136** (6.27 g, 21.0 mmol, 1 equiv) was dissolved in THF/MeOH/H_2O (6:3:1, 100 mL), and the solution was cooled to 0 °C. LiOH (2.51 g, 105 mmol, 5 equiv) was added. The mixture was stirred at 0 °C for 9 h. Aqueous HCl (1 N, 110 mL) was added at 0 °C. The solvent was then removed on a vacuum rotary evaporator to give the product as a white solid, which was used for the next step without further purification.

R_f = 0.38 (DCM/MeOH 90:10).
^{1}H NMR (DMSO-d_6, 300 MHz) δ 10.12 (br s, 2H), 7.68-7.57 (m, 2H), 7.38-7.25 (m, 3H), 4.21 (m, 1H), 3.37-3.20 (m, 2H), 2.15-1.99 (m, 1H), 1.94-1.68 (m, 3H), 1.58 (d, *J* = 6.6 Hz, 3H), 1.64-1.47 (m, 1H), 1.45-1.28 (m, 1H);

^{13}C NMR (DMSO-d_6, 300 MHz) δ 175.21, 137.40, 128.89, 128.77, 128.29, 58.57, 56.76, 46.22, 31.13, 30.86, 24.44, 20.95. **MS (ES-MS):** m/z (%) = 234 (100) [M+H$^+$], 275 (57) [MH$^+$ + MeCN], 467.1 (53) [2M+H$^+$].

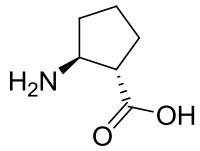

(*1S,2S*)-2-aminocyclopentanecarboxylic acid (33)[40]

The white solid compound mixture **136** was dissolved in 300 mL of 95% ethanol in a hydrogenation flask; 10% Pd-C (2.0 g) was added. The resulting mixture was shaken under H_2 (50 psi) for 48 h. After the reaction was complete (the disappearance of starting material was monitored by TLC), the mixture was filtered through Celite, and the filtrate was concentrated to obtain the HCl salt of (1*S*,2*S*)-aminocyclopentanecarboxylic acid **33** as a white solid, which was used for the next step without further purification.

^{1}H NMR (D_2O, 300 MHz) δ 3.84-3.73 (q, J = 7.5 Hz, 1H), 2.940-2.76 (m, 1H), 2.19-1.97 (m, 2H), 1.85-1.57 (m, 4H). **^{13}C NMR** (D_2O, 300 MHz) δ 177.38, 53.93, 48.40, 30.43, 28.59, 22.86;
MS (ES-MS): m/z (%) = 130 (100) [M+H$^+$], 171 (22) [MH$^+$ + MeCN].

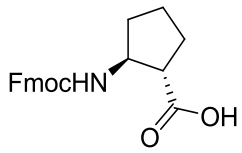

(*1S,2S*)-2-(((9H-fluoren-9-yl)methoxy)carbonylamino)cyclopentanecarboxylic acid (132)[40]

The crude **33** was dissolved in acetone/H_2O (2:1, 300 mL) and cooled to 0 °C, and Fmoc-OSu (9.2 g, 27.3 mmol, 1.1 equiv) and $NaHCO_3$ (17 g, 202 mmol, 9.6 equiv) were added. The reaction mixture was stirred at 0 °C for 1 h and was then allowed to stir at room temperature overnight. Water (100 mL) was added. The acetone was removed under reduced pressure. The aqueous residue was diluted with water (300 mL) and stirred for 1 h with diethyl ether (300 mL).The layers were separated, and the aqueous layer was acidified with 1 N aqueous HCl and extracted with ethyl acetate.

The organic layer was dried over $MgSO_4$ and concentrated to give a white solid. The crude product was purified by crystallization from *n*-hexane/CH_2Cl_2 to afford compound **132** (6.31 g, 20 mmol, 85%) as a white solid.

R_f = 0.41 (DCM/MeOH 90:10). **mp:** 164-165 °C; **[α]^{20}**(measured) = 36.5 (*c* 0.128, MeOH); (Literature **[α]^{20}** = 36.3, *c* 1.21, MeOH);

^{1}H NMR (CD_3OD, 300 MHz) δ 7.81-7.73 (d, *J* = 7.5 Hz, 2H), 7.67-7.59 (d, *J* = 7.5 Hz, 2H), 7.41-7.34 (t, *J* = 7.5 Hz, 2H), 7.33-7.26 (t, *J* = 7.5 Hz, 2H), 4.49-4.10 (m, 4H), 2.71-2.56 (q, *J* = 7.6 Hz, 1H), 2.09-1.91 (m, 2H), 1.89-1.62 (m, 3H), 1.60-1.46 (m, 1H); **^{13}C NMR** (CD_3OD, 300 MHz) δ 178.69, 158.41, 145.43, 142.64, 128.69, 128.18, 126.27, 126.21, 120.94, 67.69, 57.31, 51.53, 33.82, 29.90, 24.24;

IR (neat): 2878, 2360, 1682, 1540, 1472, 1443, 1342, 1293, 1186, 1152, 1104, 1087, 1037, 934, 774, 757, 733; **MS (ES-MS):** m/z (%) = 352 (100) [$M+H^+$], 369.1 (33) [$M+NH_4^+$], 392.9 (17) [MH^+ + MeCN], 703.3 (45) [$2M+H^+$], 720.3 (42) [$2M+NH_4^+$]. **Elemental analysis** calcd. (%) for $C_{21}H_{21}NO_4$ (351.15): C 71.78, H 6.02, N 3.99, found C 71.55, H 6.05, H 3.80.

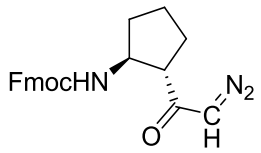

(9H-fluoren-9-yl)methyl (*1S,2S*)-2-(2-diazoacetyl)cyclopentylcarbamate (131)[39]

Compound **132** (0.56 g, 1.59 mmol, 1 equiv) was placed in a oven-dried flask containing a over-dried stir bar and dissolved in dry THF (8 ml) under a N_2 atmosphere. The solution was cooled to –15° C with ice/brine bath. N-methyl-morpholine (183 μL, 1.67 mmol, 1.1 equiv) and isobutylchloroformate (216 μL, 1.67 mmol, 1.1 equiv) were added via syringe. The mixture was stirred for 1 h and allowed to warm at 0° C. A white precipitate forming during this time. In parallel, 8 ml of a ethereal solution of diazomethane was prepared from nitrosomethylurea (0.82 g, 7.95 mmol, 5 equiv) in 2.4 ml of KOH 50 % at 0° C. After stirring for 1 h, the organic layer was separated from aqueous layer, and it was dropped slowly to the reaction mixture until the yellow color was persistent.

The flask was stoppered, placed under N_2, and stirred for 4 h, being allowed to warm from 0° C to room temperature. Glacial acetic acid (1 ml) was then added to decompose any excess diazomethane. An off-white precipitate formed at this time. The reaction mixture was diluted with CH_2Cl_2 (200 ml), washed with saturated aqueous $NaHCO_3$ (2x100 ml), aqueous HCl (1N, 100 ml) and saturated aqueous NaCl solution (100 ml). The organic layer was dried over $NaSO_4$, filtered, and concentrated. The crude product was purified by column chromatography (5% ethyl acetate in CH_2Cl_2, loaded by adsorption onto silica gel) to give compound **131** (0.42 g, 1.2 mmol, 70 %) as white solid.

R_f = 0.38 (dichloromethane/ethyl acetate 9:1). **mp:**139-140 °C; **$[\alpha]^{20}$** (measured) = 155.8 (*c* 0.102, MeOH); (**$[\alpha]^{20}$** not reported in literature).

^{1}H NMR (DMSO-*d*6, 300 MHz) δ 7.89 (d, *J* = 7.1 Hz, 2H), 7.68 (d, *J* = 7.1 Hz, 2H), 7.41 (t, *J* = 7.4 Hz, 2H), 7.32 (t, *J* = 7.4 Hz, 2H), 6.01 (s, 1H), 4.35-4.26 (d, *J* = 6.8 Hz 2H), 4.24-4.16 (t, *J* = 6.8 Hz, 1H), 4.01-3.87 (m, 1H), 2.78-2.63 (m, 1H), 1.93-1.74 (m, 2H), 1.71-1.35 (m, 4H).

^{13}C NMR (DMSO-*d*6, 300 MHz) δ196.20, 155.40, 143.79, 140.64, 127.49, 126.93, 125.01, 120.01, 65.04, 55.10, 46.66, 32.60, 27.99, 22.94. **IR** (neat): 3327, 3082, 2874, 2116, 1690, 1616, 1539, 1447, 1396, 1355, 1297, 1273, 1242, 1149, 1104, 1085, 1034, 760, 736.

MS (ES-MS): m/z (%) = 376 (100) [M+H$^+$], 348 (22) [MH$^+$-N$_2$], 393 (75) [M+NH$_4^+$], 723.3 (3) [2MH$^+$-N$_2$], 768.3 (32) [2M+NH$_4^+$]. **HR-MS (ES-MS):** 398.147 ($C_{22}H_{21}N3NaO_3$ [M+Na]$^+$: calcd. 398.1475).

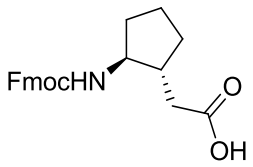

2-((*1R,2S*)-2-(((9H-fluoren-9-yl)methoxy)carbonylamino)cyclopentyl)acetic acid (130)[39]

Compound **131** (0.145 g, 0.387 mmol, 1 equiv) was dissolved in water/dioxane (1/5, 20 ml), and the flask was covered in aluminum foil to exclude light. Silver benzoate was (9 mg, 10 mol %) was added as a catalyst, and the mixture was sonicated at room temperature under N_2 for 1 h. At 0° C the solution was acidified to pH 2 with aqueous HCl (1 N).

The solution was extracted with diethyl ether (4x25 ml). The organic layer was dried over Na_2SO_4, filtered and concentrated to give a white solid. The crude was purified by column chromatography on silica gel (30% ethyl acetate in hexane). The residue was recrystallized from CH_2Cl_2/hexane to obtain a white solid (0.041 g, 0.12 mmol, 29%).

R_f = 0.43 (dichloromethane/methanol 96:4). **mp:**130-131 °C; **[α]^{20}** = +13.6 (*c* 0.124 , MeOH); (**[α]^{20}** not reported in literature). **^{1}H NMR** (CD_3OD, 300 MHz) δ 7.82-7.71 (d, *J* = 7.4 Hz, 2H), 7.67-7.57 (d, *J* = 7.4 Hz, 2H), 7.41-7.33 (t, *J* = 7.4 Hz, 2H), 7.32-7.24 (t, *J* = 7.4 Hz, 2H), 4.43-4.26 (m, 2H), 4.22-4.13 (t, *J* = 6.8 Hz, 1H), 3.59-3.46 (q, *J* = 8.1 Hz, 1H), 2.56-2.43 (dd, *J* = 3.5 Hz, 1H), 2.20-2.08 (m, 1H), 2.07-190 (m, 4H), 1.75-1.54 (m, 2H), 1.52-1.37 (m, 1H), 1.34-1.15 (m, 1H);
^{13}C NMR (CD_3OD, 300 MHz) δ176.90, 158.78, 145.44, 142.66, 128.79, 128.17, 126.25, 120.95, 67.53, 58.66, 48.61, 43.74, 38.91. **IR** (neat): 3308, 1680, 1539, 1445, 1349, 1286, 1254, 1151, 1031, 938, 758, 736. **MS (ES-MS):** m/z (%) = 365.9 (92) [M+H$^+$], 382.9 (50) [M+NH$_4^+$], 406.9 (26) [MH$^+$ + MeCN], 731.3 (98) [2M+H$^+$], 748.3 (30) [2M+NH$_4^+$]. **HR (ES-MS):** 388.1516 ($C_{22}H_{23}NNaO_4$ [M+Na]$^+$: calcd. 388.1519).

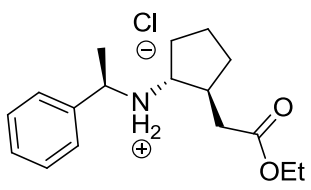

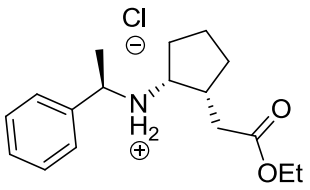

2-(2-ethoxy-2-oxoethyl)-N-((*R*)-1-phenylethyl)cyclopentanaminium chloride (150) and (151)

In a round-bottom flask fitted with a Dean-Stark-trap, ethyl 2-(2-oxocyclopentyl)acetate **138** (5.87 g, 34 mmol, 1 equiv) and R(+)-α-methylabenzylamine **139** (4.6 g , 38 mmol, 1.1 equiv) were dissolved in 34.5 ml dry benzene and refluxed for 6 h. Benzene was removed in vacuo, and the crude imine mixture **140** was used for the next step without further purification. The crude imine mixture **140** was dissolved in 34 ml of dry ethanol and cooled at 5 °C. $NaBH_4$ (385 mg, 10.2 mmol, 0.3 equiv) was added within 2 h. After that, 10 ml of water were added and the ethanol was removed in vacuo. The aqueous layer was extracted with ethyl acetate, dried over Na_2SO_4 and concentrated. The two isomers **148** and **149** were separated by column chromatography on silica gel (hexanes/ethyl acetate, 90:10), giving two yellow oils.

The resulting oils were dissolved separately in diethyl ether (110 ml for compound **148**; 63 ml for compound **149**, and 4.4 N HCl in ethyl acetate (5.5 ml for compound **148**; 3.8 ml for compound **149**) was added dropwise at room temperature with stirring. The resulting solution were stored at 0 °C for 1 h. A white precipitate formed during this time. The solid was isolated by filtration and washed with diethyl ether. The salts were recrystallized from ethanol/diethyl ether, giving compound **150**, 3.71 g, 11.9 mmol, 35 %; compound **151**, 2.1 g, 6.8 mmol, 20%. (dr (**87**/**88**) = 63:37). (below are shown also NMR information about the intermediate compound **140**, **148**, **149**)

Ethyl 2-((*E*,*Z*)-2-((*R*)-1-phenylethylimino)cyclopentyl)acetate (140)[49]

^{1}H NMR ($CDCl_3$, 300 MHz) δ 7.39-7.25 (m, 5H), 7.24-7.16 (m, 1H), 4.48-4.39 (m, 1H), 4.20-4.07 (m, 2H), 2.98-2.87 (m, 1H), 2.84-2.67 (m, 1H), 2.55-1.97 (m, 5H), 1.96-1.82 (m, 1H), 1.77-1.56 (m, 1H), 1.48-1.36 (m, 4H), 1.29-1.19 (t, *J* = 7.4 Hz, 3H). **^{13}C NMR** (CDCl3, 300MHz) δ 177.85, 177.56, 173.24, 146.15, 145.95, 128.65, 128.34, 128.29, 128.23, 127.35, 126.61, 126.51, 126.46, 126.42, 61.62, 61.47, 60.18, 60.15, 43.37, 43.16, 37.04, 30.79, 30.69, 28.70, 28.56, 24.97, 24.66, 24.50, 22.74, 22.65, 14.30, 12.26.

Ethyl 2-((*1S,2R*)-2-((*R*)-1-phenylethylamino)cyclopentyl)acetate (**148**)

R_f = 0.21 (hexanes/ethyl acetate, 90:10).

^{1}H NMR ($CDCl_3$, 300 MHz) δ 7.33-7.15 (m, 5H), 4.14-4.05 (q, *J* = 7.1 Hz, 2H), 3.85-3.76 (q, *J* = 6.5 Hz, 1H), 2.66-2.58 (q, *J* = 7.1 Hz, 1H), 2.51-2.44 (dd, *J* = 5.8 Hz, 1H), 2.22-2.10 (dd, *J* = 5.8 Hz, 1H), 2.08-1.96 (m, 1H), 1.95-1.83 (m, 1H), 1.78-1.39 (m, 4H), 1.32-1.27 (d, *J* = 6.5 Hz, 3H), 1.26-1.19 (t, *J* = 7.1 Hz, 3H), 1.22-1.10 (m, 1H). **^{13}C NMR** (CDCl3, 600 MHz) δ 173.38, 146.66, 128.29, 126.73, 126.58, 63.02, 60.149, 56.871, 42.91, 39.20, 33.34, 30.46, 24.06, 22.40, 14.23.

Ethyl 2-((*1S,2S*)-2-((*R*)-1-phenylethylamino)cyclopentyl)acetate (**149**)

R_f = 0.40 (hexanes/ethyl acetate, 90:10).

^{1}H NMR ($CDCl_3$, 300 MHz) δ 7.35-7.18 (m, 5H), 4.20-4.11 (q, *J* = 7.4 Hz, 2H), 3.77-3.69 (q, *J* = 6.9 Hz, 1H), 2.99-2.90 (m, 1H), 2.59.2.51 (dd, *J* = 6.1 Hz, 1H), 2.46-2.35 (m, 1H), 2.17-2.07 (dd, *J* = 6.1 Hz, 1H), 1.72-1.33 (m, 7 H), 1.32-1.24 (m, 7H). **^{13}C NMR** (CDCl3, 300 MHz) δ 174.21, 146.56, 128.36, 126.77, 126.67, 126.49, 60.19, 58.80, 56.43, 55.08, 38.29, 34.14, 30.86, 29.48, 24.47, 20.69, 14.33.

(*1R,2S*)-2-(2-ethoxy-2-oxoethyl)-N-((*R*)-1-phenylethyl)cyclopentanaminium chloride (**150**)

mp: 148-149 °C; **$[\alpha]^{20}$** = - 6.8 (*c* 0.176, EtOH);

^{1}H NMR (DMSO-d_6, 300 MHz) δ 9.41 (br s, 2H), 7.69-7.58 (d, *J* = 7.2 Hz, 2H), 7.49-7.35 (q, *J* = 7.2 Hz, 3H), 4.46-4.33 (q, *J* = 6.8 Hz, 1H), 4.09-3.99 (q, *J* = 6.8 Hz, 2H), 3.20-3.08 (m, 1H), 2.82-2.71 (dd, *J* = 4.1 Hz, 1H), 2.47-2.41 (m, 1H), 2.32-2.19 (m, 1H),1.97-164 (m, 4H), 1.63-1.57 (d, *J* = 6.7 Hz, 3H), 1.28-1.18 (m, 1H), 1.20-1.13 (t, *J* = 6.9 Hz, 3H).

^{13}C NMR (DMSO-d_6,300MHz) δ 171.73, 137.77, 128.75, 128.70, 127.77, 60.78, 59.79, 37.44, 30.63, 29.58, 22.80, 19.30, 14.01. **IR** (neat): 2943, 2755, 2596, 2537, 1720, 1582, 1457, 1373, 1344, 1189, 1089, 1025, 777, 713, 546. **MS (ES-MS):** m/z (%) = 275.9 (100) [$M+H^+$], 317.0 (4) [MH^+ + MeCN], 587.2 (6) [$2MH^+$ + HCl], 665.3 (8) [$2MH^+$ + TFA]. **HR (ES-MS):** 276.1955 ($C_{17}H_{26}NNO_2$ [$M+H]^+$: calcd. 276.1958).

(*1S,2S*)-2-(2-ethoxy-2-oxoethyl)-N-((*R*)-1-phenylethyl)cyclopentanaminium chloride (**151**)

mp: 150-151 °C; **[α]^{20}** (measured) = 31.8 (*c* 0.132 , EtOH); (Literature **[α]^{20}** = 34.1, *c* 1.5, EtOH). **^{1}H NMR** (DMSO-d_6, 300 MHz) δ 9.44 (br s, 2H), 7.71-7.62 (d, *J* = 7.5 Hz, 2H), 7.48-7.36 (m, 3H), 4.42-4.29 (q, *J* = 6.1 Hz, 1H), 4.14-4.04 (q, *J* = 7.2 Hz, 2H), 3.31-3.21 (m, 1H), 2.81-2.70 (dd, *J* = 3.6 Hz, 1H), 2.60-2.52 (m, 1H), 2.34-2.21 (m, 1H), 1.71-1.56 (m, 7H), 1.51-1.35(m, 2H), 1.23-1.16 (t, *J* = 7.2 Hz, 3H). **^{13}C NMR** (DMSO-$d_{6,}$300MHz) δ 171.71, 137.65, 128.76, 127.87, 59.93, 58.24, 36.09, 32.70, 28.33, 26.40, 19.70, 14.02. **IR** (neat): 2985, 2361, 2008, 1726, 1582, 1462, 1314, 1258, 1221, 1144, 1035, 765. **MS (ES-MS):** m/z (%) = 275.9 (100) [M+H$^+$], 551.2 (2) [2M+H$^+$], 587.2 (1) [2MH$^+$ + HCl], 665.3 (4) [2MH$^+$ + TFA].
HR (ES-MS): 276.1955 ($C_{17}H_{26}NNO_2$ [M+H]$^+$: calcd. 276.1958).

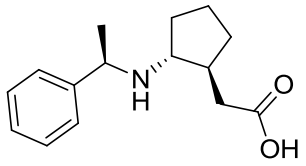

2-((*1S,2R*)-2-((*R*)-1-phenylethylamino)cyclopentyl)acetic acid (152)

Compound **150** (6.27 g, 20 mmol, 1 equiv) was dissolved in THF/MeOH/H_2O (6:3:1, 100 mL), and the solution was cooled to 0 °C. LiOH (2.4 g, 100 mmol, 5 equiv) was added. The mixture was stirred at 0 °C for 9 h. Aqueous HCl (1 N, 100 mL) was added at 0 °C. The solvent was then removed on a vacuum rotary evaporator to give the product as a white solid, which was used for the next step without further purification.

R_f = 0.35 (DCM/MeOH 9:1),
^{1}H NMR (DMSO-d_6, 300 MHz) δ 9.98 (br s, 2H), 7.72-7.63 (d, *J* = 7.3 Hz, 2H), 7.43-7.34 (m, 3H), 4.45-4.30 (q, *J* = 6.4 Hz, 1H), 3.12-3.01 (m, 1H), 2.73-2.61(dd, *J* = 4.3 Hz, 1H), 2.47-2.40 (m, 1H), 2.24-2.10 (m, 1H), 2.01-1.86 (m, 1H), 1.79-1.65 (m, 3H), 1.64-1.57 (d, *J* = 6.8 Hz, 3H), 1.53-1.41 (m, 1H), 1.36-1.13 (m, 1H);

^{13}C NMR (DMSO-d_6,300MHz) δ 173.46, 137.88, 128.70, 128.61, 127.87, 60.89, 56.41, 48.44, 38.84, 29.71, 22.92, 19.62. **MS (ES-MS):** m/z (%) = 248.2 (100) [M+H^+], 293.3 (62) [MH^+ + MeCN], 495.3.1 (33) [$2MH^+$].

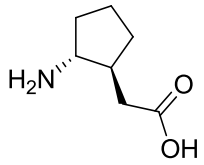

2-((*1S,2R*)-2-aminocyclopentyl)acetic acid (31)

The white solid compound **152** mixture was dissolved in 250 mL of 95% ethanol in a hydrogenation flask; 10% Pd-C (3.0 g) was added. The resulting mixture was shaken under H_2 (50 psi) at 50° C for 36 h. After the reaction was complete (the disappearance of starting material was monitored by TLC), the mixture was filtered through Celite, and the filtrate was concentrated to obtain the HCl salt of 2-((1S,2S)-2-aminocyclopentyl)acetic acid **31** as a white solid, which was used for the next step without further purification.

^{1}H NMR (D_2O, 300 MHz) δ 3.34-3.23 (q, *J* = 5.8 Hz 1H), 2.58-2.40 (m, 2H), 2.27-1.84 (m, 3H), 1.71-1.52 (m, 3H), 1.36-1.21 (m, 1H).

^{13}C NMR (D_2O,300MHz) δ 177.67, 56.80, 40.34, 37.79, 30.94, 30.61, 22.51.

MS (ES-MS): m/z (%) = 144.0 (22) [M+H^+], 185.0 (100) [MH^+ + MeCN], 287 (10) [2M+H^+].

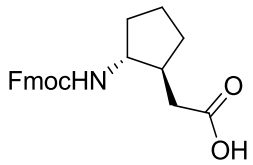

2-((*1S,2R*)-2-(((9H-fluoren-9-yl)methoxy)carbonylamino)cyclopentyl)acetic acid (153)

The crude mixture **31** was dissolved in acetone/H_2O (2:1, 300 mL) and cooled to 0 °C, and Fmoc-OSu (8.77 g, 26 mmol, 1.1 equiv) and $NaHCO_3$ (16.2 g, 19.2 mmol, 9.6 equiv) were added. The reaction mixture was stirred at 0 °C for 1 h and was then allowed to stir at room temperature overnight. Water (100 mL) was added. Acetone was removed under reduced pressure.

The aqueous residue was diluted with water (300 mL) and stirred for 1 h with diethyl ether (300 mL).

The layers were separated, and the aqueous layer was acidified with 1 N aqueous HCl and extracted with ethyl acetate. The organic layer was dried over Na_2SO_4 and concentrated to give a white solid. The crude product was purified by crystallization from *n*-hexane/CH_2Cl_2 to afford compound **153** (6.21g, 17 mmol, 85%) as a white solid.

R_f = 0.31 (DCM/MeOH 96:4). **mp:**130-131 °C; **$[\alpha]^{20}$** = -13.6 (*c* 0.16 , MeOH);

^{1}H NMR (CD_3OD, 300 MHz)) δ 7.82-7.71 (d, *J* = 7.4 Hz, 2H), 7.67-7.57 (d, *J* = 7.4 Hz, 2H), 7.41-7.33 (t, *J* = 7.4 Hz, 2H), 7.32-7.24 (t, *J* = 7.4 Hz, 2H), 4.43-4.26 (m, 2H), 4.22-4.13 (t, *J* = 6.8 Hz, 1H), 3.59-3.46 (q, *J* = 8.1 Hz, 1H), 2.56-2.43 (dd, *J* = 3.5 Hz, 1H), 2.20-2.08 (m, 1H), 2.07-190 (m, 4H), 1.75-1.54 (m, 2H), 1.52-1.37 (m, 1H), 1.34-1.15 (m, 1H);

^{13}C NMR (CD_3OD, 300 MHz) δ176.90, 158.78, 145.44, 142.66, 128.79, 128.17, 126.27, 120.95, 67.53, 58.66, 48.61, 43.74, 38.91, 32.82, 31.11, 22.58. **IR** (neat): 2959, 2363, 2008, 1938, 1680, 1560, 1440, 1360, 1280, 1149, 1105, 1080, 1038, 989, 760. **MS (ES-MS):** m/z (%) = 365.9 (93) [$M+H^+$], 383.1 (48) [$M+NH_4^+$], 407 (27) [MH^+ + MeCN], 731.3 (100) [$2MH^+$], 748.4 (30) [$2M+NH_4^+$]. **Elemental analysis** calcd. (%) for $C_{22}H_{23}NO_4$ (365.16): C 72.31, H 6.34, N 3.83, found C 71.95, H 6.35, H 3.60.

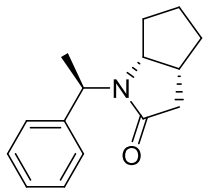

(3a*S*,6a*S*)-1-((*R*)-1-phenylethyl)hexahydrocyclopenta[b]pyrrol-2(1H)-one (141)

Compound **151** (2.6 g, 8.3 mmol, 1 equiv) was dissolved in THF/MeOH/H_2O (6:3:1, 40 mL), and the solution was cooled to 0 °C. LiOH (1 g, 41.6 mmol, 5 equiv) was added. The mixture was stirred at 0 °C for 9 h. Aqueous HCl (1 N, 43 mL) was added at 0 °C.

The solvent was then removed on a vacuum rotary evaporator to give the product **141** (1.9 g) as a colorless oil in quantitative yield.

R_f = 0.51 (Ethyl acetate), **[α]^{20}** = 31.4 (*c* 0.188, MeOH);

^{1}H NMR (DMSO-d_6, 300 MHz) δ 7.37-7.19 (m, 5H), 5.15-5.04 (q, *J* = 7.3 Hz, 1H), 3.64-3.52 (q, 1H), 2.49-2.40 (m, 1H), 2.08-1.93 (m, 1H), 1.75-1.51 (m, 4H), 1.51-1.44 (d, *J* = 7.2 Hz, 3H), 1.44-1.25 (m, 2H). **^{13}C NMR** (DMSO-$d_{6,}$300MHz) δ 173.68, 140.50, 128.29, 127.05, 126.90, 61.76, 54.95, 50.31, 34.06, 33.59, 32.80, 24.18, 18.13. **IR** (neat): 3392, 2955, 2865, 1650, 1439, 1418, 1364, 1334, 1268, 1213, 1030, 768. **MS (ES-MS):** m/z (%) = 230 (24) [M+H$^+$], 247 (6) [M+NH_4^+], 271 (48) [MH$^+$ + MeCN], 459.1 (100) [2M+H$^+$]. **HR-MS (ES-MS):** 230.1537 ($C_{15}H_{20}NO$ [M+H]$^+$: calcd. 230.1539).

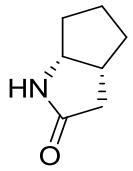

(3a*S*,6a*S*)-hexahydrocyclopenta[b]pyrrol-2(1H)-one (142)

In a flask under argon atmosphere NH_3 (55 ml) was condensed at -78° C and Li (0.266 g, 38 mmol, 4.6 equiv) was added. When the metal dissolved in NH_3, a solution containing the compound **141** (1.9 g, 8.3 mmol, 1 equiv), in dry THF- t-BuOH (17 ml of 90 : 10 mixture) was quickly added.

After 20 min powdered NH_4Cl (3.5 g) was added and the reaction mixture was stirred overnight and allowed to warm to room temperature. After that, the mixture was extracted with ethyl acetate (3 x 50 ml). The organic layer was dried over Na_2SO_4 and concentrated under reduced pressure. The residue was purified by silica gel chromatography in pure ethyl acetate giving compound **142** (0.8 g, 6.4 mmol, 77%).

R_f = 0.21 (Ethyl acetate). **mp:**187-188 °C; **$[\alpha]^{20}$** = - 16.9 (*c* 0.136, MeOH);
^{1}H NMR ($CDCl_3$, 300 MHz) δ 6.46 (br s, 1H), 4.12-4.04 (m, 1H), 2.87-2.73 (m, 1H), 2.66-2.55 (m, 1H), 2.08-1.97 (dd, *J* = 3.4 Hz, 1H), 1.85-1.55 (m, 5H), 1.53-1.43 (m, 1H).
^{13}C NMR ($CDCl_3$,300MHz) δ 178.48, 59.27, 38.03, 37.21, 34.47, 34.34, 23.72. **IR** (neat): 3288, 2952, 2864, 1649, 1420, 1321, 1301, 1270, 1179, 1148, 1108, 1043, 853.

MS (ES-MS): m/z (%) = 126 (4) [M+H$^+$], 167 (52) [MH$^+$ + MeCN], 251.1 (100) [2M+H$^+$].
HR-MS (ES-MS): 126.0911 ($C_7H_{12}NO$ [M+H]$^+$: calcd. 126.0913).

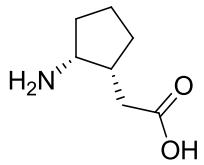

2-((*1S,2S*)-2-aminocyclopentyl)acetic acid (30)

A solution of compound **142** (0.8 g, 6.4 mmol, 1 equiv) in 1N HCl (22 ml) was stirred at 80° C for 36 h. After that, the reaction mixture was washed with DCM to remove impurities. The aqueous layer was concentrated under pressure giving compound **30** (0.5 g, 3.5 mmol, 55%) as a white solid.

mp:124-125 °C; **^{1}H NMR** (D_2O, 300 MHz) δ 7.08 (br s, 3H), 3.71-3.62 (m, 1H), 2.47-2.30 (m, 2H), 2.28-2.16 (m, 1H), 2.15-2.01 (m, 1H), 1.91-1.80 (m, 1H), 1.79-1.54 (m, 3H), 1.43-1.28 (m, 1H). **^{13}C NMR** (D_2O, 300MHz) δ 180.72, 54.72, 39.17, 37.06, 30.25, 29.34, 21.81.
MS (ES-MS): m/z (%) = 144 (28) [M+H$^+$], 185 (100) [MH$^+$ + MeCN], 287 (10) [2M+H$^+$].
HR-MS (ES-MS): 144.1021 ($C_7H_{14}NO_2$ [M+H]$^+$: calcd. 144.1019).

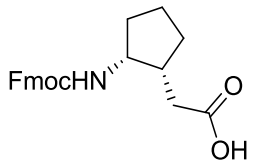

2-((*1S,2S*)-2-(((9H-fluoren-9-yl)methoxy)carbonylamino)cyclopentyl)acetic acid (143)

Crude mixture **30** was dissolved in acetone/H_2O (2:1, 92 mL) and cooled to 0 °C, and Fmoc-OSu (2.8 g, 8.32 mmol, 1.3 equiv) and $NaHCO_3$ (5.16 g, 61.4 mmol, 9.6 equiv) were added. The reaction mixture was stirred at 0 °C for 1 h and was then allowed to stir at room temperature overnight. Water (20 mL) was added. The acetone was removed under reduced pressure. The aqueous residue was diluted with water (10 mL) and stirred for 1 h with diethyl ether (20 mL). The layers were separated, and the aqueous layer was acidified with 1 N aqueous HCl and extracted with ethyl acetate. The organic layer was dried over Na_2SO_4 and concentrated to give a white solid. The crude product was purified by crystallization from *n*-hexane/CH_2Cl_2 to afford compound **143** (1.9 g, 5.2 mmol, 85%) as a white solid.

R_f = 0.28 (DCM/MeOH 96:4). **mp:**119-120 °C; **$[\alpha]^{20}$** = +10.4 (*c* 0.15 , MeOH);
^{1}H NMR (CD_3OD, 300 MHz) δ 7.80-7.73 (d, *J* = 7.2 Hz, 2H), 7.68-7.60 (d, *J* = 7.2 Hz, 2H), 7.41-7.33 (t, *J* = 7.4 Hz, 2H), 7.32-7.25 (t, *J* = 7.4 Hz, 2H), 4.47-4.38 (m, 1H), 4.34-4.25 (m, 1H), 4.22-4.15 (t, *J* = 6.4 Hz, 1H), 4.08-4.01 (q, *J* = 5.4 Hz, 1H), 2.42-2.25 (m, 2H), 2.18-2.03 (m, 1H), 2.01-1.65 (m, 3H), 1.61-1.46 (m, 2H), 1.44-1.24 (m, 1H);
^{13}C NMR (CD_3OD, 300 MHz) δ 177.11, 158.60, 145.44, 142.67, 128.79, 128.19, 126.29, 120.94, 67.49, 55.56, 48.64, 40.96, 35.51, 32.67, 30.53, 22.81. **IR** (neat): 3327, 2914, 2362, 1686, 1527, 1450, 1308, 1279, 1245, 1218, 1083, 1033, 757, 735. **MS (ES-MS):** m/z (%) = 365.9 (100) $[M+H^+]$, 383.0 (60) $[M+NH_4^+]$, 407 (18) $[MH^+$ + MeCN], 731.3 (92) $[2MH^+]$, 748.4 (45) $[2M+NH_4^+]$. **HR-MS (ES-MS):** 388.1516 ($C_{22}H_{23}NNaO_4$ $[M+Na]^+$: calcd. 388.1519).

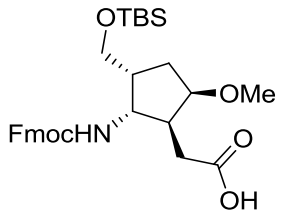

2-((*1S,2R,3R,5R*)-2-(((9H-fluoren-9-yl)methoxy)carbonylamino)-3-((tert butyldimethylsilyloxy)methyl)-5-methoxycyclopentyl)acetic acid (109)

Compound **99** (50 mg, 0.12 mmol, 1 equiv) was dissolved in DMF (5.00 ml) under inert atmosphere. After adding imidazole (50 mg, 0.7 mmol, 6 equiv), TBSCl (53 mg, 0.35 mmol, 3 equiv) and a catalytic amount of DMAP, the reaction mixture was stirred for 5 h at room temperature. Imidazole (50 mg, 0.7 mmol, 6 equiv) and TBSCl (53 mg, 0.35 mmol, 3 equiv) were then added again and the reaction was stirred for 24 h. Methanol (9.70 ml/1.1 mmol) was added and the mixture stirred for another hour. This mixture was diluted with 25% citric acid (10 ml) and extracted with ethyl acetate (3×20 ml). The combined extracts were washed with water and brine and finally dried over sodium sulfate. Evaporation of the solvent gave a viscous oil, which was purified on silica gel using a mixture of DCM/MeOH (98 : 2) as the eluent giving the final product **109** (50 mg, 0.092 mmol, 78.8%) as a white solid

mp: 74-75 °C; **$[\alpha]^{20}$** = -18.4 (*c* 0.21 , DCM).

^{1}H NMR ($CDCl_3$, 300MHz) δ 7.78-7.71 (d, *J* = 7.6 Hz, 2H), 7.61-7.55 (d, *J* = 7.6 Hz, 2H), 7.42-7.26 (m, 4H), 5.67-5.59 (d, *J* = 9.5 Hz, 1H), 4.42-4.35 (d, 2H), 4.24-4.04 (m, 2H), 3.78-3.71 (m, 2H), 3.57-3.50 (m, 1H), 3.24 (s, 3H), 2.75-2.64 (dd, *J* = 6.9 Hz, 1H), 2.55-2.45 (dd, *J* = 6.9 Hz, 1H), 2.42-2.27 (m, 1H), 2.19-2.07 (m, 1H), 2.01-1.90 (m, 1H), 1.82-1.70 (m, 1H), 0.90 (s, 9H), 0.06 (s, 6H). **^{13}C NMR** (CD_3Cl_3, 300MHz) δ178.58, 156.85, 144.04, 141.33, 127.62, 127.01, 125.06, 119.97, 80.13, 66.51, 62.87, 56.58, 56.29, 48.20, 47.35, 38.04, 31.65, 30.78, 25.83, 18.05, -5.62. **IR** (neat): 3333, 2930, 1690, 1535, 1450, 1407, 1346, 1251, 1086, 1023, 945, 836, 775, 746.

MS (ES-MS): m/z (%) = 540.2 (100) [M+H$^+$], 557.2 (30) [Mà+NH_4^+], 1079.6 (45) [2MH$^+$].

HR-MS (ES-MS): 540.278 ($C_{30}H_{42}NO_6Si$ [M+H]$^+$: calcd. 540.2776).

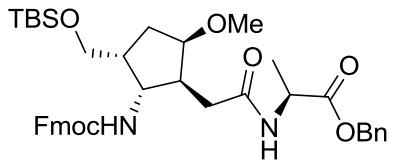

(*S*)-benzyl-2-(2-((*1S,2R,3R,5R*)-2-(((9H-fluoren-9-yl)methoxy)carbonylamino)-3-((tert-butyldimethylsilyloxy)methyl)-5-methoxycyclopentyl)acetamido)propanoate (112)

Compound **109** (100 mg, 0.186 mmol, 1 equiv) was dissolved in DCM(1ml) at 0° C. After that, EDC (40 mg, 0.2 mmol, 1.1 equiv) and HOBt (31 mg, 0.2 mmol, 1.1 equiv) were added and the mixture were strirred for 20 min at 0° C. Then, (*S*)-1-(benzyloxy)-1-oxopropan-2-aminium chloride **113** (65 mg, 0.22 mmol, 1.2 equiv) and DIPEA(0.13 ml, 0.74 mmol, 4 equiv) were added and the reaction mixture was allowed to warm at r.t. and stirred in overnight. Water (10 ml) was added and the layers were separated and the aquous layer extracted once with DCM. The combined organic layers were washed with water and brine and finally dried over Na_2SO_4 and concentrated. The crude product was purified by column chromatography (10% of ethyl acetate in DCM) giving the product as brown oil (88 mg, 0.125 mmol, 68 %).

^{1}H NMR ($CDCl_3$, 300MHz) δ 7.75-7.67 (d, *J* = 7.3 Hz, 2H), 7.59-7.52 (d, *J* = 7.2 Hz, 2H), 7.39-7.18 (m, 9H), 6.37-6.39 (d, *J* = 7.5 Hz, 1H), 5.72-5.66 (d, *J* = 9.6 Hz, 1H), 5.14-5.10 (d, J = 5.3 Hz, 2H), 4.65-4.54 (m, 1H), 4.40-4.25 (m, 2H), 4.19-4.02 (m, 2H), 3.75-3.64 (m, 2H), 3.56-3.47 (dd, 1H), 3.23-3.19 (s, 3H), 2.53-2.41 (m, 1H), 2.38-2.27 (m, 2H), 2.20-2.08 (m, 1H), 1.97-1.86 (m, 1H), 1.75-1.64 (m, 1H), 1.37-1.32 (d, *J* = 6.9 Hz, 3H), 0.08 (s, 9H), 0.03 (s, 6H). **^{13}C NMR** (CD_3Cl_3, 300MHz) δ172.99, 172.34, 156.88, 144.10, 141.31, 135.46, 129.06, 128.62, 128.25, 128.15, 127.64, 127.04, 127.02, 125.35, 125.14, 125.11, 119.97, 80.26, 66.99, 66.62, 62.82, 56.76, 56.23, 48.93, 48.04, 47.31, 38.24, 34.56, 30.41, 29.73, 25.91, 18.38, 5.54. **MS (ES-MS):** m/z (%) = 701.5 (100) [M+H$^+$], 724.4 (40) [M+NH_4^+]. **HR-MS (ES-MS):** 701.3515 ($C_{40}H_{53}N_2O_7Si$ [M+H]$^+$: calcd. 701.3527).

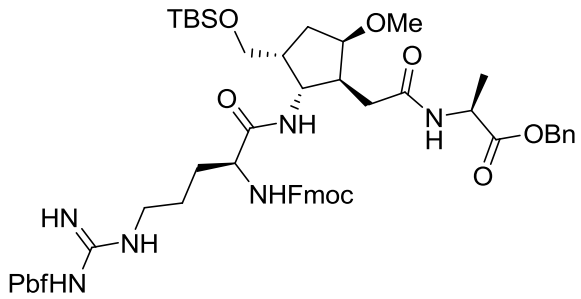

(*S*)-benzyl-2-(2-((*1S,2R,3R,5R*)-2-((*S*)-2-(((9H-fluoren-9-yl)methoxy)carbonylamino)-5-Pbf-guanidinopentanamido)-3-((tert-butyldimethylsilyloxy)methyl)-5-methoxycyclopentyl)acetamido)propanoate (115)

Compound **112**, after cleavage of Fmoc group, (50 mg, 0.025 mmol, 1 equiv) was dissolved in DCM(1ml) at 0° C. After that, EDC (15 mg, 0.073 mmol, 1.1 equiv) and HOBt (12 mg, 0.073 mmol, 1.1 equiv) were added and the mixture were strirred for 20 min at 0° C. Then, Fmoc-D-Arg(Pbf) (39 mg, 0.088 mmol, 1.2 equiv) and DIPEA(0.046 ml, 0.27 mmol, 4 equiv) were added and the reaction mixture was allowed to warm at r.t. and stirred in overnight. Water (10 ml) was added and the layers were separated and the aqueous layer extracted once with DCM. The combined organic layers were washed with water and brine and finally dried over Na_2SO_4 and concentrated. The crude product was purified by column chromatography (1% of MeOH in DCM) giving the product as brown oil (29 mg, 0.026 mmol, 40 %).

^{1}H NMR ($CDCl_3$, 300MHz) δ 7.76-7.70 (d, J = 7.4 Hz, 2H), 7.60-7.52 (m, 2H), 7.38-7.23 (m, 9H), 7.01-6.90 (d, 1H), 6.71-6.62 (br s, 2H), 6.28-6.17 (br s, 2H), 6.03-5.95 (br s, 1H), 5.15-5.05 (q, 2H), 4.54-4.07 (m, 6H), 3.72-3.48 (m, 3H), 3.33-3.26 (m, 1H), 3.24 (s, 3H), 3.20-3.10(m, 1H), 2.90 (s, 2H), 2.58 (s, 3H), 2.51 (s, 3H), 2.40-2.16 (m, 3H), 2.06 (s, 3H), 2.01-1.49 (m, 6 H), 1.42 (s, 6H), 1.35-1.32 (d, *J* = 6.9 Hz, 3H), 0.86 (s, 9H), 0.02 (s, 6H). **^{13}C NMR** (CD_3Cl_3, 300MHz) δ172.81, 171.85, 158.67, 156.51, 143.77, 141.24, 138.39, 135.33, 132.32, 128.37, 128.08, 127.70, 127.08, 125.13, 124.52, 119.92, 117.40, 86.28, 80.11, 67.14, 66.98, 62.98, 60.37, 56.03, 54.87, 53.40, 48.51, 47.05, 43.19, 38.45, 34.35, 31.90, 25.25, 23.81, 22.66, 21.02, 19.28, 18.08, 17.97, 17.92. **HR-MS (ES-MS):** 1109.5425 ($C_{59}H_{81}N_6O_{11}SSi$ $[M+H]^+$: calcd.1109.5448).

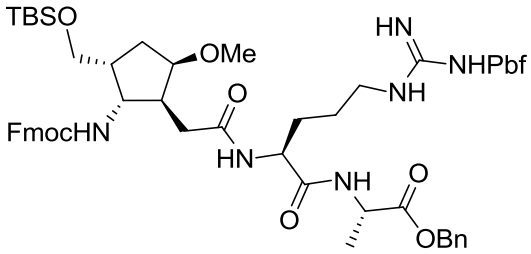

(*S*)-benzyl-2-((*S*)-2-(2-((*1S,2R,3R,5R*)-2-(((9H-fluoren-9-yl)methoxy)carbonylamino)-3-((tert-butyldimethylsilyloxy)methyl)-5-methoxycyclopentyl)acetamido)-5-(Pbf)guanidinopentanamido)propanoate (116)

Compound **109** (20 mg, 0.034 mmol, 1 equiv) was dissolved in DCM (1ml) at 0° C. After that, EDC (9.2 mg, 0.047 mmol, 1.3 equiv) and HOBt (7 mg, 0.047 mmol, 1.3 equiv) were added and the mixture were stirred for 20 min at 0° C. Then, dipeptide Arginine(Pbf)-Alanine-OBn (24 mg, 0.045 mmol, 1.2 equiv) and DIPEA(0.025 ml, 0.14 mmol, 4 equiv) were added and the reaction mixture was allowed to warm at r.t. and stirred in overnight. Water (5 ml) was added and the layers were separated and the aqueous layer extracted once with DCM. The combined organic layers were washed with water and brine and finally dried over Na_2SO_4 and concentrated. The crude product was purified by column chromatography (2% of MeOH in DCM) giving the product as colorless oil (15 mg, 0.0135 mmol, 45 %).

^{1}H NMR ($CDCl_3$, 300MHz) δ 7.77-7.70 (d, J = 7.2 Hz, 2H), 7.59-7.52 (d, J = 7.2 Hz, 2H), 7.40-7.24 (m, 9H), 6.87-6.78 (m, 1H), 6.27-6.08 (br s, 2H), 5.90-5.82 (m, 1H), 5.15-5.01 (m, 2H), 4.56-3.96 (m, 6H), 3.79-3.50 (m, 3H), 3.21 (s, 3H), 2.92 (s, 2H), 2.57 (s, 3H), 2.50 (s, 3H9), 2.40-2.14 (m, 3H), 2.07 (s, 3H), 1.97-1.53 (m, 5H), 1.47 (s, 6H), 1.22-1.18 (d, J = 6.01 Hz, 3H), 0.90 (s, 9H), 0.06 (s, 6H).). **^{13}C NMR** (CD_3Cl_3, 300MHz) δ 173.38, 172.49, 158.73, 156.94, 156.25, 143.97, 141.29, 135.38, 132.37, 128.58, 128.36, 127.65, 127.02, 125.06, 124.58, 119.97, 117.45, 86.35, 67.07, 66.66, 64.46, 56.58, 56.26, 48.49, 47.25, 43.22, 30.48, 28.60, 25.86, 25.37, 19.30, 18.08, 17.94, 17.50, 12.48, 5.57.

HR-MS (ES-MS): 1109.5425 ($C_{59}H_{81}N_6O_{11}SSi$ $[M+H]^+$: calcd.1109.5448).

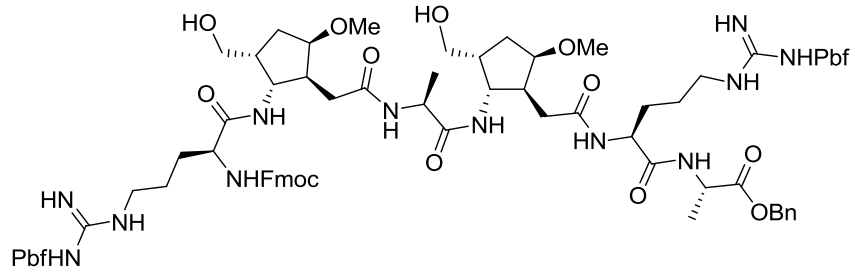

(*S*)-benzyl-2-((*S*)-2-(2-((*1S,2R,3R,5R*)-2-((S)-2-(2-((1S,2R,3R,5R)-2-((S)-2-(((9H-fluoren-9-yl)methoxy)carbonylamino)-5-guanidinopentanamido)-3-((tert-butyldimethylsilyloxy)methyl)-5-methoxycyclopentyl)acetamido)propanamido)-3-((tert-butyldimethylsilyloxy)methyl)-5-methoxycyclopentyl)acetamido)-5-guanidinopentanamido)propanoate (117)

Compound **115**, after cleavage of benzyl ester group (5.4 mg, 0.005 mmol, 1 equiv) was dissolved in DCM (1ml) at 0° C. After that, EDC (1.4 mg, 0.007 mmol, 1.3 equiv) and HOBt (1 mg, 0.007 mmol, 1.3 equiv) were added and the mixture were stirred for 20 min at 0° C. Then, compound **116**, after cleavage of Fmoc group (7 mg, 0.008 mmol, 1.2 equiv) and DIPEA(3.8 μl, 0.024 mmol, 4 equiv) were added and the reaction mixture was allowed to warm at r.t. and stirred in overnight. Water (5 ml) was added and the layers were separated and the aqueous layer extracted once with DCM. The combined organic layers were washed with water and brine and finally dried over Na_2SO_4 and concentrated. The crude product was purified by preparative HPLC giving the product as a white solid (4.9 mg, 0.003 mmol, 60 %).

HR-MS (ES-MS): 1659.7846 ($C_{84}H_{115}N_{12}O_{19}S_2$ $[M+H]^+$: calcd. 1659.7837).

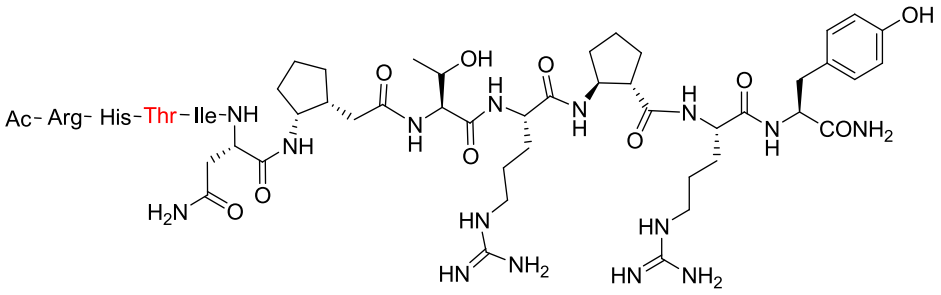

Ac-Arg^{26}-His^{27}-Thr^{28}-Ile^{29}-Asn^{30}-(*1S,2S*-ACPA)^{31}-Thr^{32}-Arg^{33}-(*1S,2S*-ACPC)^{34}-Arg^{35}-Tyr^{36}-NH$_2$ (161)

(3.21 mg, 0.00215 mmol) **HR-MS (ES-MS):** 1492.8426 ($C_{66}H_{108}N_{24}O_{16}$ $[M+4H]^{+4}$: calcd. 374.2167).

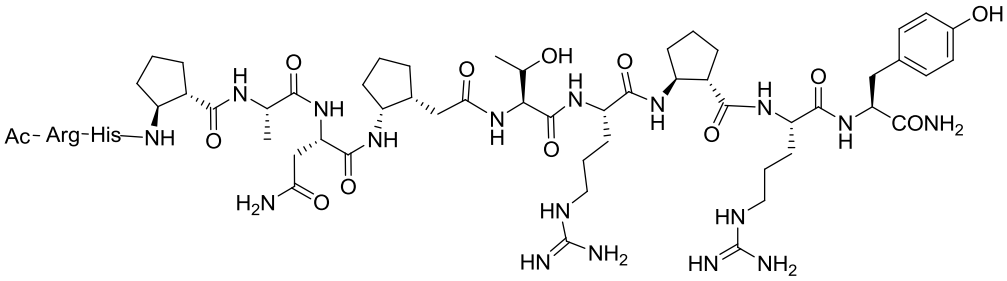

Ac-Arg^{26}-His^{27}-(*1S,2S*-ACPC)^{28}-Ile^{29}-Asn^{30}-(*1S,2S*-ACPA)^{31}-Thr^{32}-Arg^{33}-(*1S,2S*-ACPC)^{34}-Arg^{35}-Tyr^{36}-NH$_2$ (162)

(3.9 mg, 0.0026 mmol) **HR-MS (ES-MS):** 1502.8646 ($C_{68}H_{110}N_{24}O_{15}$ $[M+4H]^{+4}$: calcd. 376.7218).

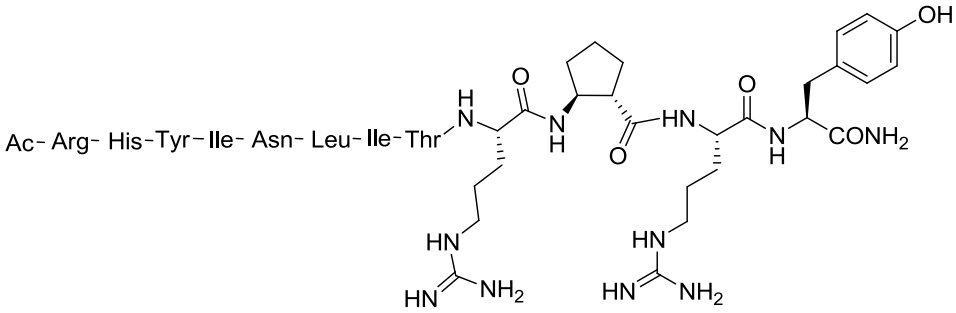

Ac-Arg^{25}-His26-Tyr^{27}-Ile^{28}-Asn^{29}-Leu^{30}-Ile^{31}-Thr^{32}-Arg^{33}-(*1S,2S*-ACPC)^{34}-Arg^{35}-Tyr^{36}-NH$_2$ (163)

(0.67 mg, 0.0004 mmol) **HR-MS (ES-MS):** 1655.9419 ($C_{76}H_{121}N_{25}O_{17}$ $[M+4H]^{+4}$: calcd. 414.9916).

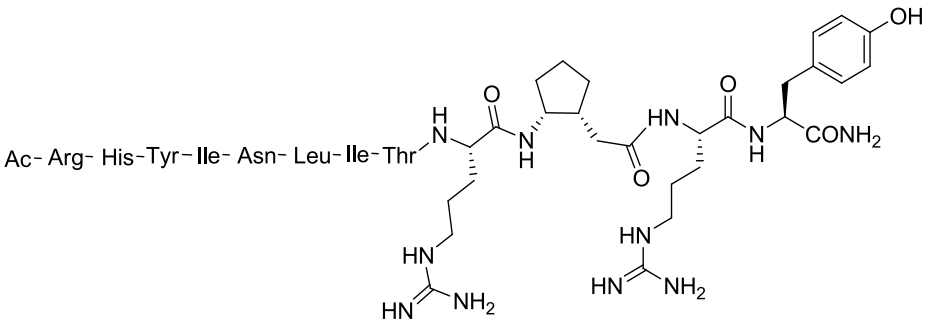

Ac-Arg^{25}-His^{26}-Tyr^{27}-Ile^{28}-Asn^{29}-Leu^{30}-Ile^{31}-Thr^{32}-Arg^{33}-(*1S,2S*-ACPA)^{34}-Arg^{35}-Tyr^{36}-NH$_2$ (164)

(0.72 mg, 0.00043 mmol) **HR-MS (ES-MS):** 1669.9586 ($C_{77}H_{123}N_{25}O_{17}$ $[M+4H]^{+4}$: calcd. 418.4955).

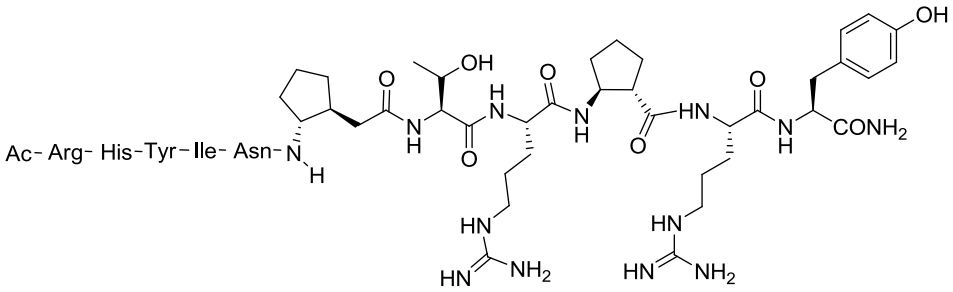

Ac-Arg^{26}-His^{27}-Tyr^{28}-Ile^{29}-Asn^{30}-(*1S,2R*-ACPA)^{31}-Thr^{32}-Arg^{33}-(*1S,2S*-ACPC)^{34}-Arg^{35}-Tyr^{36}-NH$_2$ (165)

(4.37 mg, 0.0028 mmol) **HR-MS (ES-MS):** 1554.8557 ($C_{71}H_{110}N_{24}O_{16}$ $[M+4H]^{+4}$: calcd. 389.7206).

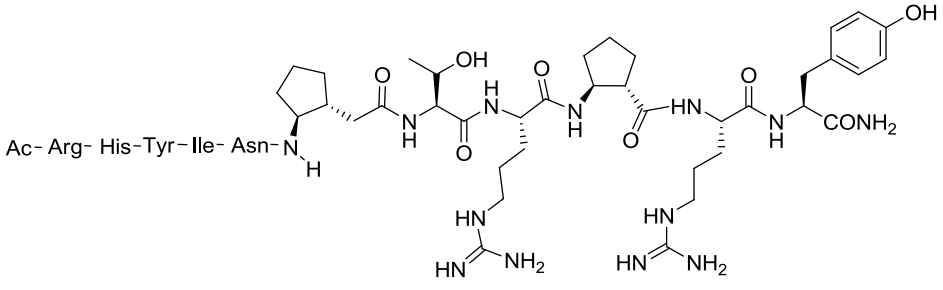

Ac-Arg^{26}-His^{27}-Tyr^{28}-Ile^{29}-Asn^{30}-(*1R,2S*-ACPA)^{31}-Thr^{32}-Arg^{33}-(*1S,2S*-ACPC)^{34}-Arg^{35}-Tyr^{36}-NH$_2$ (166)

(4.15 mg, 0.0026 mmol) **HR-MS (ES-MS):** 1554.8557 ($C_{71}H_{110}N_{24}O_{16}$ $[M+4H]^{+4}$: calcd. 389.7206)

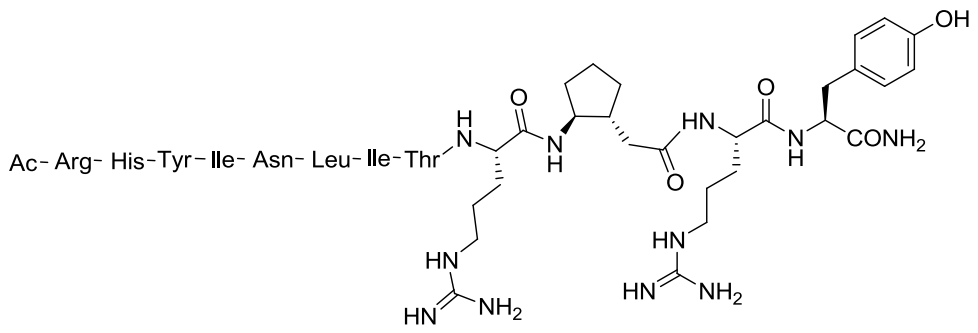

Ac-Arg^{25}-His^{26}-Tyr^{27}-Ile^{28}-Asn^{29}-Leu^{30}-Ile^{31}-Thr^{32}-Arg^{33}-(*1S,2R*-ACPA)^{34}-Arg^{35}-Tyr^{36}-NH$_2$ (167)

HR-MS (ES-MS): 1669.9586 ($C_{77}H_{123}N_{25}O_{17}$ $[M+4H]^{+4}$: calcd. 418.4955).

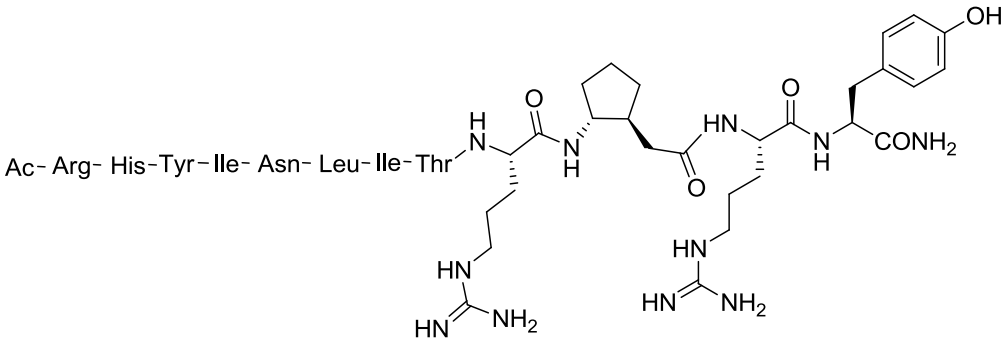

Ac-Arg^{25}-His^{26}-Tyr^{27}-Ile^{28}-Asn^{29}-Leu^{30}-Ile^{31}-Thr^{32}-Arg^{33}-(*1R,2S*-ACPA)^{34}-Arg^{35}-Tyr^{36}-NH$_2$ (168)

HR-MS (ES-MS): 1669.9586 ($C_{77}H_{123}N_{25}O_{17}$ $[M+4H]^{+4}$: calcd. 418.4955).

Appendix of NMR and X-Ray Data

NMR spectorscopic data

^{1}H-Spectra (Top of the page)

^{13}C-Spectra (Bottom of the page)

For the NPY analogues **161**, **162**, **163**, **164**, **165** and **166**, the HPLC chromatograms after purification are given.

(*1S*,*2S*)-2-(ethoxycarbonyl)-N-((*S*)-1-phenylethyl)cyclopentanaminium chloride (136)

^{1}H NMR (CD_3OD, 300MHz)

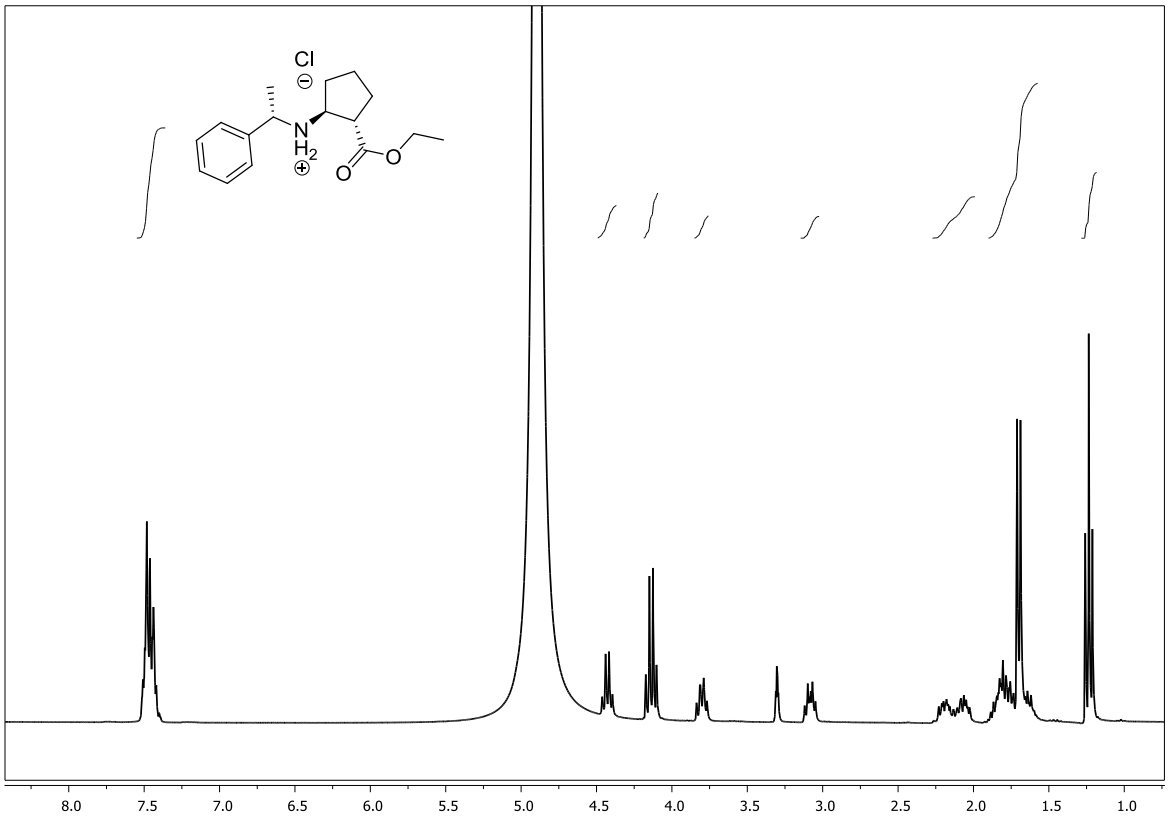

^{13}C NMR (CD_3OD, 300MHz)

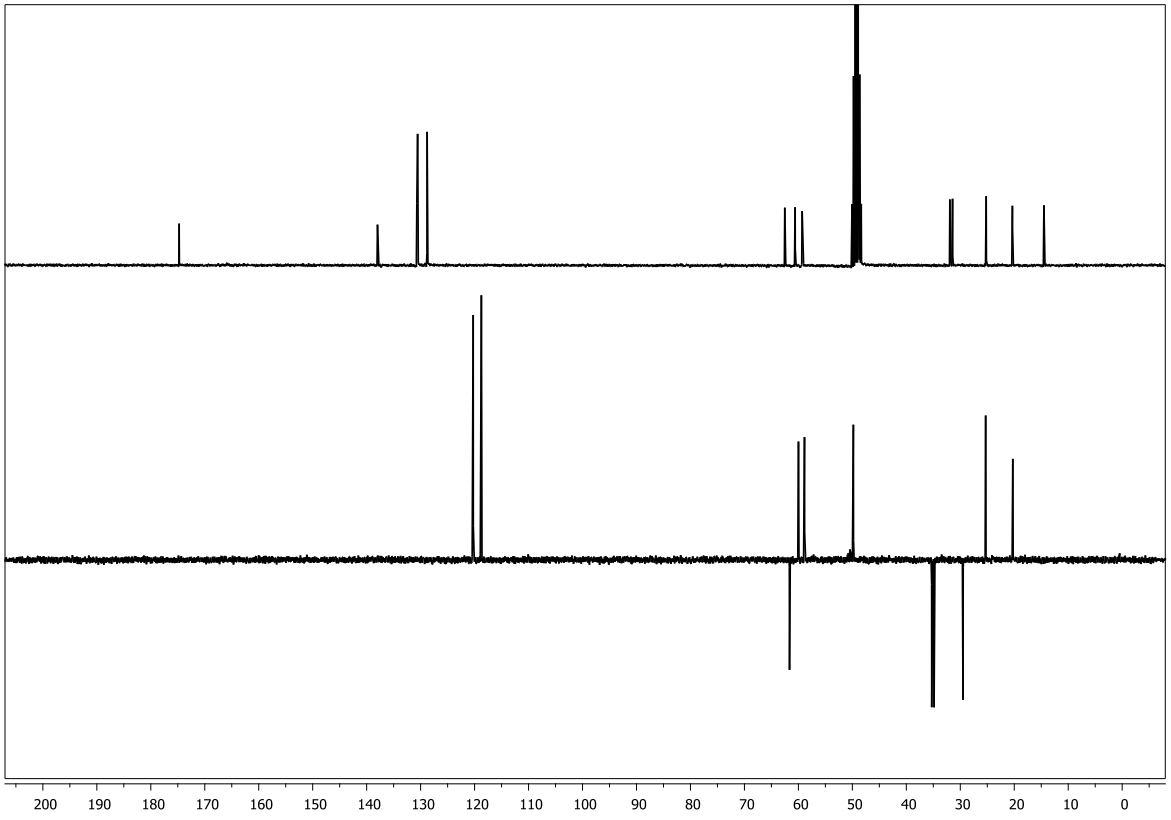

(*1S*,*2S*)-2-((*S*)-1-phenylethylamino)cyclopentanecarboxylic acid (137)

^{1}H NMR (DMSO-*d*6, 300 MHz)

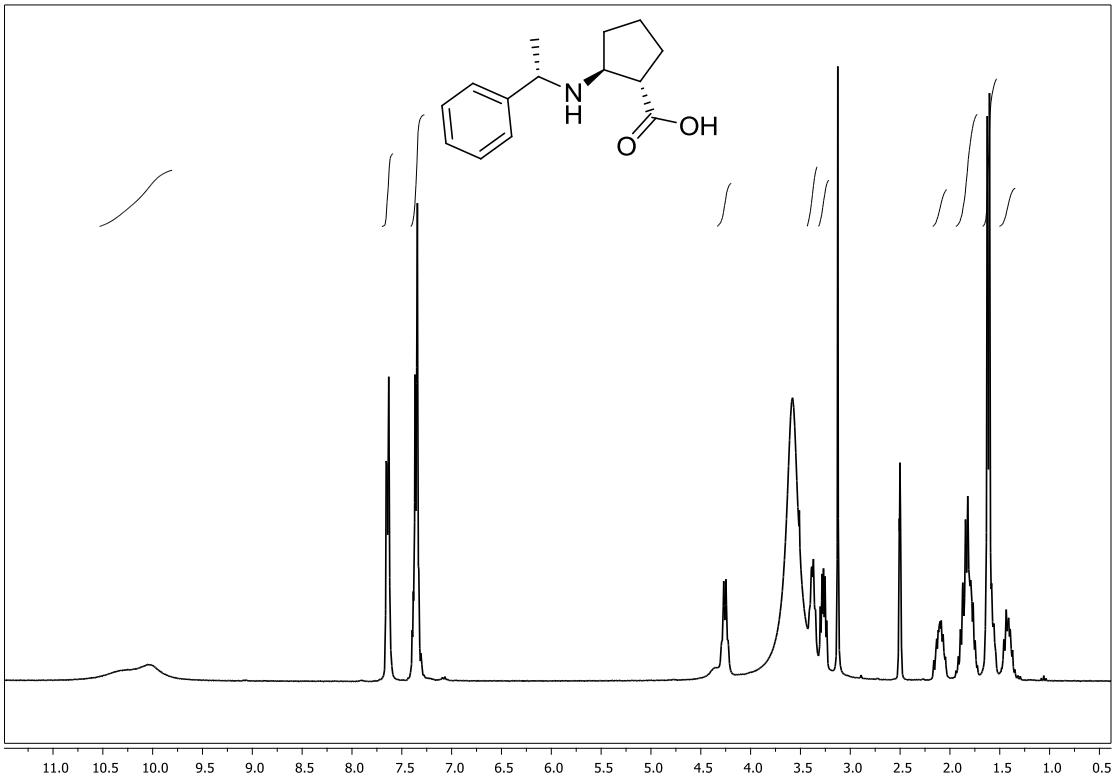

^{13}C NMR (DMSO- *d*6, 300MHz)

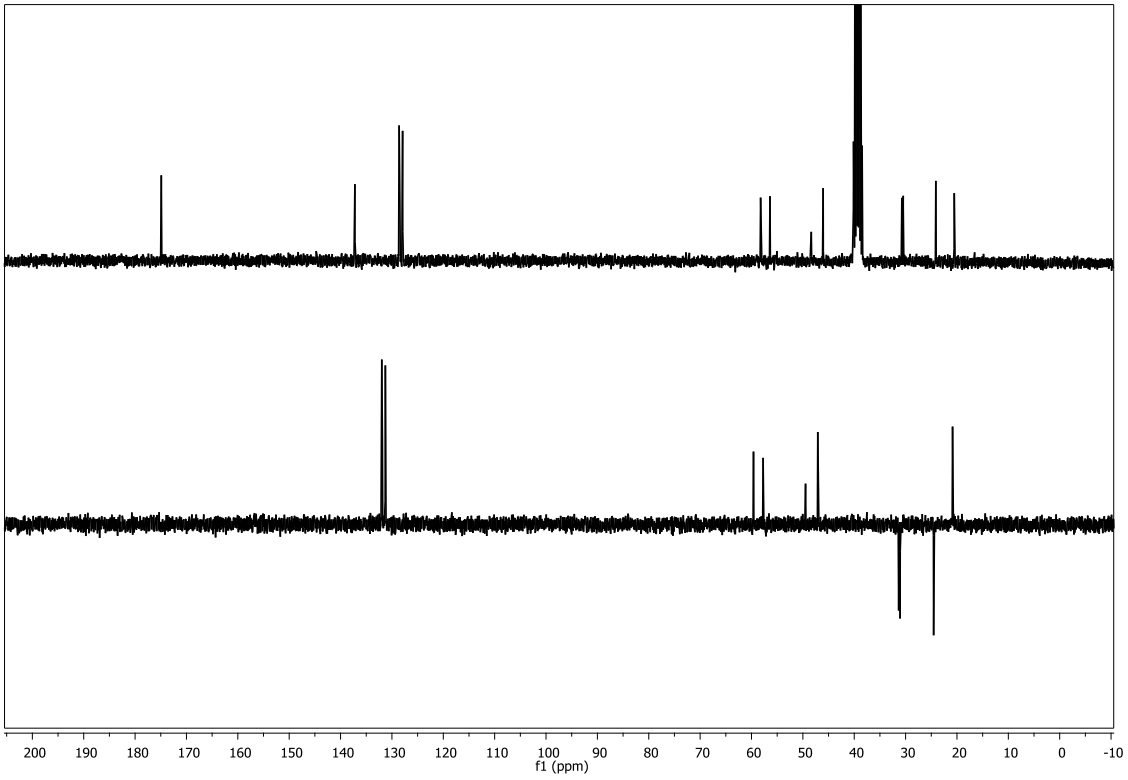

(*1S,2S*)-2-aminocyclopentanecarboxylic acid (33)

^{1}H NMR (D_2O, 300 MHz)

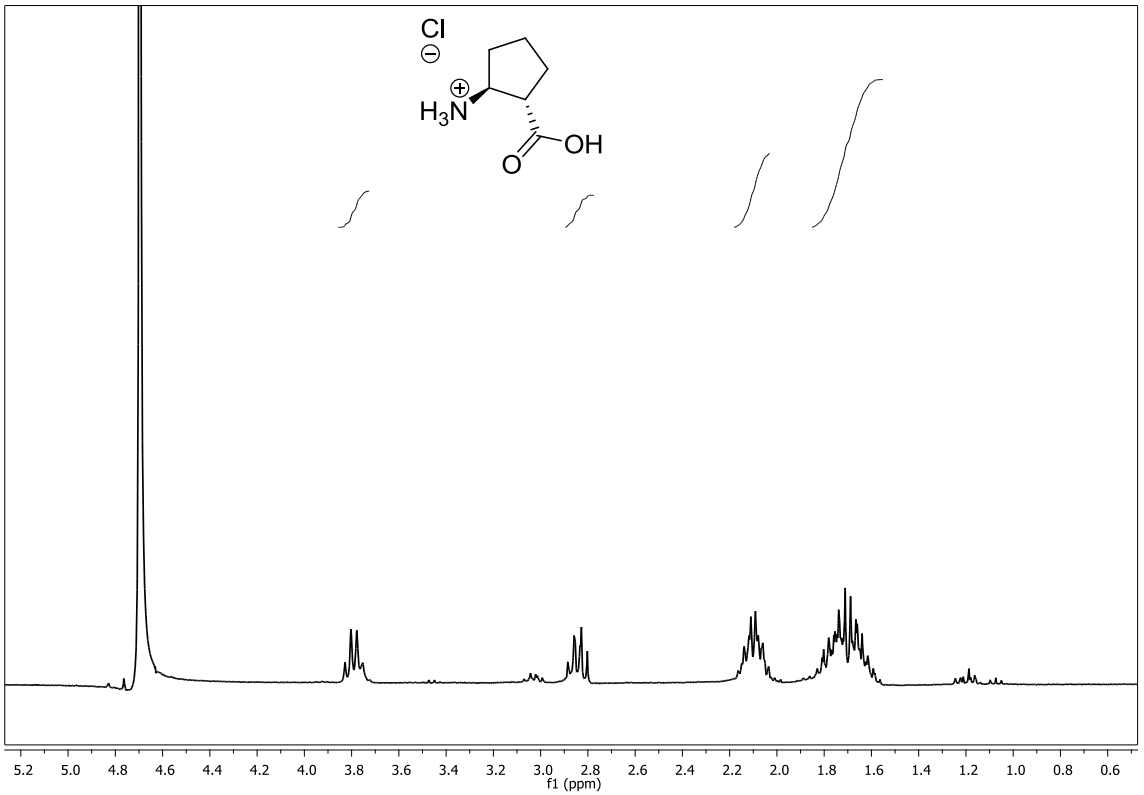

^{13}C NMR (D_2O, 300MHz)

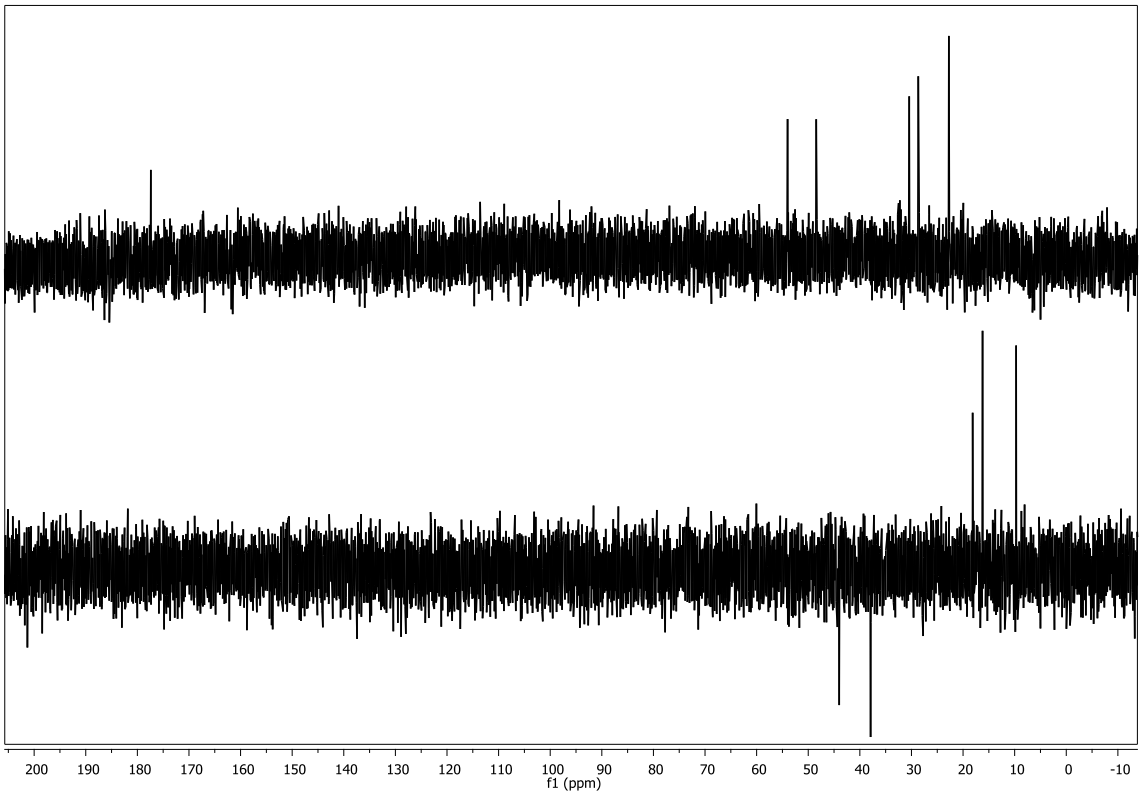

(*1S*,*2S*)-2-(((9H-fluoren-9-yl)methoxy)carbonylamino)cyclopentanecarboxylic acid (132)

^{1}H NMR (CD_3OD, 300 MHz)

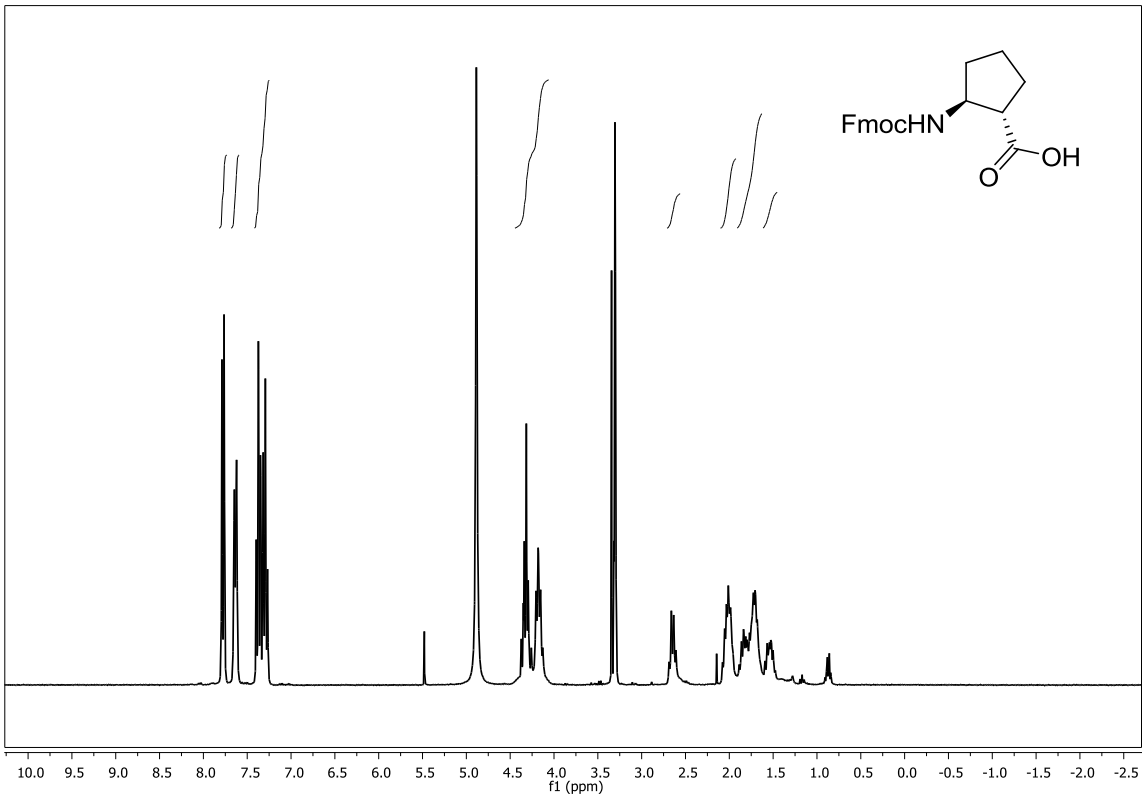

^{13}C NMR (CD_3OD, 300MHz)

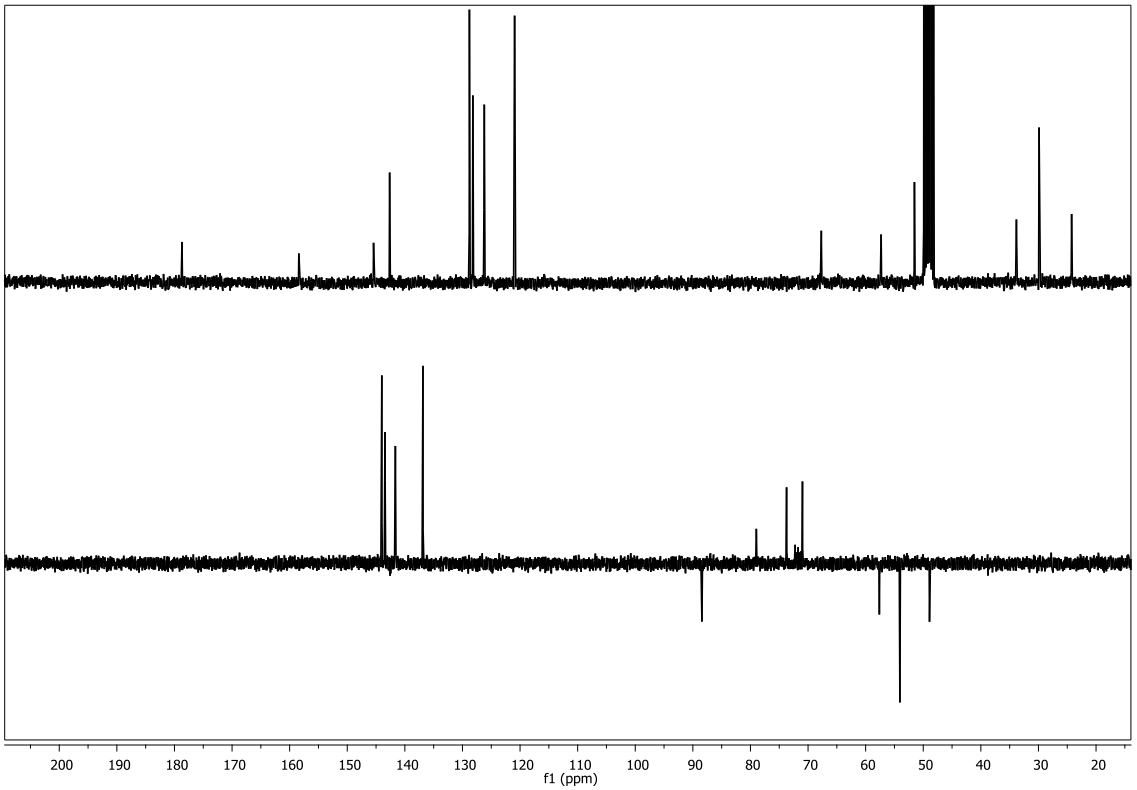

(*1S*,*2S*)-2-(((9H-fluoren-9-yl)methoxy)carbonylamino)cyclopentanecarboxylic acid (131)

^{1}H NMR (DMSO-*d*6, 300 MHz)

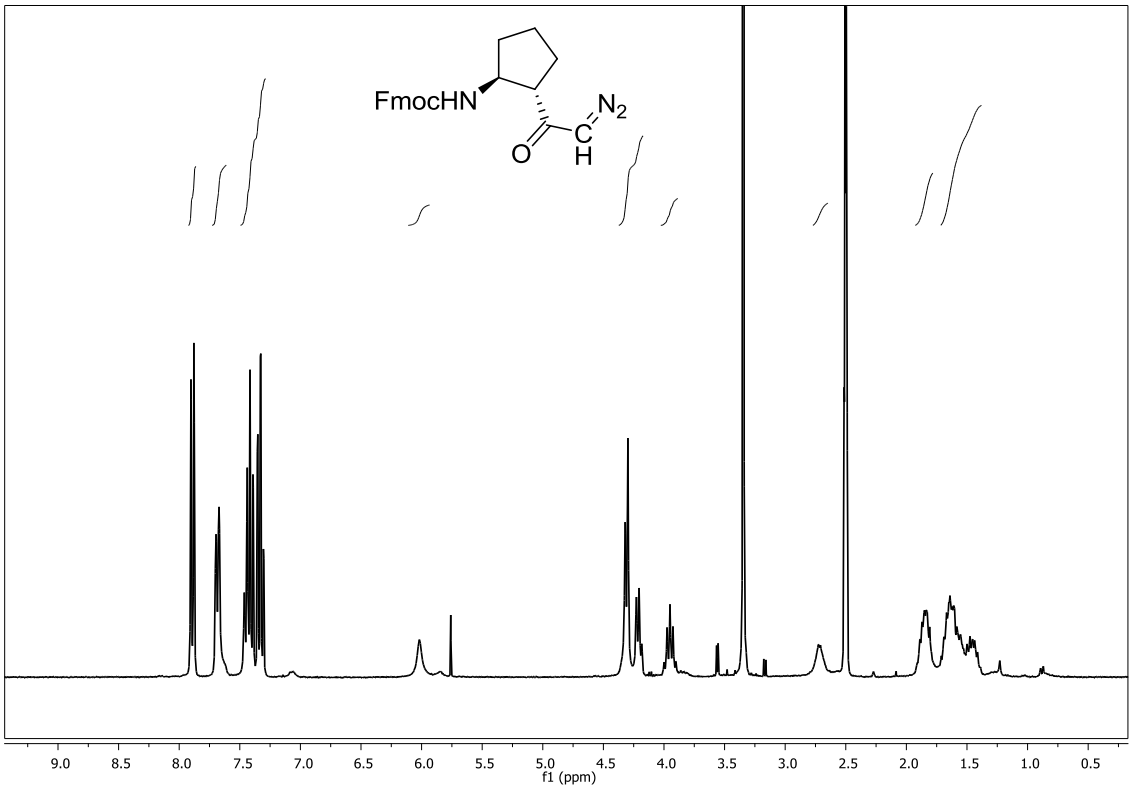

^{13}C NMR (DMSO-*d*6, 300 MHz)

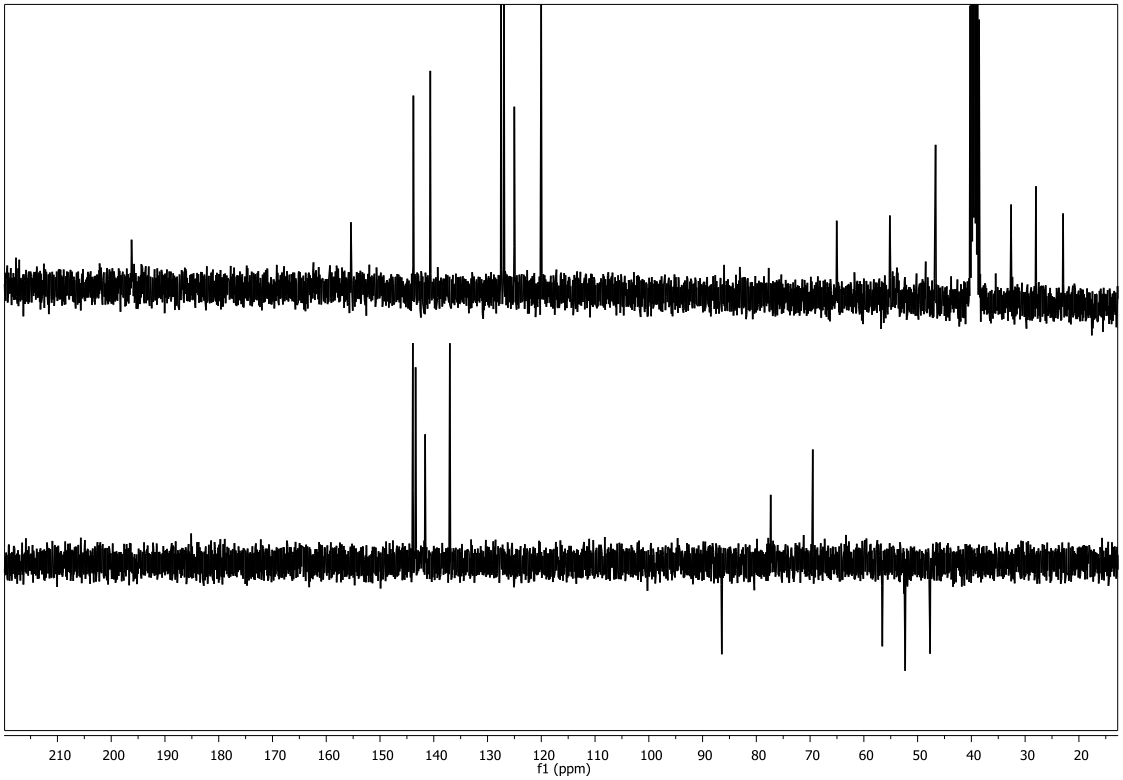

2-((*1R,2S*)-2-(((9H-fluoren-9-yl)methoxy)carbonylamino)cyclopentyl)acetic acid (130)

^{1}H NMR (CD_3OD, 300 MHz)

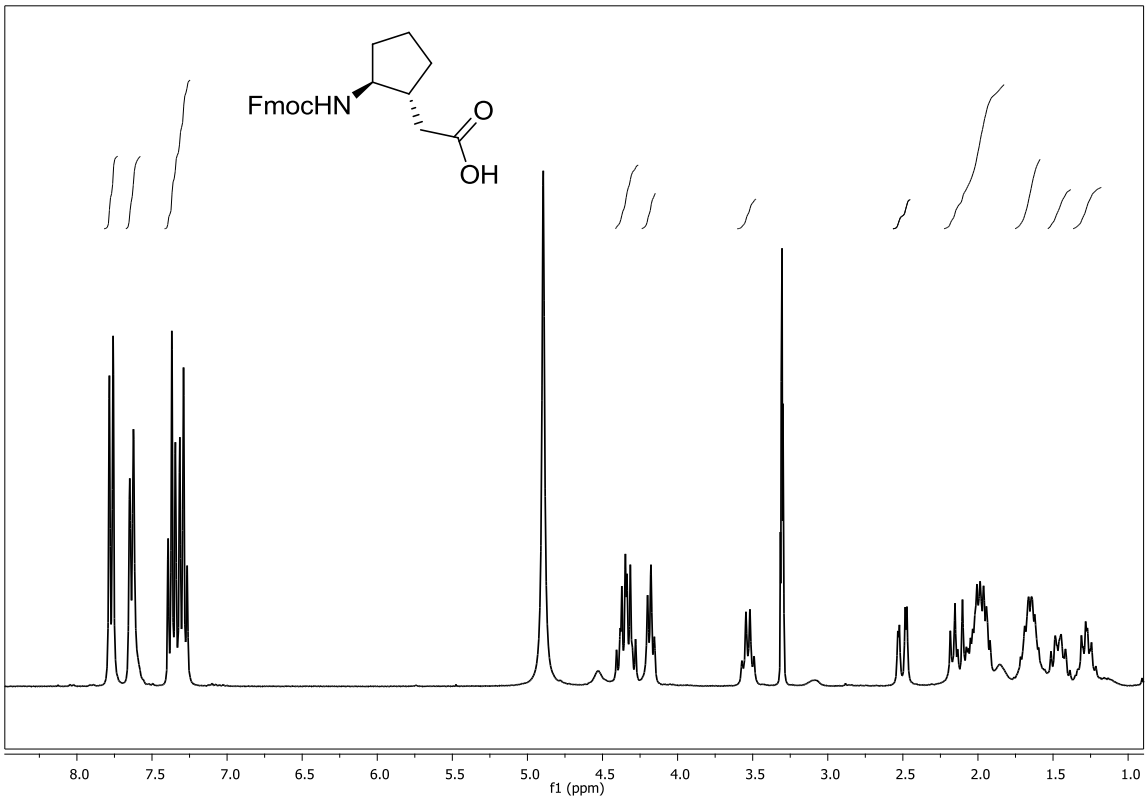

^{13}C NMR (CD_3OD, 300 MHz)

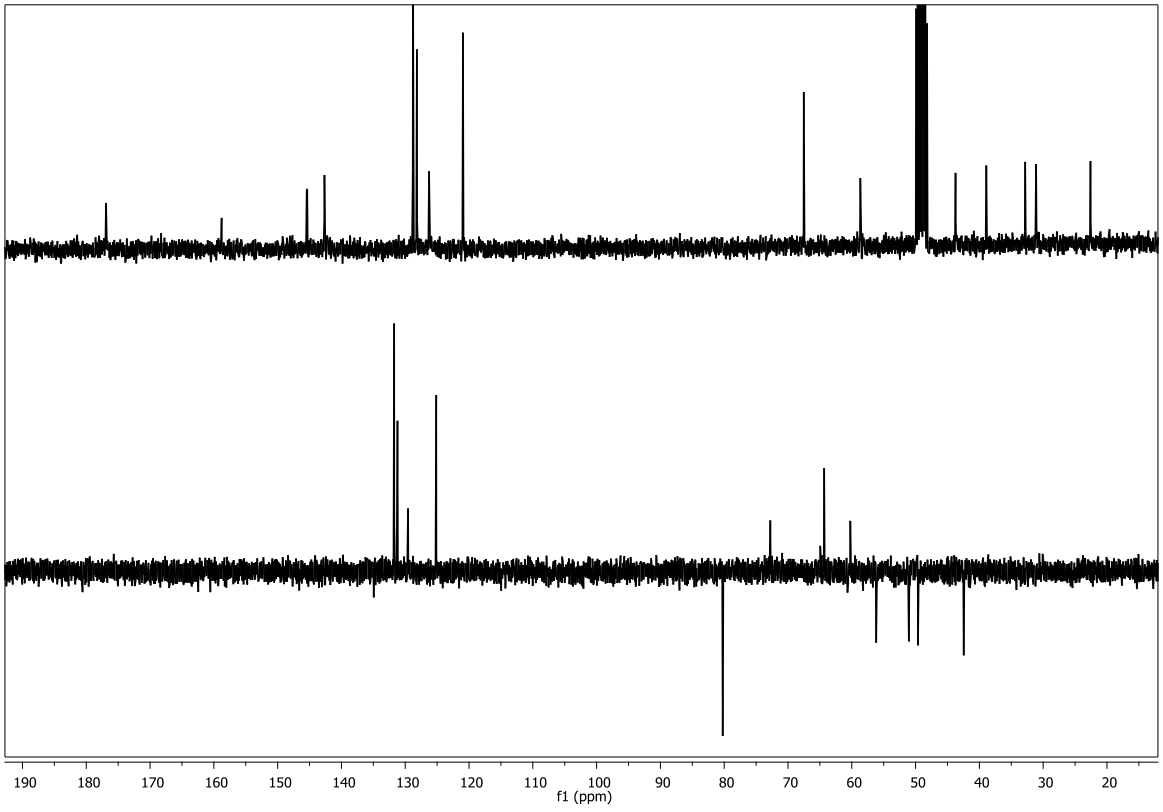

ethyl 2-((*E*,*Z*)-2-((*R*)-1-phenylethylimino)cyclopentyl)acetate (140)

^{1}H NMR ($CDCl_3$, 300 MHz)

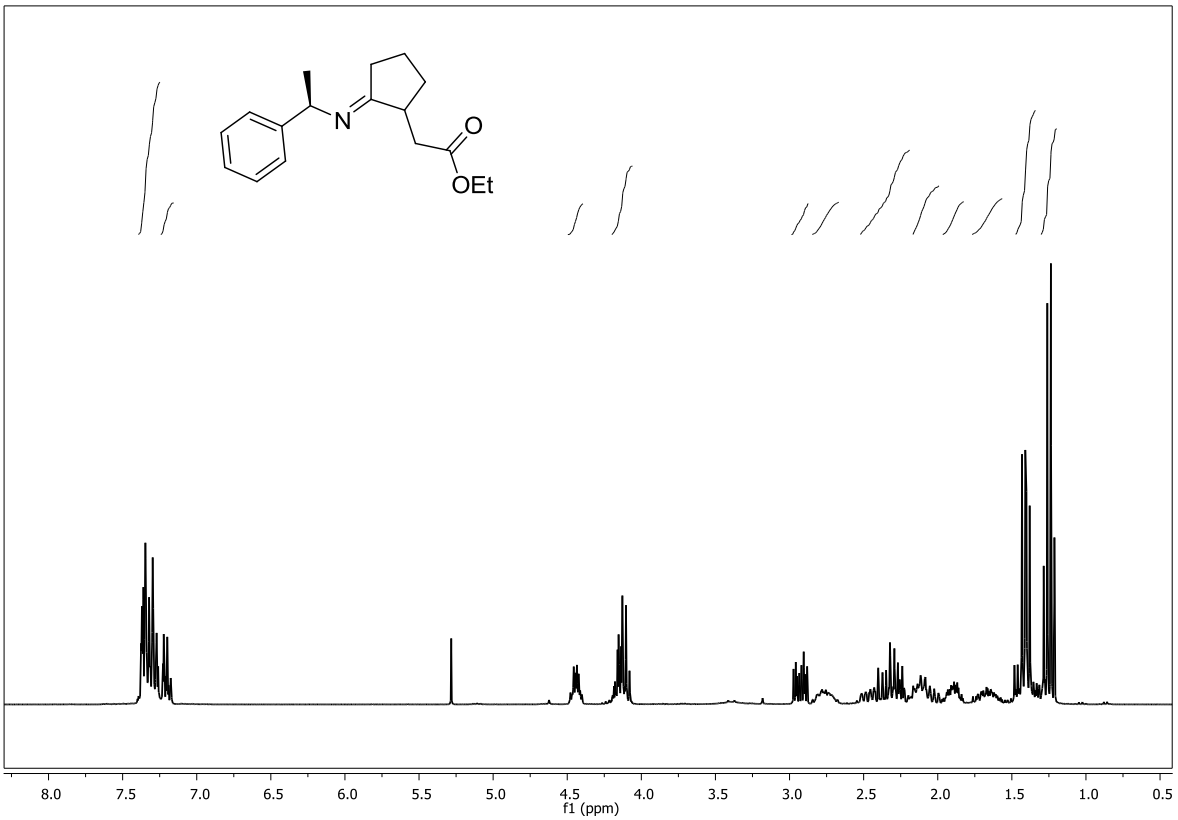

^{13}C NMR ($CDCl_3$, 300 MHz)

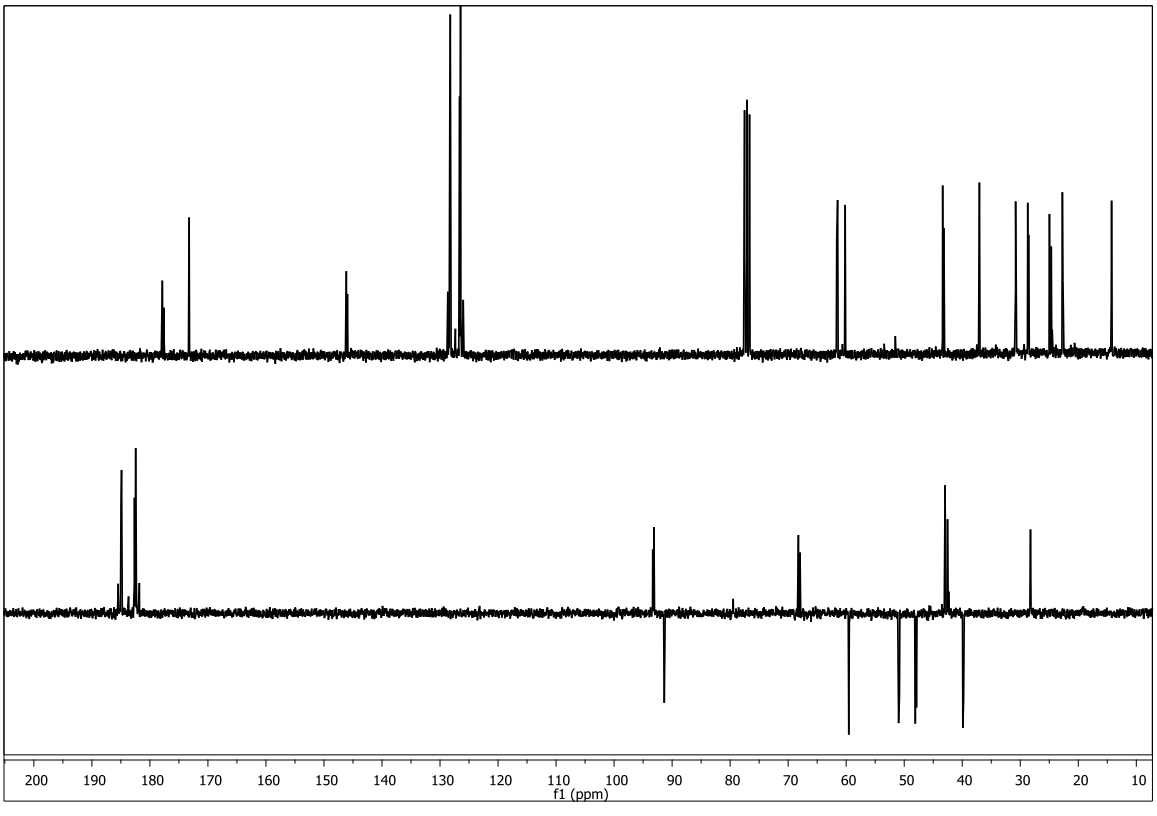

ethyl 2-((*1S,2R*)-2-((*R*)-1-phenylethylamino)cyclopentyl)acetate (148)

^{1}H NMR ($CDCl_3$, 300 MHz)

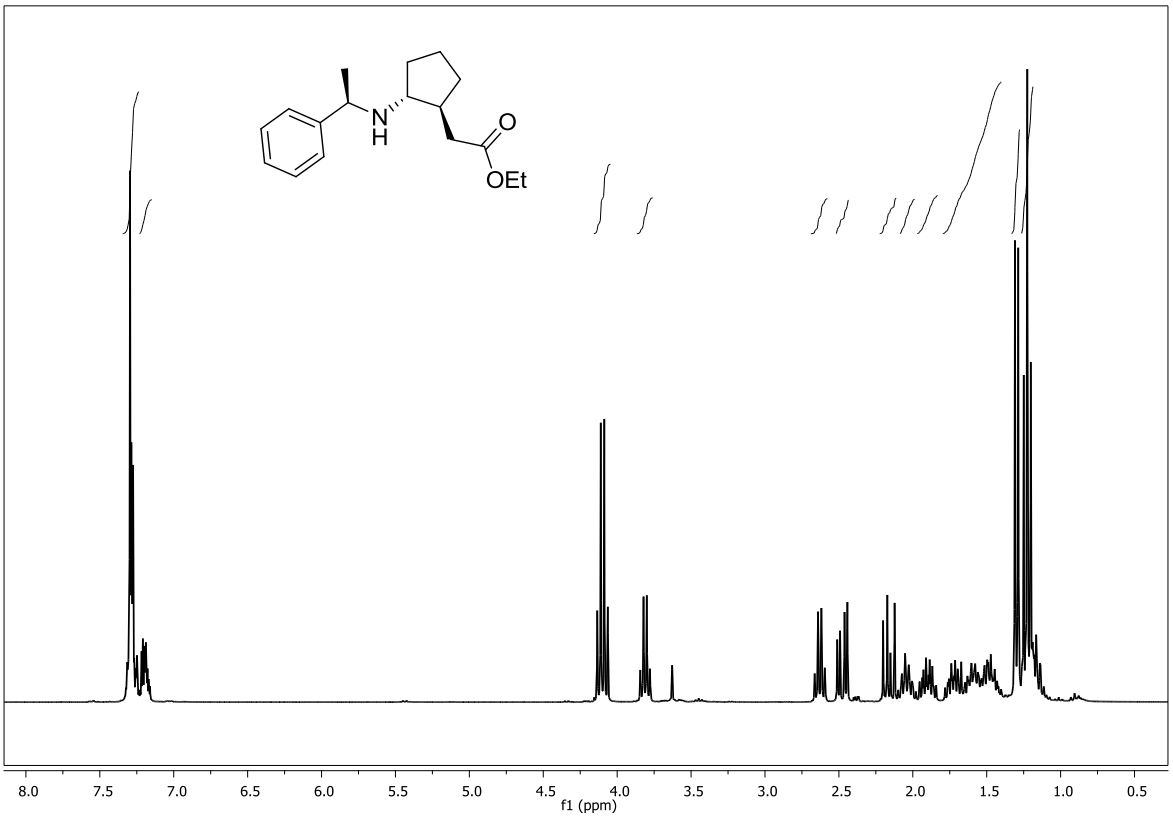

^{13}C NMR ($CDCl_3$, 300 MHz)

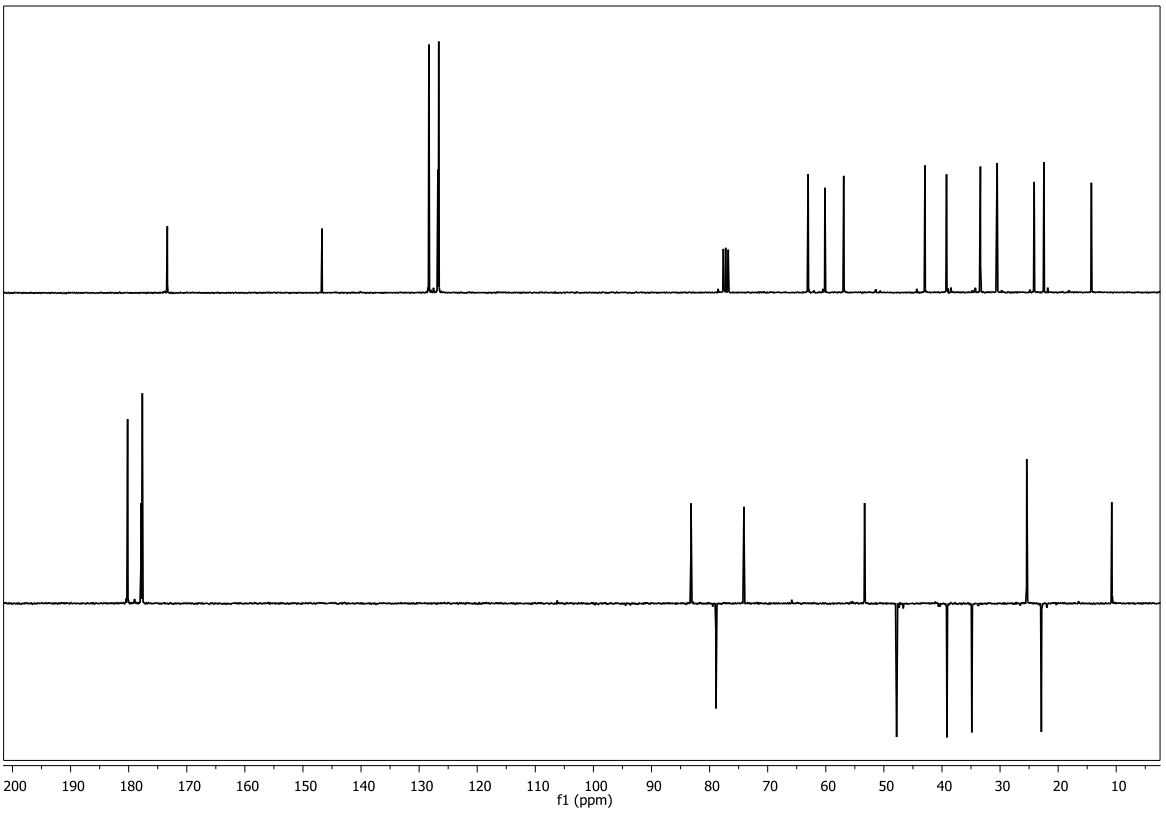

ethyl 2-((*1S,2S*)-2-((*R*)-1-phenylethylamino)cyclopentyl)acetate (149)

^{1}H NMR ($CDCl_3$, 300 MHz)

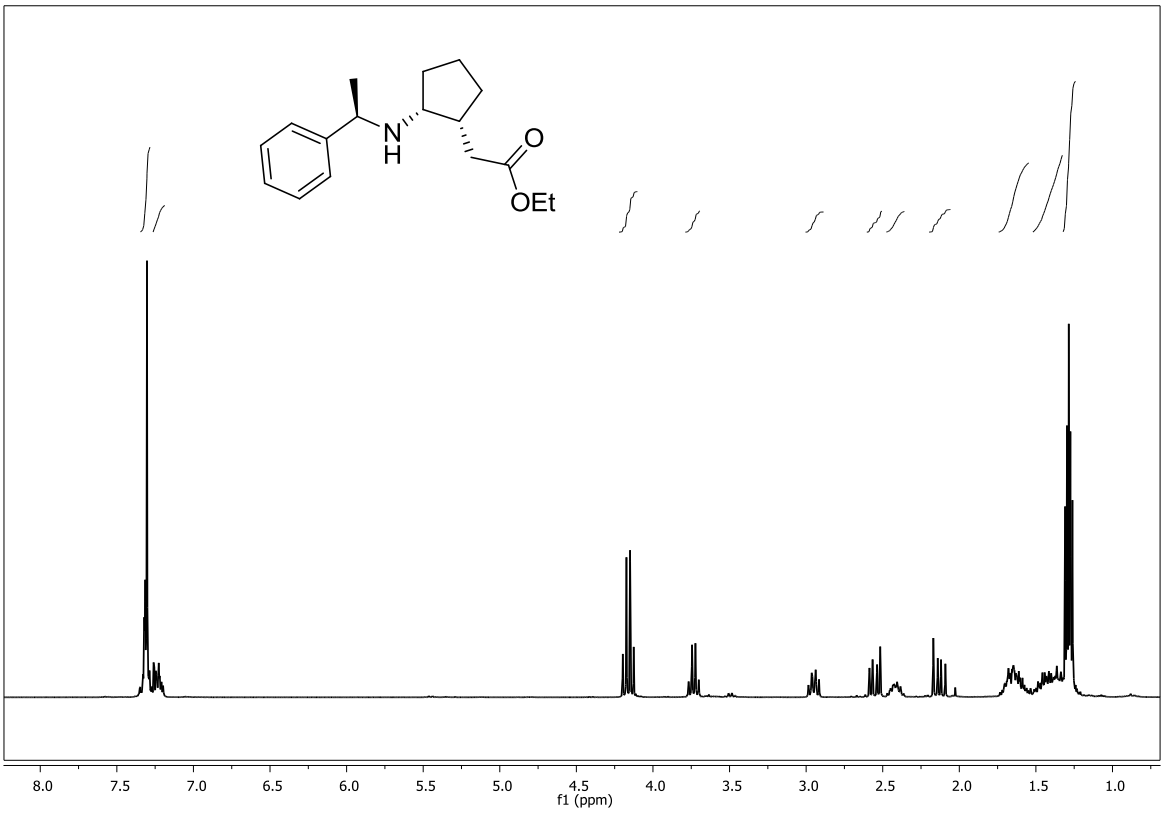

^{13}C NMR ($CDCl_3$, 300 MHz)

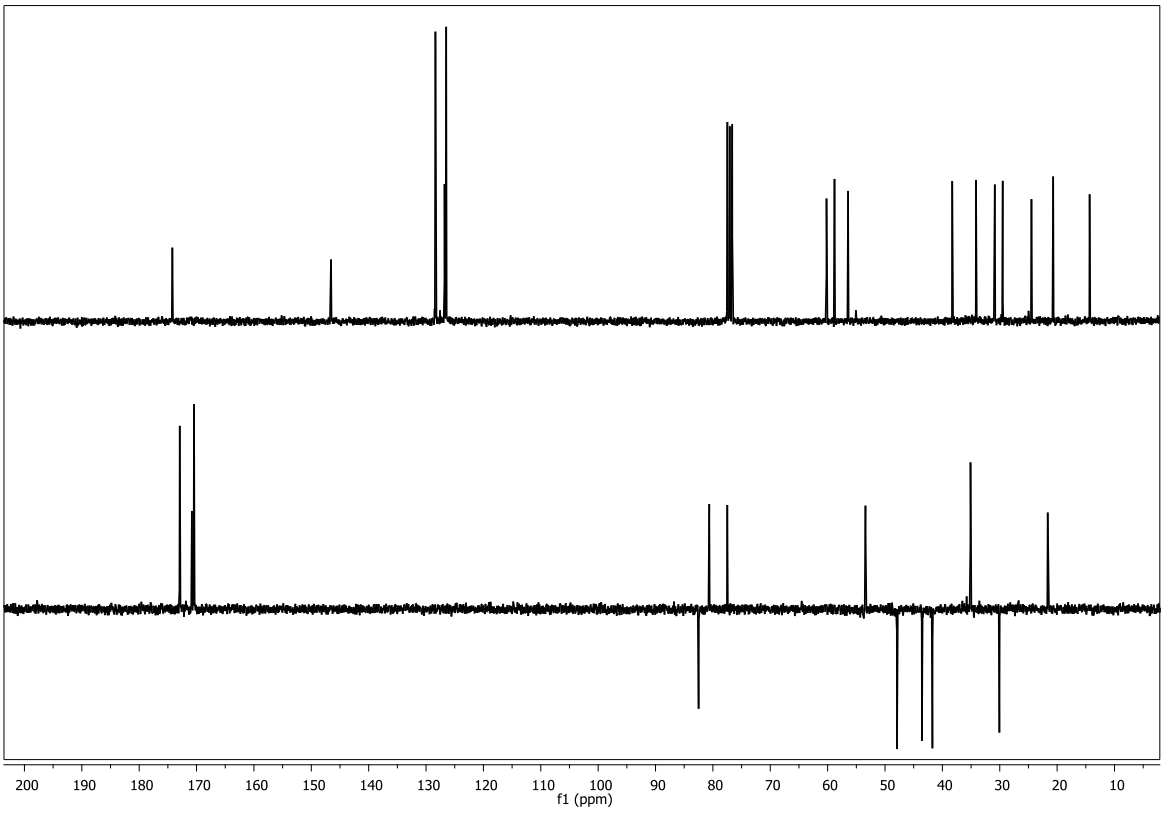

(*1R,2S*)-2-(2-ethoxy-2-oxoethyl)-N-((*R*)-1-phenylethyl)cyclopentanaminium chloride (150)

^{1}H NMR (DMSO-d_6, 300 MHz)

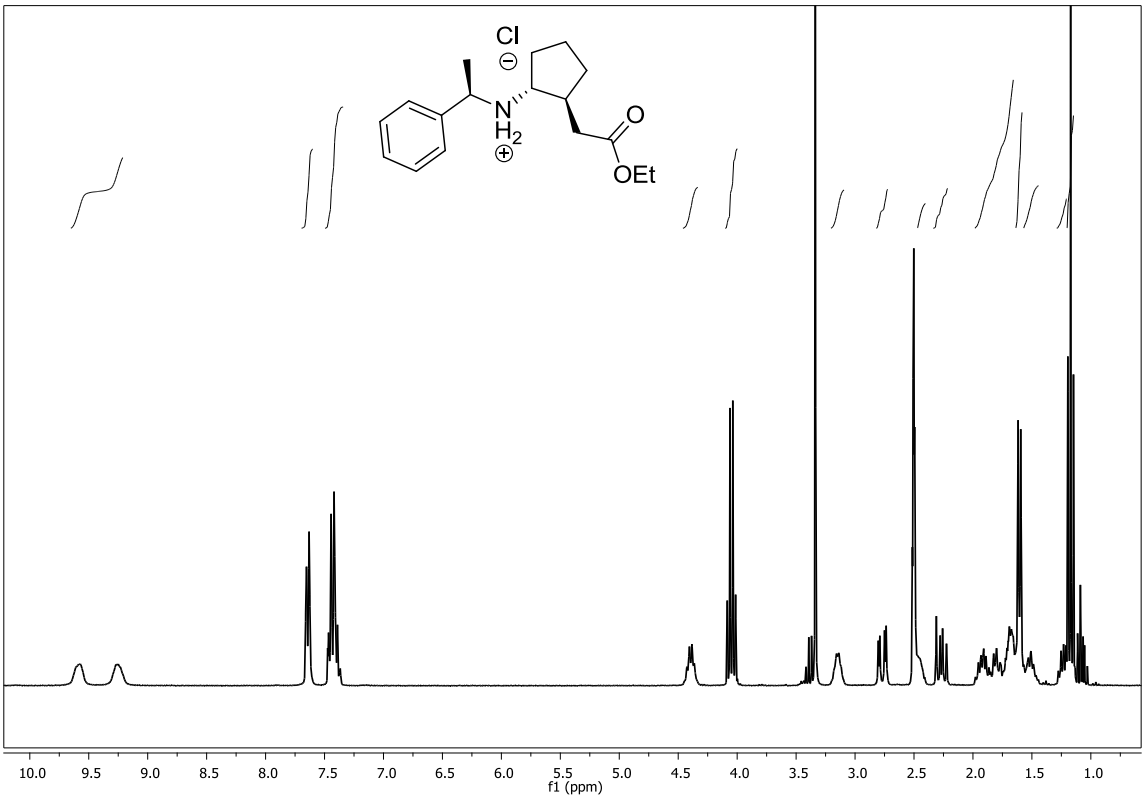

^{13}C NMR (DMSO-d_6,300MHz)

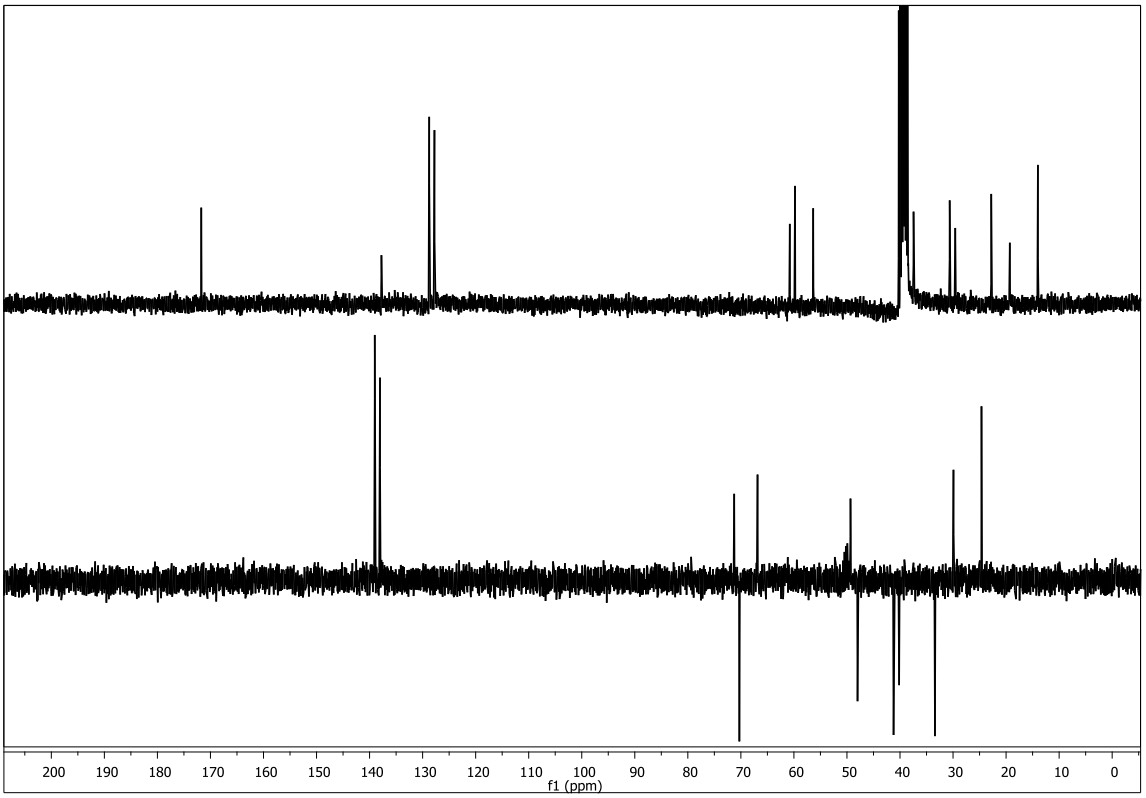

(*1S*,*2S*)-2-(2-ethoxy-2-oxoethyl)-N-((*R*)-1-phenylethyl)cyclopentanaminium chloride (151)

^{1}H NMR (DMSO-d_6, 300 MHz)

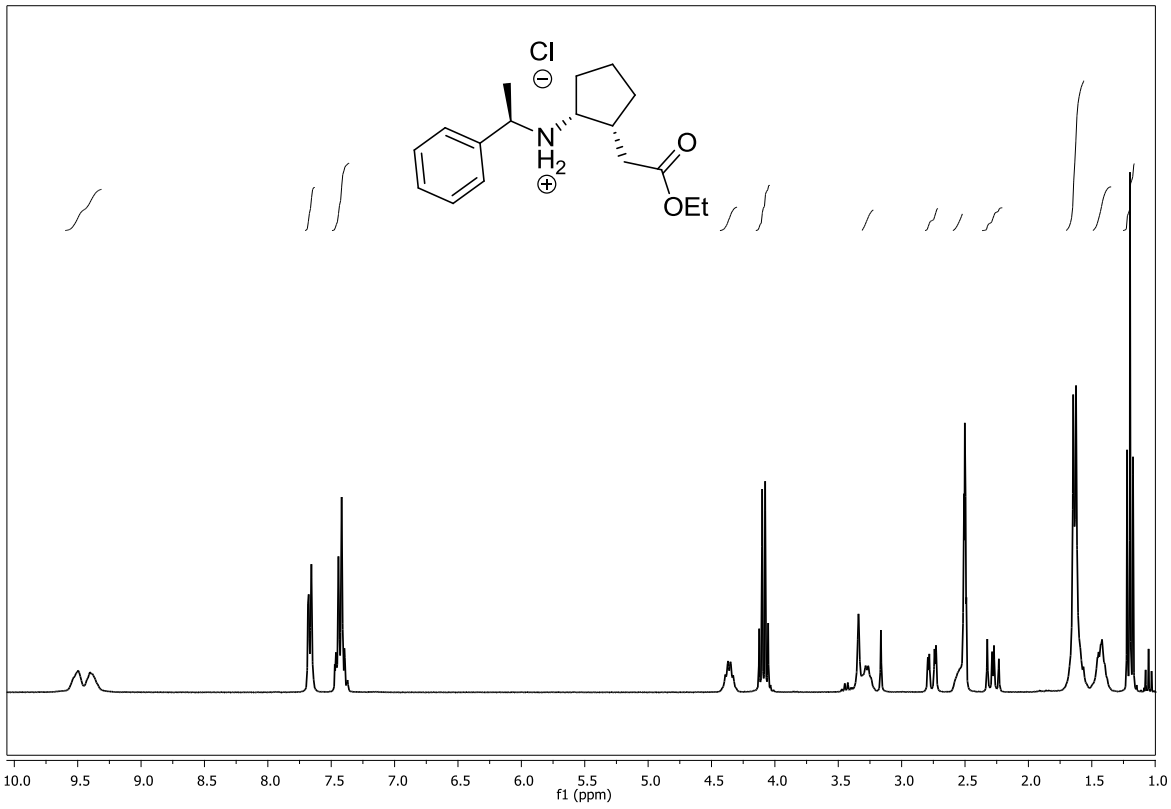

^{13}C NMR (DMSO-d_6,300MHz)

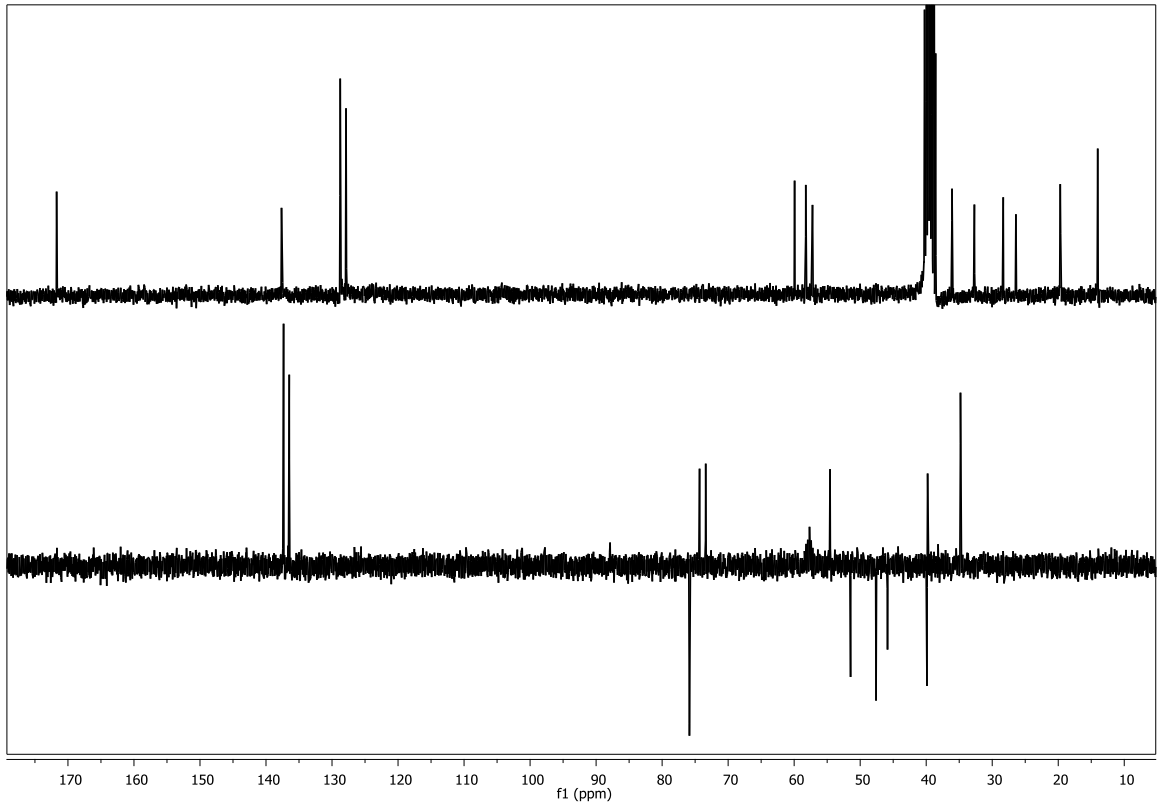

2-((*1S,2R*)-2-((*R*)-1-phenylethylamino)cyclopentyl)acetic acid (152)

^{1}H NMR (DMSO-d_6, 300 MHz)

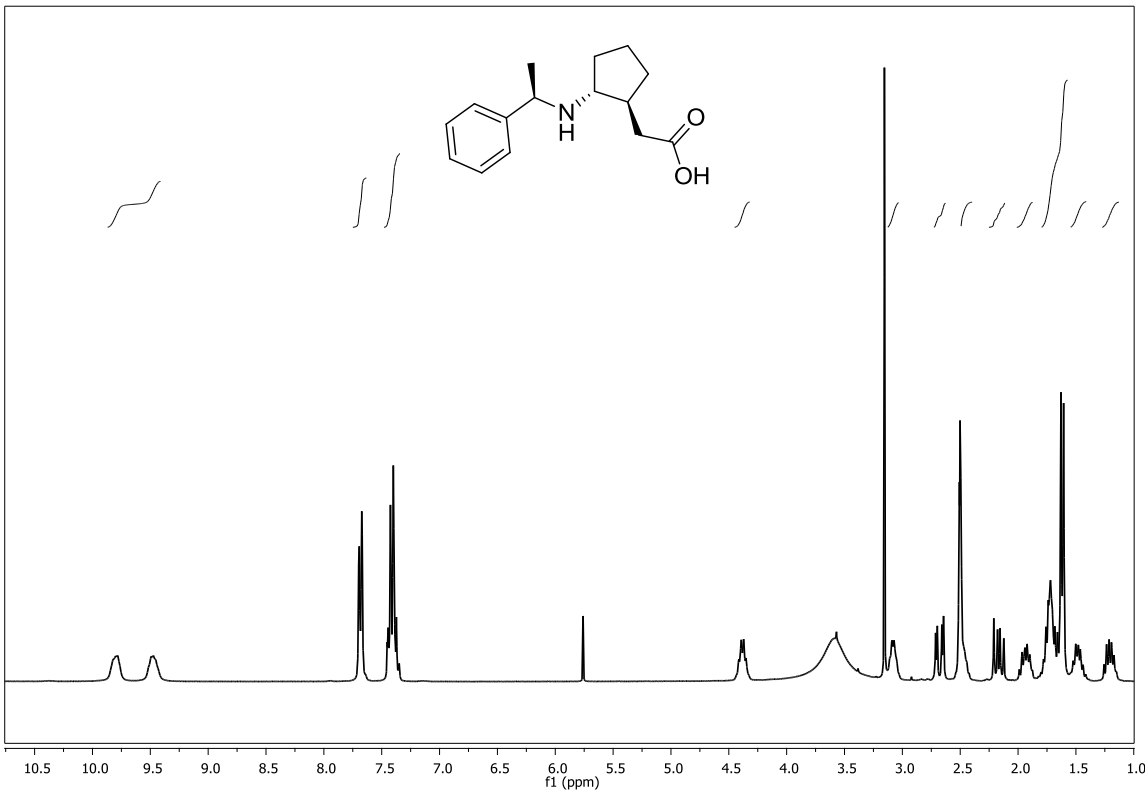

^{13}C NMR (DMSO-d_6,300MHz)

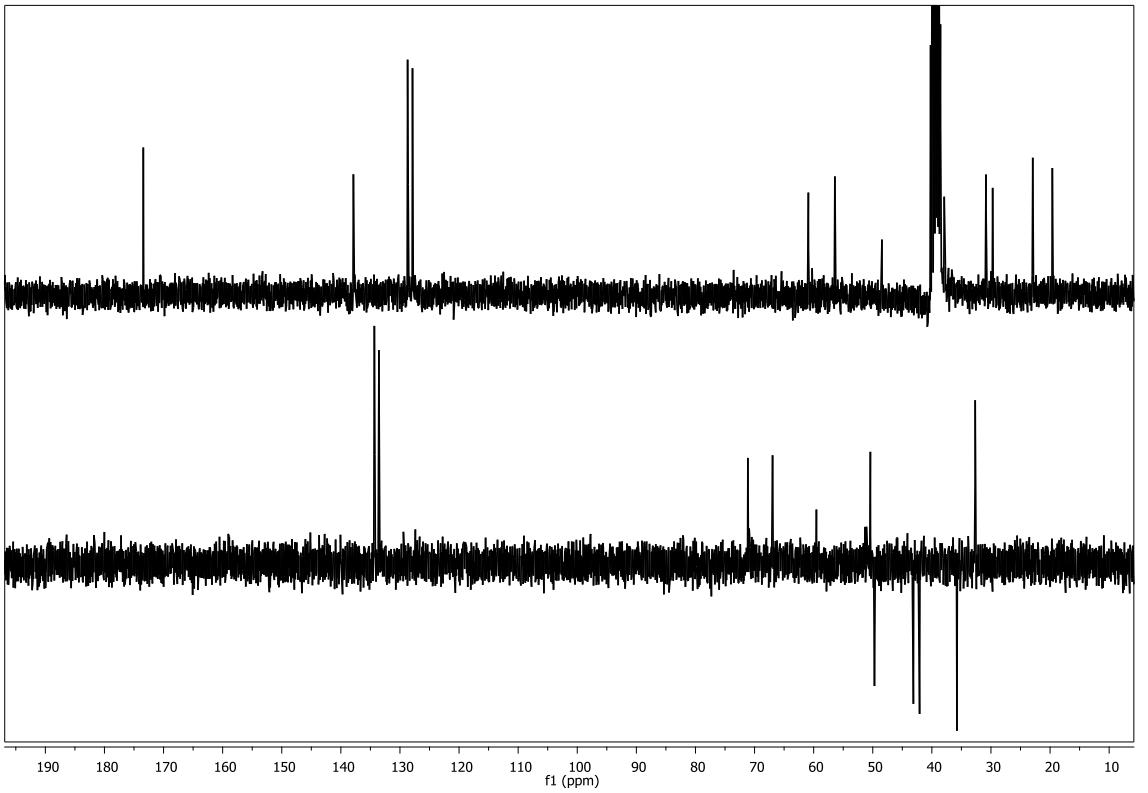

2-((*1S,2R*)-2-aminocyclopentyl)acetic acid (31)

^{1}H NMR (D_2O, 300 MHz)

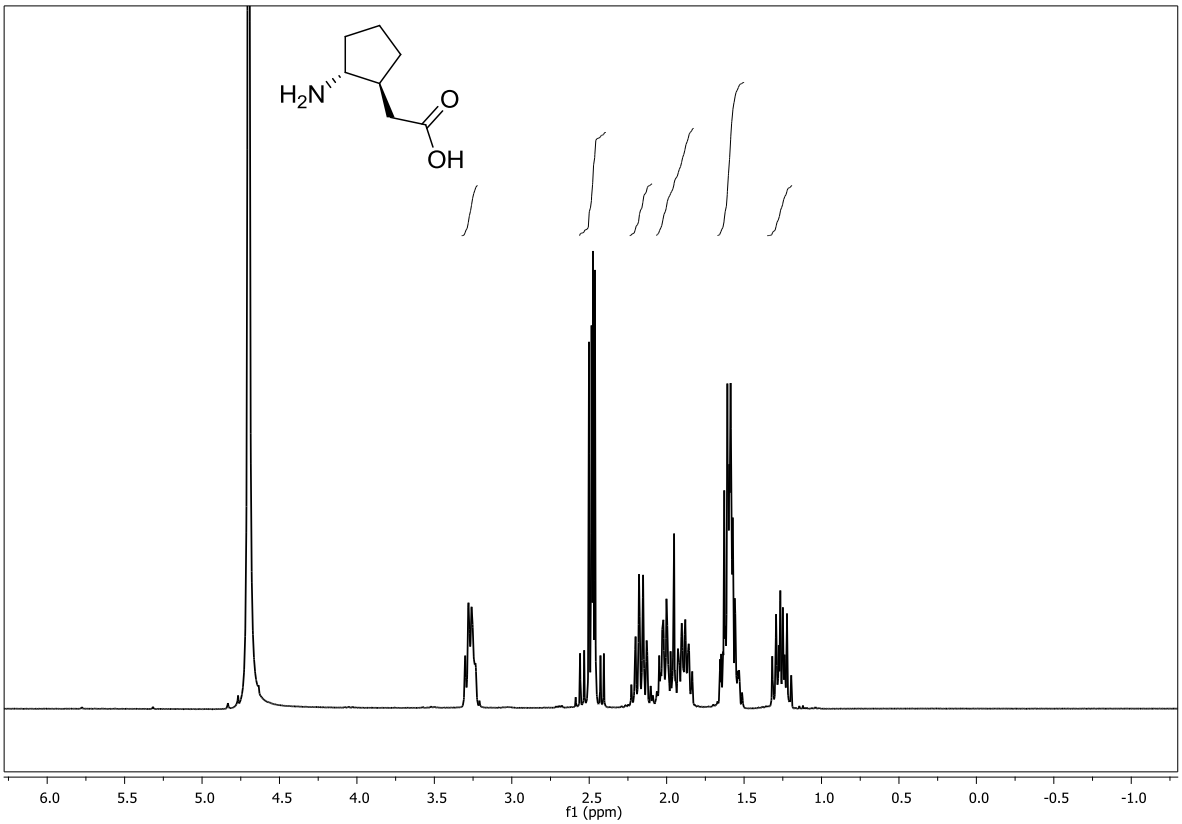

^{13}C NMR (D_2O,300MHz)

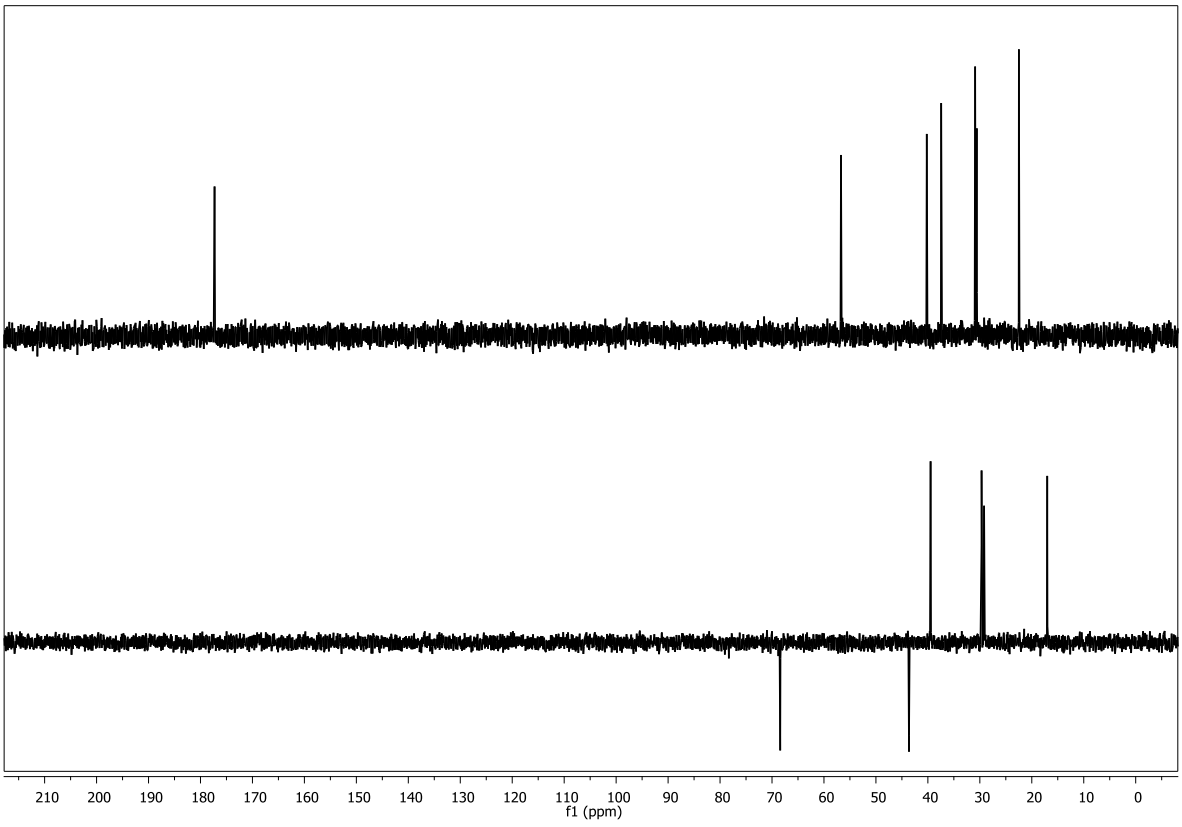

2-((*1S,2R*)-2-(((9H-fluoren-9-yl)methoxy)carbonylamino)cyclopentyl)acetic acid (153)

^{1}H NMR (CD_3OD, 300MHz)

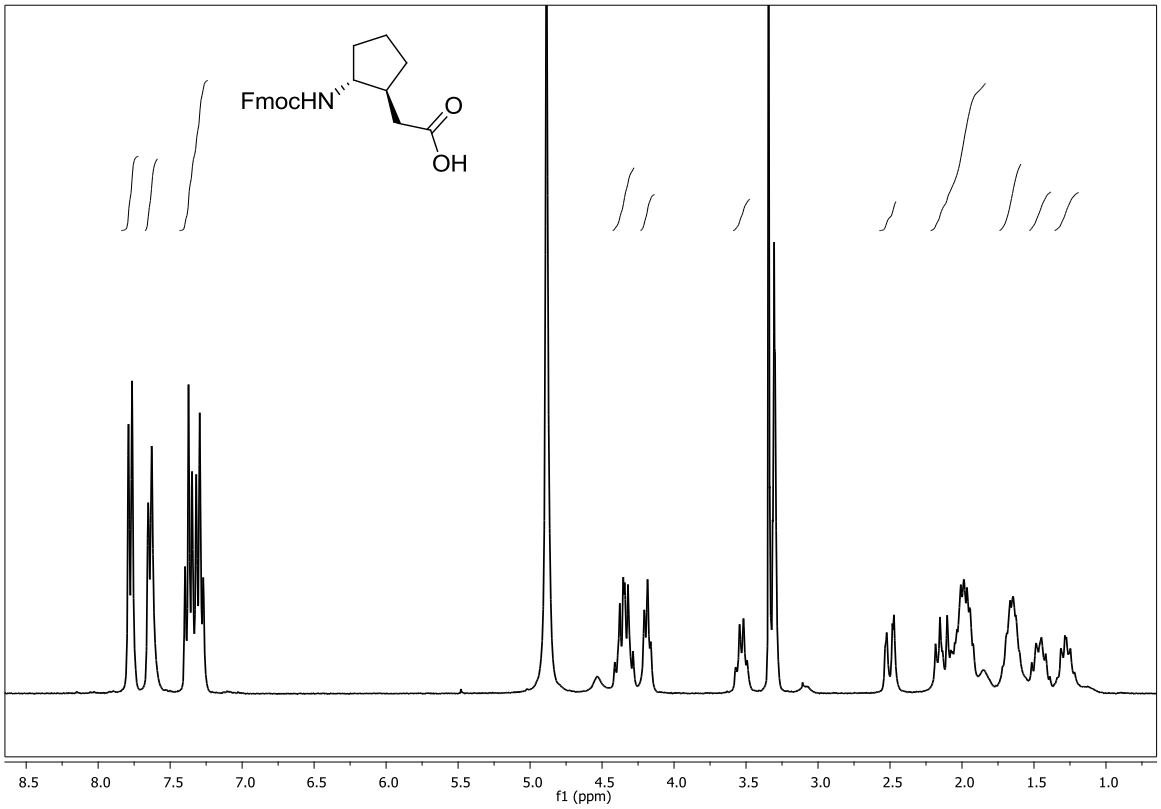

^{13}C NMR (CD_3OD, 300 MHz)

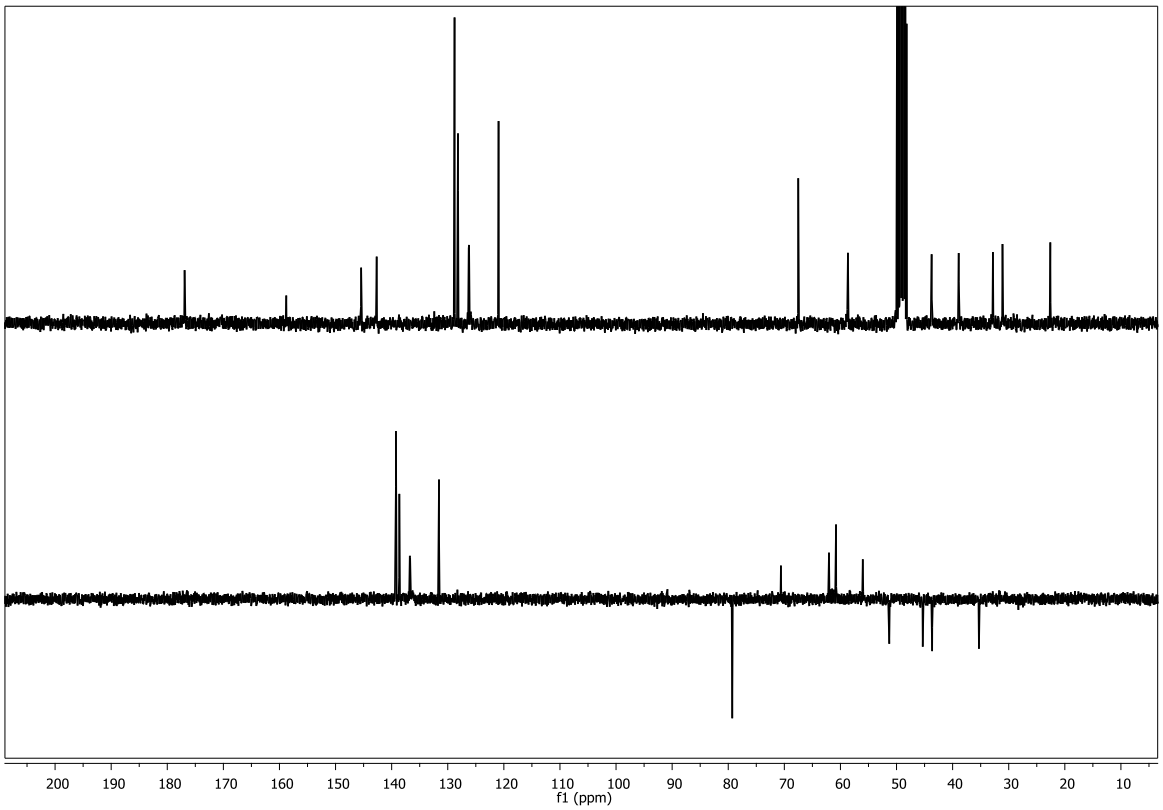

(3a*S*,6a*S*)-1-((*R*)-1-phenylethyl)hexahydrocyclopenta[b]pyrrol-2(1H)-one (141)

^{1}H NMR (DMSO-d_6, 300 MHz)

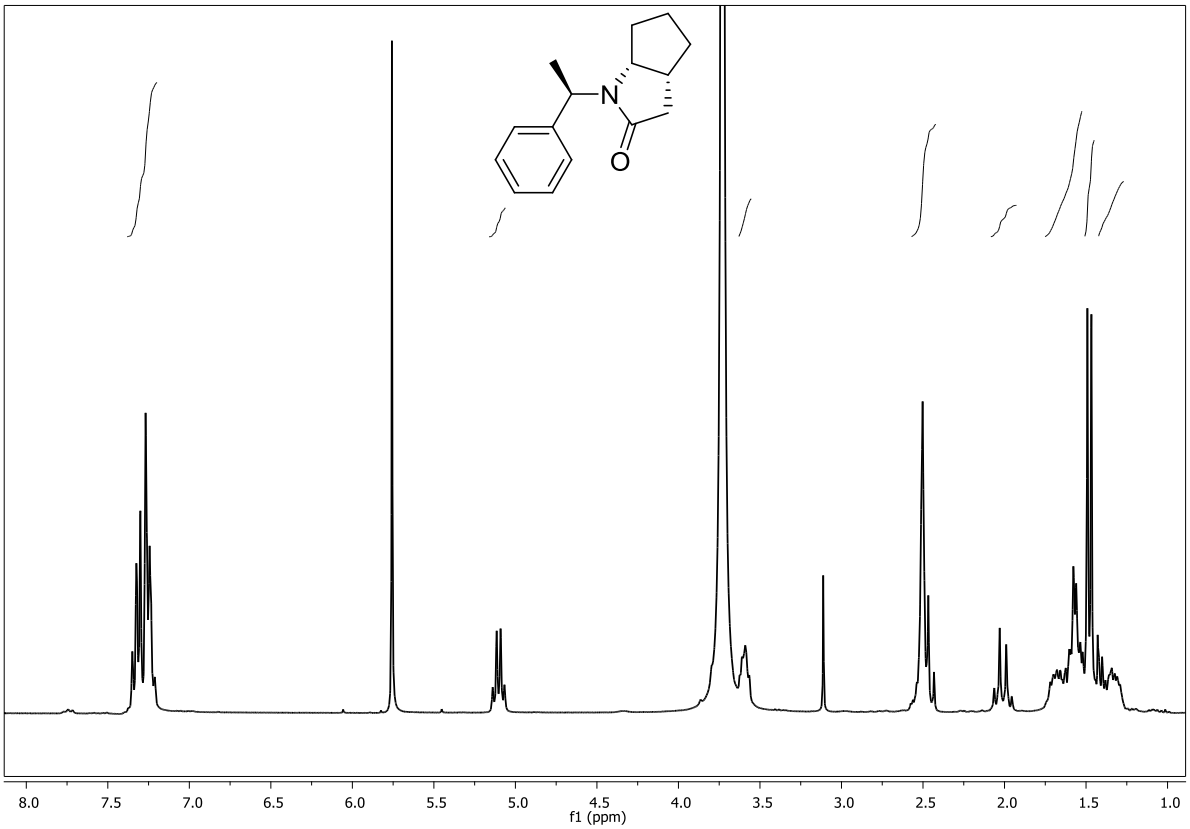

^{13}C NMR (DMSO-d_6,300MHz)

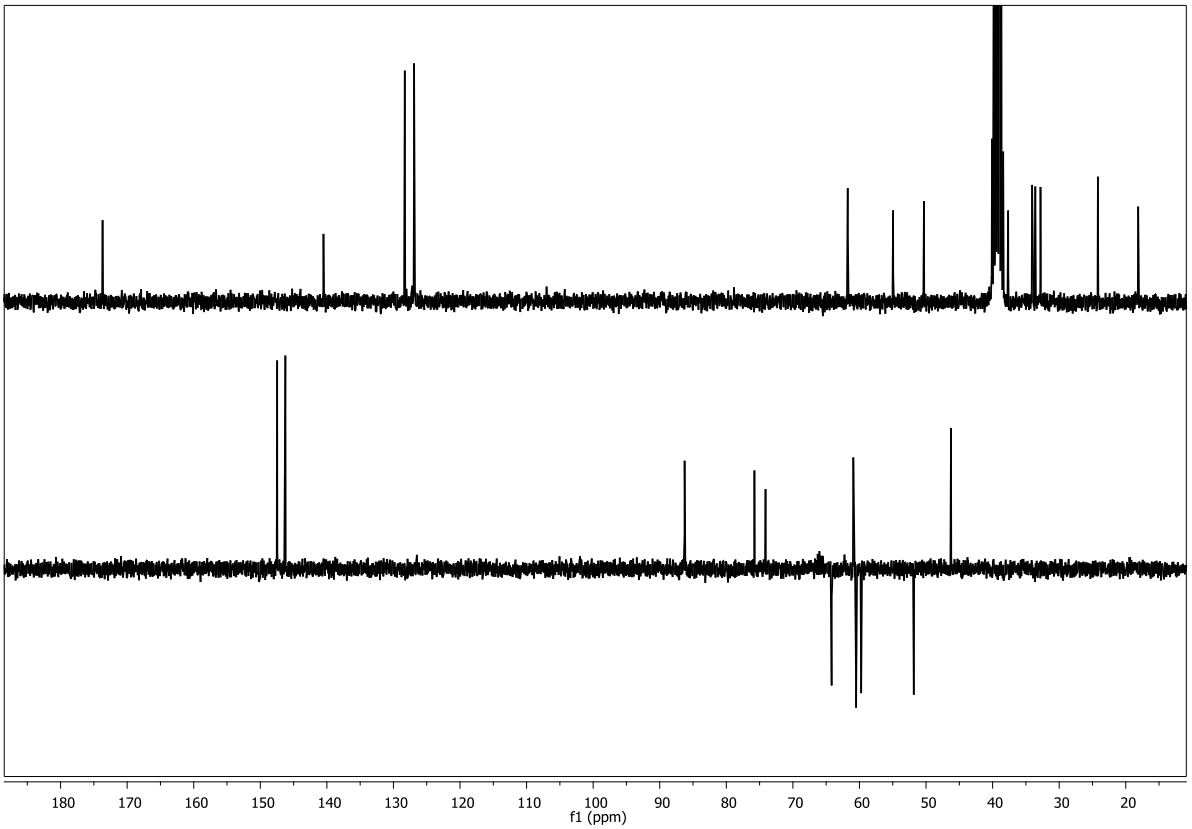

(3a*S*,6a*S*)-hexahydrocyclopenta[b]pyrrol-2(1H)-one (142)

^{1}H NMR ($CDCl_3$, 300 MHz)

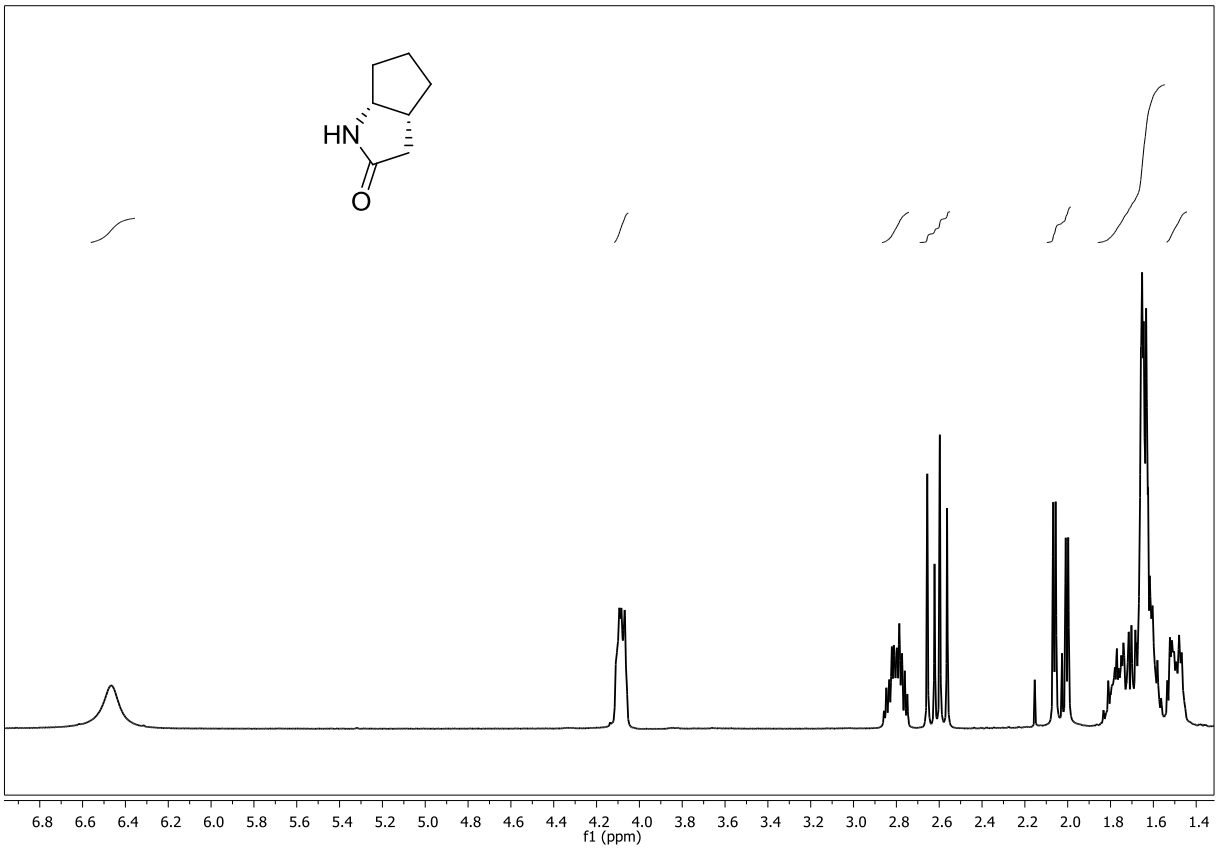

^{13}C NMR ($CDCl_3$,300MHz)

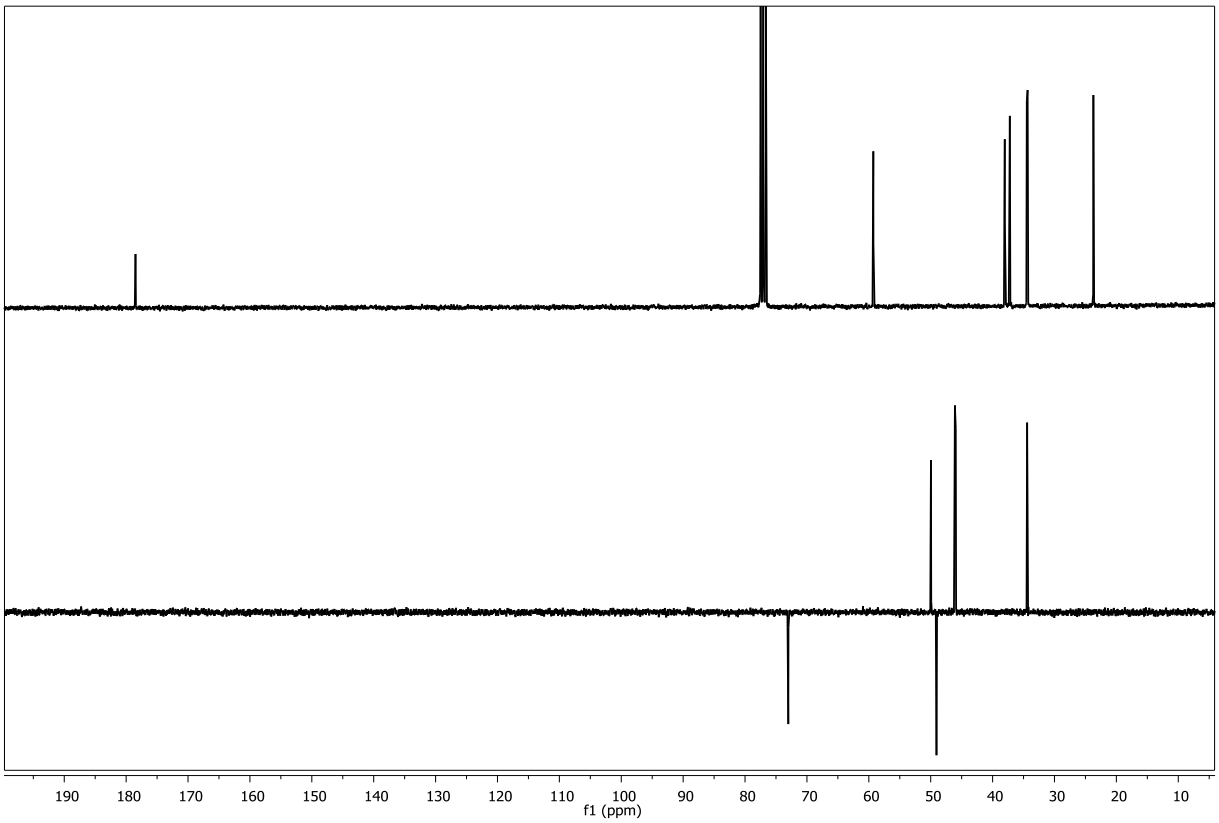

2-((*1S,2S*)-2-aminocyclopentyl)acetic acid (30)

^{1}H NMR (D_2O, 300 MHz)

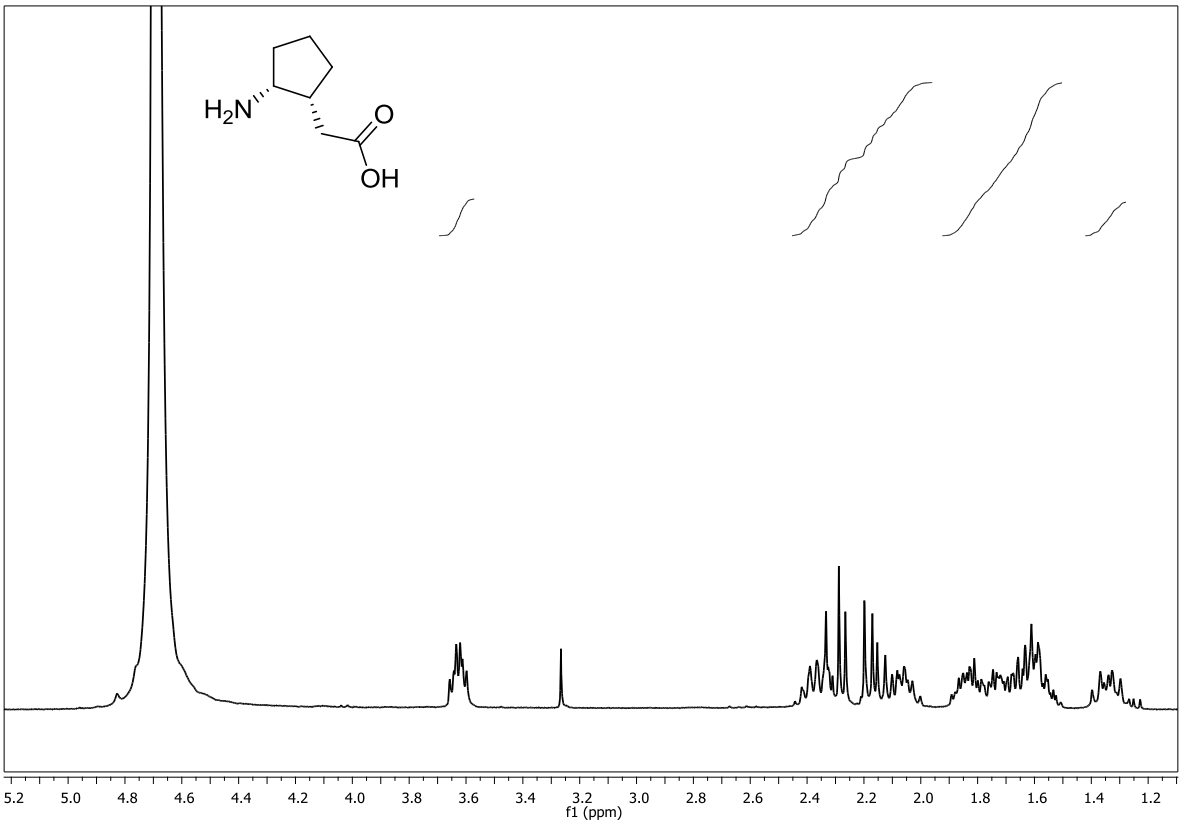

^{13}C NMR (D_2O, 300MHz)

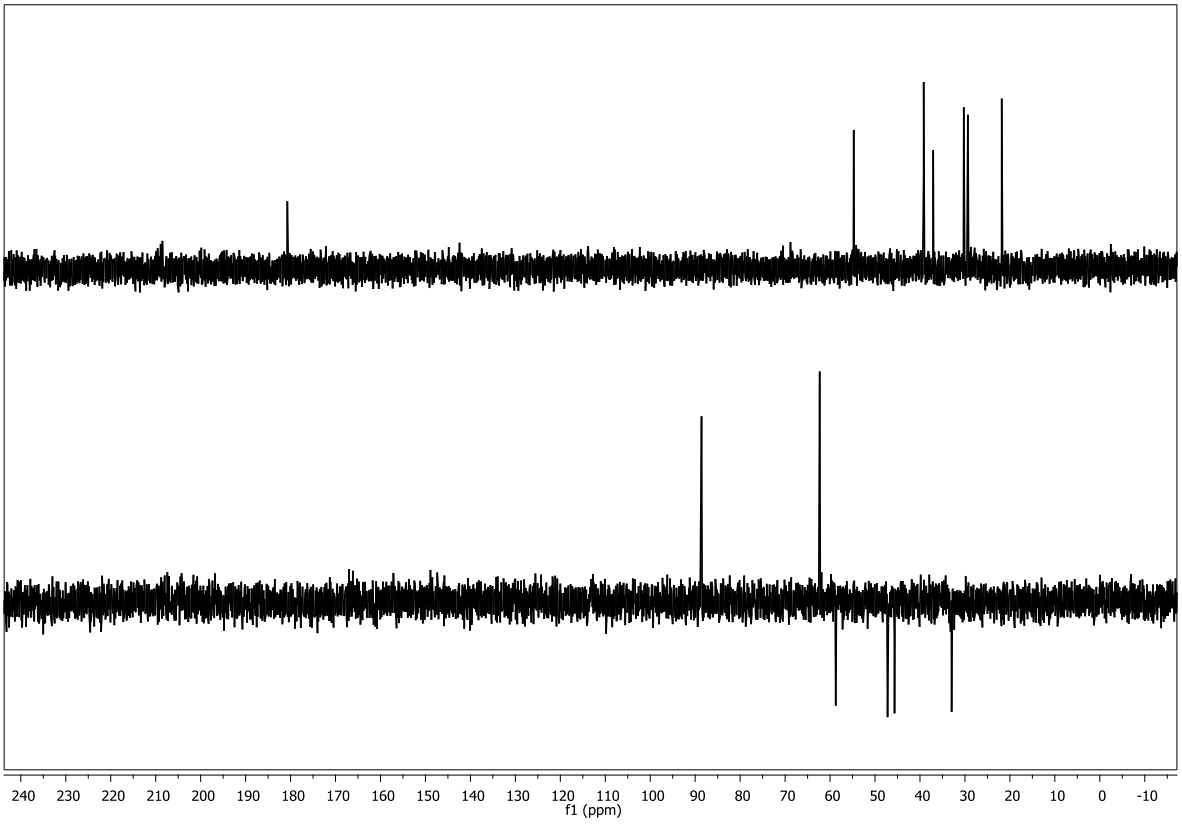

2-((*1S,2S*)-2-(((9H-fluoren-9-yl)methoxy)carbonylamino)cyclopentyl)acetic acid (143)

^{1}H NMR (CD_3OD, 300 MHz)

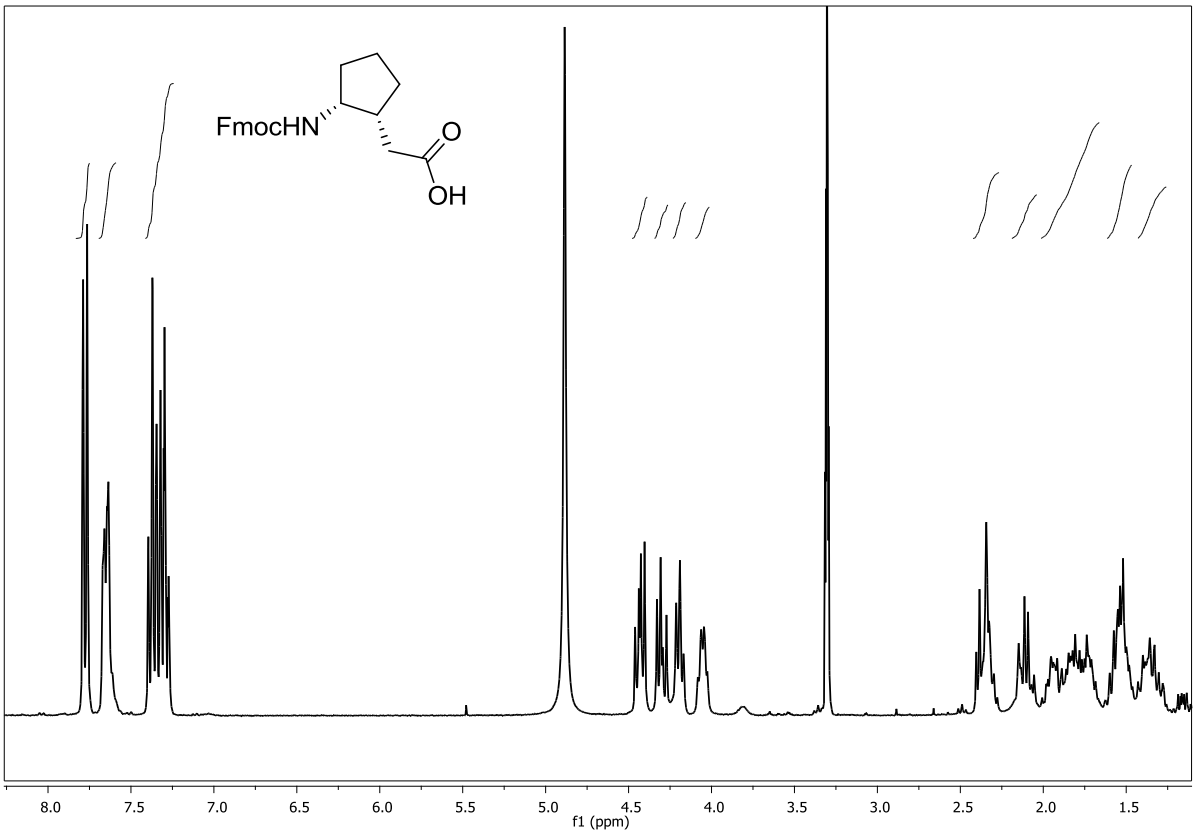

^{13}C NMR (CD_3OD, 300 MHz)

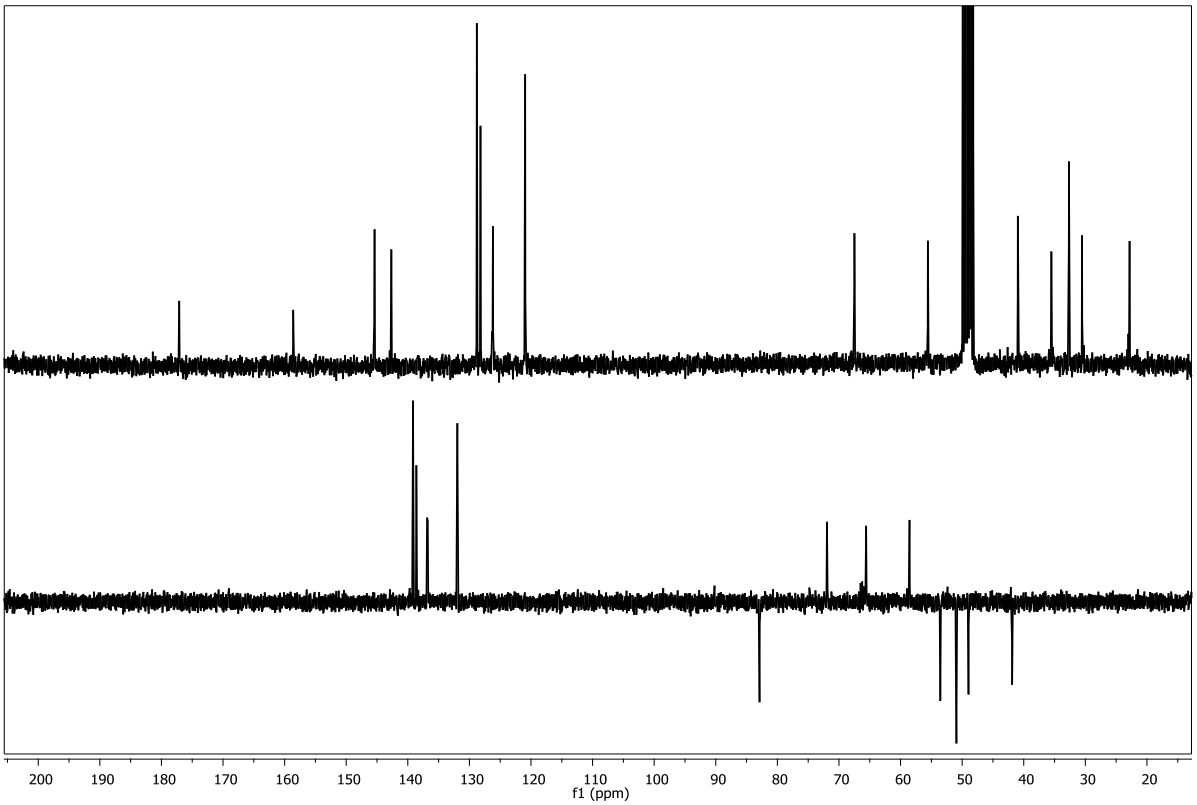

2-((*1S,2R,3R,5R*)-2-(((9H-fluoren-9-yl)methoxy)carbonylamino)-3-((tert butyldimethylsilyloxy)methyl)-5-methoxycyclopentyl)acetic acid (109)

^{1}H NMR ($CDCl_3$, 300 MHz)

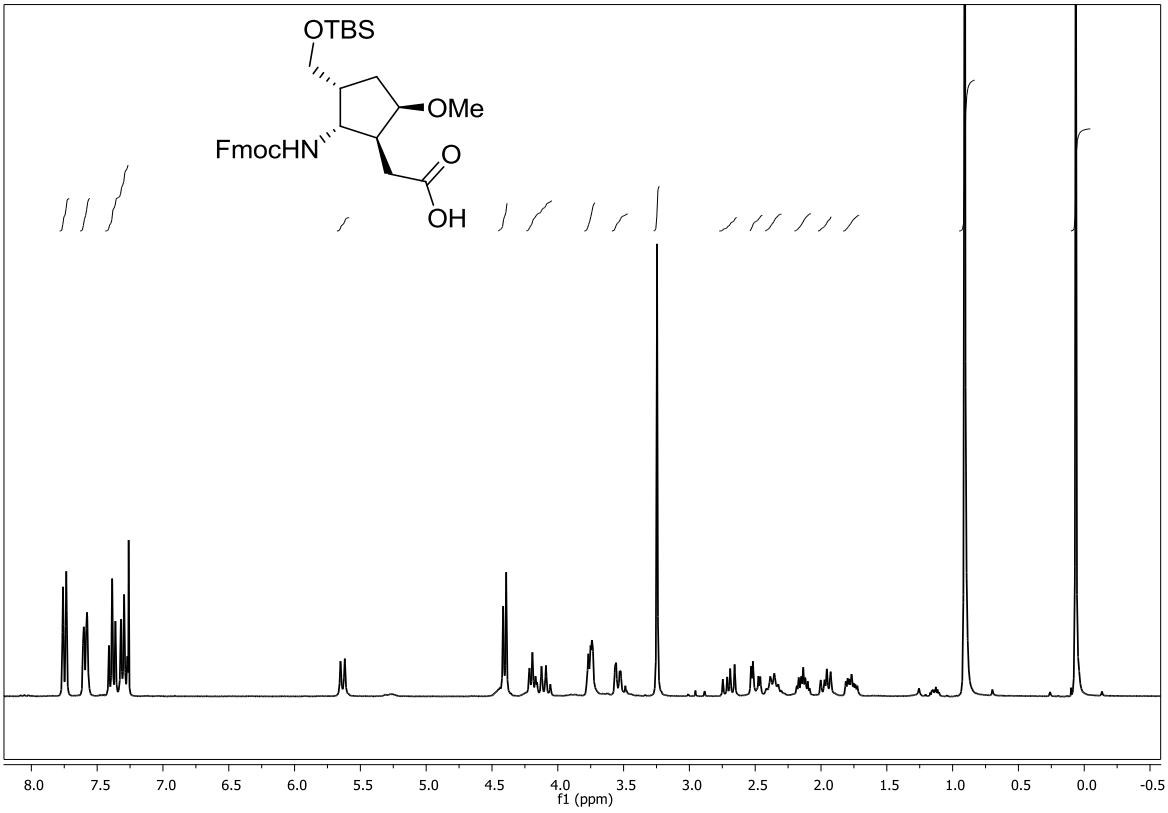

^{13}C NMR ($CDCl_3$, 300 MHz)

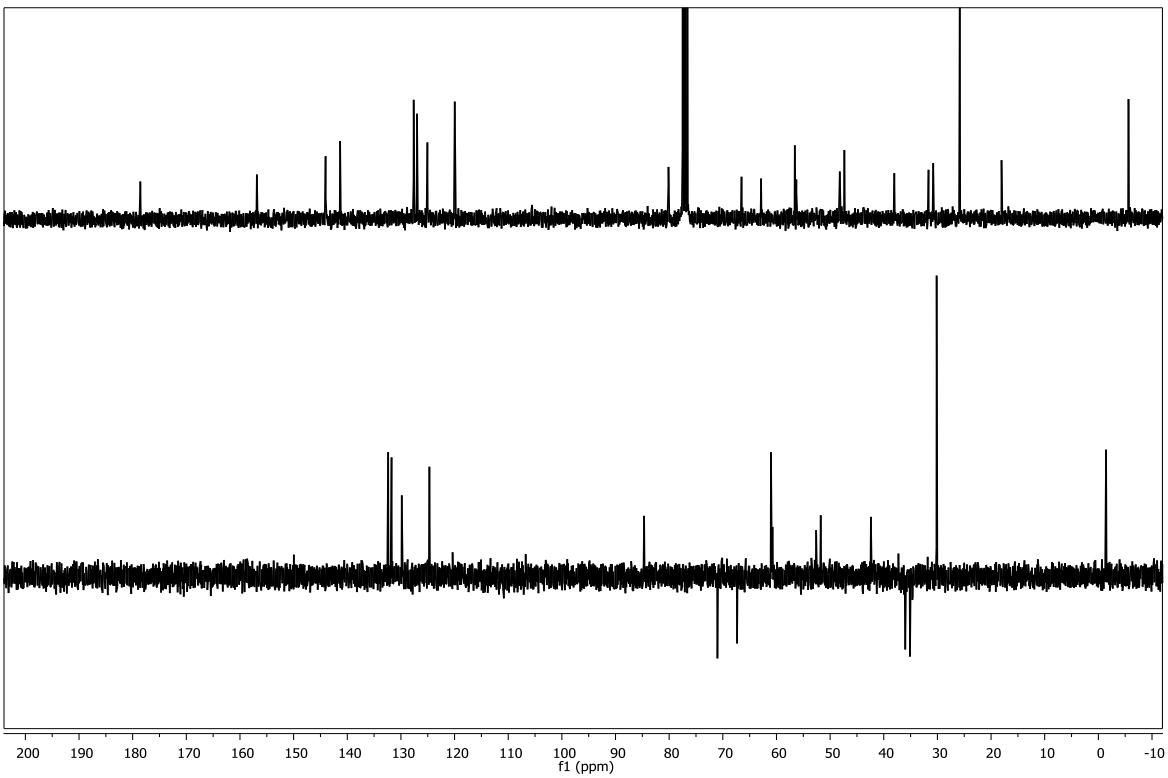

(*S*)-benzyl-2-(2-((*1S,2R,3R,5R*)-2-(((9H-fluoren-9-yl)methoxy)carbonylamino)-3-((tert-butyldimethylsilyloxy)methyl)-5-methoxycyclopentyl)acetamido)propanoate (112)

^{1}H NMR ($CDCl_3$, 300 MHz)

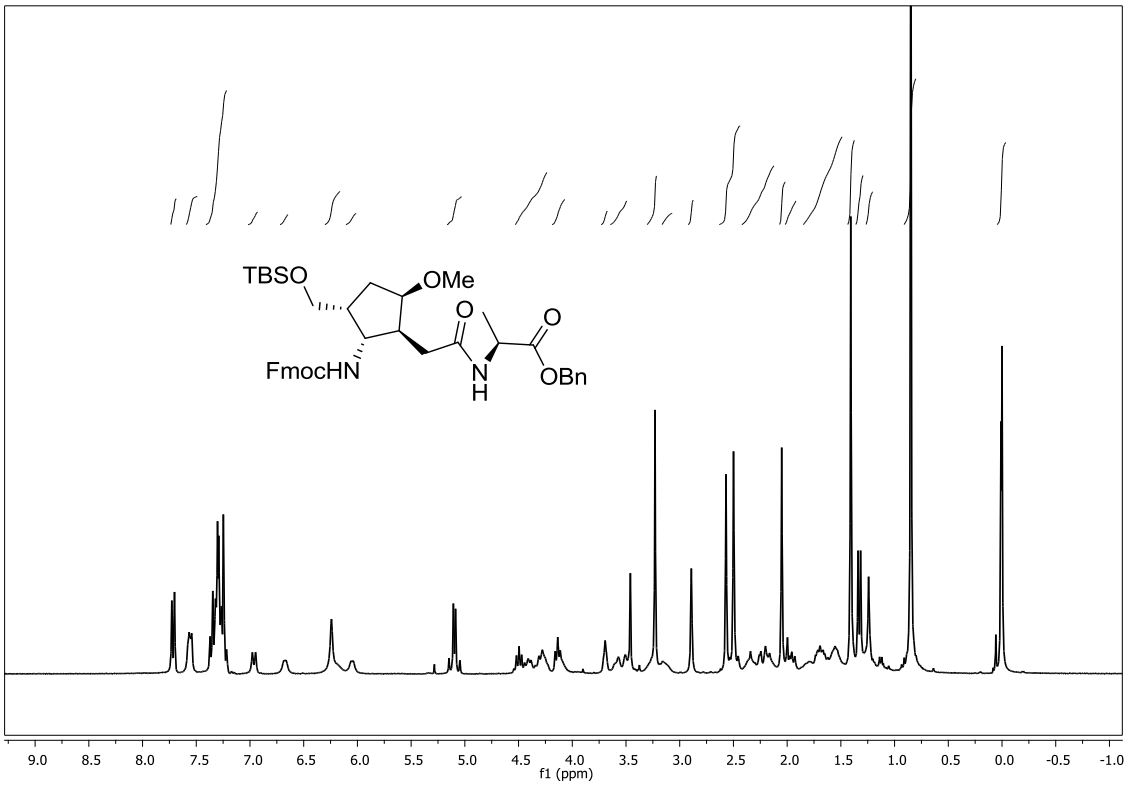

^{13}C NMR ($CDCl_3$, 300 MHz)

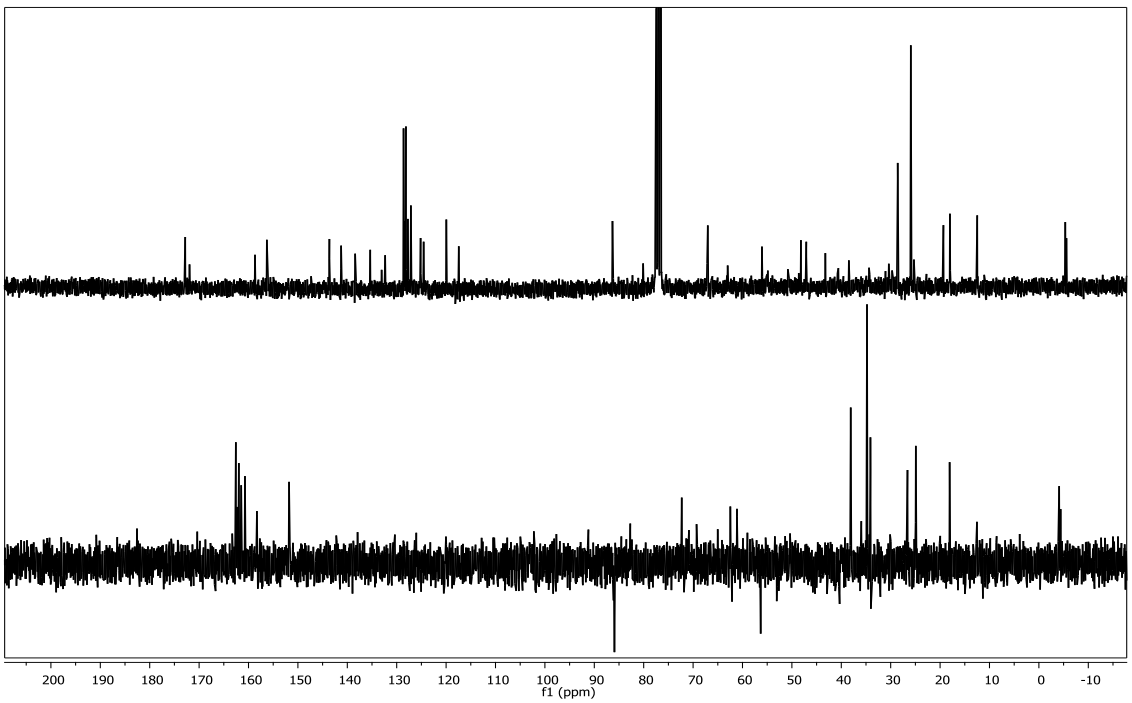

(*S*)-benzyl-2-(2-((*1S,2R,3R,5R*)-2-((*S*)-2-(((9H-fluoren-9-yl)methoxy)carbonylamino)-5-Pbf-guanidinopentanamido)-3-((tert-butyldimethylsilyloxy)methyl)-5-methoxycyclopentyl)acetamido)propanoate (115)

^{1}H NMR ($CDCl_3$, 300MHz)

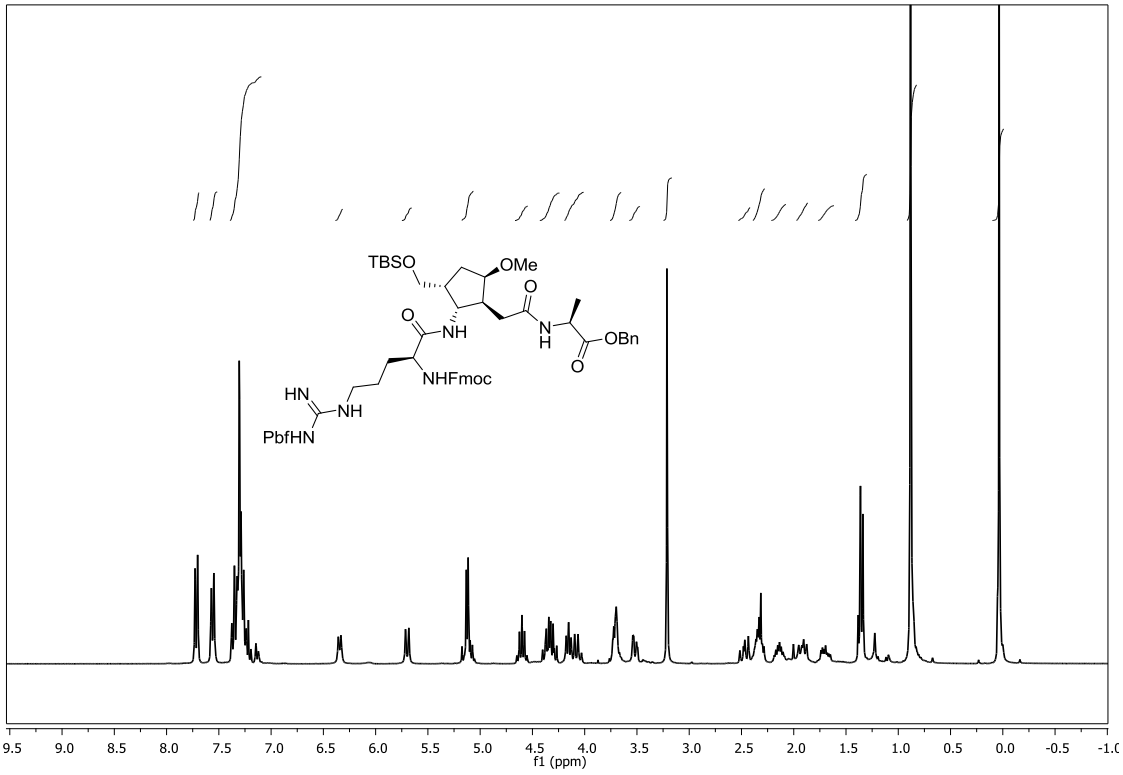

^{13}C NMR (CD_3Cl_3, 300MHz)

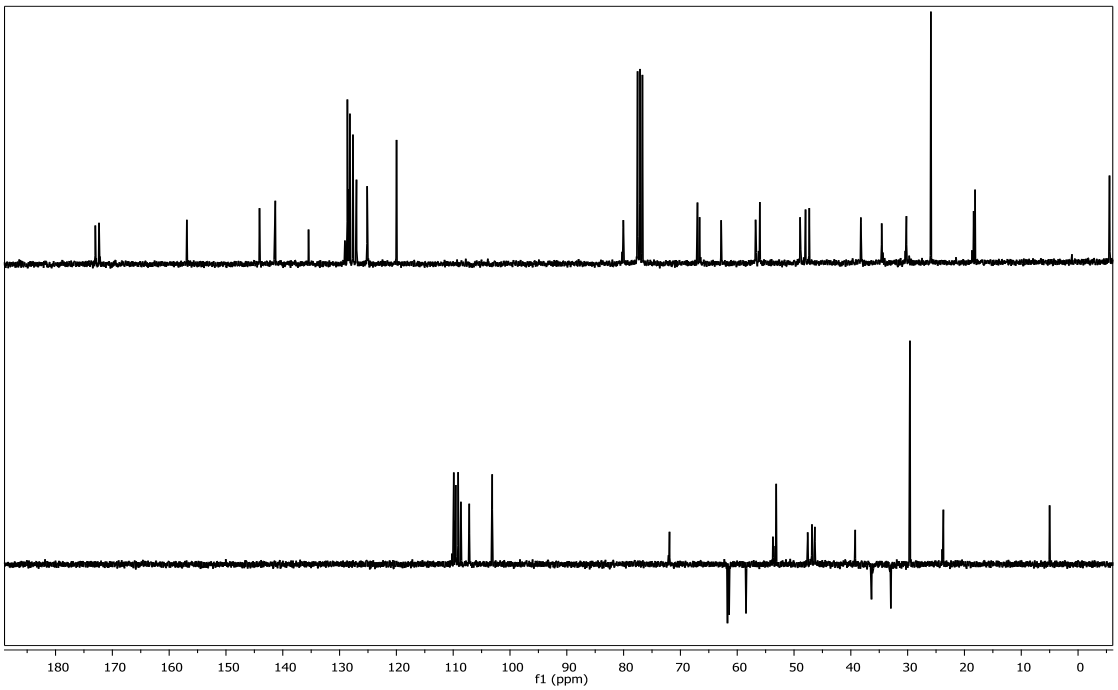

(*S*)-benzyl-2-((*S*)-2-(2-((*1S,2R,3R,5R*)-2-(((9H-fluoren-9-yl)methoxy)carbonylamino)-3-((tert-butyldimethylsilyloxy)methyl)-5-methoxycyclopentyl)acetamido)-5-(Pbf)guanidinopentanamido)propanoate (116)

^{1}H NMR ($CDCl_3$, 300MHz)

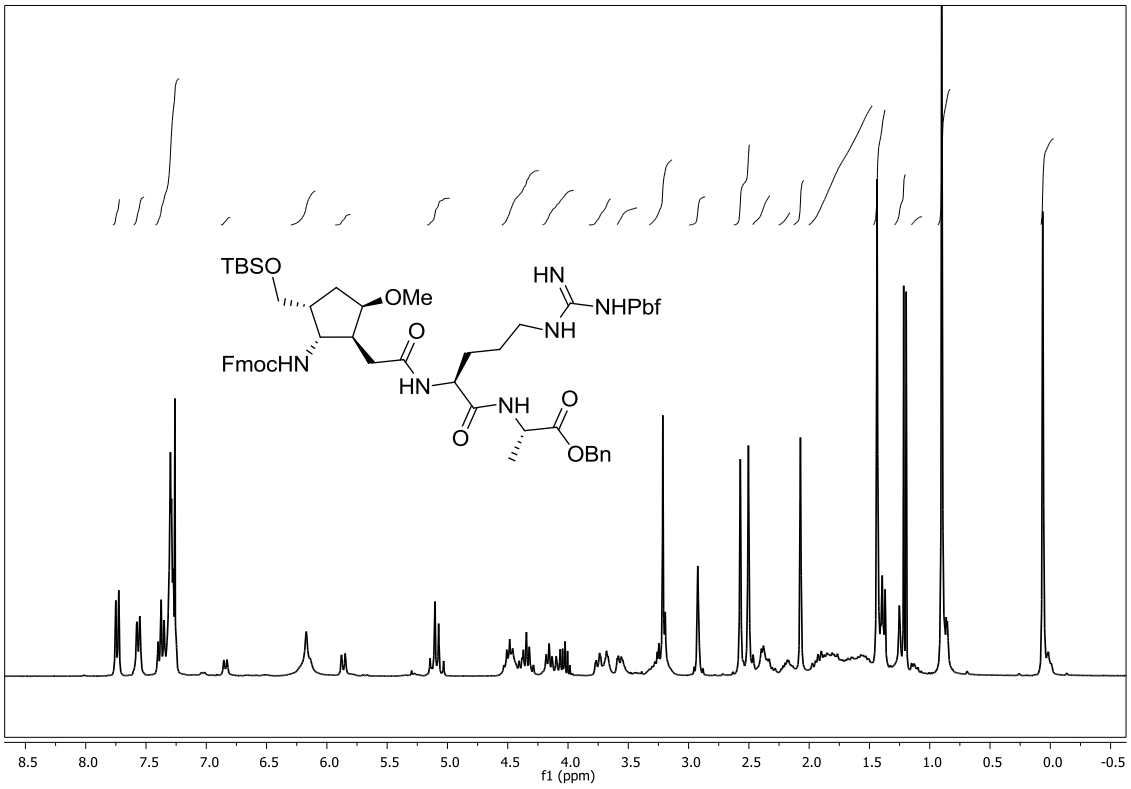

^{13}C NMR (CD_3Cl_3, 300MHz)

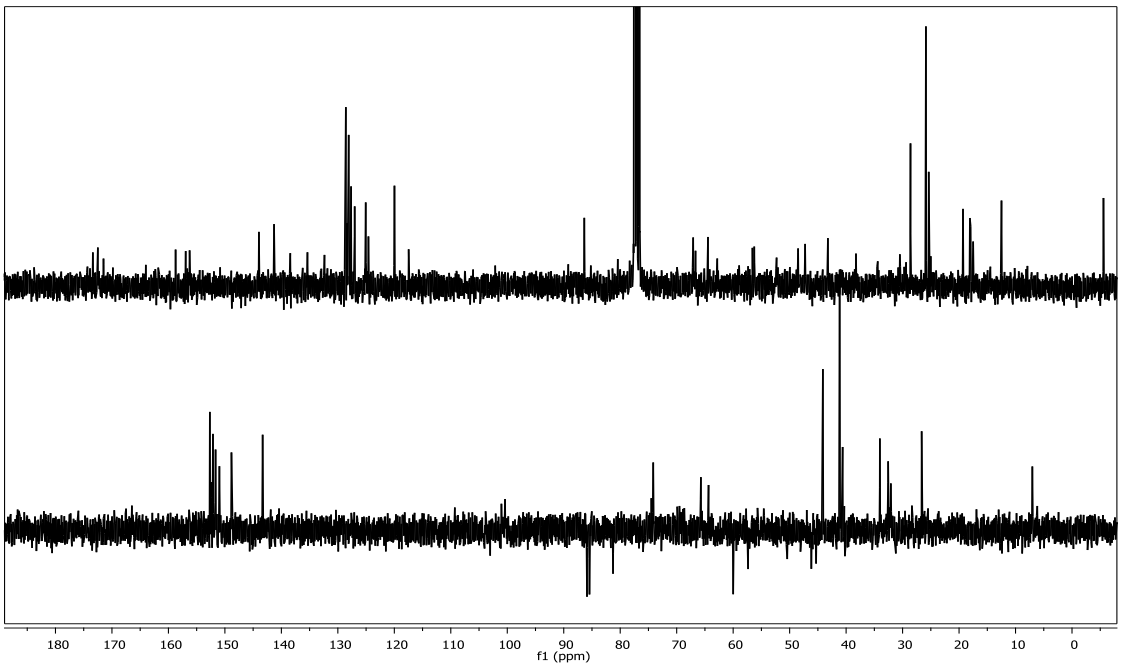

Ac-Arg^{26}-His^{27}-Thr^{28}-Ile^{29}-Asn^{30}-(*1S,2S*-ACPA)^{31}-Thr^{32}-Arg^{33}-(*1S,2S*-ACPC)^{34}-Arg^{35}-Tyr^{36}-NH_2 (161)

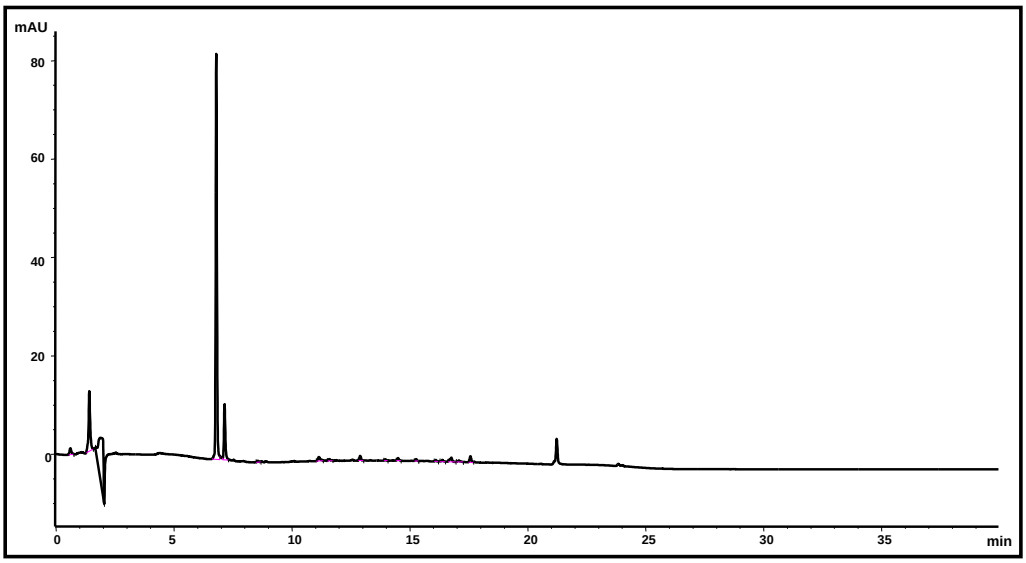

Injection 30 µl; Gradient 5-98% in 20 min, 98% for 5 min; Wavelenght = 220 nm; Retention time = 6.793 min; yield = 86,7%.

Ac-Arg^{26}-His^{27}-(*1S,2S*-ACPC)^{28}-Ile^{29}-Asn^{30}-(*1S,2S*-ACPA)^{31}-Thr^{32}-Arg^{33}-(*1S,2S*-ACPC)^{34}-Arg^{35}-Tyr^{36}-NH_2 (162)

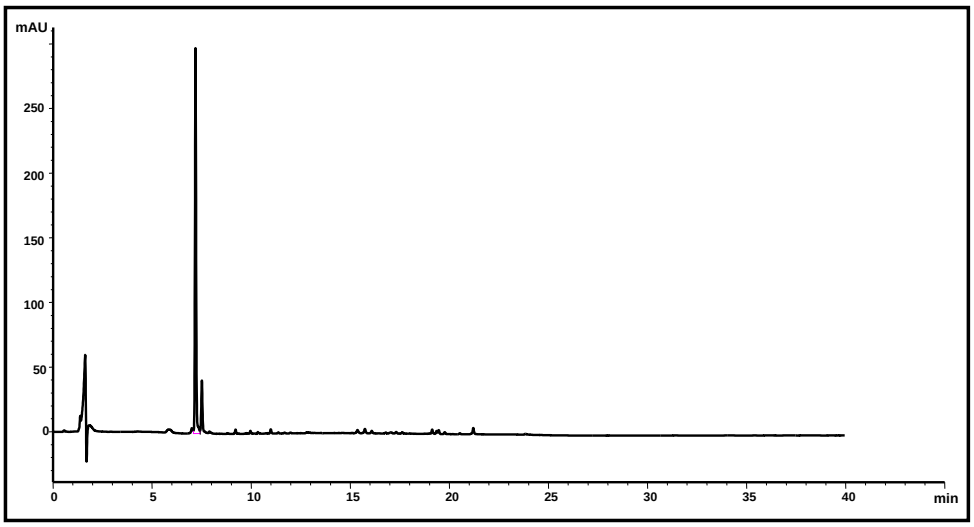

Injection 30 µl; Gradient 5-98% in 20 min, 98% for 5 min; Wavelenght = 220 nm; Retention time = 7.345 min; yield = 98%.

Ac-Arg^{25}-His26-Tyr^{27}-Ile^{28}-Asn^{29}-Leu^{30}-Ile^{31}-Thr^{32}-Arg^{33}-(*1S,2S*-ACPC)^{34}-Arg^{35}-Tyr^{36}-NH$_2$ (163)

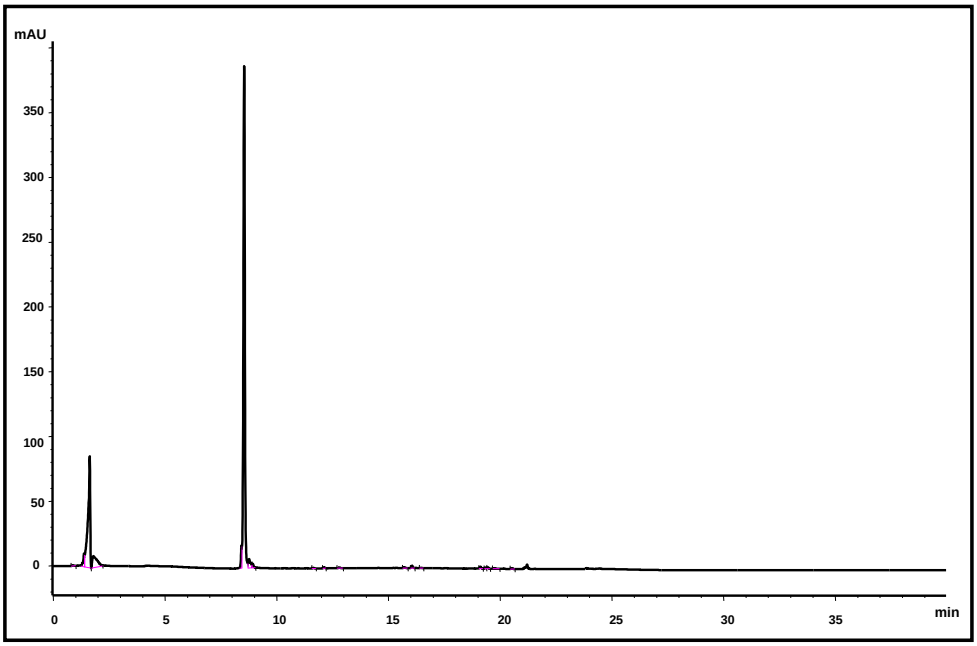

Injection 30 µl; Gradient 5-98% in 20 min, 98% for 5 min; Wavelenght = 220 nm; Retention time = 8.546 min; yield = 96.7%

Ac-Arg^{25}-His^{26}-Tyr^{27}-Ile^{28}-Asn^{29}-Leu^{30}-Ile^{31}-Thr^{32}-Arg^{33}-(*1S,2S*-ACPA)^{34}-Arg^{35}-Tyr^{36}-NH$_2$ (164)

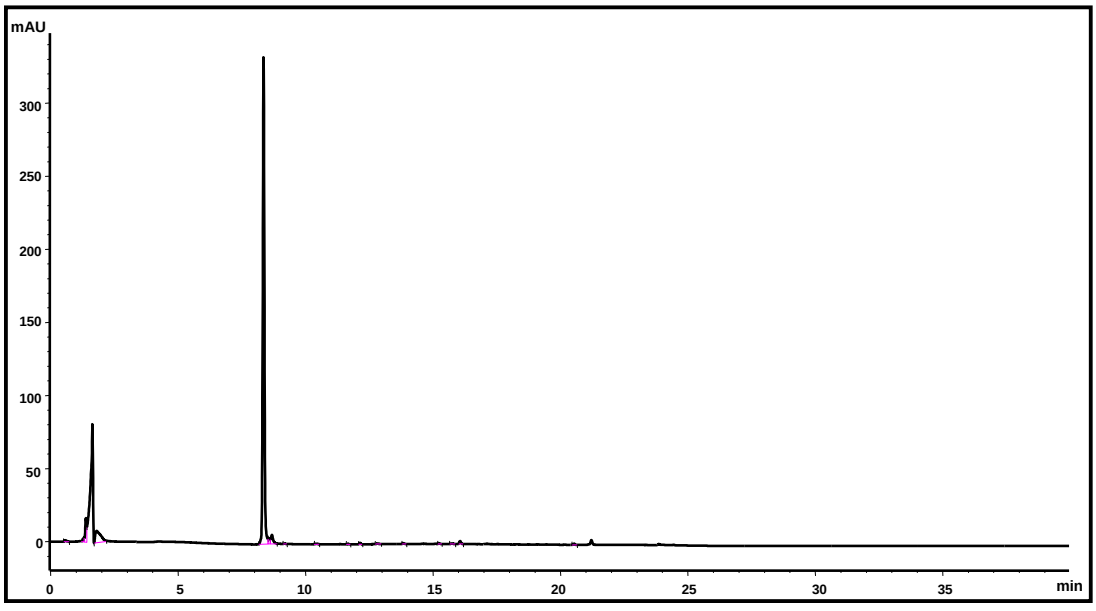

Injection 30 µl; Gradient 5-98% in 20 min, 98% for 5 min; Wavelenght = 220 nm; Retention time = 8.360 min; yield = 96.2%.

Ac-Arg^{26}-His^{27}-Tyr^{28}-Ile^{29}-Asn^{30}-(*1S,2R*-ACPA)^{31}-Thr^{32}-Arg^{33}-(*1S,2S*-ACPC)^{34}-Arg^{35}-Tyr^{36}-NH_2 (165)

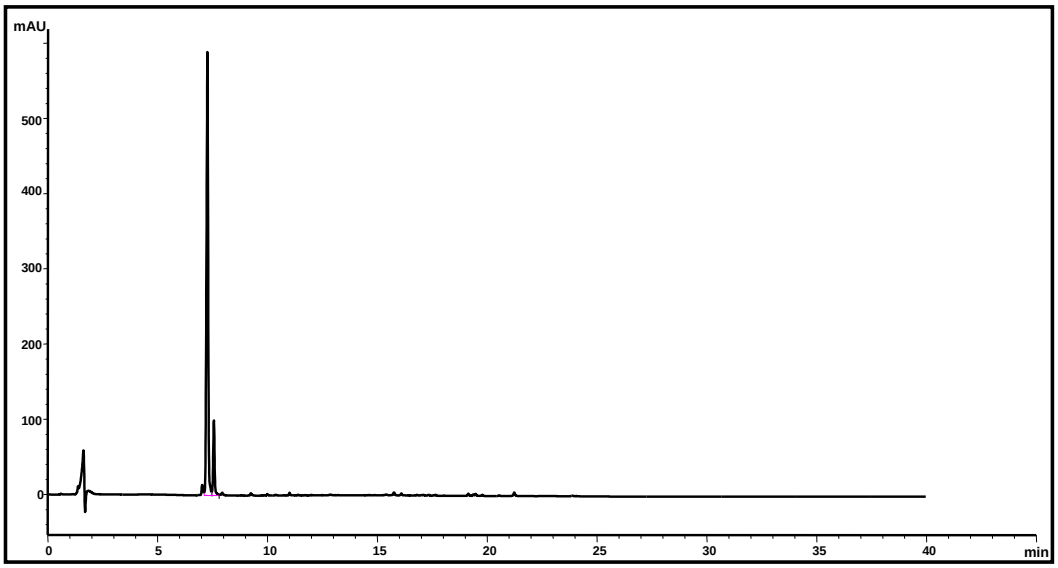

Injection 30 µl; Gradient 5-98% in 20 min, 98% for 5 min; Wavelenght = 220 nm; Retention time = 7.271 min; yield = 87.4%

Ac-Arg^{26}-His^{27}-Tyr^{28}-Ile^{29}-Asn^{30}-(*1R,2S*-ACPA)^{31}-Thr^{32}-Arg^{33}-(*1S,2S*-ACPC)^{34}-Arg^{35}-Tyr^{36}-NH_2 (166)

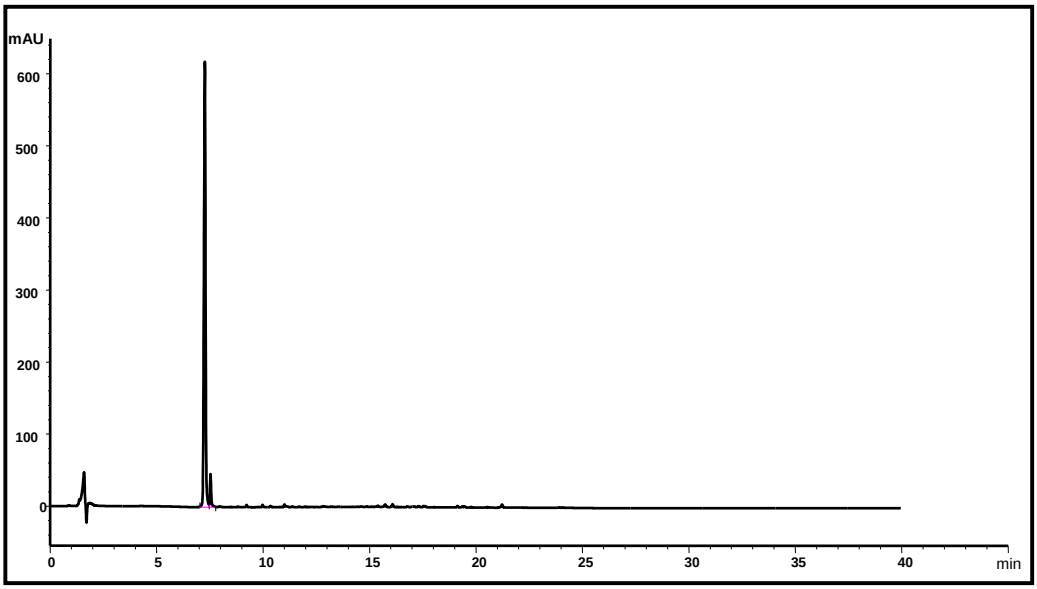

Injection 30 µl; Gradient 5-98% in 20 min, 98% for 5 min; Wavelenght = 220 nm; Retention time = 7.271 min; yield = 94,6%

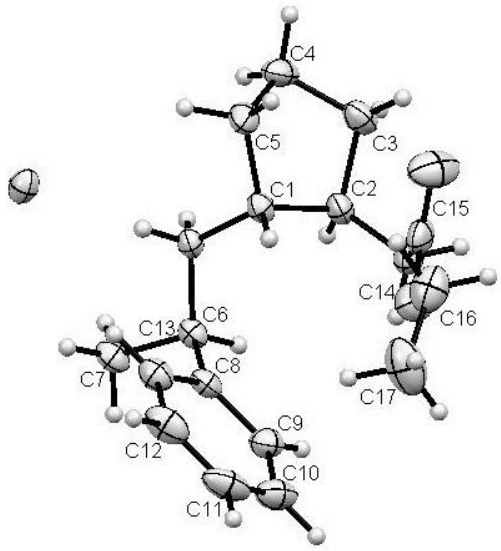

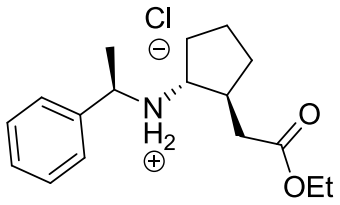

150

Crystal data of compound 150:

Empirical formula	C_{17} H_{26} N O_2, Cl
Formula weight	311.84
Crystal size	0.1545 x 0.0825 x 0.0586 mm
Crystal description	prism
Crystal colour	translucent colourless
Crystal system	Orthorhombic
Space group	C 2 2 21
Unit cell dimensions	a = 7.75993(17) Å alpha = 90 °.
	b = 16.3395(4) Å beta = 90 °.
	c = 26.7466(7) Å gamma = 90 °.
Volume	3391.29(14) $Å^3$
Z, Calculated density	8, 1.222 Mg/m^3
Absorption coefficient	2.021 mm^{-1}
F(000)	1344

Data Collection:

Measurement device type	SuperNova, Single source at offset), Atlas
Measuremnet method	\w scans
Temperature	123 K
Wavelength	1.54184 Å
Monochromator	graphite
Theta range for data collection	3.30 to 73.62 °.
Index ranges	-6<=h<=9, -20<=k<=13, -27<=l<=33
Reflections collected / unique	5942 / 3300 [R(int) = 0.0331]
Reflections greater I>2\s(I)	3168
Absorption correction	Analytical
Max. and min. transmission	0.971 and 0.943
Refinement	
Refinement method	Full-matrix least-squares on F^2
Hydrogen treatment	:
Data / restraints / parameters	3300 / 0 / 196
Goodness-of-fit on F^2	1.052
Final R indices [I>2sigma(I)]	R1 = 0.0423, wR2 = 0.1117
R indices (all data)	R1 = 0.0436, wR2 = 0.1137

Absolute structure parameter	-0.020(15)
Largest diff. peak and hole	0.289 and -0.229 e.Å^{-3}

	x	y	z	U(eq)
O(1)	7289(3)	5779(1)	3048(1)	56(1)
O(2)	8246(2)	7016(1)	2839(1)	42(1)
N(1)	5796(2)	7568(1)	4426(1)	23(1)
C(1)	6041(3)	6935(1)	4021(1)	25(1)
C(2)	7758(3)	6467(1)	4094(1)	27(1)
C(3)	7224(3)	5578(1)	4227(1)	35(1)
C(4)	5370(3)	5644(1)	4406(1)	36(1)
C(5)	4622(3)	6290(1)	4057(1)	33(1)
C(6)	6977(3)	8301(1)	4411(1)	25(1)
C(7)	6393(3)	8886(1)	4823(1)	31(1)
C(8)	7007(3)	8722(1)	3907(1)	25(1)
C(9)	8588(3)	8898(1)	3688(1)	32(1)
C(10)	8655(4)	9343(2)	3240(1)	39(1)
C(11)	7142(4)	9591(1)	3014(1)	44(1)
C(12)	5569(4)	9413(2)	3228(1)	42(1)
C(13)	5492(3)	8983(1)	3679(1)	32(1)
C(14)	8966(3)	6545(1)	3644(1)	33(1)
C(15)	8071(3)	6388(1)	3152(1)	35(1)
C(16)	7515(3)	6909(2)	2341(1)	47(1)
C(17)	7596(5)	7731(2)	2089(1)	63(1)
Cl(1)	1894(1)	8060(1)	4512(1)	30(1)

Table 2. Atomic coordinates (x 10^4) and equivalent isotropic displacement parameters (Å^2 x 10^3).
U(eq) is defined as one third of the trace of the orthogonalized Uij tensor.

O(1)-C(15)	1.199(3)	C(14)-H(14A)	0.9900
O(2)-C(15)	1.329(3)	C(14)-H(14B)	0.9900
O(2)-C(16)	1.458(3)	C(16)-H(16A)	0.9900
N(1)-C(1)	1.509(3)	C(16)-H(16B)	0.9900
N(1)-C(6)	1.509(3)	C(17)-H(17A)	0.9800
N(1)-H(1M)	0.93(3)	C(17)-H(17B)	0.9800
N(1)-H(1N)	0.91(3)	C(17)-H(17C)	0.9800
C(1)-C(2)	1.549(3)	C(15)-O(2)-C(16)	116.2(2)
C(1)-C(5)	1.528(3)	C(1)-N(1)-C(6)	116.66(15)
C(2)-C(3)	1.553(3)	H(1M)-N(1)-H(1N)	104(3)
C(2)-C(14)	1.532(3)	C(1)-N(1)-H(1N)	109.3(17)
C(3)-C(4)	1.521(3)	C(6)-N(1)-H(1M)	105.0(18)
C(4)-C(5)	1.523(3)	C(1)-N(1)-H(1M)	110.5(17)
C(6)-C(7)	1.528(3)	C(6)-N(1)-H(1N)	110.9(17)
C(6)-C(8)	1.512(3)	N(1)-C(1)-C(5)	109.69(17)
C(8)-C(9)	1.390(3)	C(2)-C(1)-C(5)	105.74(17)
C(8)-C(13)	1.392(3)	N(1)-C(1)-C(2)	110.86(16)
C(9)-C(10)	1.401(3)	C(1)-C(2)-C(14)	112.71(16)
C(10)-C(11)	1.381(4)	C(3)-C(2)-C(14)	114.84(17)

C(1)-C(2)-C(3)	105.16(18)	C(4)-C(5)-H(5A)	111.00
C(2)-C(3)-C(4)	104.90(17)	C(4)-C(5)-H(5B)	111.00
C(3)-C(4)-C(5)	102.54(18)	H(5A)-C(5)-H(5B)	109.00
C(1)-C(5)-C(4)	104.01(18)	N(1)-C(6)-H(6)	108.00
N(1)-C(6)-C(7)	1 07.28(17)	C(7)-C(6)-H(6)	108.00
N(1)-C(6)-C(8)	113.19(16)	C(8)-C(6)-H(6)	108.00
C(7)-C(6)-C(8)	111.33(16)	C(6)-C(7)-H(7A)	109.00
C(6)-C(8)-C(9)	118.9(2)	C(6)-C(7)-H(7B)	109.00
C(9)-C(8)-C(13)	119.80(19)	C(6)-C(7)-H(7C)	109.00
C(6)-C(8)-C(13)	121.1(2)	H(7A)-C(7)-H(7B)	109.00
C(8)-C(9)-C(10)	120.1(2)	H(7A)-C(7)-H(7C)	110.00
C(9)-C(10)-C(11)	119.6(3)	H(7B)-C(7)-H(7C)	109.00
C(10)-C(11)-C(12)	120.6(2)	C(8)-C(9)-H(9)	120.00
C(11)-C(12)-C(13)	120.1(3)	C(10)-C(9)-H(9)	120.00
C(8)-C(13)-C(12)	119.8(2)	C(9)-C(10)-H(10)	120.00
C(2)-C(14)-C(15)	112.97(19)	C(11)-C(10)-H(10)	120.00
O(2)-C(15)-C(14)	111.75(19)	C(10)-C(11)-H(11)	120.00
O(1)-C(15)-O(2)	123.1(2)	C(12)-C(11)-H(11)	120.00
O(1)-C(15)-C(14)	125.1(2)	C(11)-C(12)-H(12)	120.00
O(2)-C(16)-C(17)	106.6(2)	C(13)-C(12)-H(12)	120.00
N(1)-C(1)-H(1)	110.00	C(8)-C(13)-H(13)	120.00
C(2)-C(1)-H(1)	110.00	C(12)-C(13)-H(13)	120.00
C(5)-C(1)-H(1)	110.00	C(2)-C(14)-H(14A)	109.00
C(1)-C(2)-H(2)	108.00	C(2)-C(14)-H(14B)	109.00
C(3)-C(2)-H(2)	108.00	C(15)-C(14)-H(14A)	109.00
C(14)-C(2)-H(2)	108.00	C(15)-C(14)-H(14B)	109.00
C(2)-C(3)-H(3A)	111.00	H(14A)-C(14)-H(14B)	108.00
C(2)-C(3)-H(3B)	111.00	O(2)-C(16)-H(16A)	110.00
C(4)-C(3)-H(3A)	111.00	O(2)-C(16)-H(16B)	110.00
C(4)-C(3)-H(3B)	111.00	C(17)-C(16)-H(16A)	110.00
H(3A)-C(3)-H(3B)	109.00	C(17)-C(16)-H(16B)	110.00
C(3)-C(4)-H(4A)	111.00	H(16A)-C(16)-H(16B)	109.00
C(3)-C(4)-H(4B)	111.00	C(16)-C(17)-H(17A)	110.00
C(5)-C(4)-H(4A)	111.00	C(16)-C(17)-H(17B)	110.00
C(5)-C(4)-H(4B)	111.00	C(16)-C(17)-H(17C)	109.00
H(4A)-C(4)-H(4B)	109.00	H(17A)-C(17)-H(17B)	109.00
C(1)-C(5)-H(5A)	111.00	H(17A)-C(17)-H(17C)	109.00
C(1)-C(5)-H(5B)	111.00	H(17B)-C(17)-H(17C)	109.00

Table 3. Bond lengths [Å] and angles [°].

	U11	*U22*	*U33*	*U23*	*U13*	*U12*
O(1)	74(1)	59(1)	35(1)	-12(1)	4(1)	-29(1)
O(2)	45(1)	47(1)	35(1)	-2(1)	-3(1)	-4(1)
N(1)	25(1)	21(1)	23(1)	-2(1)	1(1)	3(1)
C(1)	29(1)	24(1)	23(1)	-4(1)	1(1)	2(1)
C(2)	30(1)	22(1)	29(1)	-3(1)	1(1)	5(1)
C(3)	45(1)	24(1)	38(1)	2(1)	0(1)	4(1)
C(4)	48(1)	26(1)	34(1)	-4(1)	9(1)	-11(1)
C(5)	30(1)	31(1)	39(1)	-12(1)	4(1)	-4(1)
C(6)	27(1)	21(1)	25(1)	-2(1)	-3(1)	1(1)
C(7)	40(1)	25(1)	29(1)	-6(1)	-5(1)	-1(1)
C(8)	33(1)	17(1)	25(1)	-2(1)	-3(1)	1(1)
C(9)	36(1)	27(1)	33(1)	-1(1)	1(1)	-5(1)
C(10)	54(1)	32(1)	31(1)	2(1)	4(1)	-13(1)
C(11)	77(2)	26(1)	29(1)	5(1)	-6(1)	-10(1)
C(12)	56(2)	31(1)	39(1)	5(1)	-18(1)	4(1)
C(13)	36(1)	28(1)	33(1)	0(1)	-6(1)	2(1)
C(14)	30(1)	36(1)	34(1)	-7(1)	5(1)	-1(1)
C(15)	32(1)	41(1)	2(1)	-11(1)	11(1)	-1(1)
C(16)	39(1)	65(2)	37(1)	-5(1)	-4(1)	4(1)
C(17)	77(2)	63(2)	50(2)	-1(1)	-10(2)	30(2)
Cl(1)	26(1)	36(1)	28(1)	4(1)	2(1)	4(1)

Table 4. Anisotropic displacement parameters ($Å^2$ x 10^3).
The anisotropic displacement factor exponent takes the form:
$-2\ pi^2\ [\ h^2\ a^{*2}\ U11 + ... + 2\ h\ k\ a^*\ b^*\ U12\ ]$

	x	*y*	*z*	*U(eq)*
H(1)	6017	7202	3684	30
H(1M)	5970(40)	7337(16)	4739(11)	28
H(1N)	4670(40)	7727(16)	4432(10)	28
H(2)	8357	6706	4392	33
H(3A)	7303	5219	3929	43
H(3B)	7972	5353	4493	43
H(4A)	5315	5824	4759	43
H(4B)	4756	5116	4371	43
H(5A)	3553	6527	4198	40
H(5B)	4364	6054	3725	40
H(6)	8173	8113	4490	29
H(7A)	5234	9088	4747	38
H(7B)	7194	9349	4843	38
H(7C)	6378	8596	5144	38
H(9)	9624	8716	3841	38
H(10)	9734	9474	3093	47
H(11)	7185	9887	2709	53
H(12)	4535	9582	3068	50
H(13)	4409	8868	3829	38
H(14A)	9466	7102	3640	40
H(14B)	9926	6151	3682	40
H(16A)	6307	6719	2364	57

H(16B)	8187	6500	2150	57
H(17A)	8798	7913	2070	76
H(17B)	6924	8129	2282	76
H(17C)	7119	7688	1751	76

Table 5. Hydrogen coordinates (x 10^4) and isotropic displacement parameters (Å^2 x 10^3).

C(16)-O(2)-C(15)-C(14)	176.54(18)
C(15)-O(2)-C(16)-C(17)	170.6(2)
C(16)-O(2)-C(15)-O(1)	-3.6(3)
C(6)-N(1)-C(1)-C(2)	69.9(2)
C(1)-N(1)-C(6)-C(7)	175.19(16)
C(6)-N(1)-C(1)-C(5)	-173.69(17)
C(1)-N(1)-C(6)-C(8)	52.0(2)
N(1)-C(1)-C(2)-C(14)	-121.23(18)
C(5)-C(1)-C(2)-C(14)	119.96(18)
N(1)-C(1)-C(5)-C(4)	-90.1(2)
C(5)-C(1)-C(2)-C(3)	-5.9(2)
C(2)-C(1)-C(5)-C(4)	29.5(2)
N(1)-C(1)-C(2)-C(3)	112.95(18)
C(1)-C(2)-C(3)-C(4)	-19.9(2)
C(3)-C(2)-C(14)-C(15)	72.8(2)
C(1)-C(2)-C(14)-C(15)	-47.6(2)
C(14)-C(2)-C(3)-C(4)	-144.43(19)
C(2)-C(3)-C(4)-C(5)	38.1(2)
C(3)-C(4)-C(5)-C(1)	-41.9(2)
C(7)-C(6)-C(8)-C(9)	108.7(2)
C(7)-C(6)-C(8)-C(13)	-66.9(2)
N(1)-C(6)-C(8)-C(9)	-130.35(19)
N(1)-C(6)-C(8)-C(13)	54.1(2)
C(6)-C(8)-C(9)-C(10)	-175.03(19)
C(13)-C(8)-C(9)-C(10)	0.6(3)
C(6)-C(8)-C(13)-C(12)	176.17(19)
C(9)-C(8)-C(13)-C(12)	0.6(3)
C(8)-C(9)-C(10)-C(11)	-1.3(3)
C(9)-C(10)-C(11)-C(12)	0.8(4)
C(10)-C(11)-C(12)-C(13)	0.5(4)
C(11)-C(12)-C(13)-C(8)	-1.2(3)
C(2)-C(14)-C(15)-O(1)	-56.0(3)
C(2)-C(14)-C(15)-O(2)	123.8(2)

Table 6. Torsion angles [°].

D-H...A	d(D-H)	d(H...A)	d(D...A)	<(DHA)
N(1)-H(1M)...Cl(1)#1	0.93(3)	2.23(3)	3.1399(17)	168(2)
N(1)-H(1N)...Cl(1)	0.91(3)	2.23(3)	3.1413(16)	175(2)
C(3)-H(3A)...O(1)	0.9900	2.5300	3.171(3)	122.00
C(9)-H(9)...Cl(1)#2	0.9500	2.7300	3.649(2)	162.00
C(11)-H(11)...O(1)#3	0.9500	2.5300	3.468(3)	171.00

Table 7. Hydrogen-bonds [Å and °].

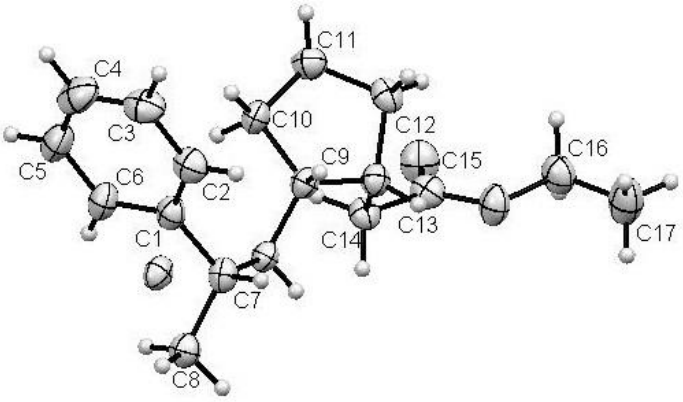

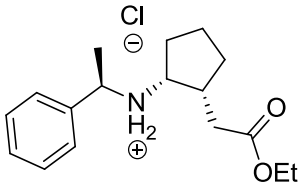

151

Crystal Data of compound 151:

Empirical formula	C_{17} H_{25} N O_2, Cl
Formula weight	310.83
Crystal size	0.2722 x 0.0343 x 0.0199 mm
Crystal description	needle
Crystal colour	translucent colourless
Crystal system	Monoclinic
Space group	P 21
Unit cell dimensions	a = 10.5439(7) Å alpha = 90 °.
	b = 6.8764(4) Å beta = 93.685(7) °.
	c = 11.9424(9) Å gamma = 90 °.
Volume	864.08(10) $Å^3$
Z, Calculated density	2, 1.195 Mg/m^3
Absorption coefficient	1.983 mm^{-1}
F(000)	334

Data Collection:

Measurement device type	SuperNova, Single source at offset), Atlas
Measuremnet method	\w scans
Temperature	123 K
Wavelength	1.54184 Å
Monochromator	graphite
Theta range for data collection	3.71 to 70.92 °.
Index ranges	-12<=h<=10, -7<=k<=8, -14<=l<=13
Reflections collected / unique	6453 / 3163 [R(int) = 0.0582]
Reflections greater I>2\s(I)	2998
Absorption correction	Analytical
Max. and min. transmission	0.990 and 0.930
Refinement	
Refinement method	Full-matrix least-squares on F^2
Hydrogen treatment	:
Data / restraints / parameters	3163 / 1 / 193
Goodness-of-fit on F^2	1.051
Final R indices [I>2sigma(I)]	R1 = 0.0679, wR2 = 0.1791
R indices (all data)	R1 = 0.0704, wR2 = 0.1840
Absolute structure parameter	-0.06(2)
Largest diff. peak and hole	0.359 and -0.569 $e.Å^{-3}$

	x	y	z	U(eq)
O(1)	-7694(3)	-1118(5)	-8578(3)	51(1)
O(2)	-8482(3)	-4152(4)	-8488(2)	44(1)
N(1)	-8522(3)	-3220(4)	-4363(2)	31(1)
C(1)	-7404(3)	-3589(6)	-2452(3)	34(1)
C(2)	-6579(4)	-5114(7)	-2206(3)	41(1)
C(3)	-5433(4)	-4815(8)	-1580(4)	48(1)
C(4)	-5121(5)	-2965(9)	-1196(4)	56(2)
C(5)	-5938(4)	-1433(7)	-1424(4)	48(1)
C(6)	-7079(4)	-1716(6)	-2055(3)	40(1)
C(7)	-8615(3)	-3944(6)	-3169(3)	32(1)
C(8)	-9795(4)	-3040(6)	-2698(3)	37(1)
C(9)	-7392(3)	-3975(5)	-4932(3)	31(1)
C(10)	-6199(3)	-2691(6)	-4739(3)	34(1)
C(11)	-5497(4)	-2862(7)	-5822(3)	39(1)
C(12)	-6214(4)	-4385(6)	-6524(3)	37(1)
C(13)	-7602(3)	-4172(5)	-6221(3)	33(1)
C(14)	-8249(4)	-2392(5)	-6790(3)	34(1)
C(15)	-8121(4)	-2436(6)	-8044(3)	38(1)
C(16)	-8197(5)	-4461(7)	-9656(4)	47(1)
C(17)	-8759(6)	-6365(8)	-9999(4)	61(2)
Cl(1)	-8705(1)	1291(1)	-4416(1)	35(1)

Table 2. Atomic coordinates (x 10^4) and equivalent isotropic displacement parameters ($Å^2$ x 10^3).
U(eq) is defined as one third of the trace of the orthogonalized Uij tensor.

O(1)-C(15)	1.212(5)	C(16)-C(17)	1.484(7)
O(2)-C(15)	1.339(5)	C(2)-H(2)	0.9500
O(2)-C(16)	1.461(5)	C(3)-H(3)	0.9500
N(1)-C(7)	1.519(4)	C(4)-H(4)	0.9500
N(1)-C(9)	1.502(4)	C(5)-H(5)	0.9500
N(1)-H(1N)	0.84(5)	C(6)-H(6)	0.9500
C(1)-C(2)	1.382(6)	C(7)-H(7)	1.0000
C(1)-C(7)	1.511(5)	C(8)-H(8A)	0.9800
C(1)-C(6)	1.407(6)	C(8)-H(8B)	0.9800
C(2)-C(3)	1.395(6)	C(8)-H(8C)	0.9800
C(3)-C(4)	1.385(8)	C(9)-H(9)	1.0000
C(4)-C(5)	1.377(7)	C(10)-H(10A)	0.9900
C(5)-C(6)	1.392(6)	C(10)-H(10B)	0.9900
C(7)-C(8)	1.530(5)	C(11)-H(11A)	0.9900
C(9)-C(10)	1.542(5)	C(11)-H(11B)	0.9900
C(9)-C(13)	1.547(5)	C(12)-H(12A)	0.9900
C(10)-C(11)	1.535(5)	C(12)-H(12B)	0.9900
C(11)-C(12)	1.513(6)	C(13)-H(13)	1.0000
C(12)-C(13)	1.537(5)	C(14)-H(14A)	0.9900
C(13)-C(14)	1.538(5)	C(14)-H(14B)	0.9900
C(14)-C(15)	1.513(5)	C(16)-H(16A)	0.9900

C(16)-H(16B)	0.9900
C(17)-H(17A)	0.9800
C(17)-H(17B)	0.9800
C(17)-H(17C)	0.9800
C(15)-O(2)-C(16)	115.8(3)
C(7)-N(1)-C(9)	114.4(3)
C(7)-N(1)-H(1N)	105(4)
C(9)-N(1)-H(1N)	110(4)
C(6)-C(1)-C(7)	121.2(3)
C(2)-C(1)-C(6)	119.1(3)
C(2)-C(1)-C(7)	119.7(4)
C(1)-C(2)-C(3)	120.9(4)
C(2)-C(3)-C(4)	119.5(5)
C(3)-C(4)-C(5)	120.3(5)
C(4)-C(5)-C(6)	120.5(4)
C(1)-C(6)-C(5)	119.6(4)
N(1)-C(7)-C(8)	108.4(3)
N(1)-C(7)-C(1)	112.1(3)
C(1)-C(7)-C(8)	113.8(3)
C(10)-C(9)-C(13)	105.2(3)
N(1)-C(9)-C(13)	114.4(3)
N(1)-C(9)-C(10)	113.4(3)
C(9)-C(10)-C(11)	105.3(3)
C(10)-C(11)-C(12)	105.6(3)
C(11)-C(12)-C(13)	104.7(3)
C(9)-C(13)-C(12)	99.5(3)
C(12)-C(13)-C(14)	112.0(3)
C(9)-C(13)-C(14)	113.6(3)
C(13)-C(14)-C(15)	110.9(3)
O(1)-C(15)-O(2)	123.8(3)
O(1)-C(15)-C(14)	124.5(4)
O(2)-C(15)-C(14)	111.6(3)
O(2)-C(16)-C(17)	106.8(4)
C(1)-C(2)-H(2)	120.00
C(3)-C(2)-H(2)	120.00
C(2)-C(3)-H(3)	120.00
C(4)-C(3)-H(3)	120.00
C(3)-C(4)-H(4)	120.00
C(5)-C(4)-H(4)	120.00
C(4)-C(5)-H(5)	120.00
C(6)-C(5)-H(5)	120.00
C(1)-C(6)-H(6)	120.00
C(5)-C(6)-H(6)	120.00
N(1)-C(7)-H(7)	107.00
C(1)-C(7)-H(7)	107.00
C(8)-C(7)-H(7)	107.00
C(7)-C(8)-H(8A)	109.00
C(7)-C(8)-H(8B)	109.00
C(7)-C(8)-H(8C)	109.00
H(8A)-C(8)-H(8B)	109.00
H(8A)-C(8)-H(8C)	109.00
H(8B)-C(8)-H(8C)	109.00
N(1)-C(9)-H(9)	108.00
C(10)-C(9)-H(9)	108.00
C(13)-C(9)-H(9)	108.00
C(9)-C(10)-H(10A)	111.00
C(9)-C(10)-H(10B)	111.00
C(11)-C(10)-H(10A)	111.00
C(11)-C(10)-H(10B)	111.00
H(10A)-C(10)-H(10B)	109.00
C(10)-C(11)-H(11A)	111.00
C(10)-C(11)-H(11B)	111.00
C(12)-C(11)-H(11A)	111.00
C(12)-C(11)-H(11B)	111.00
H(11A)-C(11)-H(11B)	109.00
C(11)-C(12)-H(12A)	111.00
C(11)-C(12)-H(12B)	111.00
C(13)-C(12)-H(12A)	111.00
C(13)-C(12)-H(12B)	111.00
H(12A)-C(12)-H(12B)	109.00
C(9)-C(13)-H(13)	110.00
C(12)-C(13)-H(13)	110.00
C(14)-C(13)-H(13)	110.00
C(13)-C(14)-H(14A)	110.00
C(13)-C(14)-H(14B)	109.00
C(15)-C(14)-H(14A)	109.00
C(15)-C(14)-H(14B)	109.00
H(14A)-C(14)-H(14B)	108.00
O(2)-C(16)-H(16A)	110.00
O(2)-C(16)-H(16B)	110.00
C(17)-C(16)-H(16A)	110.00
C(17)-C(16)-H(16B)	110.00
H(16A)-C(16)-H(16B)	109.00
C(16)-C(17)-H(17A)	109.00
C(16)-C(17)-H(17B)	109.00
C(16)-C(17)-H(17C)	109.00
H(17A)-C(17)-H(17B)	109.00
H(17A)-C(17)-H(17C)	109.00
H(17B)-C(17)-H(17C)	110.00

Table 3. Bond lengths [Å] and angles [°].

	U11	*U22*	*U33*	*U23*	*U13*	*U12*
O(1)	67(2)	44(2)	44(2)	8(1)	6(1)	-6(2)
O(2)	58(2)	46(2)	28(1)	-1(1)	1(1)	-7(1)
N(1)	30(1)	35(2)	27(1)	-2(1)	-3(1)	-1(1)
C(1)	40(2)	39(2)	24(1)	1(2)	1(1)	-3(2)
C(2)	44(2)	48(2)	32(2)	6(2)	2(2)	5(2)
C(3)	41(2)	65(3)	38(2)	12(2)	-1(2)	10(2)
C(4)	45(2)	88(4)	33(2)	7(2)	-9(2)	-11(2)
C(5)	52(2)	55(3)	35(2)	-3(2)	-4(2)	-18(2)
C(6)	48(2)	40(2)	32(2)	-3(2)	-3(2)	-8(2)
C(7)	41(2)	28(2)	27(2)	3(1)	-2(1)	-1(2)
C(8)	39(2)	36(2)	35(2)	1(1)	1(2)	-1(2)
C(9)	32(2)	31(2)	27(2)	1(1)	-2(1)	-1(1)
C(10)	36(2)	32(2)	32(2)	-3(1)	-3(1)	-5(2)
C(11)	36(2)	44(2)	38(2)	3(2)	3(2)	-1(2)
C(12)	44(2)	34(2)	32(2)	2(1)	2(1)	9(2)
C(13)	36(2)	33(2)	29(2)	-1(1)	-1(1)	0(1)
C(14)	38(2)	33(2)	32(2)	1(1)	0(1)	6(1)
C(15)	40(2)	39(2)	34(2)	7(2)	1(1)	5(2)
C(16)	55(2)	54(3)	34(2)	-2(2)	7(2)	-1(2)
C(17)	82(3)	63(3)	40(2)	-7(2)	11(2)	-21(3)
Cl(1)	38(1)	26(1)	39(1)	-1(1)	-5(1)	-1(1)

Table 4. Anisotropic displacement parameters ($Å^2$ x 10^3).
The anisotropic displacement factor exponent takes the form:
$-2\ pi^2\ [\ h^2\ a^{*2}\ U11 + ... + 2\ h\ k\ a^*\ b^*\ U12\ ]$.

	x	*y*	*z*	*U(eq)*
H(1N)	-9190(50)	-3600(80)	-4710(40)	37
H(2)	-6796	-6384	-2466	49
H(3)	-4870	-5872	-1419	58
H(4)	-4339	-2752	-773	67
H(5)	-5721	-173	-1148	57
H(6)	-7635	-652	-2217	48
H(7)	-8752	-5382	-3206	39
H(8A)	-9678	-1631	-2626	44
H(8B)	-9923	-3600	-1959	44
H(8C)	-10540	-3310	-3207	44
H(9)	-7183	-5294	-4620	37
H(10A)	-6439	-1324	-4603	40
H(10B)	-5658	-3163	-4087	40
H(11A)	-5501	-1601	-6222	47
H(11B)	-4604	-3269	-5652	47
H(12A)	-5889	-5704	-6337	44
H(12B)	-6136	-4145	-7334	44
H(13)	-8092	-5382	-6420	39
H(14A)	-9161	-2379	-6637	41
H(14B)	-7856	-1188	-6473	41
H(16A)	-7266	-4476	-9726	57

H(16B)	-8571	-3408	-10136	57
H(17A)	-9678	-6334	-9916	74
H(17B)	-8373	-7394	-9523	74
H(17C)	-8599	-6623	-10784	74

Table 5. Hydrogen coordinates (x 10^4) and isotropic displacement parameters ($Å^2$ x 10^3).

C(16)-O(2)-C(15)-C(14)	-170.2(4)
C(15)-O(2)-C(16)-C(17)	-175.8(4)
C(16)-O(2)-C(15)-O(1)	6.9(6)
C(9)-N(1)-C(7)-C(8)	179.3(3)
C(7)-N(1)-C(9)-C(10)	-88.9(3)
C(7)-N(1)-C(9)-C(13)	150.4(3)
C(9)-N(1)-C(7)-C(1)	52.9(4)
C(7)-C(1)-C(6)-C(5)	-178.1(4)
C(2)-C(1)-C(7)-N(1)	-103.2(4)
C(2)-C(1)-C(6)-C(5)	0.0(6)
C(7)-C(1)-C(2)-C(3)	177.7(4)
C(6)-C(1)-C(7)-C(8)	-48.5(5)
C(2)-C(1)-C(7)-C(8)	133.4(4)
C(6)-C(1)-C(7)-N(1)	74.9(4)
C(6)-C(1)-C(2)-C(3)	-0.5(6)
C(1)-C(2)-C(3)-C(4)	0.3(6)
C(2)-C(3)-C(4)-C(5)	0.4(7)
C(3)-C(4)-C(5)-C(6)	-0.9(7)
C(4)-C(5)-C(6)-C(1)	0.7(6)
N(1)-C(9)-C(13)-C(12)	164.8(3)
N(1)-C(9)-C(13)-C(14)	45.6(4)
C(10)-C(9)-C(13)-C(14)	-79.6(3)
C(13)-C(9)-C(10)-C(11)	-21.2(4)
C(10)-C(9)-C(13)-C(12)	39.6(3)
N(1)-C(9)-C(10)-C(11)	-147.0(3)
C(9)-C(10)-C(11)-C(12)	-6.3(4)
C(10)-C(11)-C(12)-C(13)	31.9(4)
C(11)-C(12)-C(13)-C(14)	76.5(4)
C(11)-C(12)-C(13)-C(9)	-43.9(3)
C(9)-C(13)-C(14)-C(15)	165.3(3)
C(12)-C(13)-C(14)-C(15)	53.5(4)
C(13)-C(14)-C(15)-O(1)	-126.4(4)
C(13)-C(14)-C(15)-O(2)	50.6(4)

Table 6. Torsion angles [°].

D-H...A	d(D-H)	d(H...A)	d(D...A)	<(DHA)
N(1)-H(1N)...Cl(1)#1	0.84(5)	2.39(5)	3.200(3)	163(5)
C(7)-H(7)...Cl(1)#2	1.0000	2.7100	3.598(4)	148.00
C(14)-H(14A)...Cl(1)#1	0.9900	2.8000	3.715(4)	154.00

Table 7. Hydrogen-bonds [Å and °].

Curriculum vitae

Personal information

Email	pdistefano7@googlemail.com ; ptr.dst@libero.it
Date of birth	July 7th, 1984 in Palermo, Italy
Nationality	Italian

Education and qualifications

October 2008 - July 2012: Ph.D. work in Medicinal Chemistry at the University of Regensburg under supervision of Prof. Dr. Oliver ReiserUniversity of Regensburg, Germany. "*Synthesis, applications and conformational investigations of Neuropeptide Y analogues, containing γ-aminocyclopentyl acetic acid and trans-pentacin".*

October 2008 - March 2011: associated to the research training group *Graduate College GRK 760* (Research Training Group) Medicinal Chemistry: Molecular Recognition – Ligand-Receptor Interactions.

July 2008: **Graduation**: Diploma in chemistry and pharmaceutical technology at the University of Palermo, Italy. Result of final examination: 110/110

September 2007 - July 2008: Diploma thesis in the research group of Ch.mo Prof. Patrizia Diana at the Dipartimento Farmacochimico, Tossicologico e Biologico (Univeristy of Palermo). *"7-Azaindolo[1,2-c][1,2,3]Benzotriazina: Un nuovo stistema eterociclico a potenziale attività antitumorale"* (7-Azaindole[1,2-c][1,2,3]Benzotriazine: a new heterocyclic system with potential anticancer activity).

September 2003 - July 2008: Studies in chemistry and pharmaceutical technology at the University of Palermo, Italy.

September 1998 - July 2003: Istituto tecnico industriale "Ettore Majorana", Palermo, Italy.
(High school in food chemistry). Result of final examination: 90/100.

Conferences and Courses

5th Summer School Medicinal Chemistry, University of Regensburg, September 13 - 15, 2010. Poster presentation: *"Enantioselective synthesis of new unnatural amino acids for foldamers and selective ligands for Neuropeptide Y receptors"*

Excursions in ***Bayer Shering Pharma AG***, Berlin Juli 2010, organized by *Graduate College GRK 760* (Research Training Group) Medicinal Chemistry: Molecular Recognition – Ligand-Receptor Interactions.

International Cost action workshop, University of Frankfurt am Main, 6 October 2009.
"BioMedCgem in Histamine H_4 receptors: New compounds for translational steps"

Excursions in ***Merz Pharm***, Frankfurt am Main, 5 October 2009, organized by *Graduate College GRK 760* (Research Training Group) Medicinal Chemistry: Molecular Recognition – Ligand-Receptor Interactions.

Minisymposium Histamine H_4 Receptor, University of Regensburg (Germany), February 20, 2009.

Acknowledgements

I would like to thank my Ph.D. tutor, *Prof. Dr. Oliver Reiser,* who gave me the opportunity to perform my Ph.D. in Germany. He offered me an interesting research project in the world of peptides and amino acids.

I am especially grateful to *Prof. Dr. Chiara Cabrele* for her help and suggestions with CD and NMR spectroscopy analysis on peptides. Furthermore, I thank her coworkers at the University of Bochum for the synthesis of the NPY analogues by solid phase synthesis.

A thanks to *Mr. Kastner*, *Ms. Schramm* and *Ms. Stülher* for their patience in recording 2D-NMR spectra; *Mr. Kiermeier* for recording mass-spectra and elemental analysis; Dr. *Zabel* and Ms. *Stempfhuber* for recording X-ray spectra. Additionally, I thank the group of *Prof. Dr. O. Wolfbeis* for the use of the circular dichroism spectrometer and *Dr.Vasold* for HPLC analysis.

I am grateful to *Dr. P. Kreitmeier* for his answers to any questions, K. Döring and G. Adolin for helpful contribution to some synthesis.

I am especially grateful to *Dr. Max Keller* for his help during peptide HPLC-purifications in the group of *Prof. Dr. Armin Buschauer.*

For the correction of my Ph.D. thesis I would like to thank *Prof. Dr. Chiara Cabrele, Michael Pirtsch, Georgii KachKovskyi, Ludwig Pilsl, Danette Brink.*

For the financial support I am grateful to the *Deutsche Forschungsgemeinschaft (DFG), Graduiertenkolleg GRK 760 Medicinal Chemistry.*

I am grateful to all my colleagues who contributed to my Ph.D. work either with chemistry advices or with friendship. In special case the people who worked in lab with me: *Michael Pirtsch, Georgii KachKovskyi, Tapan Maji, Michel Chiarucci, Deepak D. Jadhav.*

A special thanks to *Dr. Florian Sahr* for his help during my first months in Regensburg and also for the nice BBQ in our balcony together with *Dr. Klaus Harrar*, *Ludwig Pilsl*, *Dr. Hans Zwicknagl*, *Dr. Alexander Schätz, Dr. Tobias Olbrich, Dr. Alexander Tereshchenko, Dr. Anu Naik.*

Moreover, I would like to thank all friends that gave me, with their kind friendship, an important contribution to my experience in Regensburg:
Dr. Andrea Nobile, Dr. Fabio Baruffa, Dr. Pino D'Amico, Federico Pressacco, Dr. Allan Patrick Macabeo, Dr. Marco Durini, Dr. Mattia Marchini, Danette Brink, Salvo Tomasello, Dr. Yu-mi Sylvester, Nicola Abate, Luca Castagnini, Thomas Zannini.

For the support from a distance, I would like to thank: my parents *Rosaria* and *Gioacchino*, my sister *Maria* and my childhood friends *Adriano Russello, Tony Mangano, Alice Giocolano, Serena Argento, Fabrizio Chiodo and Nicola Prosa.*

My fiancée *Ylenia* and my parents receive my greatest wholeheartedly thank for their support, understanding, helpfulness and encouragement they gave me at any time during this experience.